Modelling and Identification of Time-domain Electromagnetic Fields of an Antenna

Rafael Rodrigues Luz Benevides

dissertação de mestrado

departamento de engenharia elétrica

UNIVERSIDADE DE BRASÍLIA

FACULDADE DE TECNOLOGIA

Universidade de Brasília
Faculdade de Tecnologia
Departamento de Engenharia Elétrica

Modelling and Identification of Time-domain Electromagnetic Fields of an Antenna

Rafael Rodrigues Luz Benevides

DISSERTAÇÃO DE MESTRADO SUBMETIDA AO PROGRAMA DE PÓS-GRADUAÇÃO EM ENGENHARIA ELÉTRICA DA UNIVERSIDADE DE BRASÍLIA COMO PARTE DOS REQUISITOS NECESSÁRIOS PARA A OBTENÇÃO DO GRAU DE MESTRE.

APROVADA POR:

Prof. Sébastien Roland Marie Joseph Rondineau, D.Sc. (ENE-UnB)
(Orientador)

Fábio César Siqueira da Silva, D.Sc. (Wavsense LLC)
(Examinador Externo)

Prof. Achiles Fontana da Mota, D.Sc. (ENE-UnB)
(Examinador Interno)

Brasília/DF, 02 de Junho de 2022.

FICHA CATALOGRÁFICA

BENEVIDES, RAFAEL RODRIGUES LUZ

Modelling and Identification of Time-domain Electromagnetic Fields of an Antenna . [Distrito Federal] 2022.

x, 113 p., 210 x 297 mm (ENE/FT/UnB, Mestre, Dissertação de Mestrado, 2022).

Universidade de Brasília, Faculdade de Tecnologia, Departamento de Engenharia Elétrica.

Departamento de Engenharia Elétrica

1. Antenna
2. Time-domain
3. Causality
4. Mode Coefficients
5. Spherical Wave Expansion
6. General Sampling Theorem
7. Self-adjoint Differential Operators
8. Compact Operators

I. ENE/FT/UnB

II. Título (série)

REFERÊNCIA BIBLIOGRÁFICA

BENEVIDES, R. R. L. (2022). Modelling and Identification of Time-domain Electromagnetic Fields of an Antenna . Dissertação de Mestrado em Engenharia Elétrica, Publicação PPGENE.DM-784/22, Departamento de Engenharia Elétrica, Universidade de Brasília, Brasília, DF, 113 p.

CESSÃO DE DIREITOS

AUTOR: Rafael Rodrigues Luz Benevides

TÍTULO: Modelling and Identification of Time-domain Electromagnetic Fields of an Antenna .

GRAU: Mestre ANO: 2022

Rafael Rodrigues Luz Benevides

Universidade de Brasília (UnB)

Campus Darcy Ribeiro

Faculdade de Tecnologia - FT

Departamento de Eng. Elétrica (ENE)

Brasília - DF CEP 70919-970

To my beloved family, Francinara, Victor and Marina.

Acknowledgements

I would like to express my most sincere gratitude...

... to Professor Sébastien and Colonel Gleidson, for the unconditional support to my academic life, for the time spent in great and productive technical discussions and for their guiding without which this work could not have come to fruition.

... to my dear wife, Francinara, for her love, patience and constant concern on the well-being of our family which brought me the necessary peace to keep my focus at this work.

... to my curious son Victor, for filling my heart with joy and happiness on a daily basis and to my yet-to-be-born daughter Marina, for bringing me hope and strength to endure any difficulty.

... to my beloved mother Sandra, for having taught me how to draw my way through science and knowledge.

... to my good friend Mario, for the uncountable hours of nice talks and helping on engineering, physics and mathematics.

I'm most certainly indebted with you.

Abstract

This works is focused on the construction of a reliable model for the time-domain propagating electromagnetic field of an antenna. Such model, which can be seen as the Green's function of an antenna setup, is based on two pillars: the first regards a dataset of phasor electric field samples from the antenna previously collected on laboratory over a collection of frequencies; while the second relies on an adaptation of the famous Nyquist sampling theorem used to perform an interpolation over the frequencies. As it is shown, the Nyquist reconstruction method is not capable of retrieving causal electric fields. For this reason, The general sampling theorem is considered and a new sampling theorem is proposed to correct the causality of the reconstructed field. Moreover, a new identification method, based on a mode-recursive algorithm inspired by the Kalman filter, is proposed and applied to estimate the mode coefficients of an antenna minimising their uncertainty and, consequently, their bias, hence leading to more reliable estimators.

Keywords: Antenna, time-domain, causality, mode coefficients, spherical wave expansion, general sampling theorem, self-adjoint differential operators, spectral theory of self-adjoint and compact operators.

Contents

List of Figures

List of Symbols

Sets

$\mathbb{N}$	Natural numbers
$\mathbb{N}_0$	$\mathbb{N} \cup \{0\}$
$\mathbb{N}_p$	Let p denote an atomic formula. Hence, $\mathbb{N}_p \stackrel{\text{def}}{=} \{n \in \mathbb{N};\ p(n)\}$. For example, $\mathbb{N}_{\leqslant m} = \{n \in \mathbb{N};\ n \leqslant m\}$ and $\mathbb{N}_{\neq m} = \{n \in \mathbb{N};\ n \neq m\}$.
$\mathbb{R}$	Real numbers
$\mathbb{R}_p$	Let p denote an atomic formula. Hence, $\mathbb{R}_p \stackrel{\text{def}}{=} \{u \in \mathbb{R};\ p(u)\}$. For example, $\mathbb{R}_{\leqslant a} = \{u \in \mathbb{R};\ u \leqslant a\}$ and $\mathbb{R}_{\neq a} = \{u \in \mathbb{R};\ u \neq a\}$.
$\mathbb{C}$	Complex numbers
$\mathcal{B}(\Omega; X)$	Class of bounded functions $\psi : \Omega \to X$.
$\mathcal{C}^0(\Omega; X)$	Class of continuous functions $\psi : \Omega \to X$.
$\mathcal{C}^m(\Omega; X)$	Class of continuous functions $\psi : \Omega \to X$ whose derivative $\psi' \in \mathcal{C}^{m-1}(\Omega; X)$.
$L^2(\Omega, \Sigma, \mu)$	Linear Space of functions $\psi : \Omega \to \mathbb{C}$ square-integrable with respect to the Lebesgue measure $\mu : \Sigma \to \mathbb{R}_{\geqslant 0}$ where Σ denotes a σ-algebra of Ω subsets.

Electromagnetism

$\overrightarrow{\mathcal{E}}, \overrightarrow{\mathrm{E}}, \overrightarrow{E}$	Time-domain, frequency-domain and Phasor electric field vector.
$\boldsymbol{\mathcal{E}}, \mathbf{E}, \boldsymbol{E}$	Components (column matrices) of the time-domain, frequency-domain and Phasor electric field vector. The reference frame over which the components are given is specified by the context.
$\mathcal{E}, \mathrm{E}, E$	Magnitude (absolute value) of the time-domain, frequency-domain and Phasor electric field vector given by the euclidian norm: $\sqrt{\boldsymbol{\mathcal{E}}^{\mathrm{T}}\boldsymbol{\mathcal{E}}}$, $\sqrt{\mathbf{E}^{\mathrm{H}}\mathbf{E}}$ and $\sqrt{\boldsymbol{E}^{\mathrm{H}}\boldsymbol{E}}$.

General Sampling

K	Kernel of the integral transform
$\mathfrak{U}$	(Gothic U) Sampling Domain
$(\mathfrak{U}, \Sigma_{\mathfrak{U}}, \mu)$	Measure space considered for the sampling domain
$\langle \cdot \vert \cdot \rangle_{\mathfrak{U}}$	Inner product on $L^2(\mathfrak{U}, \Sigma_{\mathfrak{U}}, \mu)$

$\|\cdot\|_{\mathfrak{U}}$	Norm on $L^2(\mathfrak{U}, \Sigma_{\mathfrak{U}}, \mu)$
$\mathfrak{V}$	(Gothic V) Transformed Domain
$(\mathfrak{V}, \Sigma_{\mathfrak{V}}, \mu)$	measure space considered for the transformed domain
$\langle\cdot\|\cdot\rangle_{\mathfrak{V}}$	Inner product on $L^2_w(\mathfrak{V}, \Sigma_{\mathfrak{V}}, \mu)$
$\|\cdot\|_{\mathfrak{V}}$	Norm on $L^2_w(\mathfrak{V}, \Sigma_{\mathfrak{V}}, \mu)$

Sturm-Liouville Theory

L	Sturm-Liouville Operator
v^+	Upper bound of RSLP domain
v^-	Lower bound of RSLP domain
λ	Eigenvalues
φ	Eigenfunctions

Miscellaneous

j	Imaginary unit
$[\cdot\|\cdot]$	Matrix Commutator.
$\overset{\text{a.e.}}{=}$	The equality holds almost everywhere. Let $\psi_1, \psi_2 \in L^2(\Omega, \Sigma, \mu)$, $\psi_1 \overset{\text{a.e.}}{=} \psi_2$ is written to mean that $\mu\left(\left\{u \in \Omega;\ \psi_1(u) \neq \psi_2(u)\right\}\right) = 0$.
$0, \mathbf{0}, \overrightarrow{0}$	Zero elements. $\mathbf{0}$ and $\overrightarrow{0}$ repectively denote the zero matrix (whose dimensions shall be deduced from the context) and the three-dimensional zero vector while the same symbol, 0, is used for both the scalar zero and the zero function of any function space.

List of Abbreviations

GST	General Sampling Theorem. 58–60, 62, 63, 65, 70, 71
HHE	Homogeneous Helmholtz Equation. 102, 107
WNSST	Whittaker-Nyquist-Shannon Sampling Theorem. 5, 57–61, 70, 71, 90

Glossary

Maxwell's Equations The set of partial differential equations which classically describes the electromagnetic fields created by charges. 3, 8

PLTI system Real-valued, causal, continuous-time, linear and time-invariant system. The 'P' stands for "Physical". 3, 4, 24, 92, 95–97

Chapter 1

Introduction

In general, the parameters of an antenna are described by their performance on the frequency-domain centred, in particular, at its band of operation. The reason lies mainly in the fact that the phasor form of the antenna fields, from which those parameters derive, are quite simple to handle from the mathematical perspective.

It is often the case, however, that an application (*e.g.*, radar) is focused in the time-domain response of the electromagnetic fields of an antenna. Despite what is commonly thought, and as it will be further shown, the time-domain form of a field is not easily achieved by simply taking the Inverse Fourier Transform of its phasor form. Moreover, even if that were the case, for most practical scenarios the phasor form would not be available as a function of frequency, but it would only be known at a particular discrete set of frequencies, over which the antenna has been tested and its fields were measured.

On this matter, the objective of this work shall be seen as developing a method for estimating the time-domain electromagnetic fields of an antenna given measured samples of its phasor field in different frequencies. In the way of achieving such goal, some complementary objectives have also been established: planning the set of sampling frequencies with the intention of reducing the number of tests performed over the antenna; and using the minimal set of functions (eigenspace) onto which the phasor fields are projected in order to save computational resources and improve the implementation performance.

As a first step towards such direction, this chapter intends to provide the necessary context over which this work is built and introduce the first technical aspects of it. Furthermore, it is worth emphasising that although the minimum formalism, required to robustly state and define the mathematical problem, is adopted throughout the text, it is mildly presented in the following sections.

1.1 State-of-the-Art

With respect to the construction of a mathematical model for the time-domain radiated electromagnetic field of an antenna, a central issue lies in the determination, or estimation, of its spherical mode coefficients as function of frequency, which are necessary to completely characterise such field. In this regard, [MAU13] shows that the usage of Vector Spherical Harmonics requires less mode coefficients to efficiently represent the electromagnetic field, as it

is expected since it carries more information about the vector behaviour of the field. For this reason, the vector approach is also adopted throughout this text.

Regarding the retrieving of the time-domain electromagnetic field, some techniques are worth citing: [RRF14] estimate near-field components using a FDTD solver for the case of a UWB antenna from which the far-field is obtained after a transformation while [Kli10] provides a method for determining the time-domain Poynting vector of the radiated (far-field) electromagnetic field, also based in the modal decomposition of such vector. The causality nature of those results are, nevertheless, not ensured. In this sense, [Lag21] creates model for the antenna excitation that would provide causal responses. As it is known and expected, the causality of the response, however, should be ensured by the physical properties of the model and not by a certain class of excitations. In such context, this work provides a robust causal model for the electromagnetic fields (near and far-field) produced by an antenna base in the Spherical modal expansion.

1.2 Theoretical background

In order to better understand the proposed work, it is worth reminding some fundamentals about both linear systems and antenna measurements.

1.2.1 Remark on Space and Notation of Physical Quantities

For the purpose of modelling the electromagnetic field produced by an antenna, it is enough to require the spatial space $\mathfrak{S}$ to be a three-dimensional euclidean inner product linear space over $\mathbb{R}$, where its vectors are usually thought as directions. Although all classical time-dependent vectors lie in $\mathfrak{S}$, it is also useful to define its complexification $\mathfrak{S}^{\mathbb{C}}$ – a complex extension of $\mathfrak{S}$ whose process is nicely described by [BN00, Section 2.1] – where the frequency-dependent counterparts of those vectors live.

As discussed and shown in [Rud91, Section 1.19 and Theorem 1.21], any orthonormal basis $\{\hat{\mathrm{x}}, \hat{\mathrm{y}}, \hat{\mathrm{z}}\} \subset \mathfrak{S}$, which is also an orthonormal basis in $\mathfrak{S}^{\mathbb{C}}$, induces a homeomorphism of $\mathfrak{S}^{\mathbb{C}}$ onto $\mathbb{C}^3$, which hence means that those spaces share the same topology. In fact, an arbitrary vector $\overrightarrow{a} \in \mathfrak{S}^{\mathbb{C}}$, if written as $\overrightarrow{a} = a_x\hat{\mathrm{x}} + a_y\hat{\mathrm{y}} + a_z\hat{\mathrm{y}}$, may be identified by a column matrix $\boldsymbol{a} \in \mathbb{C}^3$, given by $\boldsymbol{a} = \begin{bmatrix} a_x & a_y & a_z \end{bmatrix}^{\mathrm{T}}$, of its components with respect to such basis where a_x, a_y and a_z are, of course, complex numbers.

As it has been presented, and also for the sake of tradition and simplicity, vectors in $\mathfrak{S}^{\mathbb{C}}$ shall be represented by a regular (non-boldfaced) character with an arrow or wedge (for denoting unit vectors) above them (*e.g.*, $\overrightarrow{a}$ and $\hat{\mathrm{x}}$). On the other hand, their associated column matrices in $\mathbb{C}^3$, with respect to an orthonormal basis conveniently established by the context, shall be written using the same symbol now boldfaced but without the arrow while the wedge is kept (*e.g.*, $\boldsymbol{a}$ and $\hat{\mathbf{x}}$).

Moreover, $\mathfrak{S}^{\mathbb{C}}$ defines the inner product for its vectors as $\overrightarrow{a} \cdot \overrightarrow{b} = \boldsymbol{a}^{\mathrm{H}}\boldsymbol{b}$ to keep its metric

in accordance with the euclidean notion of distance. In this sense, the magnitude of a vector $\overrightarrow{a}$ will be denoted by its regular character, a, and given by $a = \sqrt{\overrightarrow{a} \cdot \overrightarrow{a}} = \sqrt{\boldsymbol{a}^{\mathrm{H}}\boldsymbol{a}}$. $\mathfrak{S}^{\mathbb{C}}$ also implements the cross product of its vectors as $\overrightarrow{a} \times \overrightarrow{b} \in \mathfrak{S}^{\mathbb{C}}$ associated with the matrix $[\![\boldsymbol{a}]\!]\,\boldsymbol{b} \in \mathbb{C}^3$. Still on this subject, it is worth highlighting that abuses of notation like $\boldsymbol{a} \cdot \boldsymbol{b}$ and $\boldsymbol{a} \times \boldsymbol{b}$ (respectively meaning $\boldsymbol{a}^{\mathrm{H}}\boldsymbol{b}$ and $[\![\boldsymbol{a}]\!]\,\boldsymbol{b}$) may occasionally occur when no confusion is possible to preserve the visual clarity and cleanliness of some equations.

In most cases, the scalar and vector quantities dealt in this text are time-dependent, which naturally suggests treating them as regular functions of time on the form $a : \mathbb{R} \to \mathbb{R}$ or $\overrightarrow{a} : \mathbb{R} \to \mathfrak{S}$. However, more structure is needed since the Fourier Transform of such quantities should be well defined and, of course, they must be retrieved through the Inverse Fourier Transform. Classically, such structure is reached by restricting those function to the Schwartz spaces $\mathcal{S}(\mathbb{R};\mathbb{R})$ and $\mathcal{S}(\mathbb{R};\mathfrak{S})$, *cf*. [Zem87, Theo. 7.3-2, page 183], of rapid descent functions. Nevertheless, such restriction exclude several practical and desirable cases (*e.g.*, plane waves). Such issue is not overcame in the domain of classical functions, but in the domain of tempered distributions (or slow growth distributions) defined onto those Schwartz spaces, *cf*. [Zem87, Theo. 7.4-2, page 187]. Hence, it must be required that a and $\overrightarrow{a}$ lie in the dual spaces $\mathcal{S}(\mathbb{R};\mathbb{R})^*$ and $\mathcal{S}(\mathbb{R};\mathfrak{S})^*$, respectively.

Regarding the notation and following the literature convention, no distinction will be made between a function f and its regular tempered distribution, which is the linear functional (or linear form) in the dual space of the suitable Schwartz space defined by the map

$$\varphi \;\mapsto\; \int_{\mathbb{R}} f(t)\,\varphi(t)\,dt \tag{1.1}$$

for any function φ in the said Schwartz space.

1.2.2 Antenna as a Dynamic System

In the most pragmatic fashion, consider an antenna and let $\boldsymbol{\mathcal{E}}(\boldsymbol{r},t)$ denote the electric field it produces at the position $\boldsymbol{r}$, with respect to a conveniently established frame of reference, and at the time t. Since this field is created due to the presence of a current density field $\boldsymbol{\mathcal{J}}(\boldsymbol{r},t)$ on the surface of the antenna, such device may hence be thought as a dynamic system having the current density as its input while the electric field is seen as its output, as it has been depicted in Figure 1.1.

Such system, which clearly inherits the linearity, reality and non-discreteness from Maxwell's Equations, must also, for obvious reasons, be causal. Moreover, if the antenna geometry and electromagnetic properties of the related media are assumed to not change over time, the system is also time-invariant. A system carrying all this properties will henceforth be referred as PLTI system, where "P" stands for physical (characterised by causality, reality and non-discreteness) while "LTI" is the well know acronym for "Linear and Time-invariant".

In most practical cases, the field $\boldsymbol{\mathcal{J}}$ can not be arbitrarily set. Instead, it is usually induced and controlled by a well defined scalar time-domain signal wave $\mathcal{U}$ (*e.g.*, voltage, current) input

Figure 1.1: Dynamic system block representing the antenna.

at the equipment RF chain that feeds the antenna. Such process also defines an electromagnetic dynamic system (Figure 1.2) which, for the very same previous reasons, is also considered to be PLTI. In this sense, it becomes interesting to define the operation setup of an antenna as the composition of the two systems which, of course, is a PLTI system itself as well.

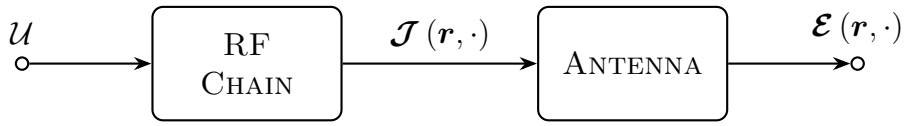

Figure 1.2: Block diagram of an antenna operation setup.

In the light of the above formalism, the main purpose of this work may be considered as finding the equivalent transfer function of such composition. Which might be done by estimating each transfer function separately and then combined them. In fact, the transfer function of the antenna block is a well established result, *cf*. [Jac99, Sec. 6.4, Eq. 6.44]. However, since only samples of $\boldsymbol{\mathcal{E}}$ and $\mathcal{U}$ are actually collected, it makes better sense identifying the composition as a whole. The next section provides a heuristic approach to the method used to reach this goal, hence working as a high-level outline of this work, whose detailed contents are developed in the following chapters.

1.2.3 Modelling the Antenna Operation Setup

The PLTI properties of the previously defined operation setup ensure that the electric field $\boldsymbol{\mathcal{E}}(\boldsymbol{r},\cdot)$ is given by the convolution of the input signal $\mathcal{U}$ with the Green's Function (or transfer function) $\boldsymbol{\mathcal{G}}(\boldsymbol{r},\cdot)$ of such setup as follows

$$\boldsymbol{\mathcal{E}}(\boldsymbol{r},t) = \int_{\mathbb{R}} \boldsymbol{\mathcal{G}}(\boldsymbol{r},t')\,\mathcal{U}(t-t')\,dt', \tag{1.2}$$

where the integral is taken in the Lebesgue sense. Of course $\boldsymbol{\mathcal{G}}$ must be real-valued since it is the electric field response to the impulse $\mathcal{U} = \delta$. Moreover, the causality requires that $\boldsymbol{\mathcal{G}}(\boldsymbol{r},t) = 0$ for any $t < 0$ in order to prevent any advanced response of the system, hence exposing the non-analytic nature of this function.

From this standpoint, it is worth noting that the objective of this work, early described in this introduction, can now be seen as estimating $\boldsymbol{\mathcal{G}}$, since it completely provides the necessary information to calculate the electric field, given an arbitrary input signal. In this direction, the start point is the result

$$\boldsymbol{\mathcal{G}}(\boldsymbol{r},t)=\frac{1}{\mathcal{U}_0}\int_{\mathbb{R}}\boldsymbol{E}(\boldsymbol{r},\nu)\,e^{j2\pi\nu t}d\nu \tag{1.3}$$

(proven in the Section 7.A) for some real constant $\mathcal{U}_0$ meaning the amplitude of the input signal over which the phasor was collected, which establishes that $\boldsymbol{\mathcal{G}}$ is directly proportional to the inverse Fourier Transform of the electric phasor field $\boldsymbol{E}(\boldsymbol{r},\nu)$, where ν denotes the frequency of the phasor. As consequence, the problem of finding $\boldsymbol{\mathcal{G}}$ is now equivalent to the problem of finding $\boldsymbol{E}$.

As it will be shown in Chapter 3, it is possible to project the electric phasor field $\boldsymbol{E}$ on the orthogonal and complete set $\left\{\boldsymbol{T}_{\ell m}\right\}_{\ell\in\mathbb{N},|m|\leqslant\ell}$, $\boldsymbol{T}_{\ell m}(\boldsymbol{r},\nu)\in\mathbb{C}^{3\times 2}$, constructed from the known spherical eigenfunctions of the vector laplacian operator. Thus, it holds that

$$\boldsymbol{E}(\boldsymbol{r},\nu)=\sum_{\ell\in\mathbb{N}}\sum_{|m|\leqslant\ell}\boldsymbol{T}_{\ell m}(\boldsymbol{r},\nu)\,\boldsymbol{q}_{\ell m}(\nu)\,, \tag{1.4}$$

where $\{\boldsymbol{q}_{\ell m}\}_{\ell\in\mathbb{N},|m|\leqslant\ell}$, $\boldsymbol{q}_{\ell m}(\nu)\in\mathbb{C}^{2\times 1}$, is a sequence of coefficient functions and the indices ℓ and m correspond to the (ℓ,m)-spherical mode.

The determination of the coefficients functions $\boldsymbol{q}_{\ell m}$ is certainly the part of this work that requires the most practical attention since they can not be directly measured. In fact, as described in Chapter 4, for a mode ℓ, it is only possible to estimate samples $\left\{\boldsymbol{q}_{\ell m}(\nu_n)\right\}_{n\in\mathbb{N}}$ at a countable set of frequencies $\{\nu_n\}_{n\in\mathbb{N}}$ over which tests were performed and electric field samples were measured. In this scenario, an interpolation method shall take place in order to estimate the value of the function $\boldsymbol{q}_{\ell m}$ at an arbitrary frequency. Most commonly, the Whittaker-Nyquist-Shannon Sampling Theorem (WNSST) is adopted to fill those gaps. However, as it is shown in the introduction of chapter 5, such procedure leads to non-causal responses $\boldsymbol{E}$. In order to avoid such problem, a generalised sampling theorem is studied in along that chapter as a template result for other sampling theorems which, leading to causal responses, are proposed in Chapter 6. In this sense, $\boldsymbol{q}_{\ell m}$ is reconstructed as

$$\boldsymbol{q}_{\ell m}(\nu)=\sum_{n\in\mathbb{N}}\boldsymbol{q}_{\ell m}(\nu_n)\,\xi_n(\nu)\,, \tag{1.5}$$

where the constructor functions $\xi_n:\mathbb{R}\to\mathbb{C}$ arise from those new sampling theorems.

Once the mode coefficient $\boldsymbol{q}_{\ell m}$ are accessible as functions, it becomes possible write the phasor electric field as

$$\boldsymbol{E}(\boldsymbol{r},\nu)=\sum_{n\in\mathbb{N}}\sum_{\ell\in\mathbb{N}}\sum_{|m|\leqslant\ell}\boldsymbol{T}_{\ell m}(\boldsymbol{r},\nu)\,\xi_n(\nu)\cdot\boldsymbol{q}_{\ell m}(\nu_n) \tag{1.6}$$

and, consequently, the Green's function may be retrieved as follows

$$\begin{aligned}\boldsymbol{\mathcal{G}}(\boldsymbol{r},t) &= \sum_{n\in\mathbb{N}}\sum_{\ell\in\mathbb{N}}\sum_{|m|\leqslant\ell}\left[\frac{1}{\mathcal{U}_0}\int_{\mathbb{R}}\boldsymbol{T}_{\ell m}(\boldsymbol{r},\nu)\,\xi_n(\nu)\,e^{\jmath 2\pi\nu t}d\nu\right]\boldsymbol{q}_{\ell m}(\nu_n)\\ &= \sum_{n\in\mathbb{N}}\sum_{\ell\in\mathbb{N}}\sum_{|m|\leqslant\ell}\left[\frac{1}{\mathcal{U}_0}\int_{\mathbb{R}}\boldsymbol{\mathcal{T}}_{\ell m}(\boldsymbol{r},t)\,\Xi_n(t-t')\,dt'\right]\boldsymbol{q}_{\ell m}(\nu_n)\\ &= \sum_{n\in\mathbb{N}}\sum_{\ell\in\mathbb{N}}\sum_{|m|\leqslant\ell}\boldsymbol{\mathcal{G}}_{\ell mn}(\boldsymbol{r},t)\,\boldsymbol{q}_{\ell m}(\nu_n),\end{aligned} \tag{1.7}$$

where $\boldsymbol{\mathcal{T}}_{\ell m}(\boldsymbol{r},\cdot)$ and Ξ_n are the inverse Fourier transforms of $\boldsymbol{T}_{\ell m}(\boldsymbol{r},\cdot)$ and ξ_n, respectively, whilst $\boldsymbol{\mathcal{G}}_{\ell mn}(\boldsymbol{r},\cdot)$ is their convolution. Thus, once the set $\left\{\boldsymbol{q}_{\ell m}(\nu_n)\right\}_{n\in\mathbb{N}}$ is know, the goal of this work becomes finding those three functions. In particular, $\boldsymbol{\mathcal{T}}_{\ell m}$ is calculated in Section 3.B and suitable Ξ_n is proposed, since it is not unique, in Section 6.3 at Equation (6.26), more precisely.

Chapter 7 is dedicated to construct $\boldsymbol{\mathcal{G}}_{\ell mn}$ and it also stores the final results of this work. As it will be seen later in that chapter, it is possible to split $\boldsymbol{\mathcal{G}}_{\ell mn}$, and consequently, $\boldsymbol{\mathcal{G}}$ in a propagating component $\boldsymbol{\mathcal{G}}^{\text{far}}$, regarding the antenna far-field, and in a reactive component $\boldsymbol{\mathcal{G}}^{\text{near}}$, associated with the near field.

Although analytic solutions for both components are found, *i.e.*, without any dependency on integrals, the results are focused on the $\boldsymbol{\mathcal{G}}^{\text{far}}$ once it is not only more interesting from the application perspective, but also it is extremely easier to be mathematically handle whilst the complexity of $\boldsymbol{\mathcal{G}}^{\text{near}}$ is remarkable. Lastly, equations (7.17), (7.18) and (7.19) form, in that order, a three-steps algorithm to construct $\boldsymbol{\mathcal{E}}$ given an arbitrary real signal $\mathcal{U}$, hence concluding the objectives.

1.3 Main Contributions

Among all the work exposing in this dissertation, two major contributions must be highlighted:

1. Minimisation of the mode coefficients uncertainty during estimation while keeping low residual energy. A mode-recursive algorithm, inspired by the performance of Kalman filter, is proposed as a method for estimating the spherical mode coefficients from the measured samples of the phasor electric field. The algorithm relies, at each iteration, in the optimisation of the Kalman Gain, hence minimising the variance of the each mode coefficients and, consequently, the accuracy of the estimation in the form of residual energy.

2. Development of sampling theorem for electromagnetic signals. Although Nyquist sampling theorem provides a reliable method to reconstruct a signal sampling in time-domain,

it fails in retrieving physical results as the reconstructed signals do not obey causality conditions. In this context, a new sampling theorem is proposed, based on the kernels created from self-adjoint differential operators, which is capable of retrieving causal signals.

1.4 Organisation of This Work

This dissertation is mainly organised as follows:

- Chapter 2 provides a brief background on the main results of electromagnetism which will be needed throughout this work.
- Chapter 3 develops in details the theory behind the spherical wave expansion of the electric field for the particular case of an antenna.
- Chapter 4 exposes the algorithms intended to estimate the spherical mode coefficients from the set of measured electric field collected in the far-field.
- Chapter 5 introduces the general sampling theorem and presents in details its conditions that will be further particularised.
- Chapter 6 is dedicates to the construction of the kernel, based on self-adjoint linear differential operators, which is used to generate the causal constructors.
- Chapter 7 reconstructs the time-domain radiated electromagnetic field and present the achieved results.

Chapter 2

Electromagnetism Background

Fundamentally, the Classical Electromagnetism Theory establishes the existence of charges, an inherent property held by material particles, and the electromagnetic field, which spans all over space. This field dynamically influences the charge carriers by means of a force, known as Lorentz Force, whilst the presence and movement of charges disturb the values of the field around them in a process elegantly described by Maxwell's Equations.

As a natural consequence of that second order dynamics, charges can exchange their kinetic energy with each other across space through waves propagating at the electromagnetic field. The described process, which also works for long distances, synthesises the idea behind antennae: material structures allowing charges to move in particular patterns over their surfaces and hence producing electromagnetic waves with different signatures.

In such context, this chapter intends to provide the basic language of Electromagnetism, mainly focused on Antenna Theory, that will be largely used throughout this text.

2.1 Time Domain, Frequency Domain and Phasors

As usual, the time domain electric field can be thought as a vector field $\boldsymbol{\mathcal{E}} : \mathbb{R}^3 \times \mathbb{R} \to \mathbb{R}^3$ where the vector $\boldsymbol{\mathcal{E}}(\boldsymbol{r}, t) \in \mathbb{R}^3$ denotes the electric field at the position $\boldsymbol{r} \in \mathbb{R}^3$ and time $t \in \mathbb{R}$. More formally, nevertheless, the electric field shall actually be associated to the tempered distribution of the field $\boldsymbol{\mathcal{E}}$ (traditionally also denoted by $\boldsymbol{\mathcal{E}}$) for which its Fourier Transform $\mathbf{E} : \mathbb{R}^3 \times \mathbb{R} \to \mathbb{C}^3$ with respect to the time and its inverse are comfortably defined as follows

$$\mathbf{E}(\boldsymbol{r}, \nu) = \int_{\mathbb{R}} \boldsymbol{\mathcal{E}}(\boldsymbol{r}, t)\, e^{-j2\pi\nu t} dt \tag{2.1}$$

$$\boldsymbol{\mathcal{E}}(\boldsymbol{r}, t) = \int_{\mathbb{R}} \mathbf{E}(\boldsymbol{r}, \nu)\, e^{j2\pi\nu t} d\nu \tag{2.2}$$

where $\nu \in \mathbb{R}$ denotes the frequency. It is worth noting that Equation (2.2) implies that $\mathrm{Re}(\mathbf{E})$ and $\mathrm{Im}(\mathbf{E})$ must respectively be even and odd functions of the frequency to ensure the reality of $\boldsymbol{\mathcal{E}}$. Hence, $\mathbf{E}(\boldsymbol{r}, -\nu) = \mathbf{E}(\boldsymbol{r}, \nu)^*$ holds true for any $\boldsymbol{r} \in \mathbb{R}^3$ and, consequently, that equation can be rewritten as

$$\boldsymbol{\mathcal{E}}(\boldsymbol{r}, t) = 2\,\mathrm{Re}\left(\int_0^{\infty} \mathbf{E}(\boldsymbol{r}, \nu)\, e^{j2\pi\nu t} d\nu \right), \tag{2.3}$$

which highlights the fact that it is enough to evaluate $\mathbf{E}$ for $\nu \geqslant 0$ to determine $\boldsymbol{\mathcal{E}}$.

The linearity of Maxwell's Equations allows the analysis of an electromagnetic problem to be performed over $\mathbf{E}$, for which the solution is usually described in a simpler fashion, and then using (2.2) or even (2.3) to retrieve the time-domain electric field. More substantially, consider an electromagnetic setup excited at a single frequency ν'. For this particular case, it holds that

$$\mathbf{E}(\boldsymbol{r}, \nu) = \boldsymbol{E}(\boldsymbol{r}, \nu) \cdot \frac{\delta(\nu - \nu') + \delta(\nu + \nu')}{2}, \tag{2.4}$$

where $\boldsymbol{E} : \mathbb{R}^3 \times \mathbb{R} \to \mathbb{C}^3$ is called the phasor electric field. It is interesting to notice that the $\boldsymbol{E}$ inherits the hermitianess of $\mathbf{E}$ due to the evenness of Dirac's distribution, which can hence be used to determine the real electric field as follows:

$$\begin{aligned}
\boldsymbol{\mathcal{E}}_{\nu'}(\boldsymbol{r}, t) &= \int_{\mathbb{R}} \boldsymbol{E}(\boldsymbol{r}, \nu) \cdot \frac{\delta(\nu - \nu') + \delta(\nu + \nu')}{2} e^{j2\pi\nu t} d\nu \\
&= \frac{1}{2}\left[\boldsymbol{E}(\boldsymbol{r}, \nu') e^{j2\pi\nu' t} + \boldsymbol{E}(\boldsymbol{r}, -\nu') e^{-j2\pi\nu' t}\right] \\
&= \frac{1}{2}\left[\boldsymbol{E}(\boldsymbol{r}, \nu') e^{j2\pi\nu_0 t} + \left(\boldsymbol{E}(\boldsymbol{r}, \nu') e^{j2\pi\nu' t}\right)^*\right] \\
&= \mathrm{Re}\left(\boldsymbol{E}(\boldsymbol{r}, \nu') e^{j2\pi\nu' t}\right).
\end{aligned} \tag{2.5}$$

From a practical standpoint, the real vector $\boldsymbol{\mathcal{E}}_{\nu'}(\boldsymbol{r}, t)$ is the one that can be physically observed, which is done by measuring the magnitude and phase of each of its components. Such information is, of course, synthesised at the complex phasor $\boldsymbol{E}(\boldsymbol{r}, \nu')$, which will henceforth have the meaning of the measured electric field sample.

2.2 The Helmholtz Equation

Let $\mathcal{Q}$ be an index set (not necessarily countable) and $\left(q_i \in \mathbb{R}\right)_{i \in \mathcal{Q}}$, be a collection of charges and let $\boldsymbol{r}_i$ and $\dot{\boldsymbol{r}}_i$ denote the position and the velocity, as functions of time, of the i-th charge, respectively. In this context, the time-domain charge ϱ and current $\boldsymbol{\mathcal{J}}$ density fields are defined as follows

$$\varrho(\boldsymbol{r}, t) = \sum_{i \in \mathcal{Q}} q_i \cdot \delta\big(\boldsymbol{r} - \boldsymbol{r}_i(t)\big) \tag{2.6}$$

$$\boldsymbol{\mathcal{J}}(\boldsymbol{r}, t) = \sum_{i \in \mathcal{Q}} q_i \cdot \dot{\boldsymbol{r}}_i(t) \cdot \delta\big(\boldsymbol{r} - \boldsymbol{r}_i(t)\big). \tag{2.7}$$

In light of such formalism, the Maxwells equations describing the fields produced by such charge and current distribution can be synthesised in time and Frequency-domain and in the phasor form as

Maxwell's Equation	Time-domain	Frequency-domain	Phasor form
Faraday's Law	$\nabla\times\boldsymbol{\mathcal{E}}+\dfrac{\partial\boldsymbol{\mathcal{B}}}{\partial t}=\mathbf{0}$	$\nabla\times\mathbf{E}+j\omega\mathbf{B}=\mathbf{0}$	$\nabla\times\boldsymbol{E}+j\omega\boldsymbol{B}=\mathbf{0}$
Ampère's Law	$\nabla\times\boldsymbol{\mathcal{H}}-\dfrac{\partial\boldsymbol{\mathcal{D}}}{\partial t}=\boldsymbol{\mathcal{J}}$	$\nabla\times\mathbf{H}-j\omega\mathbf{D}=\mathbf{J}$	$\nabla\times\boldsymbol{H}-j\omega\boldsymbol{D}=\boldsymbol{J}$
Gauss's Law for Electricity	$\nabla\cdot\boldsymbol{\mathcal{D}}=\varrho$	$\nabla\cdot\mathbf{D}=\mathrm{\rho}$	$\nabla\cdot\boldsymbol{D}=\rho$
Gauss's Law for Magnetism	$\nabla\cdot\boldsymbol{\mathcal{B}}=0$	$\nabla\cdot\mathbf{B}=0$	$\nabla\cdot\boldsymbol{B}=0$

For completeness reasons, it is worth highlighting that the electromagnetic field ends up affecting the movement of the charges themselves through the Lorentz force defined, for the i-th charge, by

$$\boldsymbol{\mathcal{F}}_i^{\mathrm{EM}}(t)=q_i\cdot\Big[\boldsymbol{\mathcal{E}}\big(\boldsymbol{r}_i(t),t\big)+\dot{\boldsymbol{r}}_i(t)\times\boldsymbol{\mathcal{B}}\big(\boldsymbol{r}_i(t),t\big)\Big]. \tag{2.8}$$

Considering a linear and non-dispersive medium, *i.e.*, $\boldsymbol{D}=\epsilon\boldsymbol{E}$ and $\boldsymbol{B}=\mu\boldsymbol{H}$, and a region of space bearing no free charges, *i.e.*, $\rho=0$ and $\boldsymbol{J}=\mathbf{0}$, it is possible to show the electromagnetic field obeys the homogeneous wave equations

$$\nabla^2\boldsymbol{\mathcal{E}}-\frac{1}{c^2}\frac{\partial^2\boldsymbol{\mathcal{E}}}{\partial t^2}=0\quad\text{and}\quad\nabla^2\boldsymbol{\mathcal{H}}-\frac{1}{c^2}\frac{\partial^2\boldsymbol{\mathcal{H}}}{\partial t^2}=0 \tag{2.9}$$

while their phasors satisfy the Homogeneous Helmholtz Equations

$$\nabla^2\boldsymbol{E}+\kappa^2\boldsymbol{E}=0\quad\text{and}\quad\nabla^2\boldsymbol{H}+\kappa^2\boldsymbol{H}=0 \tag{2.10}$$

where, most naturally, $c=\frac{1}{\sqrt{\mu\epsilon}}$ and $\kappa={}^{\omega}\!/_{c}$.

2.3 Radiated Power

About energy in an electromagnetic context, it is important to emphasise that energy and, therefore, power are concepts fundamentally associated to moving particles. In other words, the energy radiated by an electromagnetic system, as an antenna, by instance, comes from the kinetic energy of its charges. Thus, it is worth starting by studying the power $\mathcal{P}_i$ of the i-charge, defined by

$$\begin{aligned}\mathcal{P}_i(t)&=\boldsymbol{\mathcal{F}}_i^{\mathrm{EM}}(t)\cdot\dot{\boldsymbol{r}}_i(t)\\&=q_i\Big(\boldsymbol{\mathcal{E}}\big(\boldsymbol{r}_i(t),t\big)+\dot{\boldsymbol{r}}_i(t)\times\boldsymbol{\mathcal{B}}\big(\boldsymbol{r}_i(t),t\big)\Big)\cdot\dot{\boldsymbol{r}}_i(t)\\&=q_i\cdot\boldsymbol{\mathcal{E}}\big(\boldsymbol{r}_i(t),t\big)\cdot\dot{\boldsymbol{r}}_i(t).\end{aligned} \tag{2.11}$$

The total power is hence given by

$$\begin{aligned}\mathcal{P}(t) &= \sum_{i\in\mathcal{Q}} \mathcal{P}_i(t) \\ &= \sum_{i\in\mathcal{Q}} q_i \cdot \boldsymbol{\mathcal{E}}\big(\boldsymbol{r}_i(t), t\big) \cdot \dot{\boldsymbol{r}}_i(t) \\ &= \sum_{i\in\mathcal{Q}} q_i \cdot \left[\iiint_V \boldsymbol{\mathcal{E}}(\boldsymbol{r}, t)\delta\big(\boldsymbol{r} - \boldsymbol{r}_i(t)\big)dV\right] \cdot \dot{\boldsymbol{r}}_i(t) \\ &= \iiint_V \boldsymbol{\mathcal{E}}(\boldsymbol{r}, t) \sum_{i\in\mathcal{Q}} q_i \cdot \delta\big(\boldsymbol{r} - \boldsymbol{r}_i(t)\big) \cdot \dot{\boldsymbol{r}}_i(t)\, dV \\ &= \iiint_V \boldsymbol{\mathcal{E}}(\boldsymbol{r}, t) \cdot \boldsymbol{\mathcal{J}}(\boldsymbol{r}, t)\, dV, \end{aligned} \tag{2.12}$$

For a surface V holding all the charges. Thus, by using the time-domain Àmpere's Law and the Divergence Theorem on the above result, it yields the Poynting Theorem, which is presented as follows

$$\mathcal{P}(t) = \iiint_V \left(\boldsymbol{\mathcal{E}}(\boldsymbol{r}, t) \cdot \frac{\partial \boldsymbol{\mathcal{D}}}{\partial t}(\boldsymbol{r}, t) + \boldsymbol{\mathcal{H}}(\boldsymbol{r}, t) \cdot \frac{\partial \boldsymbol{\mathcal{B}}}{\partial t}(\boldsymbol{r}, t)\right) dV + \oiint_{\partial V} \Big(\boldsymbol{\mathcal{E}}(\boldsymbol{r}, t) \times \boldsymbol{\mathcal{H}}(\boldsymbol{r}, t)\Big) \cdot \hat{\boldsymbol{n}}(\boldsymbol{r})\, dA. \tag{2.13}$$

If V is static and once again considering a linear medium, the above result becomes

$$\mathcal{P}(t) = \frac{d}{dt} \iiint_V \left(\frac{\epsilon \mathcal{E}(\boldsymbol{r}, t)^2 + \mu \mathcal{H}(\boldsymbol{r}, t)^2}{2}\right) dV + \oiint_{\partial V} \Big(\boldsymbol{\mathcal{E}}(\boldsymbol{r}, t) \times \boldsymbol{\mathcal{H}}(\boldsymbol{r}, t)\Big) \cdot \hat{\boldsymbol{n}}(\boldsymbol{r})\, dA, \tag{2.14}$$

from which it becomes extremely suggestive defining the first integral as the total electromagnetic energy stored inside V while the second, which is precisely the rate at which the electromagnetic energy cross the boundary ∂V, as the total radiated power:

$$\mathcal{P}_{\text{rad}}(t) = \oiint_{\partial V} \Big(\boldsymbol{\mathcal{E}}(\boldsymbol{r}, t) \times \boldsymbol{\mathcal{H}}(\boldsymbol{r}, t)\Big) \cdot \hat{\boldsymbol{n}}(\boldsymbol{r})\, dA \tag{2.15}$$

2.3.1 Monochromatic Radiated Power

An interesting result is reached regarding the radiated power for monochromatic electromagnetic fields on the form

$$\boldsymbol{\mathcal{E}}(\boldsymbol{r}, t) = \text{Re}\Big(\boldsymbol{E}(\boldsymbol{r}, \nu)\, e^{j2\pi\nu t}\Big) \tag{2.16}$$

$$\boldsymbol{\mathcal{H}}(\boldsymbol{r}, t) = \text{Re}\Big(\boldsymbol{H}(\boldsymbol{r}, \nu)\, e^{j2\pi\nu t}\Big), \tag{2.17}$$

since

$$\begin{aligned}
\mathcal{P}_{\text{rad}}(t) &= \oiint_{\partial V} \left[\text{Re}\left(\boldsymbol{E}(\boldsymbol{r},\nu)\, e^{j2\pi\nu t}\right) \times \text{Re}\left(\boldsymbol{H}(\boldsymbol{r},\nu)\, e^{j2\pi\nu t}\right)\right] \cdot \hat{\boldsymbol{n}}(\boldsymbol{r})\, dA \\
&= \oiint_{\partial V} \left[\frac{\boldsymbol{E}(\boldsymbol{r},\nu)\, e^{j2\pi\nu t} + \boldsymbol{E}(\boldsymbol{r},\nu)^*\, e^{-j2\pi\nu t}}{2} \times \frac{\boldsymbol{H}(\boldsymbol{r},\nu)\, e^{j2\pi\nu t} + \boldsymbol{H}(\boldsymbol{r},\nu)^*\, e^{-j2\pi\nu t}}{2}\right] \cdot \hat{\boldsymbol{n}}(\boldsymbol{r})\, dA \\
&= \frac{e^{j4\pi\nu t}}{2} \oiint_{\partial V} \text{Re}\left(\boldsymbol{E}(\boldsymbol{r},\nu) \times \boldsymbol{H}(\boldsymbol{r},\nu)\right) \cdot \hat{\boldsymbol{n}}(\boldsymbol{r})\, dA \\
&\quad + \frac{1}{2} \oiint_{\partial V} \text{Re}\left(\boldsymbol{E}(\boldsymbol{r},\nu) \times \boldsymbol{H}(\boldsymbol{r},\nu)^*\right) \cdot \hat{\boldsymbol{n}}(\boldsymbol{r})\, dA.
\end{aligned}$$

The first component of $\mathcal{P}_{\text{rad}}$ also depends harmonically on time, but with a frequency twice greater than the original implying an oscillating aspect for the radiated power. Nevertheless, the second component, which does not depend on time, provides the mean behaviour of the radiated time,

$$\left\langle \mathcal{P}_{\text{rad}} \right\rangle = \frac{1}{2} \text{Re}\left[\oiint_{\partial V} \left(\boldsymbol{E}(\boldsymbol{r},\nu) \times \boldsymbol{H}(\boldsymbol{r},\nu)^*\right) \cdot \hat{\boldsymbol{n}}(\boldsymbol{r})\, dA\right], \tag{2.18}$$

in the sense that it can be said if (and how much) energy is effectively being transmitted ($\left\langle \mathcal{P}_{\text{rad}} \right\rangle > 0$) or received ($\left\langle \mathcal{P}_{\text{rad}} \right\rangle < 0$) by the distribution or even if it is an isolated system ($\left\langle \mathcal{P}_{\text{rad}} \right\rangle = 0$).

Chapter 3

Antenna Electromagnetic Fields

For the purposes of this work, and certainly for practical reasons as well, an antenna shall be seen as a material structure with desirable conducting properties and entirely confined in a finite volume $V_{\text{ant}} \subset \mathfrak{S}$. On the other hand, the complement of V_{ant}, *i.e.*, $\mathfrak{S} \setminus V_{\text{ant}}$ is assumed to bear neither free charges nor currents. The fields inside V_{ant} are of little interest while those outside that region, conversely, deserve better attention. Within this context, this Chapter aims at providing a mathematical description and also a model for the electromagnetic fields $\boldsymbol{E}$ and $\boldsymbol{H}$ created by an antenna in $\mathfrak{S} \setminus V_{\text{ant}}$.

3.1 Spherical Mode Expansion

The sought mathematical model for the antenna fields must, of course, be in accordance with the formalism of the Classical Electromagnetic Theory, which at this point is synthesised in Helmholtz Equation Equation (2.10). Since no source lies in $\mathfrak{S} \setminus V_{\text{ant}}$, that equation conveniently becomes homogeneous at that region, handing, for a fixed frequency, three eigenvalue problems to be solved. For that very reason, the idea behind solving them is an old acquaintance: find the eigenfunctions and project the solution over the corresponding eigenspace.

Before starting work in this idea, a coordinate system to describe $\mathfrak{S} \setminus V_{\text{ant}}$ must be chosen. It must be observed that the finiteness of V_{ant} indicates that the spherical coordinate system, whose a briefly description can be found at Appendix B, is the most suitable choice. Although the origin of this system and fixed unit vectors $\hat{\mathrm{x}}$, $\hat{\mathrm{y}}$ and $\hat{\mathrm{z}}$ may be chosen at will, it is highly recommended that symmetries of the antenna geometry with respect to those axes are considered while the origin must be kept inside V_{ant}. It is also worth warning that the radius vector $\boldsymbol{r}$, only as argument of function and as an abuse of notation, is used interchangeably with the tuple (r, θ, ϕ), *i.e.*, $f(\boldsymbol{r})$ and $f(r, \theta, \phi)$ not only have the same meaning, but also they represent the same mathematical object.

In this whole context, the vector eigenfunctions, as described in Appendix E and also as intuitively expected, are spherical vector waves. Thus, the electric and magnetic fields expanded

in those waves have the form

$$\boldsymbol{E}(\boldsymbol{r},\kappa) = \kappa\sqrt{\eta}\sum_{s\in\mathcal{B}}\sum_{\ell\in\mathbb{N}}\sum_{|m|\leqslant\ell}\boldsymbol{Y}_{\ell m}(\theta,\phi)\,\boldsymbol{Z}_{\ell s}(\kappa r)\,\boldsymbol{q}_{\ell ms}(\kappa)\,, \tag{3.1}$$

$$\boldsymbol{H}(\boldsymbol{r},\kappa) = \frac{j\kappa}{\sqrt{\eta}}\sum_{s\in\mathcal{B}}\sum_{\ell\in\mathbb{N}}\sum_{|m|\leqslant\ell}\boldsymbol{Y}_{\ell m}(\theta,\phi)\,\boldsymbol{Z}_{\ell s}(\kappa r)\,\boldsymbol{p}_{\ell ms}(\kappa)\,, \tag{3.2}$$

where the components of these fields are taken with respect to the spherical coordinate system unit vectors, *i.e.*,

$$\boldsymbol{E} = \begin{bmatrix}\overrightarrow{E}\cdot\hat{r}\\ \overrightarrow{E}\cdot\hat{\theta}\\ \overrightarrow{E}\cdot\hat{\phi}\end{bmatrix} \quad\text{and}\quad \boldsymbol{H} = \begin{bmatrix}\overrightarrow{H}\cdot\hat{r}\\ \overrightarrow{H}\cdot\hat{\theta}\\ \overrightarrow{H}\cdot\hat{\phi}\end{bmatrix}, \tag{3.3}$$

the matrices $\boldsymbol{Y}_{\ell m}(\theta,\phi)\in\mathbb{C}^{3\times3}$ and $\boldsymbol{Z}_{\ell s}(\kappa r)\in\mathbb{C}^{3\times2}$ compose the eigenfunction $\boldsymbol{Y}_{\ell m}(\theta,\phi)\,\boldsymbol{Z}_{\ell s}(\kappa r)$ whilst $\boldsymbol{q}_{\ell ms}(\kappa)$ and $\boldsymbol{p}_{\ell ms}(\kappa)\in\mathbb{C}^{2\times1}$ are the constants pondering each eigenfunction and they will henceforth be referred to as mode coefficients. In a pragmatic sense, the term mode will be used as a synonym for the tuple of indices (ℓ,m), which are, respectively, the degree and order of the corresponding spherical harmonics. The index s, which assume its values in $\mathcal{B}=\{3,4\}$, is described in Section D.3 and will be the focus of the Section 3.2.

If Equations (3.1) and (3.2) are applied to the phasor form of Faraday's Law, after some algebraic work it yields

$$\boldsymbol{p}_{\ell ms} = \begin{bmatrix}0 & 1\\ 1 & 0\end{bmatrix}\boldsymbol{q}_{\ell ms}, \tag{3.4}$$

meaning that it is enough to determine either $\boldsymbol{q}_{\ell ms}$ or $\boldsymbol{p}_{\ell ms}$. Traditionally, the electric field is more required, which hence makes finding $\boldsymbol{q}_{\ell ms}$ more interesting.

Moreover, the radial component of $\boldsymbol{E}$ and $\boldsymbol{H}$ are only caused by the second components of $\boldsymbol{q}_{\ell ms}$ and $\boldsymbol{p}_{\ell ms}$, respecively. Thus, assuming $\hat{r}$ as the propagation direction, if the second component of $\boldsymbol{q}_{\ell ms}$ vanishes, then the mode is said to be transverse electric (TE); analogously, if the second component of $\boldsymbol{p}_{\ell ms}$ vanishes, then the mode is transverse magnetic (TM). For that reason, the first components $\boldsymbol{q}_{\ell ms}$ and $\boldsymbol{p}_{\ell ms}$ are denoted by $q^{\mathrm{TE}}_{\ell ms}$ and $p^{\mathrm{TM}}_{\ell ms}$, respecively. On the other hand, it must be noticed from Equation (3.4) that the second component of $\boldsymbol{q}_{\ell ms}$ is $p^{\mathrm{TM}}_{\ell ms}$ itself, while the second component of $\boldsymbol{p}_{\ell ms}$ is $q^{\mathrm{TE}}_{\ell m}$. Thus, it makes better sense denoting the mode coefficients as

$$\boldsymbol{q}_{\ell ms} = \begin{bmatrix}q^{\mathrm{TE}}_{\ell ms}\\ q^{\mathrm{TM}}_{\ell ms}\end{bmatrix} \quad\text{and}\quad \boldsymbol{p}_{\ell ms} = \begin{bmatrix}p^{\mathrm{TM}}_{\ell ms}\\ p^{\mathrm{TE}}_{\ell ms}\end{bmatrix}. \tag{3.5}$$

It is worth stressing that the mode coefficients are actually functions of the wavenumber κ (or the frequency ν as one might like) and perhaps this is the most appropriated moment to point out that the core of this whole work may be seen as estimating those functions from a set of collected electric field samples. Thus, from now on, only the electric field will be studied in the next sections, even because the magnetic field might always be retrieved from electric solution due to Equation (3.4).

3.2 Transmitting and Receiving Fields

The eigenfunctions related to $s = 3$ and $s = 4$ are respectively associated with spherical waves arriving in and leaving the antenna. Since the index s carries such strong meaning, it is worth breaking apart the field solution by defining the transmitting $\boldsymbol{E}_{\text{tra}}$ and receiving fields $\boldsymbol{E}_{\text{rec}}$ as

$$\boldsymbol{E}_{\text{tra}} = \kappa\sqrt{\eta}\sum_{\ell\in\mathbb{N}}\sum_{|m|\leqslant\ell}\boldsymbol{Y}_{\ell m}\boldsymbol{Z}_{\ell 4}\boldsymbol{q}_{\ell m4}, \tag{3.6}$$

$$\boldsymbol{E}_{\text{rec}} = \kappa\sqrt{\eta}\sum_{\ell\in\mathbb{N}}\sum_{|m|\leqslant\ell}\boldsymbol{Y}_{\ell m}\boldsymbol{Z}_{\ell 3}\boldsymbol{q}_{\ell m3}, \tag{3.7}$$

from which the total field in Equation (3.1) may be easily assembled as $\boldsymbol{E} = \boldsymbol{E}_{\text{tra}} + \boldsymbol{E}_{\text{rec}}$.

While $\boldsymbol{E}_{\text{tra}}$ is naturally produced by currents inside V_{ant}, $\boldsymbol{E}_{\text{rec}}$ is most certainly not, which might raise a possible doubt about the physical meaning of this solution since $\mathfrak{S} \setminus V_{\text{ant}}$ is free of charges and currents. As a matter of fact, this solution is understood as being created by sources spotted at the infinite, hence modelling the total field produced by all the possible far away radiation emitters. Therefore, it is clear that the mode coefficient functions $\boldsymbol{q}_{\ell m3}$ are completely random and cannot be deterministically well designed.

On the other hand, the functions $\boldsymbol{q}_{\ell m4}$ are parameters of the studied antenna and might be predicted and controlled (at least in theory). In fact, the functions $\boldsymbol{q}_{\ell m4}$, if known, characterise the antenna in all of its electromagnetic aspects hence working as a mathematical signature or identity of it. One might even state that two antennae are equal if they have the same set of mode coefficient functions. Such idea may even be developed beyond this notion of equality by using the mode coefficients to define a metric, hence inducing a performance notion of distance between two antennae, under which they can be compared. Nevertheless, it must be highlighted that those functions are not invariant under translations nor under rotations on the chosen reference frame, *cf*. [Mé21].

As a final thought on this matter, it is worth bringing attention to the fact that it is completely reasonable to assume from now on that it is possible to have separately access to $\boldsymbol{E}_{\text{tra}}$ and $\boldsymbol{E}_{\text{rec}}$ rather than the total field $\boldsymbol{E}_{\text{tra}} + \boldsymbol{E}_{\text{rec}}$. This is most due to the fact that the collected samples, that will be used to estimate the electric field, will be measured either in a transmitting test or in a receiving test performed on the antenna over a supposedly controlled environment conditions.

3.3 Analytic Determination of Mode Coefficients

It is important to know that there is a sense of orthogonality between eigenfunctions on the form $\boldsymbol{Y}_{\ell m}\boldsymbol{Z}_{\ell s}$. In fact, considering the Proposition D.7, it holds that

$$\oiint \left(\boldsymbol{Y}_{\ell m}\boldsymbol{Z}_{\ell s}\right)^{\text{H}}\left(\boldsymbol{Y}_{\ell' m'}\boldsymbol{Z}_{\ell' s}\right) d\Omega = \boldsymbol{Z}_{\ell s}^{\text{H}}\boldsymbol{Z}_{\ell s}\delta_{\ell\ell'}\delta_{mm'}. \tag{3.8}$$

As usual, such orthogonality can be used to isolate the mode coefficients. In this regard, assume that $\boldsymbol{E}_{\text{tra}}$ or, more uncommon, $\boldsymbol{E}_{\text{rec}}$ are analytically known. Thus, from Equations (3.6) and (3.7), it follows that

$$\boldsymbol{q}_{\ell m4} = \frac{1}{\kappa\sqrt{\eta}} \left(\boldsymbol{Z}_{\ell 4}^{\text{H}} \boldsymbol{Z}_{\ell 4}\right)^{-1} \boldsymbol{Z}_{\ell 4}^{\text{H}} \oiint \boldsymbol{Y}_{\ell m}^{\text{H}} \boldsymbol{E}_{\text{tra}} d\Omega, \tag{3.9}$$

$$\boldsymbol{q}_{\ell m3} = \frac{1}{\kappa\sqrt{\eta}} \left(\boldsymbol{Z}_{\ell 3}^{\text{H}} \boldsymbol{Z}_{\ell 3}\right)^{-1} \boldsymbol{Z}_{\ell 3}^{\text{H}} \oiint \boldsymbol{Y}_{\ell m}^{\text{H}} \boldsymbol{E}_{\text{rec}} d\Omega. \tag{3.10}$$

It is worth noting that if the analytic forms of $\boldsymbol{E}_{\text{tra}}$ and $\boldsymbol{E}_{\text{rec}}$ used on the above equations do really represent transmitting and receiving electric fields on an antenna, respectively, then such equations will not depend on the radius r, since the mode coefficients cannot depend on it as well.

Remark. Due to the clear similarities in equations regarding the transmitting and receiving fields and also due to the fact that $\boldsymbol{Z}_{\ell 3} = \boldsymbol{Z}_{\ell 4}^{*}$, only the transmitting case will henceforth be considered. Additionally, the notation characterising that case on its associated variables will be also dropped for simplicity. Thus, from now on, bear in mind that $\boldsymbol{E} \leftarrow \boldsymbol{E}_{\text{tra}}$, $\boldsymbol{q}_{\ell m} \leftarrow \boldsymbol{q}_{\ell m4}$ and $\boldsymbol{Z}_{\ell} \leftarrow \boldsymbol{Z}_{\ell 4}$.

3.4 Radiated Power

Regarding the results that have been presented this far in the current Chapter, one might find it to be difficult to understand the mode coefficients as something more than mathematical objects and eventually argue about a possible lack of physical meaning for them. This is not really true nonetheless. As it will be shown in this section, there is indeed a close relationship between the mode coefficients and the way the electromagnetic energy is distributed among the modes.

Initially, let $V \subset \mathfrak{S}$ denote a spherical volume with arbitrary radius r, centred in the origin of the coordinate system, and such that $V_{\text{ant}} \subset V$. The mean power through the boundary ∂V that emanates from the antenna, as defined in Equation (2.18), can be calculated as

$$\begin{aligned}
\langle \mathcal{P}_{\partial V} \rangle &= \frac{1}{2} \operatorname{Re}\left[\oiint_{\partial V} \left(\boldsymbol{E} \times \boldsymbol{H}^{*}\right) \cdot \hat{\boldsymbol{r}} dA \right] \\
&= \frac{r^2}{2} \operatorname{Re}\left[\oiint \left(\boldsymbol{E} \times \boldsymbol{H}^{*}\right) \cdot \hat{\boldsymbol{r}} d\Omega \right] \\
&= \frac{r^2}{2} \operatorname{Re}\left[\oiint \boldsymbol{H}^{*} \cdot \left(\hat{\boldsymbol{r}} \times \boldsymbol{E}\right) d\Omega \right] \\
&= \frac{r^2}{2} \operatorname{Re}\left[\oiint \boldsymbol{H}^{\text{H}} [\![\hat{\boldsymbol{r}}]\!] \, \boldsymbol{E} d\Omega \right],
\end{aligned} \tag{3.11}$$

where $[\![\hat{\boldsymbol{r}}]\!] = \begin{bmatrix} 0 & 0 & 0 \\ 0 & 0 & -1 \\ 0 & 1 & 0 \end{bmatrix}$ is skew-symmetric. Considering Equation (3.6), the above integrand

may be developed as

$$\begin{aligned}
\boldsymbol{H}^{\mathrm{H}}\left[\!\left[\hat{\boldsymbol{r}}\right]\!\right]\boldsymbol{E} &= -j\kappa^2\left(\sum_{\ell\in\mathbb{N}}\sum_{|m|\leqslant\ell}\boldsymbol{Y}_{\ell m}\boldsymbol{Z}_\ell\boldsymbol{p}_{\ell m}\right)^{\mathrm{H}}\left[\!\left[\hat{\boldsymbol{r}}\right]\!\right]\left(\sum_{\ell'\in\mathbb{N}}\sum_{|m'|\leqslant\ell'}\boldsymbol{Y}_{\ell' m'}\boldsymbol{Z}_{\ell'}\boldsymbol{q}_{\ell' m'}\right)\\
&= -j\kappa^2\sum_{\ell\in\mathbb{N}}\sum_{|m|\leqslant\ell}\boldsymbol{p}_{\ell m}^{\mathrm{H}}\boldsymbol{Z}_\ell^{\mathrm{H}}\boldsymbol{Y}_{\ell m}^{\mathrm{H}}\left[\!\left[\hat{\boldsymbol{r}}\right]\!\right]\sum_{\ell'\in\mathbb{N}}\sum_{|m'|\leqslant\ell'}\boldsymbol{Y}_{\ell' m'}\boldsymbol{Z}_{\ell'}\boldsymbol{q}_{\ell' m'}\\
&= -j\kappa^2\sum_{\ell\in\mathbb{N}}\sum_{|m|\leqslant\ell}\sum_{\ell'\in\mathbb{N}}\sum_{|m'|\leqslant\ell'}\boldsymbol{p}_{\ell m}^{\mathrm{H}}\boldsymbol{Z}_\ell^{\mathrm{H}}\boldsymbol{Y}_{\ell m}^{\mathrm{H}}\left[\!\left[\hat{\boldsymbol{r}}\right]\!\right]\boldsymbol{Y}_{\ell' m'}\boldsymbol{Z}_{\ell'}\boldsymbol{q}_{\ell' m'},\\
&= -j\kappa^2\sum_{\ell\in\mathbb{N}}\sum_{|m|\leqslant\ell}\sum_{\ell'\in\mathbb{N}}\sum_{|m'|\leqslant\ell'}\boldsymbol{p}_{\ell m}^{\mathrm{H}}\boldsymbol{Z}_\ell^{\mathrm{H}}\boldsymbol{Y}_{\ell m}^{\mathrm{H}}\boldsymbol{Y}_{\ell' m'}\left[\!\left[\hat{\boldsymbol{r}}\right]\!\right]\boldsymbol{Z}_{\ell'}\boldsymbol{q}_{\ell' m'},
\end{aligned}$$

where it must be noted, from Definition D.2 and after a quick algebraic work, that $\left[\!\left[\hat{\boldsymbol{r}}\right]\!\right]$ and $\boldsymbol{Y}_{\ell' m'}$ (or $\boldsymbol{Y}_{\ell m}$) commute. Thus,

$$\begin{aligned}
\langle\mathcal{P}_{\partial V}\rangle &= -\frac{(\kappa r)^2}{2}\,\mathrm{Re}\left[j\sum_{\ell\in\mathbb{N}}\sum_{|m|\leqslant\ell}\sum_{\ell'\in\mathbb{N}}\sum_{|m'|\leqslant\ell'}\boldsymbol{p}_{\ell m}^{\mathrm{H}}\boldsymbol{Z}_\ell^{\mathrm{H}}\left(\oiint\boldsymbol{Y}_{\ell m}^{\mathrm{H}}\boldsymbol{Y}_{\ell' m'}d\Omega\right)\left[\!\left[\hat{\boldsymbol{r}}\right]\!\right]\boldsymbol{Z}_{\ell'}\boldsymbol{q}_{\ell' m'}\right]\\
&= -\frac{(\kappa r)^2}{2}\,\mathrm{Re}\left[j\sum_{\ell\in\mathbb{N}}\sum_{|m|\leqslant\ell}\sum_{\ell'\in\mathbb{N}}\sum_{|m'|\leqslant\ell'}\boldsymbol{p}_{\ell m}^{\mathrm{H}}\boldsymbol{Z}_\ell^{\mathrm{H}}\delta_{\ell\ell'}\delta_{mm'}\left[\!\left[\hat{\boldsymbol{r}}\right]\!\right]\boldsymbol{Z}_{\ell'}\boldsymbol{q}_{\ell' m'}\right]\\
&= -\frac{(\kappa r)^2}{2}\,\mathrm{Re}\left[j\sum_{\ell\in\mathbb{N}}\sum_{|m|\leqslant\ell}\boldsymbol{p}_{\ell m}^{\mathrm{H}}\boldsymbol{Z}_\ell^{\mathrm{H}}\left[\!\left[\hat{\boldsymbol{r}}\right]\!\right]\boldsymbol{Z}_\ell\boldsymbol{q}_{\ell m}\right]\\
&= -\frac{(\kappa r)^2}{2}\sum_{\ell\in\mathbb{N}}\sum_{|m|\leqslant\ell}\mathrm{Re}\left(j\boldsymbol{p}_{\ell m}^{\mathrm{H}}\boldsymbol{Z}_\ell^{\mathrm{H}}\left[\!\left[\hat{\boldsymbol{r}}\right]\!\right]\boldsymbol{Z}_\ell\boldsymbol{q}_{\ell m}\right).
\end{aligned}$$

From Definition E.4 and by remembering Equation (3.4), it can be easily proved that

$$j\boldsymbol{p}_{\ell m}^{\mathrm{H}}\boldsymbol{Z}_\ell^{\mathrm{H}}\left[\!\left[\hat{\boldsymbol{r}}\right]\!\right]\boldsymbol{Z}_\ell\boldsymbol{q}_{\ell m} = \boldsymbol{q}_{\ell m}^{\mathrm{H}}\begin{bmatrix} jz_\ell\mathcal{Z}_\ell^* & 0\\ 0 & -jz_\ell^*\mathcal{Z}_\ell\end{bmatrix}\boldsymbol{q}_{\ell m}$$

and its real part can now calculated through

$$\begin{aligned}
\mathrm{Re}\left(j\boldsymbol{p}_{\ell m}^{\mathrm{H}}\boldsymbol{Z}_\ell^{\mathrm{H}}\left[\!\left[\hat{\boldsymbol{r}}\right]\!\right]\boldsymbol{Z}_\ell\boldsymbol{q}_{\ell m}\right) &= \frac{1}{2}\left(\boldsymbol{q}_{\ell m}^{\mathrm{H}}\begin{bmatrix} jz_\ell\mathcal{Z}_\ell^* & 0\\ 0 & -jz_\ell^*\mathcal{Z}_\ell\end{bmatrix}\boldsymbol{q}_{\ell m} + \boldsymbol{q}_{\ell m}^{\mathrm{H}}\begin{bmatrix} jz_\ell\mathcal{Z}_\ell^* & 0\\ 0 & -jz_\ell^*\mathcal{Z}_\ell\end{bmatrix}^{\mathrm{H}}\boldsymbol{q}_{\ell m}\right)\\
&= \frac{1}{2}\left(\boldsymbol{q}_{\ell m}^{\mathrm{H}}\begin{bmatrix} jz_\ell\mathcal{Z}_\ell^* & 0\\ 0 & -jz_\ell^*\mathcal{Z}_\ell\end{bmatrix}\boldsymbol{q}_{\ell m} + \boldsymbol{q}_{\ell m}^{\mathrm{H}}\begin{bmatrix} -jz_\ell^*\mathcal{Z}_\ell & 0\\ 0 & jz_\ell\mathcal{Z}_\ell^*\end{bmatrix}\boldsymbol{q}_{\ell m}\right)\\
&= \frac{1}{2}\boldsymbol{q}_{\ell m}^{\mathrm{H}}\begin{bmatrix} jz_\ell\mathcal{Z}_\ell^* - jz_\ell^*\mathcal{Z}_\ell & 0\\ 0 & jz_\ell\mathcal{Z}_\ell^* - jz_\ell^*\mathcal{Z}_\ell\end{bmatrix}\boldsymbol{q}_{\ell m}\\
&= \frac{1}{2j}\left(z_\ell^*\mathcal{Z}_\ell - z_\ell\mathcal{Z}_\ell^*\right)\boldsymbol{q}_{\ell m}^{\mathrm{H}}\boldsymbol{q}_{\ell m}.
\end{aligned}$$

By using the $\mathcal{Z}_\ell = \frac{z_\ell}{u} - z'_\ell$ and the wronskian result as stated in [Nis, Eq. 10.50.1], it holds that

$$\begin{aligned}\mathrm{Re}\left(j\boldsymbol{p}_{\ell m}^{\mathrm{H}}\boldsymbol{Z}_\ell^{\mathrm{H}}\left[\!\left[\hat{\boldsymbol{r}}\right]\!\right]\boldsymbol{Z}_\ell\boldsymbol{q}_{\ell m}\right) &= \frac{1}{2j}\left(z_\ell^* z'_\ell - z_\ell z_\ell'^*\right)\boldsymbol{q}_{\ell m}^{\mathrm{H}}\boldsymbol{q}_{\ell m} \\ &= \frac{1}{2j}\mathrm{W}\left(z_\ell^*, z_\ell\right)\boldsymbol{q}_{\ell m}^{\mathrm{H}}\boldsymbol{q}_{\ell m} \\ &= \frac{1}{2j}\frac{-2j}{(kr)^2}\boldsymbol{q}_{\ell m}^{\mathrm{H}}\boldsymbol{q}_{\ell m} \\ &= \frac{-1}{(kr)^2}\boldsymbol{q}_{\ell m}^{\mathrm{H}}\boldsymbol{q}_{\ell m}. \end{aligned} \tag{3.12}$$

Finally,

$$\langle\mathcal{P}_{\partial V}\rangle = \frac{1}{2}\sum_{\ell\in\mathbb{N}}\sum_{|m|\leqslant\ell}\boldsymbol{q}_{\ell m}^{\mathrm{H}}\boldsymbol{q}_{\ell m} \tag{3.13}$$

Equation (3.13) is the main result of this section. It provides a simple method to calculate at which rate the energy of the antenna is flowing through a spherical surface ∂V and, more important, it states that such rate does not depend on the size of the surface, *i.e.*, the radius r. It is important to emphasise that, contrary to what is commonly needed, no approximation was assumed[1] to reach Equation (3.13), which hence implies that it is true at both far and near field regions. As a consequence, $\langle\mathcal{P}_{\partial V}\rangle$ can be referred, without any concern, as the antenna radiated power and hereafter it will be denoted simply by $\langle\mathcal{P}_{\mathrm{rad}}\rangle$.

Most naturally, the structure of Equation (3.13) motivates the definition of the radiated power per mode $\langle\mathcal{P}_{\mathrm{rad}}\rangle_{\ell m}$ as

$$\langle\mathcal{P}_{\mathrm{rad}}\rangle_{\ell m} \;=\; \frac{1}{2}\boldsymbol{q}_{\ell m}^{\mathrm{H}}\boldsymbol{q}_{\ell m} \;=\; \frac{1}{2}\left\|\boldsymbol{q}_{\ell m}\right\|^2 \;=\; \frac{1}{2}\left(\left|q_{\ell m}^{\mathrm{TE}}\right|^2 + \left|q_{\ell m}^{\mathrm{TM}}\right|^2\right), \tag{3.14}$$

which elegantly connects a mode coefficient to the amount of power that mode carries, endowing it with mode-filter attributes. For completeness sake,

$$\left\|\boldsymbol{q}_{\ell m}\right\| = \sqrt{2\,\langle\mathcal{P}_{\mathrm{rad}}\rangle_{\ell m}}. \tag{3.15}$$

3.5 Far and Near Fields

The second kind spherical Hankel function z_ℓ provides a key to severely simplify the analysis of the antenna fields and to better understand their meaning as well. Willing to reach these achievements, consider the following result, *cf*. [Nis, Eq. 10.49.7],

[1] Actually, all results presented so far in this Chapter are mathematically exact.

$$z_\ell(u) = j^{\ell+1}\frac{e^{-ju}}{u}\sum_{k=0}^{\ell}\frac{(2k)!}{k!}\binom{\ell+k}{\ell-k}\frac{1}{(2ju)^k} \tag{3.16}$$

$$= j^{\ell+1}\frac{e^{-ju}}{u}\cdot\left[1+\sum_{k=1}^{\ell}\frac{(2k)!}{k!}\binom{\ell+k}{\ell-k}\frac{1}{(2ju)^k}\right]$$

$$= j^{\ell+1}\frac{e^{-ju}}{u}\cdot\left[1+Q_\ell\left(\frac{1}{2ju}\right)\right]$$

$$= j^{\ell+1}\frac{e^{-ju}}{u}+j^{\ell+1}\frac{e^{-ju}}{u}Q_\ell\left(\frac{1}{2ju}\right), \tag{3.17}$$

where Q_ℓ is an ℓ-degree polynomial with real coefficients and no independent term. Now, consider the definition

$$z_\ell^{\text{far}}(u) = j^{\ell+1}\frac{e^{-ju}}{u}, \tag{3.18}$$

where the meaning of the word "far" in this context will be soon revealed. As it has been used in the proof of Equation (3.12), $\mathrm{W}\left(z_\ell^*, z_\ell\right) = {}^{-2j}/_{u^2}$. However, it can be easily proved that the wronskian of $z_\ell^{\text{far}*}$ and z_ℓ^{far} has that precisely same value, *i.e.*, $\mathrm{W}\left(z_\ell^{\text{far}*}, z_\ell^{\text{far}}\right) = {}^{-2j}/_{u^2}$. As a strong conclusion taken from this fact, one can say that if the matrix $\boldsymbol{Z}_\ell$ were constructed by using only the z_ℓ^{far} component of z_ℓ, then the antenna would radiate the same power, even though the electric field would not be the same. It becomes now clear that only the component of the electric field that decays proportionally to the factor ${}^{1}/_{\kappa r}$ does actually radiate, while the remaining components are then the responsible for the energy stored in the field surrounding the antenna. Traditionally, those components are called far and near field, respectively. This nomenclature, nevertheless, might lead to some confusion since the far field exists near the antenna, where it is even stronger, while the near field do also exist far from the antenna, even though it fades sharply faster than the far field as the distance grows.

The objective of this section is to find the form of the near and far fields. For this goal, the matrix $\boldsymbol{Z}_\ell$ must be studied. That being the case, consider the following result reached after some simple algebraic work,

$$\boldsymbol{Z}_\ell(u) = \begin{bmatrix} 0 & \sqrt{\ell(\ell+1)}\frac{z_\ell(u)}{u} \\ z_\ell(u) & 0 \\ 0 & z_{\ell-1}-\frac{z_\ell(u)}{u} \end{bmatrix}$$

$$= j^\ell\frac{e^{-ju}}{u}\begin{bmatrix}0&0\\j&0\\0&1\end{bmatrix}+j^\ell\frac{e^{-ju}}{u}\begin{bmatrix} 0 & \sqrt{\ell(\ell+1)}\frac{j}{u}\left[1+Q_\ell\left(\frac{1}{2ju}\right)\right] \\ jQ_\ell\left(\frac{1}{2ju}\right) & 0 \\ 0 & Q_{\ell-1}\left(\frac{1}{2ju}\right)+\frac{1}{ju}\left[1+Q_\ell\left(\frac{1}{2ju}\right)\right] \end{bmatrix}$$

$$= \boldsymbol{Z}_\ell^{\text{far}}(u)+\boldsymbol{Z}_\ell^{\text{near}}(u). \tag{3.19}$$

With the last definition, the far and near fields are finally achieved as

$$\boldsymbol{E}_{\text{far}} = \kappa\sqrt{\eta}\sum_{\ell\in\mathbb{N}}\sum_{|m|\leqslant\ell}\boldsymbol{Y}_{\ell m}\boldsymbol{Z}_{\ell}^{\text{far}}\boldsymbol{q}_{\ell m} \tag{3.20}$$

$$\boldsymbol{E}_{\text{near}} = \kappa\sqrt{\eta}\sum_{\ell\in\mathbb{N}}\sum_{|m|\leqslant\ell}\boldsymbol{Y}_{\ell m}\boldsymbol{Z}_{\ell}^{\text{near}}\boldsymbol{q}_{\ell m}, \tag{3.21}$$

where it must be noticed that the transmitting field can always be retrieved by $\boldsymbol{E} = \boldsymbol{E}_{\text{far}} + \boldsymbol{E}_{\text{near}}$. Still in the nomenclature matter, it is worth adding that $\boldsymbol{E}_{\text{far}}$ will also be called propagating or radiated field while, in contrast, $\boldsymbol{E}_{\text{near}}$ might be referred as non-propagating or reactive field.

Attention should be brought to the fact that the far and near fields share the same set of mode coefficients. Which clearly means that if those coefficients are estimated by only analysing the far field behaviour, then they can be used to reconstruct the near field. Therefore, this work shall hereafter concentrate its attention towards the far field, once it is substantially easier to handle and measure than the near field.

In this direction, consider the field rewritten as

$$\boldsymbol{E}_{\text{far}}(\boldsymbol{r},\kappa) = \frac{e^{-j\kappa r}}{r}\sqrt{\eta}\sum_{\ell\in\mathbb{N}}\sum_{|m|\leqslant\ell} j^{\ell}\boldsymbol{Y}_{\ell m}(\theta,\phi)\begin{bmatrix}0 & 0\\ j & 0\\ 0 & 1\end{bmatrix}\boldsymbol{q}_{\ell m}(\kappa), \tag{3.22}$$

which clearly has the form

$$\boldsymbol{E}_{\text{far}}(\boldsymbol{r},\kappa) = \frac{e^{-j\kappa r}}{r}\mathtt{E}(\theta,\phi,\kappa), \tag{3.23}$$

where $\mathtt{E}$ will be called radius-normalised electric field (or, when no confusion is possible, just electric field), even though it does not have electric field units. Equation (3.23) reveals the simple dependence of the radiated electric field on the distance r, in fact, the most important impact of it is actually changing the phase of the field. $\mathtt{E}$, on the other hand, stores the most valuable information about the radiated field regarding the radiation pattern of the antenna and, for this reason, it will become the focus of the attention for estimating the mode coefficients in the next chapter.

As a second conclusion on the far field, one must notice that it has no radial component, *i.e.*, $\boldsymbol{E}_{\text{far}}\cdot\hat{\boldsymbol{r}} = \boldsymbol{E}_{\text{far}}^{\mathrm{T}}\hat{\boldsymbol{r}} = 0$, due to the zeros in the first row of $\boldsymbol{Z}_{\ell}^{\text{far}}$. Moreover, it can be quickly proved that

$$[\![\boldsymbol{r}]\!]\begin{bmatrix}0 & 0\\ j & 0\\ 0 & 1\end{bmatrix} = j\begin{bmatrix}0 & 0\\ j & 0\\ 0 & 1\end{bmatrix}\begin{bmatrix}0 & 1\\ 1 & 0\end{bmatrix},$$

which, alongside the already used fact that $[\![\boldsymbol{r}]\!]$ and $\boldsymbol{Y}_{\ell m}$ commute, can be used to evaluate the

following

$$\begin{aligned}
\boldsymbol{r}\times\boldsymbol{E}_{\text{far}} &= [\![\boldsymbol{r}]\!]\,\boldsymbol{E}_{\text{far}}\\
&= \frac{e^{-j\kappa r}}{r}\sqrt{\eta}\sum_{\ell\in\mathbb{N}}\sum_{|m|\leqslant\ell} j^{\ell}\,[\![\boldsymbol{r}]\!]\,\boldsymbol{Y}_{\ell m}(\theta,\phi)\begin{bmatrix}0&0\\j&0\\0&1\end{bmatrix}\boldsymbol{q}_{\ell m}(\kappa)\\
&= \frac{e^{-j\kappa r}}{r}\sqrt{\eta}\sum_{\ell\in\mathbb{N}}\sum_{|m|\leqslant\ell} j^{\ell}\boldsymbol{Y}_{\ell m}(\theta,\phi)\,[\![\boldsymbol{r}]\!]\begin{bmatrix}0&0\\j&0\\0&1\end{bmatrix}\boldsymbol{q}_{\ell m}(\kappa)\\
&= j\frac{e^{-j\kappa r}}{r}\sqrt{\eta}\sum_{\ell\in\mathbb{N}}\sum_{|m|\leqslant\ell} j^{\ell}\boldsymbol{Y}_{\ell m}(\theta,\phi)\begin{bmatrix}0&0\\j&0\\0&1\end{bmatrix}\begin{bmatrix}0&1\\1&0\end{bmatrix}\boldsymbol{q}_{\ell m}(\kappa)\\
&= j\frac{e^{-j\kappa r}}{r}\sqrt{\eta}\sum_{\ell\in\mathbb{N}}\sum_{|m|\leqslant\ell} j^{\ell}\boldsymbol{Y}_{\ell m}(\theta,\phi)\begin{bmatrix}0&0\\j&0\\0&1\end{bmatrix}\boldsymbol{p}_{\ell m}(\kappa)\\
&= \eta\boldsymbol{H}_{\text{far}}(\boldsymbol{r},\kappa).
\end{aligned}$$

Hence,

$$\boldsymbol{H}_{\text{far}} = \frac{1}{\eta}\boldsymbol{r}\times\boldsymbol{E}_{\text{far}}, \tag{3.24}$$

implying that the radiated magnetic field $\boldsymbol{H}$ also does not have a radial component. Which leads to one more nice property of the far fields: the propagation is transverse electromagnetic (TEM). It must be observerd that, from Equation (3.24), the complex Poynting vector becomes

$$\boldsymbol{E}_{\text{far}}\times\boldsymbol{H}^{*}_{\text{far}} = \frac{1}{\eta}\big(\boldsymbol{E}^{\text{H}}_{\text{far}}\boldsymbol{E}_{\text{far}}\big)\hat{\boldsymbol{r}} = \frac{1}{\eta}\big\|\boldsymbol{E}_{\text{far}}\big\|^{2}\hat{\boldsymbol{r}} = \frac{1}{\eta r^{2}}\,\|\mathtt{E}\|^{2}\,\hat{\boldsymbol{r}}, \tag{3.25}$$

reassuring the already assumed direction of the energy flux to be radial.

At this point, since $\mathtt{E}(\theta,\phi,\kappa) = \begin{bmatrix}0 & \mathtt{E}_{\theta}(\theta,\phi,\kappa) & \mathtt{E}_{\phi}(\theta,\phi,\kappa)\end{bmatrix}^{\text{T}}$, the equations involving $\mathtt{E}$ will be simplified by ignoring its first element, *i.e.*, from now on, it will be considered that $\mathtt{E}(\theta,\phi,\kappa)\in\mathbb{C}^{2\times 1}$ where

$$\mathtt{E}(\theta,\phi) = \begin{bmatrix}\mathtt{E}_{\theta}(\theta,\phi,\kappa) & \mathtt{E}_{\phi}(\theta,\phi,\kappa)\end{bmatrix}^{\text{T}}. \tag{3.26}$$

Thus,

$$\begin{aligned}
\mathtt{E}(\theta,\phi,\kappa) &= \sum_{\ell\in\mathbb{N}}\sum_{|m|\leqslant\ell}\frac{j^{\ell}\sqrt{\eta}}{\sqrt{\ell(\ell+1)}}\begin{bmatrix}\dfrac{jmY^{m}_{\ell}}{\sin\theta} & \dfrac{\partial Y^{m}_{\ell}}{\partial\theta}\\ -\dfrac{\partial Y^{m}_{\ell}}{\partial\theta} & \dfrac{jmY^{m}_{\ell}}{\sin\theta}\end{bmatrix}\begin{bmatrix}j&0\\0&1\end{bmatrix}\boldsymbol{q}_{\ell m}(\kappa)\\
&= \sum_{\ell\in\mathbb{N}}\sum_{|m|\leqslant\ell}\frac{j^{\ell}\sqrt{\eta}}{\sqrt{\ell(\ell+1)}}\begin{bmatrix}\dfrac{-mY^{m}_{\ell}}{\sin\theta} & \dfrac{\partial Y^{m}_{\ell}}{\partial\theta}\\ -j\dfrac{\partial Y^{m}_{\ell}}{\partial\theta} & \dfrac{jmY^{m}_{\ell}}{\sin\theta}\end{bmatrix}\boldsymbol{q}_{\ell m}.
\end{aligned} \tag{3.27}$$

By defining the matrix

$$\boldsymbol{T}_{\ell m}(\theta,\phi)=\frac{j^{\ell}\sqrt{\eta}}{\sqrt{\ell(\ell+1)}}\begin{bmatrix}\dfrac{-mY_{\ell}^{m}}{\sin\theta} & \dfrac{\partial Y_{\ell}^{m}}{\partial\theta}\\ -j\dfrac{\partial Y_{\ell}^{m}}{\partial\theta} & \dfrac{jmY_{\ell}^{m}}{\sin\theta}\end{bmatrix}, \tag{3.28}$$

the last equation can be compactly rewritten as

$$\mathtt{E}(\theta,\phi,\kappa)=\sum_{\ell\in\mathbb{N}}\sum_{|m|\leqslant\ell}\boldsymbol{T}_{\ell m}(\theta,\phi)\,\boldsymbol{q}_{\ell m}(\kappa). \tag{3.29}$$

It is interesting to notice that $\boldsymbol{T}_{\ell m}$ inherits the orthogonality of $\boldsymbol{Y}_{\ell m}$ in the sense that

$$\oiint\boldsymbol{T}_{\ell m}^{\mathrm{H}}\boldsymbol{T}_{\ell' m'}d\Omega=\eta\delta_{\ell\ell'}\delta_{mm'}, \tag{3.30}$$

from which the mode coefficients can now be determined if $\mathtt{E}$ is analytically available through the following expression

$$\boldsymbol{q}_{\ell m}=\frac{1}{\eta}\oiint\boldsymbol{T}_{\ell m}^{\mathrm{H}}\mathtt{E}d\Omega, \tag{3.31}$$

which is surely simpler than Equation (3.9).

3.6 Antenna Properties

In practice, one is interested in the description of the most common antenna properties that are useful as classical figures of merit to analyse and compare the antenna performance. Those properties, of course, may also be derived from the above formalism involving the mode coefficients. This section is dedicated to register such properties as functions the mode coefficients.

Firstly, it is interesting to see from Equation (3.25) that the radiated power, once again calculated on a spherical surface of radius r, can also be expressed as

$$\begin{aligned}\langle\mathcal{P}_{\mathrm{rad}}\rangle&=\frac{r^2}{2}\operatorname{Re}\left(\oiint(\boldsymbol{E}_{\mathrm{far}}\times\boldsymbol{H}_{\mathrm{far}})\cdot\hat{\boldsymbol{r}}d\Omega\right)\\&=\frac{1}{2\eta}\operatorname{Re}\left(\oiint\|\mathtt{E}\|^2d\Omega\right)\\&=\frac{1}{2\eta}\oiint\|\mathtt{E}\|^2d\Omega,\end{aligned} \tag{3.32}$$

even though its value have already been calculated at (3.13).

3.6.1 Radiation Intensity

The antenna radiation intensity $\mathsf{U}(\theta,\phi,\kappa)\in\mathbb{R}_{\geqslant 0}$ is defined with the intention to provide the idea of how much power is radiated in each direction. Hence, it makes sense defining it as

a "directional" density of radiated power, *i.e.*, the radiated power per solid angle as

$$\mathsf{U} = \frac{\left\|\mathsf{E}\right\|^2}{2\eta} = \frac{1}{2\eta}\sum_{\ell,m}\sum_{\ell',m'} \boldsymbol{q}^{\mathrm{H}}_{\ell m}\boldsymbol{T}^{\mathrm{H}}_{\ell m}\boldsymbol{T}_{\ell' m'}\boldsymbol{q}_{\ell' m'}, \tag{3.33}$$

where $\sum_{\ell,m}$ is the contraction form for $\sum_{\ell\in\mathbb{N}}\sum_{|m|\leqslant\ell}$. The graph in spherical coordinates of U, which is a 3-dimensional plot, is said to be the radiation pattern of the antenna.

3.6.2 Normalised and Directive Gains

In order to perform a relative analysis of the spherical radiation distribution, it is worth studying a normalised version of the radiation intensity. The finiteness of the radiated power implies that $\mathsf{U}(\theta,\phi,\kappa)$ must reach a maximum at some diretion $(\theta_\circ,\phi_\circ)$. By assuming that the series in Equation (3.33) converges to a differentiable function, such direction would then be one of the solutions of

$$\frac{\partial \mathsf{U}}{\partial\theta}(\theta,\phi) = 0 \quad \text{and} \quad \frac{\partial \mathsf{U}}{\partial\phi}(\theta,\phi) = 0. \tag{3.34}$$

Once $(\theta_\circ,\phi_\circ)$ is known, the radiation intensity can then be normalised by $\mathsf{U}(\theta_\circ,\phi_\circ)$ and this ratio is defined as the normalised gain $\mathsf{g}(\theta,\phi)$. Thus,

$$\mathsf{g}(\theta,\phi) = \frac{\mathsf{U}(\theta,\phi)}{\mathsf{U}(\theta_\circ,\phi_\circ)}. \tag{3.35}$$

Since solving Equation (3.34) may become too complex, the direction $(\theta_\circ,\phi_\circ)$ may not be always available. Alternatively, it is possible to normalise the radiation intensity by using the isotropic radiation intensity U_I, which would come to be the radiation intensity of an isotropic antenna, if it were real, that would radiate the same power of the real antenna. Hence,

$$\mathsf{U}_I = \frac{\langle \mathcal{P}_{\mathrm{rad}}\rangle}{4\pi} = \frac{1}{8\pi}\sum_{\ell,m}\left\|\boldsymbol{q}_{\ell m}\right\|^2. \tag{3.36}$$

When the radiation intensity is normalised by such factor, it is called directive gain and denoted by

$$\mathsf{D}(\theta,\phi) = 8\pi\cdot\frac{\mathsf{U}(\theta,\phi)}{\sum\limits_{\ell,m}\left\|\boldsymbol{q}_{\ell m}\right\|^2} = \frac{4\pi}{\eta}\cdot\frac{\sum\limits_{\ell,m}\sum\limits_{\ell',m'}\boldsymbol{q}^{\mathrm{H}}_{\ell m}\boldsymbol{T}^{\mathrm{H}}_{\ell m}\boldsymbol{T}_{\ell' m'}\boldsymbol{q}_{\ell' m'}}{\sum\limits_{\ell,m}\left\|\boldsymbol{q}_{\ell m}\right\|^2}. \tag{3.37}$$

The maximum value of D, *i.e.*, $\mathsf{D}(\theta_\circ,\phi_\circ)$ is commonly called directivity of the antenna.

3.7 Causality Requirements for Mode Coefficients

Causality is an important aspect of this work since it aims to attain a model for the time-domain Electric Field of an antenna. Even though the causality, by itself, does not provide enough information to perform the reconstruction of the Electric field, it establishes the rules this reconstruction must obey.

As it has been explained in subsection 1.2.2, an antenna might be thought as a PLTI system and $\boldsymbol{E}(\boldsymbol{r},\cdot)$ would be the Fourier transform of its time-domain impulse response at position $\boldsymbol{r}$, *i.e.*, $\boldsymbol{E}(\boldsymbol{r},\cdot)$ is the frequency-domain impulse response. Therefore, whenever the inverse Fourier transform is applied in $\boldsymbol{E}(\boldsymbol{r},\cdot)$, the result $\boldsymbol{\mathcal{E}}(\boldsymbol{r},\cdot)$ must correspond to a causal system, *i.e.*, $\boldsymbol{\mathcal{E}}(\boldsymbol{r},t) \in \mathbb{R}^3$ for any time $t \in \mathbb{R}$ and $t < 0$ must imply in $\boldsymbol{\mathcal{E}}(\boldsymbol{r},t) = \boldsymbol{0}$. In this section, it will be studied over which condition the coefficient modes $\boldsymbol{q}_{\ell m}$ lead to a causal response of the antenna.

It should be noticed that the complete form of the electric field, *i.e.*, $\boldsymbol{E} = \boldsymbol{E}_{\text{far}} + \boldsymbol{E}_{\text{near}}$ as described in Equation (3.6), shall be used to analyse the causality of the antenna, since requiring causality only for $\boldsymbol{E}_{\text{far}}$ does not imply a causal $\boldsymbol{E}_{\text{near}}$.

The Appendix A establishes important results about causality in the context of a general PLTI system and most of them will be necessary to understand this section. For this reason, the reader is encouraged to refer to that appendix whenever its results are used or even to read it previously.

3.7.1 Hermitianness of the Electric Field

The first, and easiest, aspect of the causality that will be observed is the hermitianness of the Electric Field, which is a necessary condition for causality, but not sufficient, as concluded in Lemma A.2. Mathematically, it means that $\boldsymbol{E}(\boldsymbol{r},-\kappa) = \boldsymbol{E}(\boldsymbol{r},\kappa)^*$ must hold for any $\kappa \in \mathbb{R}$ at any $\boldsymbol{r} \in \mathbb{R}^3 \setminus V_{\text{ant}}$. Before applying this condition to Equation (3.6), consider its left hand side as

$$\boldsymbol{E}(\boldsymbol{r},-\kappa) = -\kappa\sqrt{\eta}\sum_{\ell\in\mathbb{N}}\sum_{|m|\leqslant\ell} \boldsymbol{Y}_{\ell m}(\theta,\phi)\,\boldsymbol{Z}_\ell(-\kappa r)\,\boldsymbol{q}_{\ell m}(-\kappa)\,, \tag{3.38}$$

which clearly requires $\boldsymbol{Z}_\ell$ to be defined for negative values. This definition can be done by considering the analytic continuation of z_ℓ which leads, as described in Proposition E.1, to

$$\boldsymbol{Z}_\ell(-\kappa r) = (-1)^\ell\,\boldsymbol{Z}_\ell(\kappa r)^*\begin{bmatrix}1 & 0\\ 0 & -1\end{bmatrix}, \tag{3.39}$$

However, to keep the equations as small as possible, this formula will be saved for later and $\boldsymbol{Z}_\ell(-\kappa r)$ will continue to be written for now. For the right hand side, consider the Proposition D.6, which establishes that $\boldsymbol{Y}^*_{\ell m} = (-1)^m\,\boldsymbol{Y}_{\ell,-m}$. Thus,

$$\begin{aligned}\boldsymbol{E}(\boldsymbol{r},\kappa)^* &= \kappa\sqrt{\eta}\sum_{\ell\in\mathbb{N}}\sum_{|m|\leqslant\ell} \boldsymbol{Y}_{\ell m}(\theta,\phi)^*\,\boldsymbol{Z}_\ell(\kappa r)^*\,\boldsymbol{q}_{\ell m}(\kappa)^*\\ &= \kappa\sqrt{\eta}\sum_{\ell\in\mathbb{N}}\sum_{|m|\leqslant\ell} (-1)^m\,\boldsymbol{Y}_{\ell,-m}(\theta,\phi)\,\boldsymbol{Z}_\ell(\kappa r)^*\,\boldsymbol{q}_{\ell m}(\kappa)^*\,.\end{aligned} \tag{3.40}$$

Since Equations (3.38) and (3.40) must be equal, then

$$\sum_{\ell\in\mathbb{N}}\sum_{|m|\leqslant\ell}\left[(-1)^m\,\boldsymbol{Y}_{\ell,-m}(\theta,\phi)\,\boldsymbol{Z}_\ell(\kappa r)^*\,\boldsymbol{q}_{\ell m}(\kappa)^* + \boldsymbol{Y}_{\ell m}(\theta,\phi)\,\boldsymbol{Z}_\ell(-\kappa r)\,\boldsymbol{q}_{\ell m}(-\kappa)\right] = \boldsymbol{0}$$

must hold for any r, θ, ϕ and κ. However, since the matrices $\boldsymbol{Y}_{\ell m}$ are orthogonal, Proposition D.7, it must be true that

$$(-1)^m \boldsymbol{Z}_\ell(\kappa r)^* \boldsymbol{q}_{\ell,-m}(\kappa)^* + \boldsymbol{Z}_\ell(-\kappa r)\boldsymbol{q}_{\ell m}(-\kappa) = \boldsymbol{0}$$

for any tuple of indices (ℓ, m) where $\ell \in \mathbb{N}$ and $|m| \leqslant \ell$. The Equation (3.39) can finally be applied to the last result yielding

$$(-1)^m \boldsymbol{Z}_\ell(\kappa r)^* \boldsymbol{q}_{\ell,-m}(\kappa)^* + (-1)^\ell \boldsymbol{Z}_\ell(\kappa r)^* \begin{bmatrix} 1 & 0 \\ 0 & -1 \end{bmatrix} \boldsymbol{q}_{\ell m}(-\kappa) = \boldsymbol{0}$$

or

$$\boldsymbol{Z}_\ell(\kappa r)^* \left((-1)^m \boldsymbol{q}_{\ell,-m}(\kappa)^* + (-1)^\ell \begin{bmatrix} 1 & 0 \\ 0 & -1 \end{bmatrix} \boldsymbol{q}_{\ell m}(-\kappa) \right) = \boldsymbol{0}.$$

Since it is valid for any value of r, the only left possibility is

$$\boldsymbol{q}_{\ell m}(-\kappa) = (-1)^{\ell+m} \begin{bmatrix} -1 & 0 \\ 0 & 1 \end{bmatrix} \boldsymbol{q}_{\ell,-m}(\kappa)^*. \tag{3.41}$$

The last equation is the desired result. It establishes how the mode coefficients should be define for negative values of wavenumber (or frequency) so that $\boldsymbol{E}$ could be hermitian.

3.7.2 Kramers-Kronig relations for the Electric Field

Another necessary condition for causality that must be explored are the Kramers-Kronig relations. In fact, as stated in Corollary A.1, this condition and the hermitianness are together sufficient to ensure the causality of the antenna. In this sense, the electric field $\boldsymbol{E}(\boldsymbol{r}, \cdot)$ must obey for any r

$$\boldsymbol{E}(\boldsymbol{r}, \kappa) = -\frac{1}{j\pi} \mathsf{PV} \int_{\mathbb{R}} \frac{\boldsymbol{E}(\boldsymbol{r}, \kappa')}{\kappa' - \kappa} d\kappa'. \tag{3.42}$$

Considering once again Equation (3.6), the above condition becomes

$$\sum_{\ell \in \mathbb{N}} \sum_{|m| \leqslant \ell} \boldsymbol{Y}_{\ell m}(\theta, \phi) \left[\kappa \boldsymbol{Z}_\ell(\kappa r) \boldsymbol{q}_{\ell m}(\kappa) + \frac{1}{j\pi} \mathsf{PV} \int_{\mathbb{R}} \frac{\kappa' \boldsymbol{Z}_\ell(\kappa' r) \boldsymbol{q}_{\ell m}(\kappa')}{\kappa' - \kappa} d\kappa' \right] = \boldsymbol{0}.$$

And since the matrices $\boldsymbol{Y}_{\ell m}$ are orthogonal, the following must hold for all modes

$$\kappa \boldsymbol{Z}_\ell(\kappa r) \boldsymbol{q}_{\ell m}(\kappa) + \frac{1}{j\pi} \mathsf{PV} \int_{\mathbb{R}} \frac{\kappa' \boldsymbol{Z}_\ell(\kappa' r) \boldsymbol{q}_{\ell m}(\kappa')}{\kappa' - \kappa} d\kappa' = \boldsymbol{0}.$$

The above result implies that the class of function on the form $\kappa \boldsymbol{Z}_\ell(\kappa r) \boldsymbol{q}_{\ell m}(\kappa)$ must obey Kramers-Kronig for all modes and for any $\boldsymbol{r}$. It is interesting to notice that such functions do not individually correspond to causal systems since they are not hermitian in general.

At this point, it is worth considering each component of $\kappa \boldsymbol{Z}_\ell(\kappa r) \boldsymbol{q}_{\ell m}(\kappa)$ separatedly. However, one must be able to notice that the third component can be obtained through the first,

hence they carry the same information. Thus, for simplicity, only the first and second components are considered leading to

$$\kappa z_\ell\left(\kappa r\right) q_{\ell m}^{\mathrm{TE}}\left(\kappa\right) + \frac{1}{j\pi}\mathsf{PV}\int_{\mathbb{R}} \frac{\kappa' z_\ell\left(\kappa' r\right) q_{\ell m}^{\mathrm{TE}}\left(\kappa'\right)}{\kappa' - \kappa} d\kappa' = 0, \tag{3.43}$$

$$z_\ell\left(\kappa r\right) q_{\ell m}^{\mathrm{TM}}\left(\kappa\right) + \frac{1}{j\pi}\mathsf{PV}\int_{\mathbb{R}} \frac{z_\ell\left(\kappa' r\right) q_{\ell m}^{\mathrm{TM}}\left(\kappa'\right)}{\kappa' - \kappa} d\kappa' = 0. \tag{3.44}$$

The second kind spherical Hankel function z_ℓ can be expanded in its Laurent series around zero, *cf*. [Nis, Eq. 10.53.1-10.53.2], *i.e*. it converges at any element of $\mathbb{C} \setminus \{0\}$, where it has a pole of order $\ell + 1$. After some organisation, this series can be written as

$$z_\ell\left(u\right) = \sum_{a=0}^{\ell} C_a u^{2a-\ell-1} + \sum_{a=\ell}^{\infty} D_a u^a$$

where it is worth noting that the series has coefficient zero associated with the terms $u^{-\ell}$, $u^{-\ell+2}$, $u^{-\ell+4}$, $\cdots$, $u^{\ell-2}$ and also that the presented coefficients C_a and D_a do not vanish (their value are actually not important for the following analysis). If z_ℓ is replaced by its series in Equations (3.43) and (3.44), they become

$$\sum_{a=0}^{\ell} C_a \left(\kappa^{2a-\ell} q_{\ell m}^{\mathrm{TE}}\left(\kappa\right) + \frac{1}{j\pi}\mathsf{PV}\int_{\mathbb{R}} \frac{\kappa'^{2a-\ell} q_{\ell m}^{\mathrm{TE}}\left(\kappa'\right)}{\kappa' - \kappa} d\kappa' \right) r^{2a-\ell-1}$$
$$+ \sum_{a=\ell}^{\infty} D_a \left(\kappa^{a+1} q_{\ell m}^{\mathrm{TE}}\left(\kappa\right) + \frac{1}{j\pi}\mathsf{PV}\int_{\mathbb{R}} \frac{\kappa'^{a+1} q_{\ell m}^{\mathrm{TE}}\left(\kappa'\right)}{\kappa' - \kappa} d\kappa' \right) r^a = 0$$

$$\sum_{a=0}^{\ell} C_a \left(\kappa^{2a-\ell-1} q_{\ell m}^{\mathrm{TM}}\left(\kappa\right) + \frac{1}{j\pi}\mathsf{PV}\int_{\mathbb{R}} \frac{\kappa'^{2a-\ell-1} q_{\ell m}^{\mathrm{TM}}\left(\kappa'\right)}{\kappa' - \kappa} d\kappa' \right) r^{2a-\ell-1}$$
$$+ \sum_{a=\ell}^{\infty} D_a \left(\kappa^{a} q_{\ell m}^{\mathrm{TM}}\left(\kappa\right) + \frac{1}{j\pi}\mathsf{PV}\int_{\mathbb{R}} \frac{\kappa'^{a} q_{\ell m}^{\mathrm{TM}}\left(\kappa'\right)}{\kappa' - \kappa} d\kappa' \right) r^a = 0,$$

which must hold for any valid r. Due to the uniqueness of Laurent series, *cf*. [Net05, Ch. IV, Theorem. 8, Page 211], all coefficients of the series above must vanish. Thus, for any $a \in \mathbb{N}_{\leqslant \ell} \cup \{0\}$

$$\kappa^{2a-\ell} q_{\ell m}^{\mathrm{TE}}\left(\kappa\right) = -\frac{1}{j\pi}\mathsf{PV}\int_{\mathbb{R}} \frac{\kappa'^{2a-\ell} q_{\ell m}^{\mathrm{TE}}\left(\kappa'\right)}{\kappa' - \kappa} d\kappa' \tag{3.45}$$

$$\kappa^{2a-\ell-1} q_{\ell m}^{\mathrm{TM}}\left(\kappa\right) = -\frac{1}{j\pi}\mathsf{PV}\int_{\mathbb{R}} \frac{\kappa'^{2a-\ell-1} q_{\ell m}^{\mathrm{TM}}\left(\kappa'\right)}{\kappa' - \kappa} d\kappa' \tag{3.46}$$

shall hold for any $a \in \mathbb{N}_{\geqslant \ell}$, while

$$\kappa^{a+1} q_{\ell m}^{\mathrm{TE}}\left(\kappa\right) = -\frac{1}{j\pi}\mathsf{PV}\int_{\mathbb{R}} \frac{\kappa'^{a+1} q_{\ell m}^{\mathrm{TE}}\left(\kappa'\right)}{\kappa' - \kappa} d\kappa' \tag{3.47}$$

$$\kappa^{a} q_{\ell m}^{\mathrm{TM}}\left(\kappa\right) = -\frac{1}{j\pi}\mathsf{PV}\int_{\mathbb{R}} \frac{\kappa'^{a} q_{\ell m}^{\mathrm{TM}}\left(\kappa'\right)}{\kappa' - \kappa} d\kappa' \tag{3.48}$$

must also be true. The four above conditions are the main results of this subsection. If one is able to ensure them, alongside Equation (3.41), then the antenna will surely be causal.

A sufficient condition, but it must be emphasised that it is not actually necessary, to guarantee that the above functions satisfy Kramers-Kronig relations is established in Theorem A.1. Such condition, nevertheless, requires extending the functions to an open set $D \subseteq \mathbb{C}$ containing $\overline{\mathbb{C}_+} = \left\{\varkappa \in \mathbb{C};\ \mathrm{Im}\,(\varkappa) \geqslant 0\right\}$ over which they must be holomorphic (or analytic in this context) as described in the said Theorem. Thus, if

$$\varkappa^{2a-\ell} q_{\ell m}^{\mathrm{TE}}(\varkappa) \quad \text{and} \quad \varkappa^{2a-\ell-1} q_{\ell m}^{\mathrm{TM}}(\varkappa), \quad \forall a \in \mathbb{N}_{\leqslant \ell} \cup \{0\} \tag{3.49}$$

and

$$\varkappa^{a+1} q_{\ell m}^{\mathrm{TE}}(\varkappa) \quad \text{and} \quad \varkappa^{a} q_{\ell m}^{\mathrm{TM}}(\varkappa), \quad \forall a \in \mathbb{N}_{\geqslant \ell} \tag{3.50}$$

are analytic in D and they vanishes as $\varkappa \to \infty$ on $\overline{\mathbb{C}_+}$, then they obey Kramers-Kronig relations. Of course the analyticity required above does not determine the sought functions, but it can provide some clues about they form.

The most obvious characteristic of $q_{\ell m}^{\mathrm{TE}}$ and $q_{\ell m}^{\mathrm{TM}}$ comes from the (3.49) at $a = 0$, which $q_{\ell m}^{\mathrm{TE}}$ and $q_{\ell m}^{\mathrm{TM}}$ must have at least ℓ and $\ell + 1$ zeros at $\varkappa = 0$, respectively. Thus,

$$q_{\ell m}^{\mathrm{TE}}(\varkappa) = \varkappa^{\ell} f_{\ell m}^{\mathrm{TE}}(\varkappa) \quad \text{and} \quad q_{\ell m}^{\mathrm{TM}}(\varkappa) = \varkappa^{\ell+1} f_{\ell m}^{\mathrm{TM}}(\varkappa)$$

where the auxiliary $f_{\ell m}^{\mathrm{TE}}$ and $f_{\ell m}^{\mathrm{TM}}$ should also be analytic in D. This conclusion would suffice if it were not for the requirement of vanishing as $\varkappa \to \infty$ on $\overline{\mathbb{C}_+}$. Actually, given an exponent b, constructing auxiliary functions so that such that

$$\lim_{\varkappa \to \infty} \varkappa^{\ell+b} f_{\ell m}^{\mathrm{TE}}(\varkappa) = 0 \quad \text{and} \quad \lim_{\varkappa \to \infty} \varkappa^{\ell+b} f_{\ell m}^{\mathrm{TM}}(\varkappa) = 0$$

is not hard whatsoever. Consider $f_{\ell m}^{\mathrm{TE}}$ for example. It would be enough choosing $\ell + b + 1$ (or more) poles $\left\{\varkappa_i\right\}_{i \in \mathbb{N}_{\leqslant \ell+b+1}}$ in the lower half-plane and defining

$$f_{\ell m}^{\mathrm{TE}}(\varkappa) = \frac{1}{(\varkappa - \varkappa_1)(\varkappa - \varkappa_2) \cdots (\varkappa - \varkappa_{\ell+b+1})}.$$

In fact, if $\varkappa = Re^{j\theta}$, then

$$\begin{aligned} \left| \varkappa^b q_{\ell m}^{\mathrm{TE}}(\varkappa) \right| &= \frac{R^{\ell+b}}{\left|Re^{j\theta} - \varkappa_1\right| \left|Re^{j\theta} - \varkappa_2\right| \cdots \left|Re^{j\theta} - \varkappa_{\ell+b+1}\right|} \\ &= \frac{1}{\left|e^{j\theta} - \frac{\varkappa_1}{R}\right| \left|e^{j\theta} - \frac{\varkappa_2}{R}\right| \cdots \left|e^{j\theta} - \frac{\varkappa_{\ell+b}}{R}\right| \left|Re^{j\theta} - \varkappa_{\ell+b+1}\right|}, \end{aligned}$$

from which it is clear that $\lim_{R \to \infty} \left| \varkappa^b q_{\ell m}^{\mathrm{TE}}(\varkappa) \right| = 0$. Moreover, notice that the chosen $f_{\ell m}^{\mathrm{TE}}$ is also suitable for any exponent less than b. This approach would suffice it were not for the fact that b must be as great as one might want, due to (3.50), and, most certainly, the auxiliary functions should not depend on b. Nevertheless, the above discussion provides the insight on how to proceed.

Before continuing, it is worth analysing another candidate for the auxiliary functions. Given the exponential nature of the problem difficulty, one may be wondering if choosing $f_{\ell m}^{\mathrm{TE}}(\varkappa) = e^{j\alpha\varkappa}$, for some $\alpha > 0$, would work. Well, it would not. The reason is that

$$\left|\varkappa^b q_{\ell m}^{\mathrm{TE}}(\varkappa)\right| = R^{\ell+b} e^{-\alpha R \sin\theta}$$

only converges to zero as $R \to \infty$ if $\theta \in (0, \pi)$, hence it does not contemplate the real frequency (or wavenumber) case. Attempts to adapt this approach commonly leads to non-analytical auxiliary functions.

One solution, motivated by the above discussion, is to consider a sequence $\{\varkappa_i\}_{i\in\mathbb{N}}$ on the lower half-plane without accumulation point and project an entire function[2] h with simple zeros at the sequence, *i.e.*, $h(\varkappa_i) = 0\ \forall i \in \mathbb{N}$. The Weierstrass Factorisation Theorem, *cf.* [Net05, Ch. V, Corollary, page 364], ensures that there is an entire function g so that h has the form

$$h(\varkappa) = e^{g(\varkappa)} \prod_{i\in\mathbb{N}} \left(1 - \frac{\varkappa}{\varkappa_i}\right),$$

which converges on any compact subset of $\mathbb{C}$. At this point, it is enough defining $f_{\ell m}^{\mathrm{TE}}$ (and also $f_{\ell m}^{\mathrm{TM}}$) as

$$f_{\ell m}^{\mathrm{TE}}(\kappa) = \frac{1}{h(\kappa)} = \frac{e^{-g(\varkappa)}}{\displaystyle\prod_{i\in\mathbb{N}} \left(1 - \frac{\varkappa}{\varkappa_i}\right)}.$$

Finally, if $q_{\ell m}^{\mathrm{TE}}$ and $q_{\ell m}^{\mathrm{TM}}$ are assumed to be analytic, then they may have the following aspect

$$q_{\ell m}^{\mathrm{TE}}(\varkappa) = \frac{\varkappa^\ell e^{-g_{\ell m}^{\mathrm{TE}}(\varkappa)}}{\displaystyle\prod_{i\in\mathbb{N}} \left(1 - \frac{\varkappa}{\varkappa_{i\ell m}^{\mathrm{TE}}}\right)} \quad \text{and} \quad q_{\ell m}^{\mathrm{TM}}(\varkappa) = \frac{\varkappa^{\ell+1} e^{-g_{\ell m}^{\mathrm{TM}}(\varkappa)}}{\displaystyle\prod_{i\in\mathbb{N}} \left(1 - \frac{\varkappa}{\varkappa_{i\ell m}^{\mathrm{TM}}}\right)}, \tag{3.51}$$

where all poles must have negative imaginary part and they cannot be arbitrarily close to each other.

As models for the mode coefficients, it is worth remembering the forms constructed above are not unique. In fact, a finite number of zeros, even at $\varkappa = 0$, or entire functions, like $e^{j\varkappa}$ to ensure the convergence to zero on the upper half-plane, can still be put into the those models and they would still imply causality. This uncertainty on the their form and the fact that infinitely many poles, for each mode, needs to be estimated most certainly discourage their utilisation.

3.A Computational form of $T_{\ell m}$ Matrix

Given the relevance of the $\boldsymbol{T}_{\ell m}$ to describe the radiated field and the antenna properties, it is important to have a more explicit form for it that does not involves the derivative in θ. This

[2] A complex-valued function of one complex variable is said to be entire if it is holomorphic on $\mathbb{C}$.

brief appendix develops such form in aiming its computational implementation. The starting point is to develop Equation (3.28) as follows

$$\begin{aligned}\boldsymbol{T}_{\ell m}(\theta,\phi) &= \frac{j^{\ell}\sqrt{\eta}}{\sqrt{\ell(\ell+1)}}\begin{bmatrix}\dfrac{-mY_{\ell}^{m}}{\sin\theta} & \dfrac{\partial Y_{\ell}^{m}}{\partial\theta}\\ -j\dfrac{\partial Y_{\ell}^{m}}{\partial\theta} & \dfrac{jmY_{\ell}^{m}}{\sin\theta}\end{bmatrix}\\ &= \frac{j^{\ell}\sqrt{\eta}}{\sqrt{\ell(\ell+1)}}\begin{bmatrix}0 & -1\\ j & 0\end{bmatrix}\begin{bmatrix}-\dfrac{\partial Y_{\ell}^{m}}{\partial\theta} & \dfrac{mY_{\ell}^{m}}{\sin\theta}\\ \dfrac{mY_{\ell}^{m}}{\sin\theta} & -\dfrac{\partial Y_{\ell}^{m}}{\partial\theta}\end{bmatrix}\\ &= \frac{j^{\ell}\sqrt{\eta}}{\sqrt{\ell(\ell+1)}}\begin{bmatrix}0 & -1\\ j & 0\end{bmatrix}\left(\frac{mY_{\ell}^{m}}{\sin\theta}\mathbf{O}_2-\frac{\partial Y_{\ell}^{m}}{\partial\theta}\mathbf{I}_2\right),\end{aligned} \tag{3.52}$$

where $\mathbf{O}_2=\begin{bmatrix}0 & 1\\ 1 & 0\end{bmatrix}$ is an auxiliary matrix.

Due to the sine in the denominator, it is important to analyse the behaviour of $\boldsymbol{T}_{\ell m}$ at $\theta=0$ and $\theta=\pi$. As stated in Proposition D.2, it holds that

$$\frac{\partial Y_{\ell}^{m}}{\partial\theta}(0,\phi)=\frac{\partial Y_{\ell}^{m}}{\partial\theta}(\pi,\phi)=0. \tag{3.53}$$

Besides, from the Definition C.1, the ratio $\dfrac{Y_{\ell}^{m}}{\sin\theta}$ is well defined (removable singularity) whenever $m\neq 0$ and the following holds

$$\lim_{\theta\to 0}\frac{Y_{\ell}^{m}(\theta,\phi)}{\sin\theta}=\lim_{\theta\to\pi}\frac{Y_{\ell}^{m}(\theta,\phi)}{\sin\theta}=\begin{cases}0, & \text{if } \ell>1\\ \frac{1}{2}\sqrt{\frac{3}{2\pi}}e^{-j\phi}, & \text{if } \ell=1 \text{ and } m=-1\\ -\frac{1}{2}\sqrt{\frac{3}{2\pi}}e^{j\phi}, & \text{if } \ell=1 \text{ and } m=1\end{cases}. \tag{3.54}$$

However, for those particular cases where $m=0$, the term $\dfrac{mY_{\ell}^{m}}{\sin\theta}$ is beforehand zero. Thus,

$$\boldsymbol{T}_{\ell m}(0,\phi)=\boldsymbol{T}_{\ell m}(\pi,\phi)=\begin{cases}\mathbf{0}_{2\times 2}, & \text{if } m=0 \text{ or } \ell>1\\ -j\begin{bmatrix}0 & -1\\ j & 0\end{bmatrix}\dfrac{m}{4}\sqrt{\dfrac{3\eta}{\pi}}e^{j\phi}\mathbf{O}_2, & \text{if } m\neq 0 \text{ and } \ell=1\end{cases}. \tag{3.55}$$

For any other case, *i.e.*, $\theta\in(0,\pi)$, the Proposition D.2 can be used to go further by doing

$$\begin{aligned}\boldsymbol{T}_{\ell m}(\theta,\phi) &= \frac{j^{\ell}\sqrt{\eta}}{\sqrt{\ell(\ell+1)}}\begin{bmatrix}0 & -1\\ j & 0\end{bmatrix}\left(\frac{mY_{\ell}^{m}}{\sin\theta}\mathbf{O}_2-\ell\frac{\cos\theta}{\sin\theta}Y_{\ell}^{m}\mathbf{I}_2+\frac{C_{\ell m}}{\sin\theta}Y_{\ell-1}^{m}\mathbf{I}_2\right)\\ &= \frac{j^{\ell}\sqrt{\eta}}{\sqrt{\ell(\ell+1)}}\frac{1}{\sin\theta}\begin{bmatrix}0 & -1\\ j & 0\end{bmatrix}\left(mY_{\ell}^{m}\mathbf{O}_2-\ell\cos\theta Y_{\ell}^{m}\mathbf{I}_2+C_{\ell m}Y_{\ell-1}^{m}\mathbf{I}_2\right),\end{aligned} \tag{3.56}$$

where $C_{\ell m}=\sqrt{\frac{2\ell+1}{2\ell-1}}\sqrt{\ell^2-m^2}$ is an auxiliary coefficient defined to prevent overloading the equations more than it is necessary.

3.B Results on Fourier Transform of the Spherical Hankel Function

The main objective of this appendix is to construct the inverse Fourier transform of the $\boldsymbol{Z}_\ell$. To simplify the following equations, the argument of such function will be frequency-like variable $u = \kappa r = \frac{2\pi r}{c}\nu$. Thus,

$$\begin{aligned}\mathcal{F}^{-1}\left(\boldsymbol{Z}_\ell\right)(t) &= \int_{\mathbb{R}} \boldsymbol{Z}_\ell\left(\frac{2\pi r}{c}\nu\right) e^{2\pi j\nu t} d\nu \\ &= \frac{c}{2\pi r}\int_{\mathbb{R}} \boldsymbol{Z}_\ell(u)\, e^{2\pi j u \frac{ct}{2\pi r}} du \\ &= \frac{c}{2\pi r}\int_{\mathbb{R}} \boldsymbol{Z}_\ell(u)\, e^{2\pi j u\tau} du \end{aligned} \tag{3.57}$$

where $\tau = \frac{ct}{2\pi r}$ is the counterpart time-like variable. The first step towards such result is, of course, calculate the inverse Fourier transform of the second kind spherical Hankel function z_ℓ. For this intermediary goal, consider the following auxiliary results, documented as lemmas, about the inverse Fourier transform.

Lemma 3.1. $\mathcal{F}^{-1}\left(\dfrac{1}{u^{k+1}}\right)(\tau) = j\pi \cdot \dfrac{(j2\pi\tau)^k}{k!} \cdot \operatorname{sgn}(\tau)$

Proof. It is enough to observe that

$$\frac{d^k}{dv^k}\left(\frac{1}{u}\right) = \frac{d^{k-1}}{dv^{k-1}}\left(-\frac{1}{u^2}\right) = \frac{d^{k-2}}{dv^{k-2}}\left(\frac{2}{u^3}\right) = \cdots = (-1)^k \frac{k!}{u^{k+1}}.$$

Using that $\mathcal{F}^{-1}\Big(f^{(k)}(u)\Big)(\tau) = (-j2\pi\tau)^k \mathcal{F}^{-1}\Big(f(u)\Big)(\tau)$, it becomes

$$\mathcal{F}^{-1}\left((-1)^k \frac{k!}{u^{k+1}}\right)(\tau) = (-j2\pi\tau)^k \mathcal{F}^{-1}\left(\frac{1}{u}\right)(\tau).$$

Finally, since $\mathcal{F}^{-1}\left(\frac{1}{u}\right)(\tau) = j\pi \cdot \operatorname{sgn}(\tau)$,

$$\mathcal{F}^{-1}\left((-1)^k \frac{k!}{u^{k+1}}\right)(\tau) = (-j2\pi\tau)^k \cdot j\pi \cdot \operatorname{sgn}(\tau),$$

from which the yielded result follows. ∎

Lemma 3.2. $\mathcal{F}^{-1}\left(z_\ell\right)(\tau) = -j^\ell \pi \sum_{k=0}^{\ell} \pi^k \binom{2k}{k}\binom{\ell+k}{\ell-k} \cdot \left(\tau - 1/2\pi\right)^k \cdot \operatorname{sgn}\left(\tau - 1/2\pi\right)$

Proof. Once again considering the expansion of z_ℓ, *cf.* [Nis, Eq. 10.49.7],

$$z_\ell(u) = j^{\ell+1} e^{-ju} \sum_{k=0}^{\ell} \frac{1}{(2j)^k} \frac{(2k)!}{k!} \binom{\ell+k}{\ell-k} \frac{1}{u^{k+1}},$$

the following holds

$$\begin{aligned}
\mathcal{F}^{-1}\left(z_\ell\right)(\tau) &= \int_{\mathbb{R}} z_\ell(u)\, e^{2\pi j u\tau} du \\
&= j^{\ell+1} \sum_{k=0}^{\ell} \frac{1}{(2j)^k} \frac{(2k)!}{k!} \binom{\ell+k}{\ell-k} \int_{\mathbb{R}} \frac{e^{-ju}}{u^{k+1}} e^{2\pi j u\tau} du \\
&= j^{\ell+1} \sum_{k=0}^{\ell} \frac{1}{(2j)^k} \frac{(2k)!}{k!} \binom{\ell+k}{\ell-k} \int_{\mathbb{R}} \frac{1}{u^{k+1}} e^{2\pi j u(\tau-1/2\pi)} du \\
&= j^{\ell+1} \sum_{k=0}^{\ell} \frac{1}{(2j)^k} \frac{(2k)!}{k!} \binom{\ell+k}{\ell-k} \mathcal{F}^{-1}\left(\frac{1}{u^{k+1}}\right)(\tau - 1/2\pi) \\
&= j^{\ell+1} \sum_{k=0}^{\ell} \frac{1}{(2j)^k} \frac{(2k)!}{k!} \binom{\ell+k}{\ell-k} \cdot j\pi \cdot \frac{\left(j2\pi\left(\tau - 1/2\pi\right)\right)^k}{k!} \cdot \operatorname{sgn}\left(\tau - 1/2\pi\right) \\
&= -j^{\ell}\pi \sum_{k=0}^{\ell} \pi^k \frac{(2k)!}{(k!)^2} \binom{\ell+k}{\ell-k} \cdot \left(\tau - 1/2\pi\right)^k \cdot \operatorname{sgn}\left(\tau - 1/2\pi\right). \qquad \blacksquare
\end{aligned}$$

Lemma 3.3. $\mathcal{F}^{-1}\left(\frac{z_\ell(u)}{u}\right)(\tau) = -2j^{\ell+1}\pi^2 \sum_{k=0}^{\ell} \pi^k \binom{2k}{k} \binom{\ell+k}{\ell-k} \cdot \frac{\left(\tau - 1/2\pi\right)^{k+1}}{k+1} \cdot \operatorname{sgn}\left(\tau - 1/2\pi\right)$

Proof. Once again,

$$\begin{aligned}
\mathcal{F}^{-1}\left(\frac{z_\ell(u)}{u}\right)(\tau) &= \int_{\mathbb{R}} \frac{z_\ell(u)}{u} e^{2\pi j u\tau} du \\
&= j^{\ell+1} \sum_{k=0}^{\ell} \frac{1}{(2j)^k} \frac{(2k)!}{k!} \binom{\ell+k}{\ell-k} \int_{\mathbb{R}} \frac{e^{-ju}}{u^{k+2}} e^{2\pi j u\tau} du \\
&= j^{\ell+1} \sum_{k=0}^{\ell} \frac{1}{(2j)^k} \frac{(2k)!}{k!} \binom{\ell+k}{\ell-k} \int_{\mathbb{R}} \frac{1}{u^{k+2}} e^{2\pi j u(\tau-1/2\pi)} du \\
&= j^{\ell+1} \sum_{k=0}^{\ell} \frac{1}{(2j)^k} \frac{(2k)!}{k!} \binom{\ell+k}{\ell-k} \mathcal{F}^{-1}\left(\frac{1}{u^{k+2}}\right)(\tau - 1/2\pi) \\
&= j^{\ell+1} \sum_{k=0}^{\ell} \frac{1}{(2j)^k} \frac{(2k)!}{k!} \binom{\ell+k}{\ell-k} \cdot j\pi \cdot \frac{\left(j2\pi\left(\tau - 1/2\pi\right)\right)^{k+1}}{(k+1)!} \cdot \operatorname{sgn}\left(\tau - 1/2\pi\right) \\
&= -2j^{\ell+1}\pi \sum_{k=0}^{\ell} \pi^{k+1} \frac{(2k)!}{(k+1)! \cdot k!} \binom{\ell+k}{\ell-k} \cdot \left(\tau - 1/2\pi\right)^{k+1} \cdot \operatorname{sgn}\left(\tau - 1/2\pi\right). \blacksquare
\end{aligned}$$

At this point, it must be noticed that

$$\mathcal{F}^{-1}\left(\frac{z_\ell(u)}{u}\right)(\tau) = -2j^{\ell+1}\pi^2 \cdot \mathsf{pol}_\ell\left(\tau - 1/2\pi\right) \cdot \operatorname{sgn}\left(\tau - 1/2\pi\right), \tag{3.58}$$

where pol_ℓ is polynomial of degree $\ell+1$, and

$$\mathcal{F}^{-1}\left(z_\ell(u)\right)(\tau) = -j^{\ell}\pi \cdot \mathsf{pol}'_\ell\left(\tau - 1/2\pi\right) \cdot \operatorname{sgn}\left(\tau - 1/2\pi\right), \tag{3.59}$$

implying a quite nice relationship between the two transforms. Now, it is possible to calculate the inverse Fourier transform of $\boldsymbol{Z}_\ell$ as follows

$$\begin{aligned}
\int_{\mathbb{R}} \boldsymbol{Z}_\ell(u)\, e^{2\pi j u\tau} du &= \int_{\mathbb{R}} \begin{bmatrix} 0 & \sqrt{\ell(\ell+1)}\frac{z_\ell(u)}{u} \\ z_\ell(u) & 0 \\ 0 & z_{\ell-1}(u) - \frac{z_\ell(u)}{u} \end{bmatrix} e^{2\pi j u\tau} du \\
&= \begin{bmatrix} 0 & \sqrt{\ell(\ell+1)}\displaystyle\int_{\mathbb{R}} \frac{z_\ell(u)}{u} e^{2\pi j u\tau} du \\ \displaystyle\int_{\mathbb{R}} z_\ell(u)\, e^{2\pi j u\tau} du & 0 \\ 0 & \displaystyle\int_{\mathbb{R}} z_{\ell-1}(u)\, e^{2\pi j u\tau} du - \int_{\mathbb{R}} \frac{z_\ell(u)}{u} e^{2\pi j u\tau} du \end{bmatrix} \\
&= \begin{bmatrix} 0 & -2j^{\ell+1}\pi^2\sqrt{\ell(\ell+1)}\mathsf{pol}_\ell\left(\tau - 1/2\pi\right) \\ -j^{\ell}\pi \cdot \mathsf{pol}'_\ell\left(\tau - 1/2\pi\right) & 0 \\ 0 & -j^{\ell-1}\pi \cdot \mathsf{pol}'_{\ell-1}\left(\tau - 1/2\pi\right) + 2j^{\ell+1}\pi^2\mathsf{pol}_\ell\left(\tau - 1/2\pi\right) \end{bmatrix} \\
&\quad \cdot \operatorname{sgn}\left(\tau - 1/2\pi\right).
\end{aligned} \tag{3.60}$$

Finally,

$$\mathcal{F}^{-1}\left(\boldsymbol{Z}_\ell\right)(t) = \boldsymbol{\mathcal{Z}}_\ell\left(r, \frac{ct}{2\pi r} - \frac{1}{2\pi}\right) \cdot \operatorname{sgn}\left(\frac{ct}{2\pi r} - \frac{1}{2\pi}\right), \tag{3.61}$$

where

$$\boldsymbol{\mathcal{Z}}_\ell(r,\tau) = j^\ell \frac{c}{2r} \begin{bmatrix} 0 & -2\pi j\sqrt{\ell(\ell+1)} \cdot \mathsf{pol}_\ell(\tau) \\ -\mathsf{pol}'_\ell(\tau) & 0 \\ 0 & j \cdot \mathsf{pol}'_{\ell-1}(\tau) + 2\pi j \cdot \mathsf{pol}_\ell(\tau) \end{bmatrix} \tag{3.62}$$

and

$$\mathsf{pol}_\ell(\tau) = \sum_{k=0}^{\ell} \pi^k \binom{2k}{k} \binom{\ell+k}{\ell-k} \cdot \frac{\tau^{k+1}}{k+1}. \tag{3.63}$$

Lastly, it is also worth calculating $\mathcal{F}^{-1}\left(\nu \boldsymbol{Z}_\ell\right)(t)$, which can be done as

$$\begin{aligned}
\mathcal{F}^{-1}\left(\nu \boldsymbol{Z}_\ell\right)(t) &= \frac{1}{2\pi j}\frac{d}{dt}\mathcal{F}^{-1}\left(\boldsymbol{Z}_\ell\right)(t) \\
&= \frac{1}{2\pi j}\frac{d}{dt}\left(\boldsymbol{\mathcal{Z}}_\ell\left(r, \frac{ct}{2\pi r} - \frac{1}{2\pi}\right) \cdot \operatorname{sgn}\left(\frac{ct}{2\pi r} - \frac{1}{2\pi}\right)\right) \\
&= \frac{1}{2\pi j}\left[\frac{c}{2\pi r}\partial_t \boldsymbol{\mathcal{Z}}_\ell\left(r, \frac{ct}{2\pi r} - \frac{1}{2\pi}\right) \cdot \operatorname{sgn}\left(\frac{ct}{2\pi r} - \frac{1}{2\pi}\right)\right. \\
&\quad \left. + 2\frac{c}{2\pi r}\boldsymbol{\mathcal{Z}}_\ell\left(r, \frac{ct}{2\pi r} - \frac{1}{2\pi}\right) \cdot \delta\left(\frac{ct}{2\pi r} - \frac{1}{2\pi}\right)\right] \\
&= \frac{1}{2\pi j}\left[\frac{c}{2\pi r}\partial_t \boldsymbol{\mathcal{Z}}_\ell\left(r, \frac{ct}{2\pi r} - \frac{1}{2\pi}\right) \cdot \operatorname{sgn}\left(\frac{ct}{2\pi r} - \frac{1}{2\pi}\right) + 2\boldsymbol{\mathcal{Z}}_\ell\left(r, \frac{ct}{2\pi r} - \frac{1}{2\pi}\right) \cdot \delta\left(t - \frac{r}{c}\right)\right] \\
&= \frac{c}{j4\pi^2 r}\partial_t \boldsymbol{\mathcal{Z}}_\ell\left(r, \frac{ct}{2\pi r} - \frac{1}{2\pi}\right) \cdot \operatorname{sgn}\left(\frac{ct}{2\pi r} - \frac{1}{2\pi}\right) + \frac{1}{j\pi}\boldsymbol{\mathcal{Z}}_\ell\left(r, \frac{ct}{2\pi r} - \frac{1}{2\pi}\right) \cdot \delta\left(t - \frac{r}{c}\right)
\end{aligned} \tag{3.64}$$

Chapter 4

Estimation of the Mode Coefficients

Although the theory presented in the previous chapter provides a simple and ingenious method for representing the electric field emitted by an antenna, it is not fully prepared to be applied in practice. To that end, some challenges must be overcome. The most obvious issue regards the fact that the series in Equation (3.29) must be truncated in a finite number of modes in order to be computationally implemented. Additionally, a mode coefficient function $\boldsymbol{q}_{\ell m}$ is not, and can not be, directly measured, hence it must be observed from samples of the phasor electric field collected during tests performed on the antenna.

In this chapter, and also in light of the difficulties exposed above, a stochastic and truncated model for the phasor electric field samples is developed and an asymptotically unbiased estimator for the mode coefficients is proposed based on the minimisation of their covariances.

4.1 Truncation of Phasor Electric Field

As it has been shown in Chapter 3, The phasor electric field transmitted by an antenna can be understood as the linear combination of countably infinite spherical waves, each one described by a mode. However, it is not possible to compute an infinite number of modes and, consequently, the usage of Equation (3.29) to model samples of the electric field is conditioned to the choice of a finite number of modes over which this field will be projected.

In this regard, it is suggestive considering an upper bound for the degree of the modes, which would constrain the order as well. In this direction, consider $k \in \mathbb{N}$ to be such bound and let $\mathtt{E}_k$ and $\boldsymbol{\varepsilon}_k^{\mathrm{tru}}$ denote the electric field in Equation (3.29) truncated up to the k-th degree and the truncation error given by $\mathtt{E} - \mathtt{E}_k$, respectively. Hence, it can be written that

$$\mathtt{E}_k(\theta, \phi, \nu) = \sum_{\ell \in \mathbb{N}_{\leqslant k}} \sum_{|m| \leqslant \ell} \boldsymbol{T}_{\ell m}(\theta, \phi)\, \boldsymbol{q}_{\ell m}(\nu)\,, \tag{4.1}$$

$$\boldsymbol{\varepsilon}_k^{\mathrm{tru}}(\theta, \phi, \nu) = \sum_{\ell \in \mathbb{N}_{>k}} \sum_{|m| \leqslant \ell} \boldsymbol{T}_{\ell m}(\theta, \phi)\, \boldsymbol{q}_{\ell m}(\nu)\,. \tag{4.2}$$

It is important to compute, of course, the total number of modes N_k over which the field is about to be projected. Surely, it can be easily calculated by summing the first k odd numbers starting from 3 as follows

$$N_k = 3 + 5 + 7 + \cdots + (2k+1) = k^2 + 2k. \tag{4.3}$$

Moreover, Equation (4.1) encourages the definition of the matrices $\mathbf{T}_k(\theta,\phi) \in \mathbb{C}^{2\times 2N_k}$ and $\mathbf{q}_k(\nu) \in \mathbb{C}^{2N_k\times 1}$, given by

$$\mathbf{T}_k = \begin{bmatrix} \boldsymbol{T}_{(1,-1)} & \boldsymbol{T}_{(1,0)} & \boldsymbol{T}_{(1,1)} & \boldsymbol{T}_{(2,-2)} & \cdots & \boldsymbol{T}_{(k,k)} \end{bmatrix}, \tag{4.4}$$

$$\mathbf{q}_k = \begin{bmatrix} \boldsymbol{q}^{\mathrm{T}}_{(1,-1)} & \boldsymbol{q}^{\mathrm{T}}_{(1,0)} & \boldsymbol{q}^{\mathrm{T}}_{(1,1)} & \boldsymbol{q}^{\mathrm{T}}_{(2,-2)} & \cdots & \boldsymbol{q}^{\mathrm{T}}_{(k,k)} \end{bmatrix}^{\mathrm{T}}, \tag{4.5}$$

so that the $\mathtt{E}_k$ can be written as the linear form

$$\mathtt{E}_k(\theta,\phi,\nu) = \mathbf{T}_k(\theta,\phi)\,\mathbf{q}_k(\nu), \tag{4.6}$$

which is not only more compact and clear than Equation (4.1), but it also better supports the computational implementation of the estimators further developed.

4.2 Modelling the Measured Samples

At this point, let $\boldsymbol{\varepsilon}^{\mathrm{mea}}(\theta,\phi,\nu)$ denote the measurement noise introduced by the sensor when measuring the electric field in the direction (θ,ϕ) and at the frequency ν. Hence, the observed phasor electric field can be modelled after the random variable $\widetilde{\mathtt{E}}$ at the form

$$\begin{aligned} \widetilde{\mathtt{E}}(\theta,\phi,\nu) &= \mathtt{E}(\theta,\phi,\nu) + \boldsymbol{\varepsilon}^{\mathrm{mea}}(\theta,\phi,\nu) \\ &= \mathtt{E}_k(\theta,\phi,\nu) + \boldsymbol{\varepsilon}^{\mathrm{tru}}_k(\theta,\phi,\nu) + \boldsymbol{\varepsilon}^{\mathrm{mea}}(\theta,\phi,\nu) \\ &= \mathbf{T}_k(\theta,\phi)\,\mathbf{q}_k(\nu) + \boldsymbol{\varepsilon}_k(\theta,\phi,\nu), \end{aligned} \tag{4.7}$$

where $\boldsymbol{\varepsilon}_k$ denote the total noise defined as the sum of the deterministic variable $\boldsymbol{\varepsilon}^{\mathrm{tru}}_k$ with the random variable $\boldsymbol{\varepsilon}^{\mathrm{mea}}$, from which the samples inherit their stochastic characteristics.

Naturally, the sensor is assumed to be calibrated, hence implying that $\big\langle \boldsymbol{\varepsilon}^{\mathrm{mea}}(\theta,\phi,\nu) \big\rangle = \mathbf{0} \in \mathbb{C}^{2\times 1}$ for any tuple (θ,ϕ,ν). Besides, it is reasonable to suppose that components of $\boldsymbol{\varepsilon}^{\mathrm{mea}}$ are uncorrelated and that the nature of this noise does not depend on the direction, while the independence on the frequency is assumed by simplicity. Therefore, $\mathrm{cov}\big(\boldsymbol{\varepsilon}^{\mathrm{mea}}(\theta,\phi,\nu)\big) = \sigma^2\mathbf{I}_2$, where $\sigma^2 \in \mathbb{R}$ is constant. In the context of those assumptions, it holds that $\big\langle \boldsymbol{\varepsilon}_k(\theta,\phi,\nu) \big\rangle = \boldsymbol{\varepsilon}^{\mathrm{tru}}_k(\theta,\phi,\nu)$, which easily leads to $\mathrm{cov}\big(\boldsymbol{\varepsilon}_k(\theta,\phi,\nu)\big) = \sigma^2\mathbf{I}_2$.

In light of the background established above, assume that a collection of $M \in \mathbb{N}$ directions, denoted by $\big\{(\theta_i,\phi_i)\big\}_{i\in\mathbb{N}_{\leqslant M}}$, has been chosen and consider that samples of the phasor electric field $\big\{\widetilde{\mathtt{E}}(\theta_i,\phi_i,\nu)\big\}_{i\in\mathbb{N}_{\leqslant M}}$ were measured in those directions at an arbitrary frequency ν. In this context, consider the matrices $\widetilde{\mathbf{E}}(\nu) \in \mathbb{C}^{2M\times 1}$, $\boldsymbol{\Upsilon}_k \in \mathbb{C}^{2M\times 2N_k}$ and $\boldsymbol{\epsilon}_k(\nu) \in \mathbb{C}^{2M\times 1}$ defined by the blocks

$$\widetilde{\mathbf{E}}(\nu) = \begin{bmatrix} \widetilde{\mathtt{E}}(\theta_1,\phi_1,\nu) \\ \widetilde{\mathtt{E}}(\theta_2,\phi_2,\nu) \\ \widetilde{\mathtt{E}}(\theta_3,\phi_3,\nu) \\ \vdots \\ \widetilde{\mathtt{E}}(\theta_M,\phi_M,\nu) \end{bmatrix}, \quad \boldsymbol{\Upsilon}_k = \begin{bmatrix} \mathbf{T}_k(\theta_1,\phi_1) \\ \mathbf{T}_k(\theta_2,\phi_2) \\ \mathbf{T}_k(\theta_3,\phi_3) \\ \vdots \\ \mathbf{T}_k(\theta_M,\phi_M) \end{bmatrix} \quad \text{and} \quad \boldsymbol{\epsilon}_k(\nu) = \begin{bmatrix} \boldsymbol{\varepsilon}_k(\theta_1,\phi_1,\nu) \\ \boldsymbol{\varepsilon}_k(\theta_2,\phi_2,\nu) \\ \boldsymbol{\varepsilon}_k(\theta_3,\phi_3,\nu) \\ \vdots \\ \boldsymbol{\varepsilon}_k(\theta_M,\phi_M,\nu) \end{bmatrix}, \tag{4.8}$$

from which Equation (4.7) can be modified into

$$\widetilde{\mathbf{E}}(\nu) = \boldsymbol{\Upsilon}_k \mathbf{q}_k(\nu) + \boldsymbol{\epsilon}_k(\nu). \tag{4.9}$$

It is worth highlighting that Equation (4.9) synthesises the model for the samples containing all the information on the electric field at the frequency ν that has been collected. For this reason, such model will further been used in the next sections to create estimators for the mode coefficient $\mathbf{q}_k(\nu)$.

Remark. In order to keep the visual clarity of the equations, the frequency argument of $\widetilde{\mathbf{E}}$, $\mathbf{q}$ and $\boldsymbol{\epsilon}$ and its variations might be henceforth omitted when no confusion is possible.

4.3 Batch Estimation of the Mode Coefficients

Let $\widehat{\mathbf{q}}_k$ denote an estimator for the deterministic value $\mathbf{q}_k$. Of course, one is interested in retrieving the electric field by simply doing

$$\widehat{\mathbf{E}}_k = \boldsymbol{\Upsilon}_k \widehat{\mathbf{q}}_k. \tag{4.10}$$

Due to the linearity of the model in (4.9), the most intuitive approach to find such estimator would be choosing the one that minimises the residual energy, given by

$$\mathscr{E}_k^{\text{res}} = \left(\widetilde{\mathbf{E}} - \widehat{\mathbf{E}}_k\right)^{\text{H}} \left(\widetilde{\mathbf{E}} - \widehat{\mathbf{E}}_k\right), \tag{4.11}$$

hence leading to the well known linear regression, *cf*. [Lju99, Ch. 7, Eq. 7.34],

$$\widehat{\mathbf{q}}_k = \left[\boldsymbol{\Upsilon}_k^{\text{H}} \boldsymbol{\Upsilon}_k\right]^{-1} \cdot \boldsymbol{\Upsilon}_k^{\text{H}} \widetilde{\mathbf{E}}, \tag{4.12}$$

if the moment matrix $\boldsymbol{\Upsilon}_k^{\text{H}} \boldsymbol{\Upsilon}_k$ could be inverted, which shall be assumed from now on unless stated otherwise.

Although the minimum possible residual energy is achieved by this method, the quality of the regression shall actually be analysed by studying the bias and the covariance of the estimators, which regard the accuracy and precision of them, respectively.

4.3.1 Estimator bias

It is important to notice that the estimators $\widehat{\mathbf{q}}_k$ and $\widehat{\mathbf{E}}_k$ are actually biased due to the truncation error. In fact, from Equations (4.9) and (4.12), consider the following

$$\begin{aligned} \widehat{\mathbf{q}}_k &= \left[\boldsymbol{\Upsilon}_k^{\text{H}} \boldsymbol{\Upsilon}_k\right]^{-1} \cdot \boldsymbol{\Upsilon}_k^{\text{H}} \left(\boldsymbol{\Upsilon}_k \mathbf{q}_k + \boldsymbol{\epsilon}_k\right) \\ &= \mathbf{q}_k + \left[\boldsymbol{\Upsilon}_k^{\text{H}} \boldsymbol{\Upsilon}_k\right]^{-1} \cdot \boldsymbol{\Upsilon}_k^{\text{H}} \boldsymbol{\epsilon}_k, \end{aligned} \tag{4.13}$$

from which the expected value of the $\widehat{\mathbf{q}}$ can be simply calculated as

$$\begin{aligned}\left\langle \widehat{\mathbf{q}}_k \right\rangle &= \mathbf{q}_k + \left[\boldsymbol{\Upsilon}_k^{\mathrm{H}}\boldsymbol{\Upsilon}_k\right]^{-1} \cdot \boldsymbol{\Upsilon}_k^{\mathrm{H}} \left\langle \boldsymbol{\epsilon}_k \right\rangle \\ &= \mathbf{q}_k + \left[\boldsymbol{\Upsilon}_k^{\mathrm{H}}\boldsymbol{\Upsilon}_k\right]^{-1} \cdot \boldsymbol{\Upsilon}_k^{\mathrm{H}} \boldsymbol{\epsilon}_k^{\mathrm{tru}}. \end{aligned} \tag{4.14}$$

Hence, the biases of $\widehat{\mathbf{q}}_k$ and $\widehat{\mathbf{E}}_k$, which are defined by $\mathrm{bias}\big(\widehat{\mathbf{q}}_k\big) = \langle \widehat{\mathbf{q}}_k \rangle - \mathbf{q}$ and $\mathrm{bias}\big(\widehat{\mathbf{E}}_k\big) = \left\langle \widehat{\mathbf{E}}_k \right\rangle - \widehat{\mathbf{E}}_k$, will be given by

$$\mathrm{bias}\big(\widehat{\mathbf{q}}_k\big) = \left[\boldsymbol{\Upsilon}_k^{\mathrm{H}}\boldsymbol{\Upsilon}_k\right]^{-1}\boldsymbol{\Upsilon}_k^{\mathrm{H}}\boldsymbol{\epsilon}_k^{\mathrm{tru}}, \tag{4.15}$$

$$\mathrm{bias}\big(\widehat{\mathbf{E}}_k\big) = \boldsymbol{\Upsilon}_k\left[\boldsymbol{\Upsilon}_k^{\mathrm{H}}\boldsymbol{\Upsilon}_k\right]^{-1}\boldsymbol{\Upsilon}_k^{\mathrm{H}}\boldsymbol{\epsilon}_k^{\mathrm{tru}}, \tag{4.16}$$

that clearly do not vanish for a finite value of k. However, they can be made as small as required by just increasing k, which controls the number of modes where the collected data will be projected. Thus, the accuracy of the estimators can be controlled as well.

4.3.2 Estimator Covariance

The covariance of the $\widehat{\mathbf{q}}_k$ can be evaluated by using Equations (4.13) and (4.14) through the quantity

$$\begin{aligned}\widehat{\mathbf{q}}_k - \left\langle \widehat{\mathbf{q}}_k \right\rangle &= \left[\boldsymbol{\Upsilon}_k^{\mathrm{H}}\boldsymbol{\Upsilon}_k\right]^{-1}\boldsymbol{\Upsilon}_k^{\mathrm{H}}\Big(\boldsymbol{\epsilon}_k - \boldsymbol{\epsilon}_k^{\mathrm{tru}}\Big) \\ &= \left[\boldsymbol{\Upsilon}_k^{\mathrm{H}}\boldsymbol{\Upsilon}_k\right]^{-1}\boldsymbol{\Upsilon}_k^{\mathrm{H}}\boldsymbol{\epsilon}^{\mathrm{mea}}, \end{aligned}$$

since, by definition, it holds that

$$\begin{aligned}\mathrm{cov}\left(\widehat{\mathbf{q}}_k\right) &= \left\langle \Big(\widehat{\mathbf{q}}_k - \left\langle \widehat{\mathbf{q}}_k \right\rangle\Big)\Big(\widehat{\mathbf{q}}_k - \left\langle \widehat{\mathbf{q}}_k \right\rangle\Big)^{\mathrm{H}} \right\rangle \\ &= \left[\boldsymbol{\Upsilon}_k^{\mathrm{H}}\boldsymbol{\Upsilon}_k\right]^{-1}\boldsymbol{\Upsilon}_k^{\mathrm{H}} \left\langle \boldsymbol{\epsilon}^{\mathrm{mea}}\boldsymbol{\epsilon}^{\mathrm{meaH}} \right\rangle \boldsymbol{\Upsilon}_k\left[\boldsymbol{\Upsilon}_k^{\mathrm{H}}\boldsymbol{\Upsilon}_k\right]^{-1} \\ &= \left[\boldsymbol{\Upsilon}_k^{\mathrm{H}}\boldsymbol{\Upsilon}_k\right]^{-1}\boldsymbol{\Upsilon}_k^{\mathrm{H}} \cdot \mathrm{cov}\left(\boldsymbol{\epsilon}^{\mathrm{mea}}\right) \cdot \boldsymbol{\Upsilon}_k\left[\boldsymbol{\Upsilon}_k^{\mathrm{H}}\boldsymbol{\Upsilon}_k\right]^{-1}. \end{aligned}$$

At this moment, it is worth introducing the traditional notations $\mathbf{P}_k = \mathrm{cov}\left(\widehat{\mathbf{q}}_k\right)$ and $\mathbf{R} = \mathrm{cov}\left(\boldsymbol{\epsilon}^{\mathrm{mea}}\right)$, from which the last equation becomes

$$\mathbf{P}_k = \left[\boldsymbol{\Upsilon}_k^{\mathrm{H}}\boldsymbol{\Upsilon}_k\right]^{-1}\boldsymbol{\Upsilon}_k^{\mathrm{H}} \cdot \mathbf{R} \cdot \boldsymbol{\Upsilon}_k\left[\boldsymbol{\Upsilon}_k^{\mathrm{H}}\boldsymbol{\Upsilon}_k\right]^{-1}. \tag{4.17}$$

Moreover, the whiteness of the measurement noise implies that $\mathbf{R} = \sigma^2\mathbf{I}_{2M}$. Thus, Equation (4.17) can be compactly rewritten as

$$\mathbf{P}_k = \left[\boldsymbol{\Upsilon}_k^{\mathrm{H}}\boldsymbol{\Upsilon}_k\right]^{-1}\sigma^2. \tag{4.18}$$

Even though Equation (4.18) is only defined when the matrix moment is invertible, it is intuitive and interesting to see the covariance as infinite when that matrix can not be inverted. Hence

stressing the fact that uncertainty on the values of the parameters becomes too large the regressors are ill conditioned. Finally, the covariance of the $\widehat{\mathbf{E}}_k$ can be easily calculated leading to the result

$$\operatorname{cov}\left(\widehat{\mathbf{E}}_k\right) = \boldsymbol{\Upsilon}_k \mathbf{P}_k \boldsymbol{\Upsilon}_k^{\mathrm{H}} = \boldsymbol{\Upsilon}_k \left[\boldsymbol{\Upsilon}_k^{\mathrm{H}} \boldsymbol{\Upsilon}_k\right]^{-1} \boldsymbol{\Upsilon}_k^{\mathrm{H}} \sigma^2, \tag{4.19}$$

from where it must be noticed[1] that $\operatorname{tr}\left(\operatorname{cov}\left(\widehat{\mathbf{E}}_k\right)\right) = 2N_k\sigma^2$. Since $\widehat{\mathbf{E}}_k$ is an array of $2M$ estimators, it can be said that the mean value of the variance of a scalar estimator is approximately given by ${}^{N_k\sigma^2}/_{M}$. Hence, it is also possible to control the precision of the electric field estimation by changing the number of the modes and the number of the collected samples.

4.3.3 Tikhonov Regularisation

As previously commented, the usage of the Equation (4.12) revolves around the existence of the inverse of the moment matrix. Numerically, however, it is also important that such matrix is not even near-singular, which can be avoided by preventing that two or more modes become too close to each other. Despite the fact that the modes are linearly independent, it is impossible to ensure those conditions for a finite number of chosen directions. It is mainly caused by the fact that the spatial frequency of the spherical harmonics increases indefinitely as more modes are considered in the regression. Hence, in practice, N_k and, therefore, k are bounded from above.

Such difficulty can be detected whenever the covariance of the parameters, the main diagonal of $\mathbf{P}_k$, is sharply increased by the addition of modes, which is usually associated to an overfitting of the model over the samples. The most common workaround for this issue is to consider an estimator on the form

$$\widehat{\mathbf{q}}_k = \left[\boldsymbol{\Upsilon}_k^{\mathrm{H}} \boldsymbol{\Upsilon}_k + \mathbf{A}\right]^{-1} \cdot \boldsymbol{\Upsilon}_k^{\mathrm{H}} \widetilde{\mathbf{E}} \tag{4.20}$$

where the square matrix $\mathbf{A}$ must be positive definite to ensure that $\boldsymbol{\Upsilon}_k^{\mathrm{H}} \boldsymbol{\Upsilon}_k + \mathbf{A}$ can be inverted. Hence, it is natural to consider a matrix $\boldsymbol{\Lambda} \in \mathbb{C}^{d \times 2N_k}$, with an arbitrary number of rows d, and define $\mathbf{A} = \boldsymbol{\Lambda}^{\mathrm{H}} \boldsymbol{\Lambda}$. This method is called Tihkonov Regularisation and the estimator, that can now be written as

$$\widehat{\mathbf{q}}_k = \left[\boldsymbol{\Upsilon}_k^{\mathrm{H}} \boldsymbol{\Upsilon}_k + \boldsymbol{\Lambda}^{\mathrm{H}} \boldsymbol{\Lambda}\right]^{-1} \cdot \boldsymbol{\Upsilon}_k^{\mathrm{H}} \widetilde{\mathbf{E}}, \tag{4.21}$$

minimises the quantity $\left(\widetilde{\mathbf{E}} - \widehat{\mathbf{E}}_k\right)^{\mathrm{H}} \left(\widetilde{\mathbf{E}} - \widehat{\mathbf{E}}_k\right) + \left(\boldsymbol{\Lambda}\widehat{\mathbf{q}}_k\right)^{\mathrm{H}} \left(\boldsymbol{\Lambda}\widehat{\mathbf{q}}_k\right)$, whose right term is related with the radiated power, as described in Equation (3.13), when $\boldsymbol{\Lambda} = \lambda \mathbf{I}$ for a scalar λ. Hence, it can be said that Tikhonov Regularisation minimises a trade-off between the residual energy and the radiated energy in each mode.

The statistical characteristics of this new estimator can be calculated as it has been done

[1] By using the property $\operatorname{tr}(AB) = \operatorname{tr}(BA)$.

in the last section. In fact,

$$\begin{aligned}\widehat{\mathbf{q}}_k &= \left[\boldsymbol{\Upsilon}_k^{\mathrm{H}}\boldsymbol{\Upsilon}_k + \boldsymbol{\Lambda}^{\mathrm{H}}\boldsymbol{\Lambda}\right]^{-1}\boldsymbol{\Upsilon}_k^{\mathrm{H}}\left(\boldsymbol{\Upsilon}_k\mathbf{q}_k + \boldsymbol{\epsilon}_k\right)\\ &= \left[\boldsymbol{\Upsilon}_k^{\mathrm{H}}\boldsymbol{\Upsilon}_k + \boldsymbol{\Lambda}^{\mathrm{H}}\boldsymbol{\Lambda}\right]^{-1}\left[\boldsymbol{\Upsilon}_k^{\mathrm{H}}\boldsymbol{\Upsilon}_k\mathbf{q}_k + \boldsymbol{\Upsilon}_k^{\mathrm{H}}\boldsymbol{\epsilon}_k\right]\\ &= \left[\boldsymbol{\Upsilon}_k^{\mathrm{H}}\boldsymbol{\Upsilon}_k + \boldsymbol{\Lambda}^{\mathrm{H}}\boldsymbol{\Lambda}\right]^{-1}\left[\left(\boldsymbol{\Upsilon}_k^{\mathrm{H}}\boldsymbol{\Upsilon}_k + \boldsymbol{\Lambda}^{\mathrm{H}}\boldsymbol{\Lambda}\right)\mathbf{q}_k - \boldsymbol{\Lambda}^{\mathrm{H}}\boldsymbol{\Lambda}\mathbf{q}_k + \boldsymbol{\Upsilon}_k^{\mathrm{H}}\boldsymbol{\epsilon}_k\right]\\ &= \mathbf{q}_k + \left[\boldsymbol{\Upsilon}_k^{\mathrm{H}}\boldsymbol{\Upsilon}_k + \boldsymbol{\Lambda}^{\mathrm{H}}\boldsymbol{\Lambda}\right]^{-1}\left[\boldsymbol{\Upsilon}_k^{\mathrm{H}}\boldsymbol{\epsilon}_k - \boldsymbol{\Lambda}^{\mathrm{H}}\boldsymbol{\Lambda}\mathbf{q}_k\right].\end{aligned} \tag{4.22}$$

Hence, the expected value of is now given by

$$\langle\widehat{\mathbf{q}}_k\rangle = \mathbf{q}_k + \left[\boldsymbol{\Upsilon}_k^{\mathrm{H}}\boldsymbol{\Upsilon}_k + \boldsymbol{\Lambda}^{\mathrm{H}}\boldsymbol{\Lambda}\right]^{-1}\left[\boldsymbol{\Upsilon}_k^{\mathrm{H}}\boldsymbol{\epsilon}_k^{\mathrm{tru}} - \boldsymbol{\Lambda}^{\mathrm{H}}\boldsymbol{\Lambda}\mathbf{q}_k\right], \tag{4.23}$$

from which one concludes that such estimator is also biased, but this time such bias can not be directly controlled by just increasing the number of modes. Furthermore, the new covariance matrix can be calculated by noting that

$$\widehat{\mathbf{q}}_k - \langle\widehat{\mathbf{q}}_k\rangle = \left[\boldsymbol{\Upsilon}_k^{\mathrm{H}}\boldsymbol{\Upsilon}_k + \boldsymbol{\Lambda}^{\mathrm{H}}\boldsymbol{\Lambda}\right]^{-1}\boldsymbol{\Upsilon}_k^{\mathrm{H}}\boldsymbol{\epsilon}^{\mathrm{mea}}. \tag{4.24}$$

Thus,

$$\mathbf{P}_k = \left[\boldsymbol{\Upsilon}_k^{\mathrm{H}}\boldsymbol{\Upsilon}_k + \boldsymbol{\Lambda}^{\mathrm{H}}\boldsymbol{\Lambda}\right]^{-1}\boldsymbol{\Upsilon}_k^{\mathrm{H}}\boldsymbol{\Upsilon}_k\left[\boldsymbol{\Upsilon}_k^{\mathrm{H}}\boldsymbol{\Upsilon}_k + \boldsymbol{\Lambda}^{\mathrm{H}}\boldsymbol{\Lambda}\right]^{-1}\sigma^2. \tag{4.25}$$

With this last result, it becomes clear that comparing the performance of the regularisation for the whole set of $\boldsymbol{\Gamma}$ possibilities would be quite sophisticated from the mathematical standpoint. Such comparison, however, shall further be done numerically for a few chosen of $\boldsymbol{\Lambda} = \lambda\mathbf{I}$. On this matter, it is worth saying that even though $\boldsymbol{\Lambda}$ introduces several new control parameters that might be tuned to improve the estimation results, it is most commonly adopted $\boldsymbol{\Lambda} = \lambda\mathbf{I}$ for simplicity. By doing this, the bias and the covariance of $\widehat{\mathbf{q}}_k$ become

$$\begin{aligned}\mathrm{bias}\left(\widehat{\mathbf{q}}_k\right) &= \left[\boldsymbol{\Upsilon}_k^{\mathrm{H}}\boldsymbol{\Upsilon}_k + |\lambda|^2\mathbf{I}\right]^{-1}\left[\boldsymbol{\Upsilon}_k^{\mathrm{H}}\boldsymbol{\epsilon}_k^{\mathrm{tru}} - |\lambda|^2\mathbf{q}_k\right]\\ &= \left[\boldsymbol{\Upsilon}_k^{\mathrm{H}}\boldsymbol{\Upsilon}_k + |\lambda|^2\mathbf{I}\right]^{-1}\boldsymbol{\Upsilon}_k^{\mathrm{H}}\boldsymbol{\epsilon}_k^{\mathrm{tru}} - \left[\boldsymbol{\Upsilon}_k^{\mathrm{H}}\boldsymbol{\Upsilon}_k + |\lambda|^2\mathbf{I}\right]^{-1}|\lambda|^2\mathbf{q}_k\\ &= \left[\boldsymbol{\Upsilon}_k^{\mathrm{H}}\boldsymbol{\Upsilon}_k + |\lambda|^2\mathbf{I}\right]^{-1}\boldsymbol{\Upsilon}_k^{\mathrm{H}}\boldsymbol{\epsilon}_k^{\mathrm{tru}} - \left[\frac{1}{|\lambda|^2}\boldsymbol{\Upsilon}_k^{\mathrm{H}}\boldsymbol{\Upsilon}_k + \mathbf{I}\right]^{-1}\mathbf{q}_k\end{aligned} \tag{4.26}$$

and

$$\mathbf{P}_k = \left[\boldsymbol{\Upsilon}_k^{\mathrm{H}}\boldsymbol{\Upsilon}_k + |\lambda|^2\mathbf{I}\right]^{-1}\boldsymbol{\Upsilon}_k^{\mathrm{H}}\boldsymbol{\Upsilon}_k\left[\boldsymbol{\Upsilon}_k^{\mathrm{H}}\boldsymbol{\Upsilon}_k + |\lambda|^2\mathbf{I}\right]^{-1}\sigma^2. \tag{4.27}$$

The above results make it clear that high values of $|\lambda|^2$ increases the precision of the estimator as $\lim_{|\lambda|^2\to\infty}\mathbf{P}_k = \mathbf{0}$, while the accuracy decreases as $\lim_{|\lambda|^2\to\infty}\mathrm{bias}\left(\widehat{\mathbf{q}}_k\right) = \mathbf{q}_k$, implying that $\widehat{\mathbf{q}}_k \to \mathbf{0}$. This result is in accordance with the sole minimisation of $\widehat{\mathbf{q}}_k^{\mathrm{H}}\widehat{\mathbf{q}}_k$, as expected. Hence, it can be said that $|\lambda|^2$ controls the balance between precision and accuracy.

4.4 Mode-Recursive Estimation Algorithm

Considering the statistical limitations of the estimator in Equation (4.21) discussed in the last section, this work proposes a method, inspired by the algorithm behind the Kalman Filter, for estimating the mode coefficients $\mathbf{q}_k$ where precision and accuracy can both be controlled by increasing the number of modes. This sections is dedicated to document such method, which is synthesised in a mode-recursive algorithm instead of a single equation as in the batch estimation.

In order to introduce the main idea of the method, assume that an estimator $\widehat{\mathbf{q}}_k$ and its covariance $\mathbf{P}_k$ are available beforehand and such information must be used to increase the number of modes by constructing a new estimator $\widehat{\mathbf{q}}_{k+1}$ with covariance $\mathbf{P}_{k+1}$. At first, let ΔN_{k+1} denote the number of added modes, which can be computed by using Equation (4.3) as

$$\Delta N_{k+1} = N_{k+1} - N_k = 2k + 3. \tag{4.28}$$

Intuitively, the most natural guess for $\widehat{\mathbf{q}}_{k+1}$ and $\mathbf{P}_{k+1}$ would have the form

$$\widehat{\mathbf{q}}_{k+1} = \begin{bmatrix} \widehat{\mathbf{q}}_k \\ \Delta\widehat{\mathbf{q}}_{k+1} \end{bmatrix} \quad \text{and} \quad \mathbf{P}_{k+1} = \begin{bmatrix} \mathbf{P}_k & \mathbf{0} \\ \mathbf{0}^{\mathrm{T}} & \Delta\mathbf{P}_{k+1} \end{bmatrix}, \tag{4.29}$$

where $\Delta\widehat{\mathbf{q}}_{k+1} \in \mathbb{C}^{2\Delta N_{k+1}\times 1}$ is a guess that must be made on the new coefficients while its covariance $\Delta\mathbf{P}_{k+1} = \operatorname{cov}\left(\Delta\widehat{\mathbf{q}}_{k+1}\right) \in \mathbb{C}^{2\Delta N_{k+1}\times 2\Delta N_{k+1}}$ shall be seen as measure of the uncertainty of such guess.

As a first thought, it could be said that the guess $\widehat{\mathbf{q}}_{k+1}$ in Equation (4.29) is a rough estimation since the introduction of new modes should not add more energy, but redistribute it among the old and the new modes. On the other hand, if the energy acquired by the new modes is low enough if compared with the total, hence implying that they could be neglected, such could then be considered good estimator for the mode coefficients.

The quality of $\widehat{\mathbf{q}}_{k+1}$ must, of course, be evaluated by analysing the residual of the electric field it predicts. With this in mind, consider the definitions $\widehat{\mathbf{E}}_{k+1} = \boldsymbol{\Upsilon}_{k+1}\widehat{\mathbf{q}}_{k+1}$ and $\mathbf{r}_{k+1} = \widetilde{\mathbf{E}} - \widehat{\mathbf{E}}_{k+1}$, from which a correction to $\widehat{\mathbf{q}}_{k+1}$ might be designed as

$$\widehat{\mathbf{q}}^{+}_{k+1} = \widehat{\mathbf{q}}_{k+1} + \mathbf{K}_{k+1}\mathbf{r}_{k+1}, \tag{4.30}$$

where the superscript + will be used to denote an estimator that has been corrected. In contrast, the superscript − shall also be used from now on to denote a variable before its correction. Once the corrected estimator $\widehat{\mathbf{q}}^{+}_{k+1}$ has been obtained, a new prediction $\widehat{\mathbf{E}}^{+}_{k+1} = \boldsymbol{\Upsilon}_{k+1}\widehat{\mathbf{q}}^{+}_{k+1}$ and its residual $\mathbf{r}^{+}_{k+1}$ become available.

About the above equation, it is interesting to think that each row of the gain matrix $\mathbf{K}_{k+1} \in \mathbb{C}^{2N_{k+1}\times 2M}$, which is commonly known as Kalman gain, weighs the residuals and corrects the corresponding value in the guess. Thus, a low residual implies low correction, meaning that guess has some quality, while a high residual implies high correction on the guess. Such

nice ideas involving $\mathbf{K}_{k+1}$ naturally lead to the question on how it should be chosen, which is answered in the next subsection.

With the intention of synthesising the algorithm that has been designed so far, consider

$$\widehat{\mathbf{q}}_{k+1}^{-} = \mathbf{F}_{k+1}\widehat{\mathbf{q}}_{k}^{+} + \mathbf{G}_{k+1}\Delta\widehat{\mathbf{q}}_{k+1} \qquad \text{(Mode Coeff. Propagation)}$$

$$\mathbf{P}_{k+1}^{-} = \mathbf{F}_{k+1}\mathbf{P}_{k}^{+}\mathbf{F}_{k+1}^{\mathrm{T}} + \mathbf{G}_{k+1}\Delta\mathbf{P}_{k+1}\mathbf{G}_{k+1}^{\mathrm{T}} \qquad \text{(Covariance Propagation)}$$

$$\widehat{\mathbf{E}}_{k+1}^{-} = \boldsymbol{\Upsilon}_{k+1}\widehat{\mathbf{q}}_{k+1}^{-} \qquad (A\ \textit{priori}\ \text{estimate})$$

$$\mathbf{r}_{k+1}^{-} = \widetilde{\mathbf{E}} - \widehat{\mathbf{E}}_{k+1}^{-} \qquad \text{(Innovation)}$$

$$\widehat{\mathbf{q}}_{k+1}^{+} = \widehat{\mathbf{q}}_{k+1}^{-} + \mathbf{K}_{k+1}\mathbf{r}_{k+1}^{-} \qquad \text{(Mode Coeff. Correction)}$$

$$\widehat{\mathbf{E}}_{k+1}^{+} = \boldsymbol{\Upsilon}_{k+1}\widehat{\mathbf{q}}_{k+1}^{+} \qquad (A\ \textit{posteriori}\ \text{estimate})$$

$$\mathbf{r}_{k+1}^{+} = \widetilde{\mathbf{E}} - \widehat{\mathbf{E}}_{k+1}^{+} \qquad \text{(Residual)}$$

where the auxiliary matrices

$$\mathbf{F}_{k+1} = \begin{bmatrix} \mathbf{I}_{2N_k} \\ \mathbf{0}_{2\Delta N_{k+1}\times 2N_k} \end{bmatrix} \quad \text{and} \quad \mathbf{G}_{k+1} = \begin{bmatrix} \mathbf{0}_{2N_k\times 2\Delta N_{k+1}} \\ \mathbf{I}_{2\Delta N_{k+1}} \end{bmatrix} \tag{4.31}$$

are defined to better support the some calculations.

4.4.1 Correction of the Covariance

As usual, the process of calculating the covariance matrix begins with the determination of the auxiliary quantity

$$\widehat{\mathbf{q}}_{k+1}^{+} - \left\langle \widehat{\mathbf{q}}_{k+1}^{+} \right\rangle = \widehat{\mathbf{q}}_{k+1}^{-} - \left\langle \widehat{\mathbf{q}}_{k+1}^{-} \right\rangle + \mathbf{K}_{k+1}\Big(\mathbf{r}_{k+1}^{-} - \left\langle \mathbf{r}_{k+1}^{-} \right\rangle \Big). \tag{4.32}$$

Since the above term involves the residual, it will be useful write it in the form

$$\begin{aligned} \mathbf{r}_{k+1}^{-} &= \widetilde{\mathbf{E}} - \widehat{\mathbf{E}}_{k+1}^{-} \\ &= \boldsymbol{\Upsilon}_{k+1}\mathbf{q}_{k+1} + \boldsymbol{\epsilon}_{k+1} - \boldsymbol{\Upsilon}_{k+1}\widehat{\mathbf{q}}_{k+1}^{-} \\ &= -\boldsymbol{\Upsilon}_{k+1}\Big(\widehat{\mathbf{q}}_{k+1}^{-} - \mathbf{q}_{k+1} \Big) + \boldsymbol{\epsilon}_{k+1}, \end{aligned} \tag{4.33}$$

from where it can be seen that its expected value is simply given by

$$\left\langle \mathbf{r}_{k+1}^{-} \right\rangle = -\boldsymbol{\Upsilon}_{k+1}\Big(\left\langle \widehat{\mathbf{q}}_{k+1}^{-} \right\rangle - \mathbf{q}_{k+1} \Big) + \boldsymbol{\epsilon}_{k+1}^{\mathrm{tru}}. \tag{4.34}$$

Hence,

$$\mathbf{r}_{k+1}^{-} - \left\langle \mathbf{r}_{k+1}^{-} \right\rangle = -\boldsymbol{\Upsilon}_{k+1}\Big(\widehat{\mathbf{q}}_{k+1}^{-} - \left\langle \widehat{\mathbf{q}}_{k+1}^{-} \right\rangle \Big) + \boldsymbol{\epsilon}^{\mathrm{mea}} \tag{4.35}$$

and

$$\widehat{\mathbf{q}}_{k+1}^{+} - \left\langle \widehat{\mathbf{q}}_{k+1}^{+} \right\rangle = \widehat{\mathbf{q}}_{k+1}^{-} - \left\langle \widehat{\mathbf{q}}_{k+1}^{-} \right\rangle + \mathbf{K}_{k+1}\left(-\boldsymbol{\Upsilon}_{k+1}\Big(\widehat{\mathbf{q}}_{k+1}^{-} - \left\langle \widehat{\mathbf{q}}_{k+1}^{-} \right\rangle \Big) + \boldsymbol{\epsilon}^{\mathrm{mea}} \right). \tag{4.36}$$

Let $\mathbf{C}_{k+1}^{-} = \left\langle \left[\widehat{\mathbf{q}}_{k+1}^{-} - \left\langle \widehat{\mathbf{q}}_{k+1}^{-} \right\rangle\right] \boldsymbol{\epsilon}^{\mathrm{meaH}} \right\rangle$ and consider the corrected covariance $\mathbf{P}_{k+1}^{+}$ calculated as follows

$$
\begin{aligned}
\mathbf{P}_{k+1}^{+} &= \left\langle \left[\widehat{\mathbf{q}}_{k+1}^{+} - \left\langle \widehat{\mathbf{q}}_{k+1}^{+} \right\rangle\right] \left[\widehat{\mathbf{q}}_{k+1}^{+} - \left\langle \widehat{\mathbf{q}}_{k+1}^{+} \right\rangle\right]^{\mathrm{H}} \right\rangle \\
&= \left\langle \left[\widehat{\mathbf{q}}_{k+1}^{-} - \left\langle \widehat{\mathbf{q}}_{k+1}^{-} \right\rangle\right] \left[\widehat{\mathbf{q}}_{k+1}^{-} - \left\langle \widehat{\mathbf{q}}_{k+1}^{-} \right\rangle\right]^{\mathrm{H}} \right\rangle \\
&\quad + \mathbf{K}_{k+1} \left[- \boldsymbol{\Upsilon}_{k+1} \left\langle \left[\widehat{\mathbf{q}}_{k+1}^{-} - \left\langle \widehat{\mathbf{q}}_{k+1}^{-} \right\rangle\right] \left[\widehat{\mathbf{q}}_{k+1}^{-} - \left\langle \widehat{\mathbf{q}}_{k+1}^{-} \right\rangle\right]^{\mathrm{H}} \right\rangle + \left\langle \boldsymbol{\epsilon}^{\mathrm{mea}} \left[\widehat{\mathbf{q}}_{k+1}^{-} - \left\langle \widehat{\mathbf{q}}_{k+1}^{-} \right\rangle\right]^{\mathrm{H}} \right\rangle \right] \\
&\quad + \left[- \left\langle \left[\widehat{\mathbf{q}}_{k+1}^{-} - \left\langle \widehat{\mathbf{q}}_{k+1}^{-} \right\rangle\right] \left[\widehat{\mathbf{q}}_{k+1}^{-} - \left\langle \widehat{\mathbf{q}}_{k+1}^{-} \right\rangle\right]^{\mathrm{H}} \right\rangle \boldsymbol{\Upsilon}_{k+1}^{\mathrm{H}} + \left\langle \left[\widehat{\mathbf{q}}_{k+1}^{-} - \left\langle \widehat{\mathbf{q}}_{k+1}^{-} \right\rangle\right] \boldsymbol{\epsilon}^{\mathrm{meaH}} \right\rangle \right] \mathbf{K}_{k+1}^{\mathrm{H}} \\
&\quad + \mathbf{K}_{k+1} \left\langle \left(-\boldsymbol{\Upsilon}_{k+1} \left(\widehat{\mathbf{q}}_{k+1}^{-} - \left\langle \widehat{\mathbf{q}}_{k+1}^{-} \right\rangle \right) + \boldsymbol{\epsilon}^{\mathrm{mea}} \right) \left(-\boldsymbol{\Upsilon}_{k+1} \left(\widehat{\mathbf{q}}_{k+1}^{-} - \left\langle \widehat{\mathbf{q}}_{k+1}^{-} \right\rangle \right) + \boldsymbol{\epsilon}^{\mathrm{mea}} \right)^{\mathrm{H}} \right\rangle \mathbf{K}_{k+1}^{\mathrm{H}} \\
&= \mathbf{P}_{k+1}^{-} + \mathbf{K}_{k+1} \left[-\boldsymbol{\Upsilon}_{k+1} \mathbf{P}_{k+1}^{-} + \mathbf{C}_{k+1}^{-\mathrm{H}} \right] + \left[-\mathbf{P}_{k+1}^{-} \boldsymbol{\Upsilon}_{k+1}^{\mathrm{H}} + \mathbf{C}_{k+1}^{-} \right] \mathbf{K}_{k+1}^{\mathrm{H}} \\
&\quad + \mathbf{K}_{k+1} \left[\boldsymbol{\Upsilon}_{k+1} \mathbf{P}_{k+1}^{-} \boldsymbol{\Upsilon}_{k+1}^{\mathrm{H}} + \mathbf{R} - \boldsymbol{\Upsilon}_{k+1} \mathbf{C}_{k+1}^{-} - \mathbf{C}_{k+1}^{-\mathrm{H}} \boldsymbol{\Upsilon}_{k+1}^{\mathrm{H}} \right] \mathbf{K}_{k+1}^{\mathrm{H}}. \qquad (4.37)
\end{aligned}
$$

Ideally, the algorithm must be such that uncertainty of the parameters becomes smaller after each iteration, thus implying the estimator becomes better. Therefore, it is logical to require that $\mathrm{tr}\left(\mathbf{P}_{k+1}^{+}\right)$ becomes as small as it is possible. As explained in Section 4.A, such minimal trace exists under the assumption of positive definiteness of the leading term of the quadratic form, from which it is shown, at Equation (4.58), that the optimal gain is given by

$$
\mathbf{K}_{k+1} = \left(\mathbf{P}_{k+1}^{-} \boldsymbol{\Upsilon}_{k+1}^{\mathrm{H}} - \mathbf{C}_{k+1}^{-}\right) \left(\boldsymbol{\Upsilon}_{k+1} \mathbf{P}_{k+1}^{-} \boldsymbol{\Upsilon}_{k+1}^{\mathrm{H}} + \mathbf{R} - \boldsymbol{\Upsilon}_{k+1} \mathbf{C}_{k+1}^{-} - \left(\boldsymbol{\Upsilon}_{k+1} \mathbf{C}_{k+1}^{-}\right)^{\mathrm{H}} \right)^{-1}. \qquad \text{(Kalman Gain)}
$$

Now, using the result stated at Equation (4.59), the optimal corrected covariance is written as

$$
\begin{aligned}
\mathbf{P}_{k+1}^{+} &= \mathbf{P}_{k+1}^{-} - \mathbf{K}_{k+1} \left(\mathbf{P}_{k+1}^{-} \boldsymbol{\Upsilon}_{k+1}^{\mathrm{H}} - \mathbf{C}_{k+1}^{-}\right)^{\mathrm{H}} \\
&= \left(\mathbf{I} - \mathbf{K}_{k+1} \boldsymbol{\Upsilon}_{k+1}\right) \mathbf{P}_{k+1}^{-} - \mathbf{K}_{k+1} \mathbf{C}_{k+1}^{-\mathrm{H}}. \qquad \text{(Covariance Correction)}
\end{aligned}
$$

4.4.2 Covariance Between the Estimator and the Measurement Noise

Since the auxiliary matrix $\mathbf{C}_{k+1}^{-}$ became necessary to calculate the Kalman gain in Kalman Gain and, posteriorly, the covariance correction in Covariance Correction, it must also be calculated in each iteration. This subsection is then intended to provide propagating equations for that matrix.

Initially, it is reasonable to assume that guesses $\Delta\widehat{\mathbf{q}}_{k+1}$ and the measurement noise are statistical uncorrelated, *i.e.*, $\left\langle \Delta\widehat{\mathbf{q}}_{k+1} \boldsymbol{\epsilon}^{\mathrm{meaH}} \right\rangle = \mathbf{0}$. From this assumption and the Mode Coeff.

Propagation, it can be written that

$$\begin{aligned}\mathbf{C}_{k+1}^{-} &= \left\langle \left[\widehat{\mathbf{q}}_{k+1}^{-} - \left\langle \widehat{\mathbf{q}}_{k+1}^{-} \right\rangle \right] \boldsymbol{\epsilon}^{\mathrm{meaH}} \right\rangle \\ &= \mathbf{F}_{k+1} \left\langle \left[\widehat{\mathbf{q}}_{k}^{+} - \left\langle \widehat{\mathbf{q}}_{k}^{+} \right\rangle \right] \boldsymbol{\epsilon}^{\mathrm{meaH}} \right\rangle \\ &= \mathbf{F}_{k+1}\mathbf{C}_{k}^{+}. \qquad \text{(Auxiliary Cov. Propagation)}\end{aligned}$$

On the other hand, the Equation (4.36), that is now better rewritten as

$$\widehat{\mathbf{q}}_{k+1}^{+} - \left\langle \widehat{\mathbf{q}}_{k+1}^{+} \right\rangle = \left(\mathbf{I} - \mathbf{K}_{k+1}\boldsymbol{\Upsilon}_{k+1}\right)\left(\widehat{\mathbf{q}}_{k+1}^{-} - \left\langle \widehat{\mathbf{q}}_{k+1}^{-} \right\rangle\right) + \mathbf{K}_{k+1}\boldsymbol{\epsilon}^{\mathrm{mea}}, \tag{4.38}$$

can once again be used to calculate the correction $\mathbf{C}_{k+1}^{+}$ as follows

$$\begin{aligned}\mathbf{C}_{k+1}^{+} &= \left\langle \left[\widehat{\mathbf{q}}_{k+1}^{+} - \left\langle \widehat{\mathbf{q}}_{k+1}^{+} \right\rangle \right] \boldsymbol{\epsilon}^{\mathrm{meaH}} \right\rangle \\ &= \left(\mathbf{I} - \mathbf{K}_{k+1}\boldsymbol{\Upsilon}_{k+1}\right)\left\langle \left[\widehat{\mathbf{q}}_{k+1}^{-} - \left\langle \widehat{\mathbf{q}}_{k+1}^{-} \right\rangle \right] \boldsymbol{\epsilon}^{\mathrm{meaH}} \right\rangle + \mathbf{K}_{k+1}\left\langle \boldsymbol{\epsilon}^{\mathrm{mea}}\boldsymbol{\epsilon}^{\mathrm{meaH}} \right\rangle \\ &= \left(\mathbf{I} - \mathbf{K}_{k+1}\boldsymbol{\Upsilon}_{k+1}\right)\mathbf{C}_{k+1}^{-} + \mathbf{K}_{k+1}\mathbf{R} \qquad \text{(Auxiliary Cov. Correction)}\end{aligned}$$

At this moment, it is worth highlighting once again that the convergence of the algorithm depends on the matrix $\boldsymbol{\Upsilon}_{k+1}\mathbf{P}_{k+1}^{-}\boldsymbol{\Upsilon}_{k+1}^{\mathrm{H}} + \mathbf{R}$ has a greater spectral radius than $\boldsymbol{\Upsilon}_{k+1}\mathbf{C}_{k+1}^{-} + \left(\boldsymbol{\Upsilon}_{k+1}\mathbf{C}_{k+1}^{-}\right)^{\mathrm{H}}$. Nevertheless, checking if this condition is satisfied in each iteration would certainly become troublesome due to a high increasing in computational resources and in the execution time. As a workaround, the convergence of the residual energy alongside the convergence of the trace of the corrected covariance can be used as an evidence of regression performance.

4.4.3 Bias Propagation and Correction

Even though the bias can not be observed, it is possible to infer some properties about its convergence. Initially, with the reasonable assumption of an unbiased guess, *i.e.*, bias $\left(\Delta\widehat{\mathbf{q}}_{k+1}\right) = 0$, it can be easily proven that

$$\mathrm{bias}\left(\widehat{\mathbf{q}}_{k+1}^{-}\right) = \mathbf{F}_{k+1}\mathrm{bias}\left(\widehat{\mathbf{q}}_{k}^{+}\right) \tag{4.39}$$

$$\mathrm{bias}\left(\widehat{\mathbf{q}}_{k+1}^{+}\right) = \left(\mathbf{I} - \mathbf{K}_{k+1}\boldsymbol{\Upsilon}_{k+1}\right)\mathrm{bias}\left(\widehat{\mathbf{q}}_{k+1}^{-}\right) + \mathbf{K}_{k+1}\boldsymbol{\epsilon}_{k+1}^{\mathrm{tru}}. \tag{4.40}$$

It is interesting to notice the resemblance of the last equation to the Auxiliary Cov. Correction and to the Covariance Correction. Thus, if the algorithm converges, which is mostly characterised by $\mathbf{K}_{k+1} \to \mathbf{0}$ while the spectral radius of $\mathbf{I} - \mathbf{K}_{k+1}\boldsymbol{\Upsilon}_{k+1}$ is kept less than one, then the bias and the covariances would converge as well.

4.4.4 Algorithm Initialisation and Guessing Strategy

Since the proposed algorithm is recursive, it must have its parameters initialised. Although it is possible starting it at $k = 1$ with an initial guess like $\widehat{\mathbf{q}}_{1}^{+} = \mathbf{0}$ and a high value for $\mathbf{P}_1$, as it

is commonly done for parametric identifications, those choices would certainly lead to a poor performance with respect to the execution time and computational resources. It is also worth highlighting that each iteration would take longer than the previous one since the dimensions of the matrices involved in the regression increase as more modes are added.

In this scenario, the employment of the algorithm is constrained to an effective initialisation of its parameters. Such effectiveness can be achieved by using the batch regression for a minimal required number of modes. In fact, let k_0 denote the maximum initial degree of the mode coefficients. The initial parameters might hence be chosen by considering the Equations (4.21), (4.24) and (4.27) as follows

$$\widehat{\mathbf{q}}_{k_0}^{+} = \left[\boldsymbol{\Upsilon}_{k_0}^{\mathrm{H}}\boldsymbol{\Upsilon}_{k_0} + |\lambda|^2\,\mathbf{I}\right]^{-1}\boldsymbol{\Upsilon}_{k_0}^{\mathrm{H}}\widetilde{\mathbf{E}}, \tag{4.41}$$

$$\mathbf{C}_{k_0}^{+} = \left[\boldsymbol{\Upsilon}_{k_0}^{\mathrm{H}}\boldsymbol{\Upsilon}_{k_0} + |\lambda|^2\,\mathbf{I}\right]^{-1}\boldsymbol{\Upsilon}_{k_0}^{\mathrm{H}}\sigma^2, \tag{4.42}$$

$$\mathbf{P}_{k_0}^{+} = \left[\boldsymbol{\Upsilon}_{k_0}^{\mathrm{H}}\boldsymbol{\Upsilon}_{k_0} + |\lambda|^2\,\mathbf{I}\right]^{-1}\boldsymbol{\Upsilon}_{k_0}^{\mathrm{H}}\boldsymbol{\Upsilon}_{k_0}\left[\boldsymbol{\Upsilon}_{k_0}^{\mathrm{H}}\boldsymbol{\Upsilon}_{k_0} + |\lambda|^2\,\mathbf{I}\right]^{-1}\sigma^2. \tag{4.43}$$

A strategy for choosing the guesses, on the other hand, could be quite more subjective than choosing the initial parameters. For this task, it is worth remembering that as more modes are added, it is expected that they have less energy than the previous modes. Even for that reason, the certainty of this fact also grows at each iteration. Thus, reasonable choices for the guesses and their uncertainty would be

$$\Delta\widehat{\mathbf{q}}_{k+1} = \mathbf{0}_{2\Delta N_{k+1}\times 1}, \tag{4.44}$$

$$\Delta\mathbf{P}_{k+1} = \alpha_{k+1}\mathbf{I}_{2\Delta N_{k+1}}, \tag{4.45}$$

where positive constants in $\left\{\alpha_k\right\}_{k\in\mathbb{N}_{\leqslant k_0}}$ should form a monotonically decreasing sequence. It could be said that a natural and wise choice for those constants is $\alpha_{k+1} = \max\left(\operatorname{diag}\left(\mathbf{P}_k^{+}\right)\right)$.

4.4.5 Implementation

By considering the definitions and results that have been developed so far in the current and previous sections, the proposed algorithm is finally ready to be used. With this intention in mind, the block diagram shown in Figure 4.1 was created to better support the computational implementation of the algorithm.

In short, the diagram depicts the workflow that has been designed for one iteration and, therefore, it also works as an outline for this whole section. Moreover, it is interesting to compare it with a dynamical system where $\widehat{\mathbf{q}}^{+}$, $\mathbf{C}^{+}$ and $\mathbf{P}^{+}$ must be seen as an internal state, $\Delta\widehat{\mathbf{q}}$, $\Delta\mathbf{P}$ and $\widetilde{\mathbf{E}}$ would be the external inputs while the residual energy alongside the trace of the covariance would compose the outputs, which are particularly used as a metric to the quality of the regression.

About the computational resources, particular attention should be drawn to Regressors block, which not only serves several other blocks, but also grows accelerated since its number of

columns $2N_k$ quadratically depends on k. For that reason, before the usage of this algorithm, it is strongly encouraged that a maximum value $k_{\max}$ is defined and $\boldsymbol{\Upsilon}_{k_{\max}}$ is precompiled and locally stored in disk in order to save time. By doing this, each $\boldsymbol{\Upsilon}_k$ becomes nothing more than a slice of $\boldsymbol{\Upsilon}_{k_{\max}}$, hence it is enough to load the later before running the iteration. Still on this matter, it is worth stressing that the calculated regressor matrix does not depend on the electric field samples. So, it could be reused for different sets of samples, if they were collected at the same set of directions, which is often the case for tests performed in the same antenna but in different frequencies.

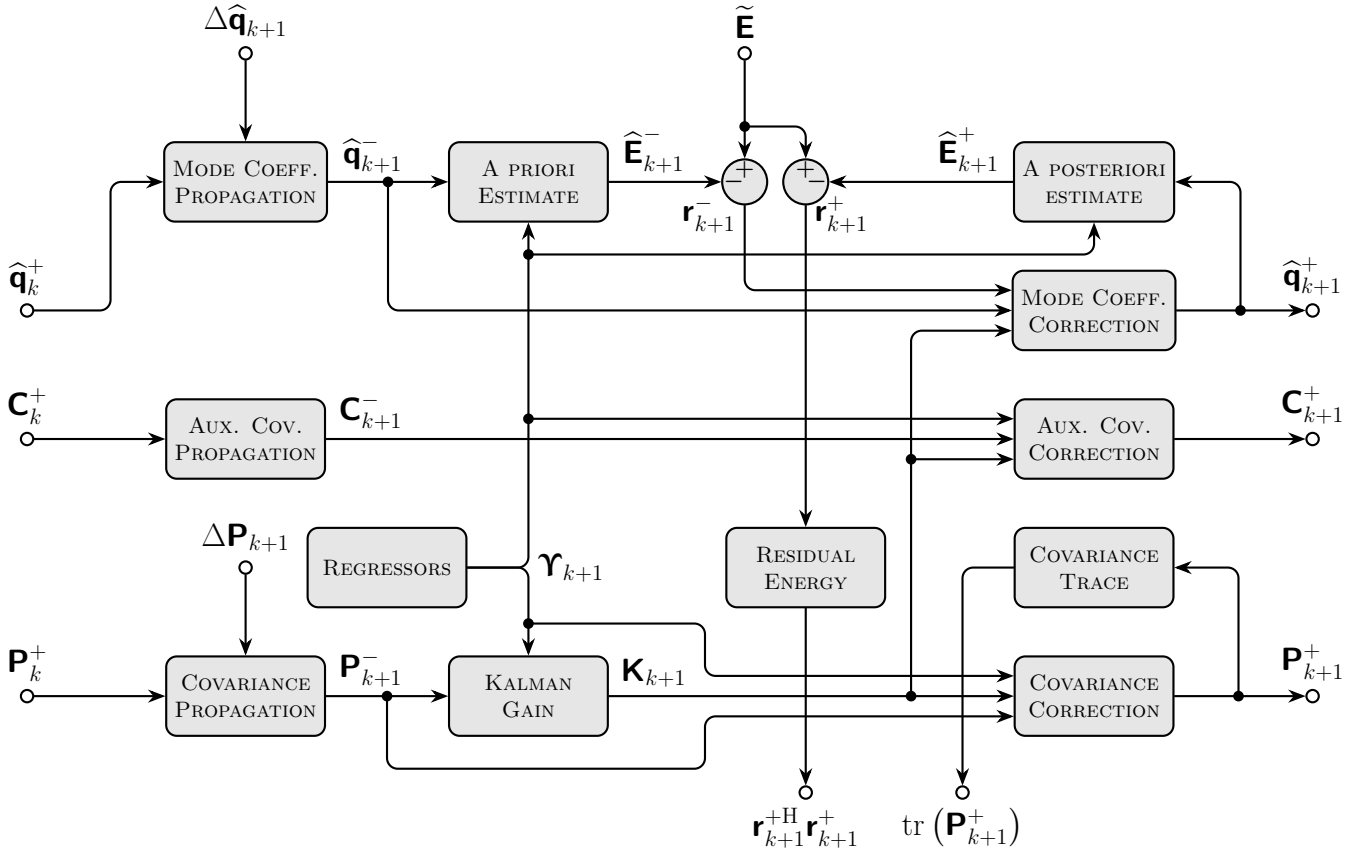

Figure 4.1: Block diagram describing the schematics of an iteration of the proposed regression algorithm. Each block corresponds to an equation previously described in this Chapter.

4.5 Results

The algorithm has been implemented and applied to a data set of collected electric field samples of a real antenna provided by the *Institut d'Electronique et des Technologies du Numérique* (IETR) of the University of Rennes. The data is composed by a collection of 61 tests performed at different frequencies, from 230 GHz to 290 GHz with step of 1 GHz, and at $M = 4900$ different directions (θ, ϕ) composing a grid where

$$(\theta, \phi) \in \Big\{\big(3.6^\circ \cdot i,\ 3.6^\circ \cdot (j-1)\big);\ i \in \mathbb{N}_{\leqslant 49} \wedge j \in \mathbb{N}_{\leqslant 100}\Big\}. \tag{4.46}$$

In order to evaluate the performance of the regressions methods, so they can be later compared to each other, two metrics were defined. The first is the Relative Residual Energy ρ_k given by

$$\rho_k = \frac{\left\|\widetilde{\mathbf{E}} - \widehat{\mathbf{E}}_k\right\|^2}{\left\|\widetilde{\mathbf{E}}\right\|^2} = \frac{\left(\widetilde{\mathbf{E}} - \widehat{\mathbf{E}}_k\right)^{\mathrm{H}}\left(\widetilde{\mathbf{E}} - \widehat{\mathbf{E}}_k\right)}{\widetilde{\mathbf{E}}^{\mathrm{H}}\widetilde{\mathbf{E}}}, \tag{4.47}$$

which measures how good the estimated mode coefficients are in explaining the collected samples. As it has already been commented in subsection 4.3.3, it is also important to evaluate the precision of the the estimator, which is made by checking the trace of its covariance matrix. Since the number of elements in the main diagonal of this matrix is linearly related to the number of modes, it makes better sense using the Normalised Variance per Mode ς_k, defined as

$$\varsigma_k = \frac{\mathrm{tr}\left(\mathbf{P}_k\right)}{N_k \cdot \sigma^2}, \tag{4.48}$$

as the indicator for the precision of the estimator. In order to analyse the behaviour of each regression, the metrics were applied for several values of k, even for batch methods. Moreover, since those behaviours are quite alike at different frequencies, the samples associated with frequency 260 GHz were taken as example and considered for the results.

The first presented result, which is shown in Figure 4.2 (mind the log scale for the metrics), regards the performance of the non-regularised batch method, *i.e.*, $|\lambda|^2 = 0$. It is worth noticing that both metrics decrease as more modes are added to regression, hence increasing its quality up to the mode $k = 50$, when an overfitting occurs. Such overfitting is highlighted by a sharply increased variance (or uncertainty), meaning the estimator is no longer reliable.

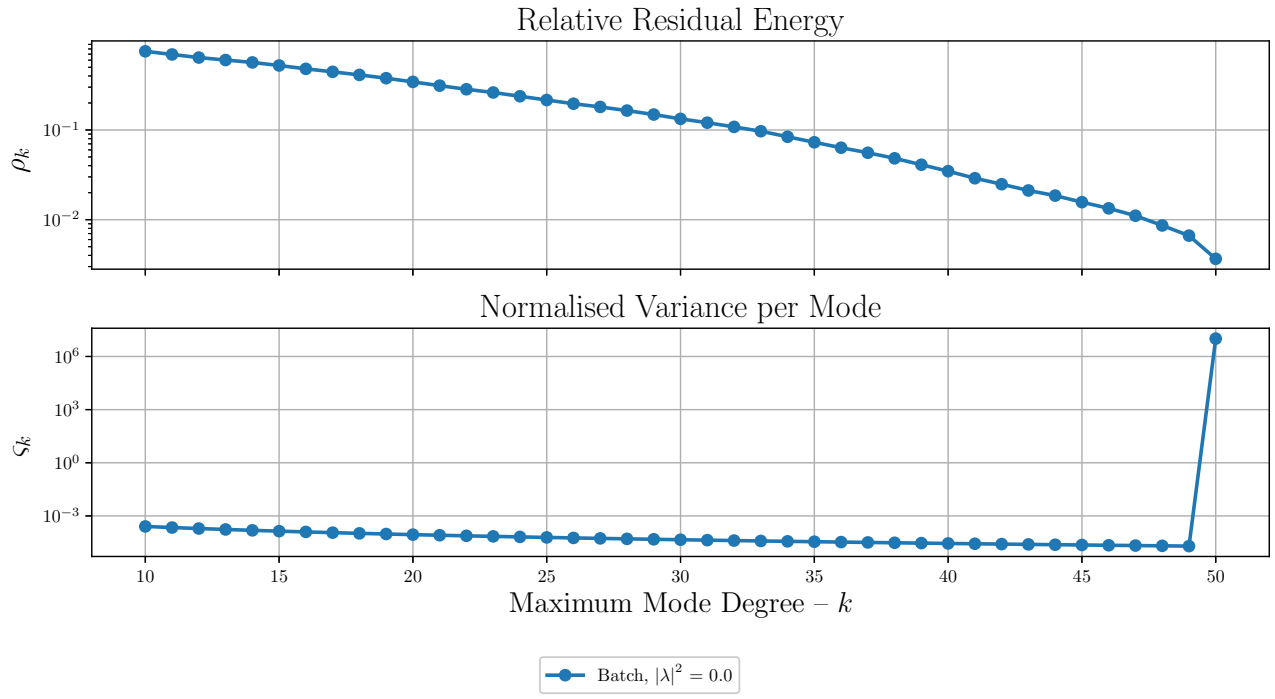

Figure 4.2: Performance of the batch regression without regularisation at 260 GHz. An overfitting occurs when $k = 50$ meaning that this regression method is only applicable up to $k = 49$.

The estimated coefficients can be visualised by considering the fraction of the radiated power (or signal energy, as it would be defined in Signal Processing) per mode as it is depicted in Figure 4.3. It must be noticed some slightly concentrated energy around $\ell = 50$ and $m = 0$, which are actually artefacts from the regression and are associated with the high uncertainty.

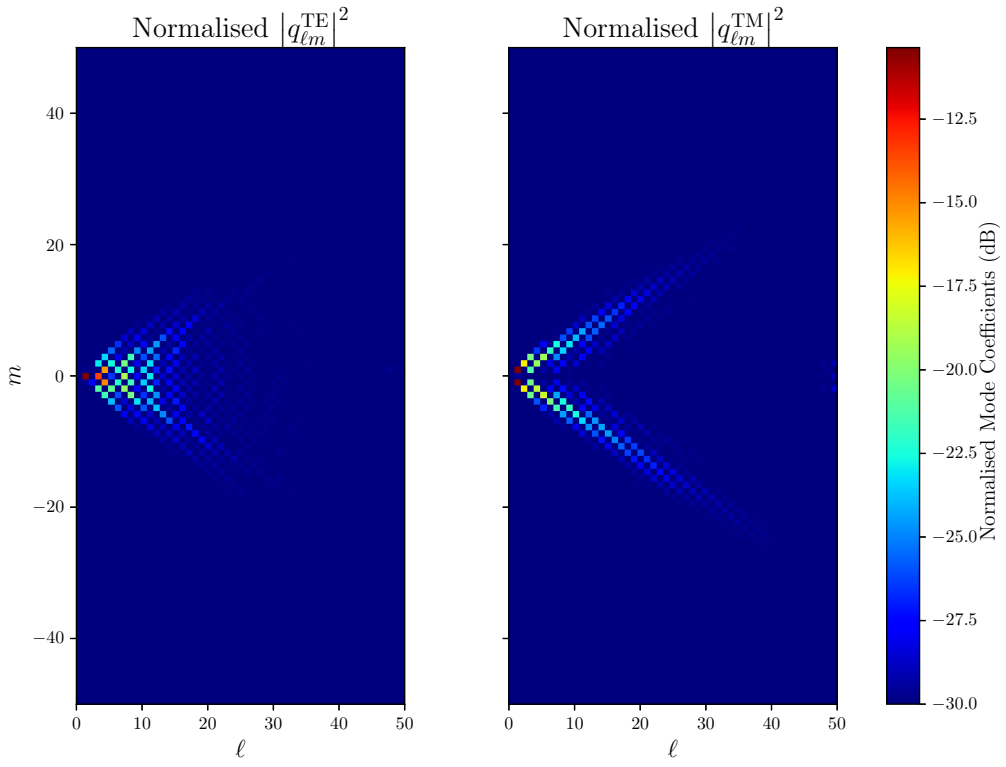

Figure 4.3: Energy distribution per mod at 260 GHz. Estimated using non-regularised batch regression method with $k = 50$.

At this point, it is worth comparing the last results with the regularised methods, as it shown in Figure 4.4. For regularisation parameters up around $|\lambda|^2 \approx 100$, the results are pretty much similar. Hence, it has been considered orders of magnitude greater or equal than 100. As it was expected, the relative residual energy becomes larger as $|\lambda|^2$ grows due to the also growing bias of the estimator. Additionally, even though the normalised variance per mode decreases, it must be noticed that such result is stepwise more related with the certainty that the parameters are able to minimise the radiated power than the residual energy itself, hence its increasing.

As result, the overfitting still occurs as artefacts still figure in the energy distribution, *cf*. Figures 4.5, 4.6 and 4.7, but it can no longer be detected through the mean variance per mode indicator. It is worth saying that those artefacts become even more accentuated, *i.e.*, they concentrate more energy, if a larger value for k is used.

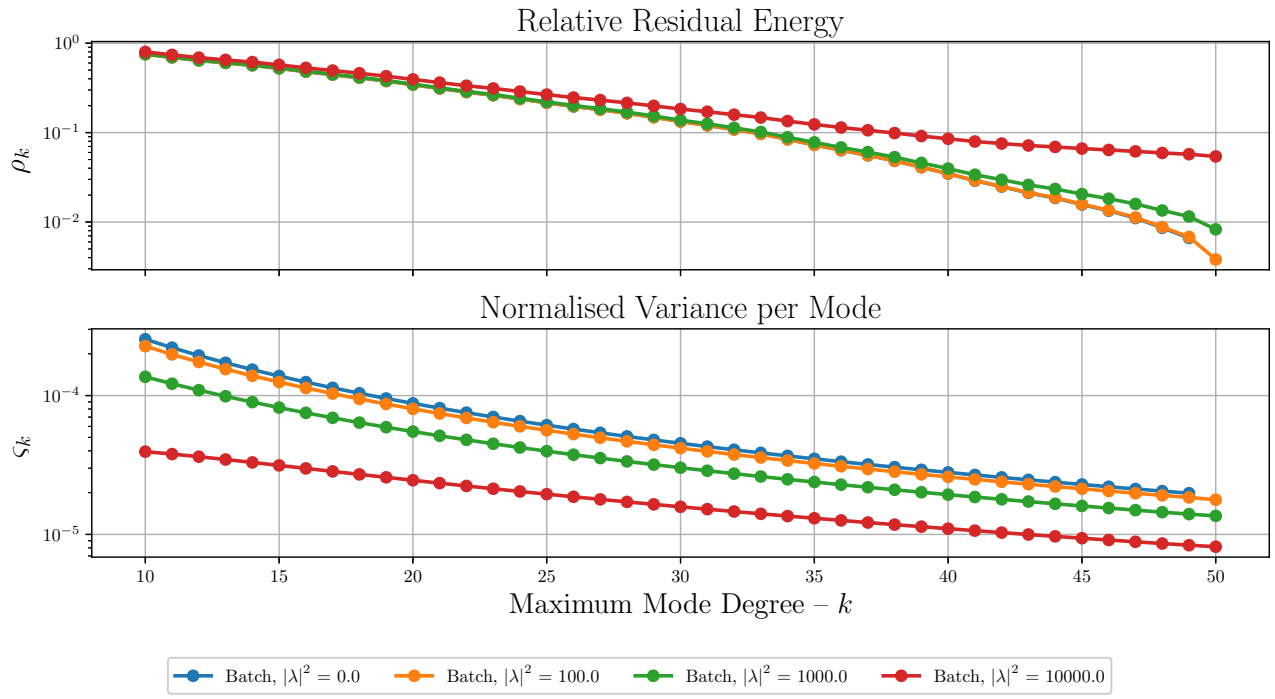

Figure 4.4: Comparison of the performance of the non-regularised and regularised batch regression methods.

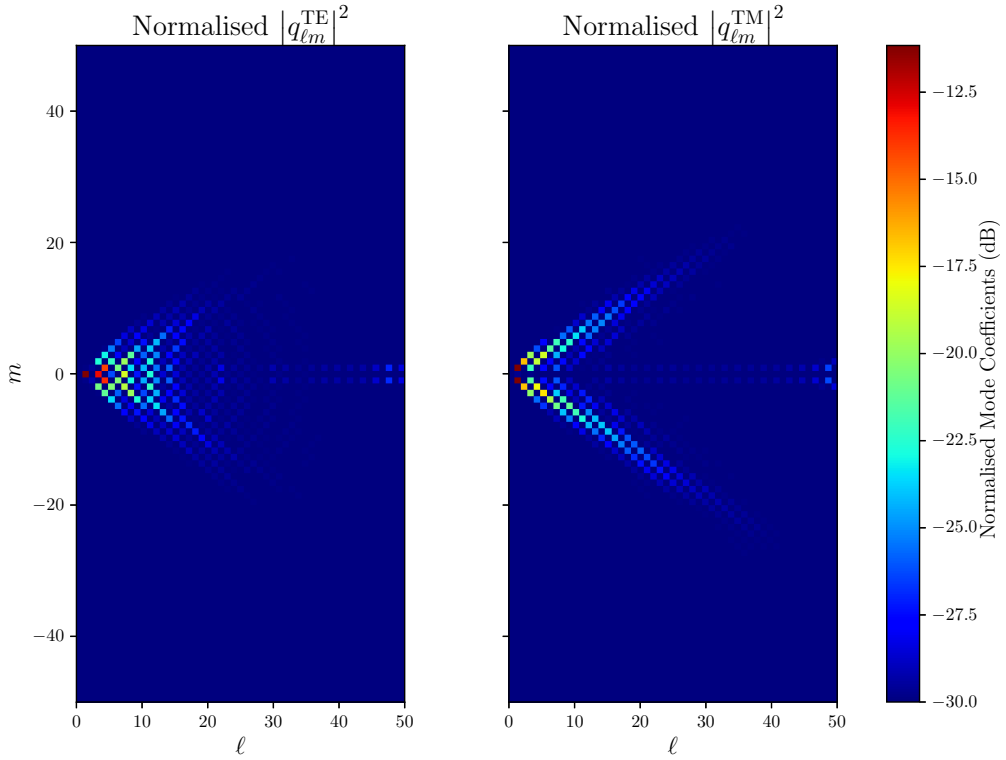

Figure 4.5: Energy distribution per mode at 260 GHz. Estimated using batch regularised regression method with $|\lambda|^2 = 100$ and $k = 50$.

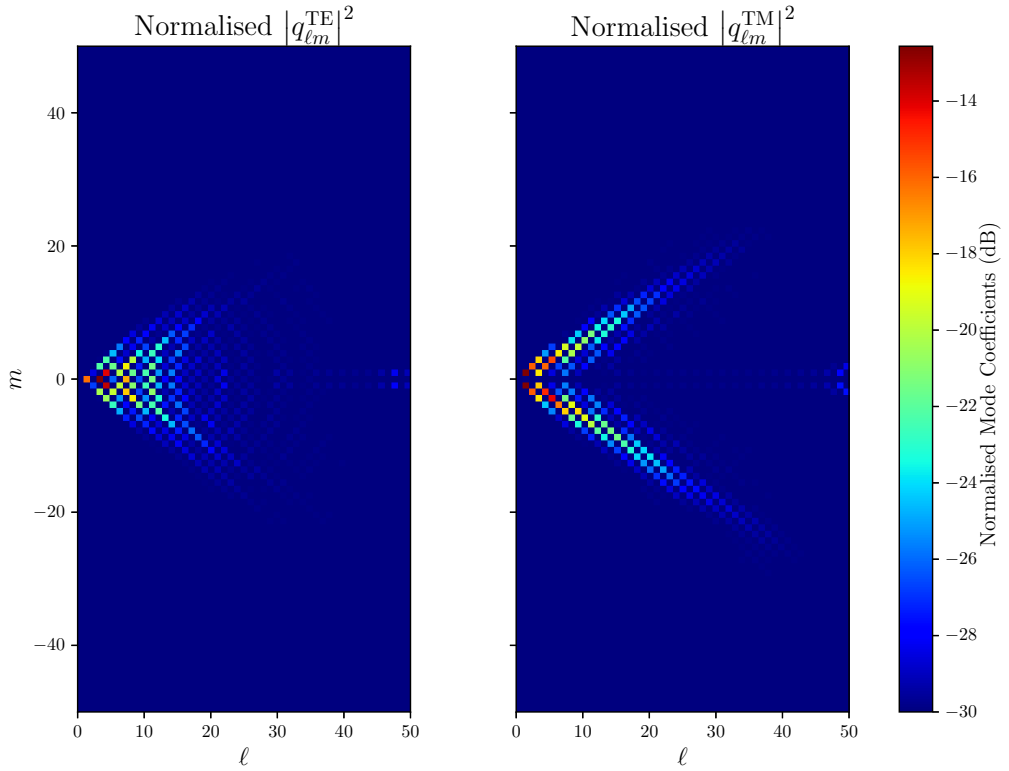

Figure 4.6: Energy Distribution per mode at 260 GHz. Estimated using batch regularised regression method with $|\lambda|^2 = 1000$ and $k = 50$.

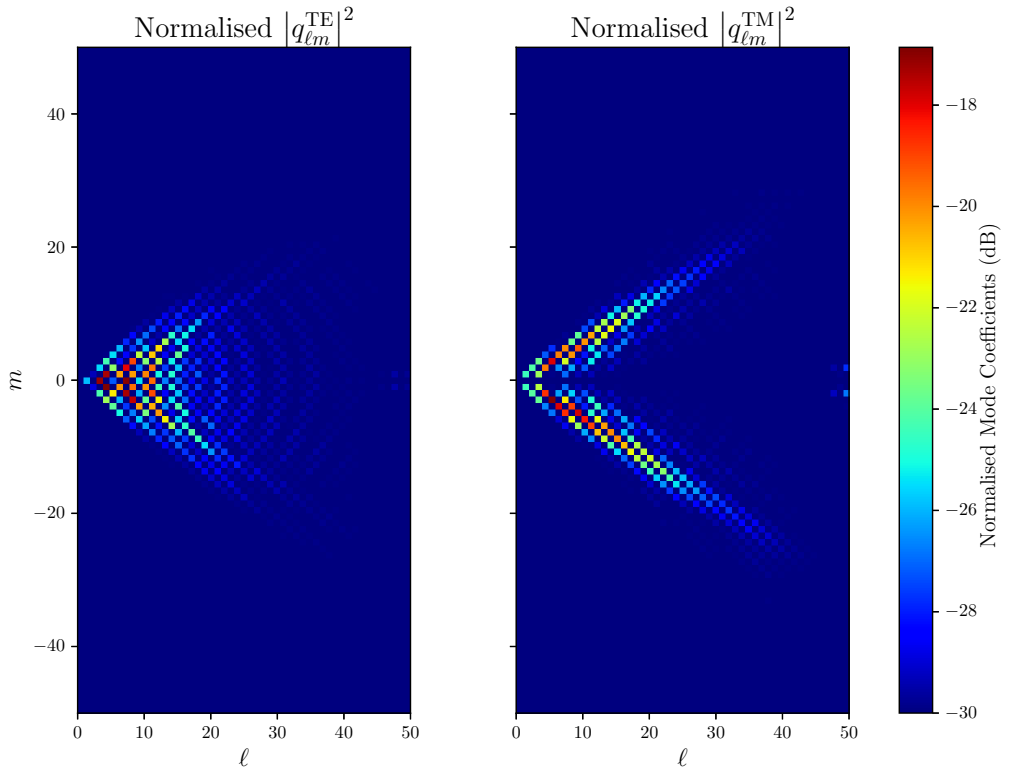

Figure 4.7: Energy Distribution per mode at 260 GHz. Estimated using batch regularised regression method with $|\lambda|^2 = 10000$ and $k = 50$.

In order to finally exemplify the usage of the recursive method, consider an initialisation of the parameters using the non-regularised batch method with $k_0 = 30$. Hence, Equations (4.41), (4.42) and (4.43) become

$$\widehat{\mathbf{q}}_{30}^{+} = \left[\boldsymbol{\Upsilon}_{30}^{\mathrm{H}}\boldsymbol{\Upsilon}_{30}\right]^{-1}\boldsymbol{\Upsilon}_{30}^{\mathrm{H}}\widetilde{\mathbf{E}}, \tag{4.49}$$

$$\mathbf{C}_{30}^{+} = \left[\boldsymbol{\Upsilon}_{30}^{\mathrm{H}}\boldsymbol{\Upsilon}_{30}\right]^{-1}\boldsymbol{\Upsilon}_{30}^{\mathrm{H}}\sigma^2, \tag{4.50}$$

$$\mathbf{P}_{30}^{+} = \left[\boldsymbol{\Upsilon}_{30}^{\mathrm{H}}\boldsymbol{\Upsilon}_{30}\right]^{-1}\sigma^2. \tag{4.51}$$

The performance of this method can be seen in Figure 4.8 (in purple). It must be noticed that the relative residual energy reaches the same order of magnitude of the batch method, hence keeping the same quality in explaining the data, while its normalised variance per mode is substantially better than in the batch methods. Of course, such difference in the certainty of the mode coefficients estimator is caused by the minimisation strategy each method uses: while the batch methods minimises a trade-off between residual energy and radiated power, the proposed recursive method only minimises the normalised variance per mode itself (through the trace of the covariance matrix). Hence, achieving a better level of certainty, which naturally implies the residual energy to be low.

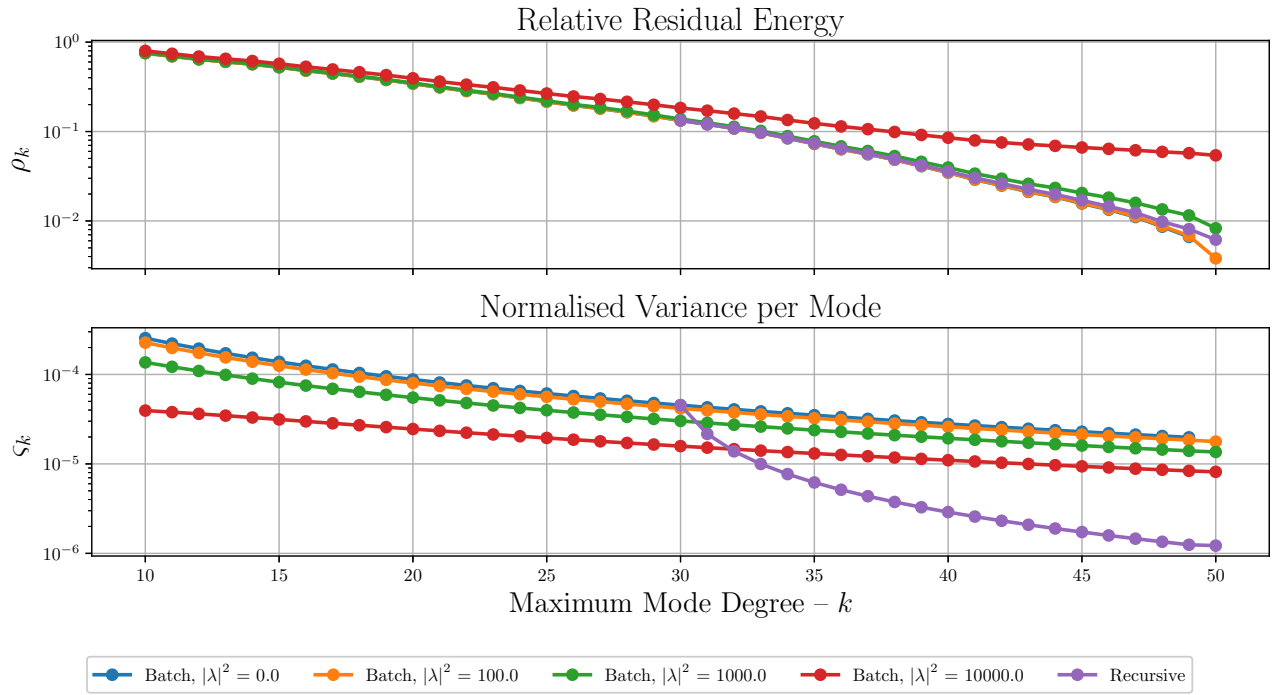

Figure 4.8: Comparison between the recursive regression algorithm with the batch methods.

An important consequence of using the recursive method to also be noticed is the fact that it does not create artefacts in the energy distribution per mode, as it can be visualised in Figure 4.9. Such fact is too a natural implication of the strategy used in this algorithm, which is clear from Mode Coeff. Correction: the modes are corrected only if they justify a

lower variance, in contrast to the batch methods where the modes are neither propagated nor corrected (since the algorithm is not recursive) but, once again, are estimated by minimising a trade-off between residual energy and radiated power.

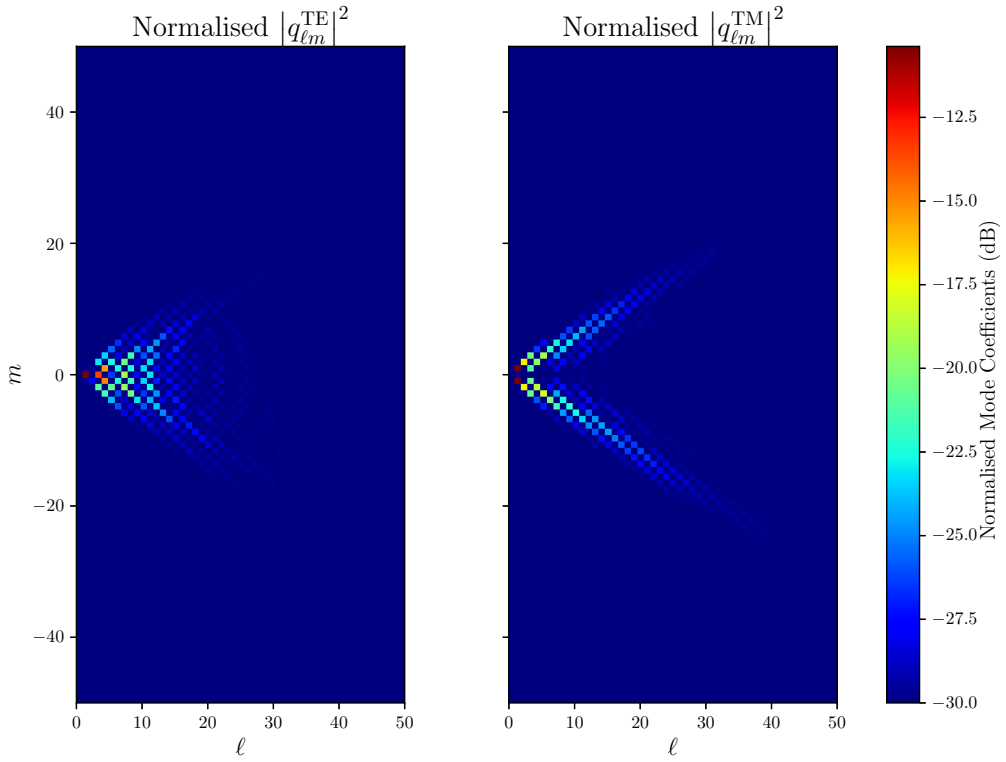

Figure 4.9: Energy distribution per mode at 260 GHz. Estimated using recursive regression method, which does not generate any artefacts.

Finally, to ensure the quality of the estimation, figures 4.10, 4.11, 4.12, 4.13 and 4.14 presents a visual comparison between the measured electric field and the reconstructed field using the estimated mode coefficients at five different frequencies spread over the measured band and the respective relative residual energy of the estimation field.

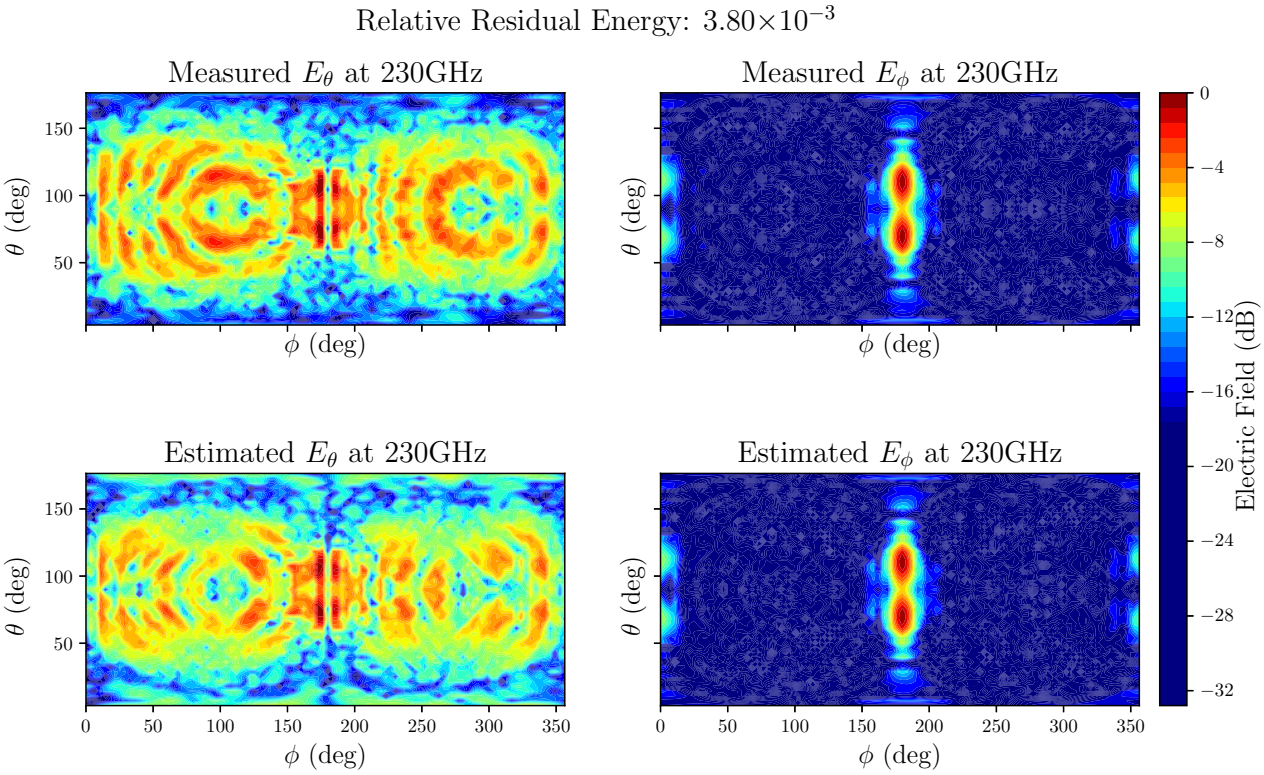

Figure 4.10: Comparison between the measured and estimated phasor field at 230 GHz.

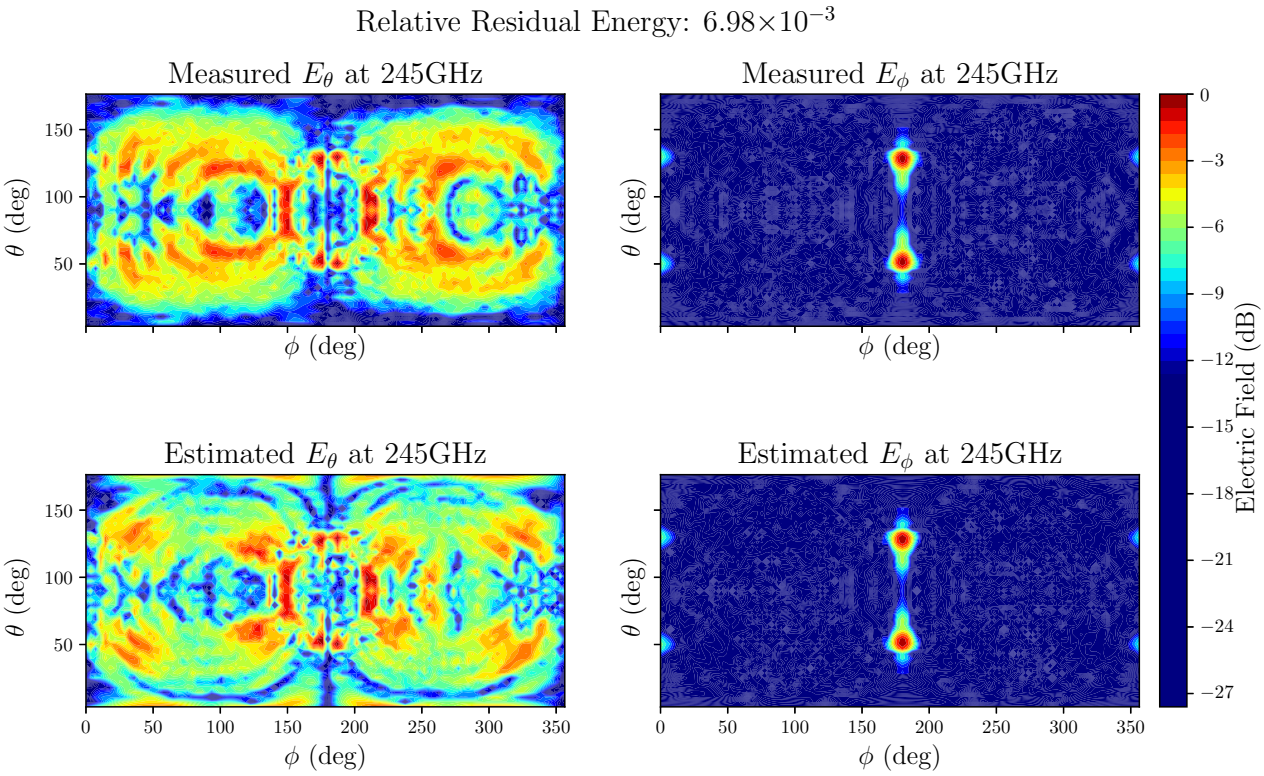

Figure 4.11: Comparison between the measured and estimated phasor field at 245 GHz.

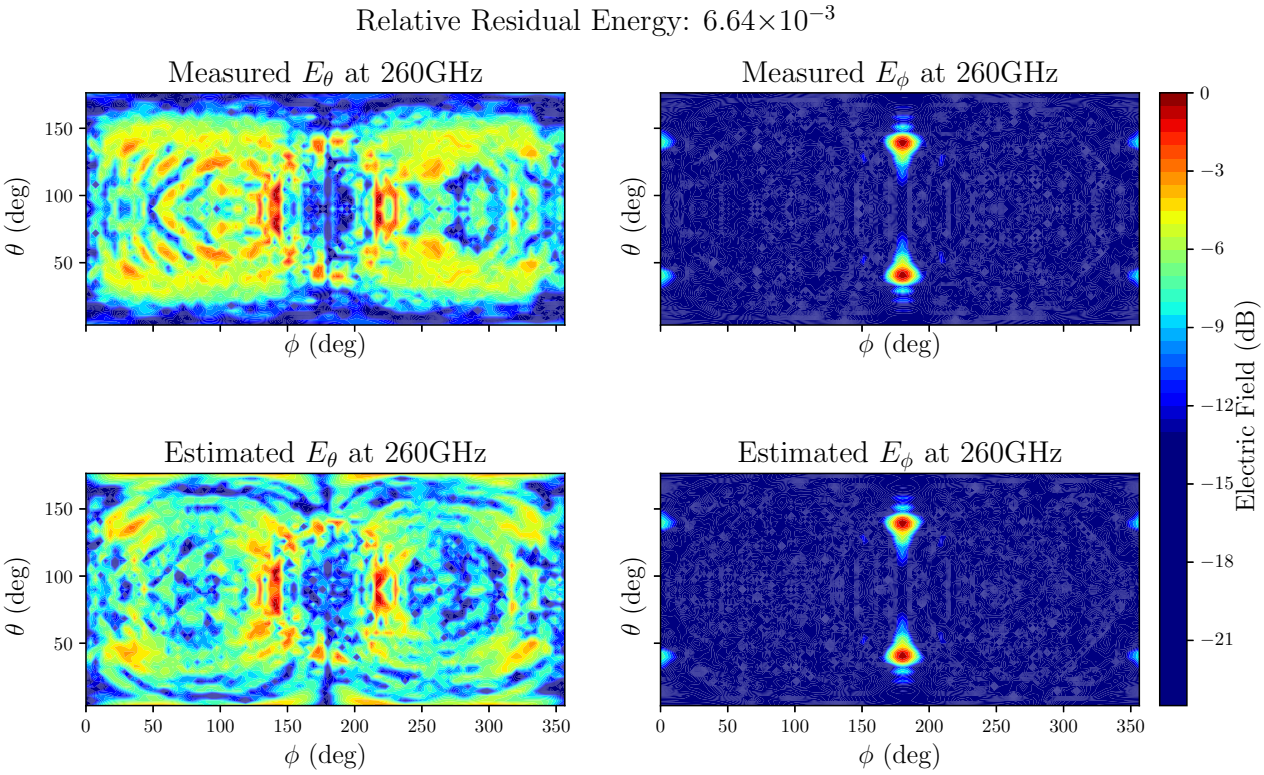

Figure 4.12: Comparison between the measured and estimated phasor field at 260 GHz.

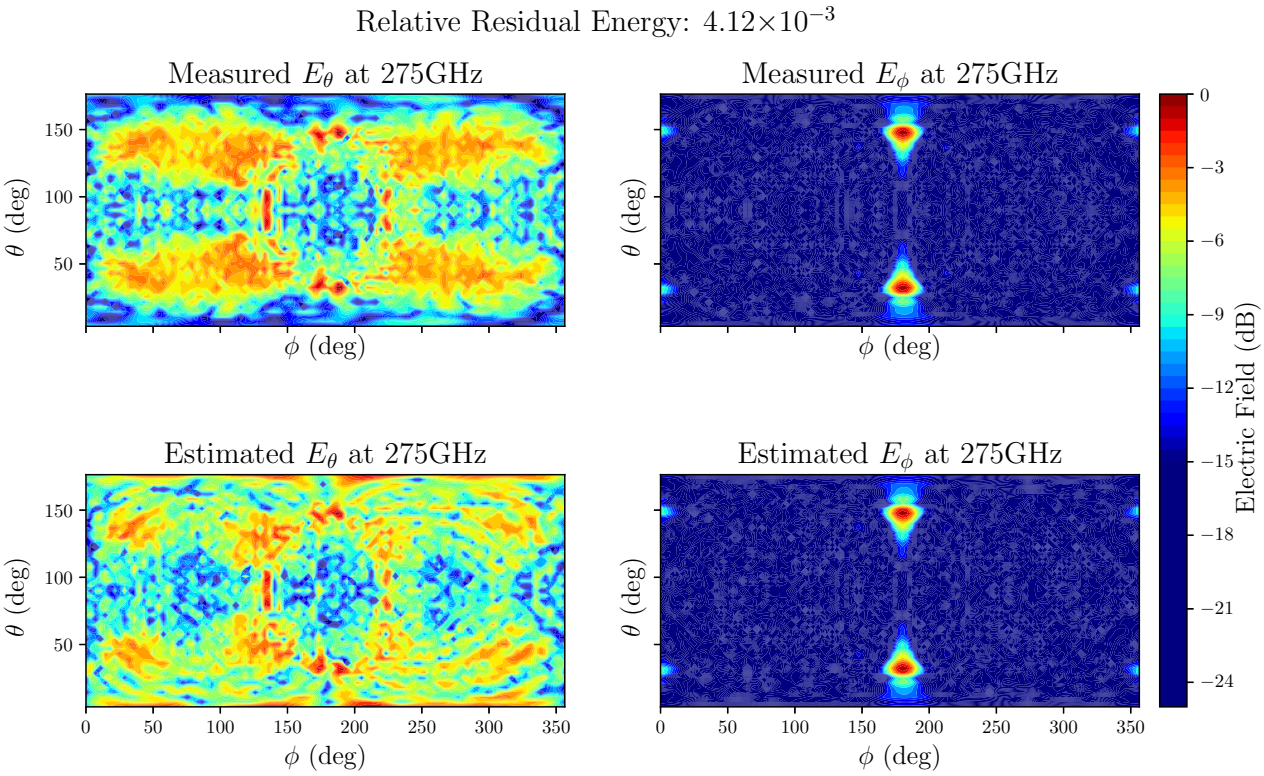

Figure 4.13: Comparison between the measured and estimated phasor field at 275 GHz.

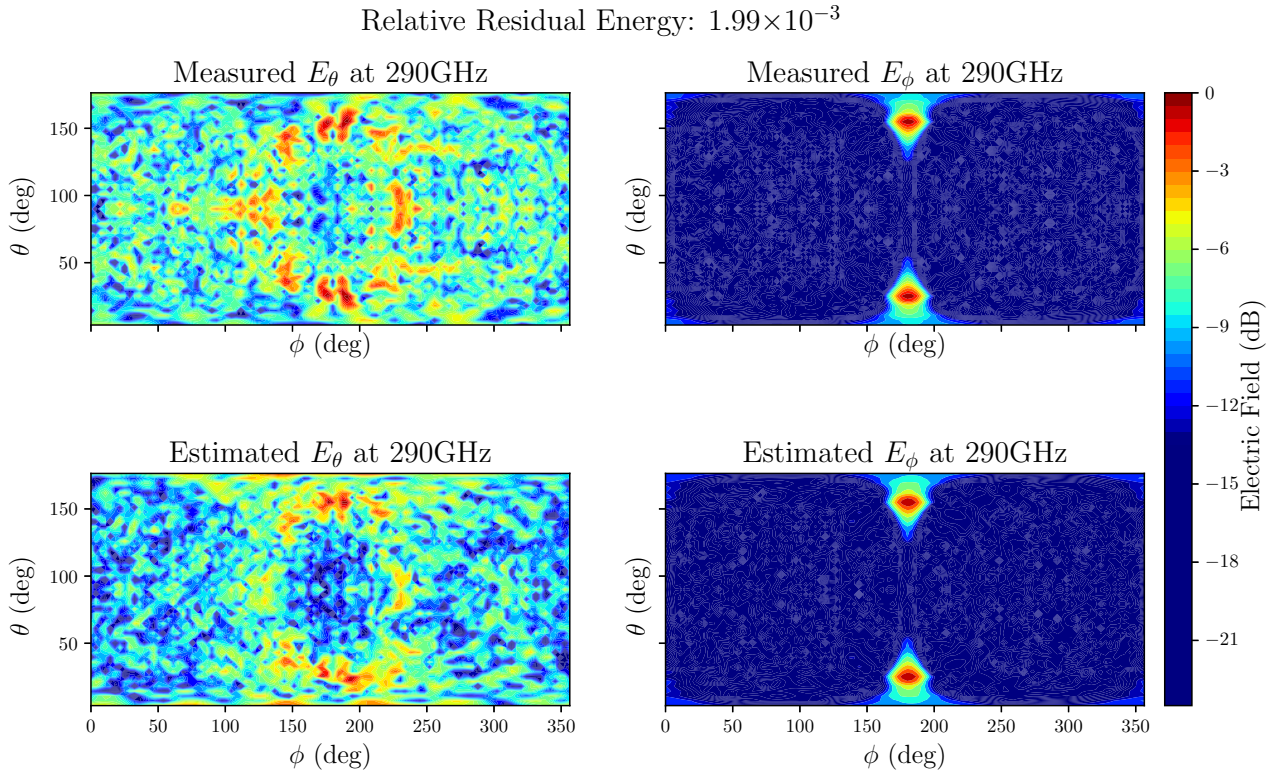

Figure 4.14: Comparison between the measured and estimated phasor field at 290 GHz.

4.A Kalman Gain

Consider once again the Equation (4.37), whose indices and wedges will be suppressed in the following equations so them are kept clear, and let the corrected covariance $\mathbf{P}^+$ be seen as a quadratic form function of the gain $\mathbf{K}$ as follows

$$\begin{aligned}\mathbf{P}^+(\mathbf{K}) &= \mathbf{P}^- + \mathbf{K}\left(\mathbf{C}^- - \mathbf{P}^-\boldsymbol{\Upsilon}^{\mathrm{H}}\right)^{\mathrm{H}} + \left(\mathbf{C}^- - \mathbf{P}^-\boldsymbol{\Upsilon}^{\mathrm{H}}\right)\mathbf{K}^{\mathrm{H}} + \mathbf{K}\left(\boldsymbol{\Upsilon}\mathbf{P}^-\boldsymbol{\Upsilon}^{\mathrm{H}} + \mathbf{R} - \boldsymbol{\Upsilon}\mathbf{C}^- - \left(\boldsymbol{\Upsilon}\mathbf{C}^-\right)^{\mathrm{H}}\right)\mathbf{K}^{\mathrm{H}} \\ &= \mathbf{P}^- + \mathbf{K}\mathbf{B}^{\mathrm{H}} + \mathbf{B}\mathbf{K}^{\mathrm{H}} + \mathbf{K}\mathbf{A}\mathbf{K}^{\mathrm{H}}. \end{aligned} \tag{4.52}$$

From this standpoint, the goal of this appendix is to find an optimal gain $\mathbf{K}^\circ$ such that $\mathrm{tr}\left(\mathbf{P}^+(\mathbf{K})\right)$ is minimal. In order to reach this goal, it is first necessary to ensure the existence of such point, which can be done by requiring the leading term $\mathbf{A}$ to be positive definite, so that the quadratic form would surely be convex. It is worth noting that this requirement can be achieved by assuming that the largest eigenvalue of $\boldsymbol{\Upsilon}\mathbf{P}^-\boldsymbol{\Upsilon}^{\mathrm{H}} + \mathbf{R}$, which is positive semidefinite since $\mathbf{P}^-$ and $\mathbf{R}$ are covariance matrices (and consequently hermitian), is greater than the largest eigenvalue of $\boldsymbol{\Upsilon}\mathbf{C}^- + \left(\boldsymbol{\Upsilon}\mathbf{C}^-\right)^{\mathrm{H}}$, which is hermitian.

By considering this assumption, it is safe to say that the stationary point of $\mathrm{tr}\left(\mathbf{P}^+\right)$ is minimal and the problem becomes now finding that point denoted by $\left(\mathbf{K}^\circ, \mathrm{tr}\left(\mathbf{P}^-(\mathbf{K}^\circ)\right)\right)$. Let h be the composition defined by $h(\mathbf{K}) = \mathrm{tr}\left(\mathbf{P}^-(\mathbf{K})\right)$, then this problem can be solved by founding $\mathbf{K}^\circ$ such that the Gâteaux variation $\delta h(\mathbf{K}^\circ; \mathbf{V})$ vanishes for any matrix direction $\mathbf{V}$, *cf.* [Tro96,

Ch. 3, proposition 3.3]. To that end, let ϵ denote a real number and consider the result

$$\delta h\left(\mathbf{K};\mathbf{V}\right)=\frac{d}{d\epsilon}\Bigg[h\left(\mathbf{K}+\epsilon\mathbf{V}\right)\Bigg]_{\epsilon=0}, \tag{4.53}$$

cf. [Tro96, Ch. 2, equation 7], through which the variation can be calculated, and the application

$$h\left(\mathbf{K}+\epsilon\mathbf{V}\right)=\mathrm{tr}\left(\mathbf{P}^{-}+\left(\mathbf{K}+\epsilon\mathbf{V}\right)\mathbf{B}^{\mathrm{H}}+\mathbf{B}\left(\mathbf{K}+\epsilon\mathbf{V}\right)^{\mathrm{H}}+\left(\mathbf{K}+\epsilon\mathbf{V}\right)\mathbf{A}\left(\mathbf{K}+\epsilon\mathbf{V}\right)^{\mathrm{H}}\right) \tag{4.54}$$

whose derivative with respect to the variable ϵ is given by

$$\frac{d}{d\epsilon}\Bigg[h\left(\mathbf{K}+\epsilon\mathbf{V}\right)\Bigg]=\mathrm{tr}\left(\mathbf{V}\mathbf{B}^{\mathrm{H}}+\mathbf{B}\mathbf{V}^{\mathrm{H}}+\mathbf{V}\mathbf{A}\left(\mathbf{K}+\epsilon\mathbf{V}\right)^{\mathrm{H}}+\left(\mathbf{K}+\epsilon\mathbf{V}\right)\mathbf{A}\mathbf{V}^{\mathrm{H}}\right).$$

Thus,

$$\begin{aligned}\delta h\left(\mathbf{K};\mathbf{V}\right)&=\mathrm{tr}\left(\mathbf{V}\mathbf{B}^{\mathrm{H}}+\mathbf{B}\mathbf{V}^{\mathrm{H}}+\mathbf{V}\mathbf{A}\mathbf{K}^{\mathrm{H}}+\mathbf{K}\mathbf{A}\mathbf{V}^{\mathrm{H}}\right)\\&=\mathrm{tr}\left(\left[\mathbf{B}+\mathbf{K}\mathbf{A}\right]\mathbf{V}^{\mathrm{H}}+\mathbf{V}\left[\mathbf{B}+\mathbf{K}\mathbf{A}\right]^{\mathrm{H}}\right)\end{aligned}$$

At this point, it is worth defining the auxiliary matrix $\mathbf{U}=\mathbf{B}+\mathbf{K}\mathbf{A}$ so the above expression can be rewritten as $\delta h\left(\mathbf{K};\mathbf{V}\right)=\mathrm{tr}\left(\mathbf{U}\mathbf{V}^{\mathrm{H}}+\mathbf{V}\mathbf{U}^{\mathrm{H}}\right)$. An element $\left[\mathbf{U}\mathbf{V}^{\mathrm{H}}+\mathbf{V}\mathbf{U}^{\mathrm{H}}\right]_{ij}$ of that matrix will generically have the form

$$\begin{aligned}\left[\mathbf{U}\mathbf{V}^{\mathrm{H}}+\mathbf{V}\mathbf{U}^{\mathrm{H}}\right]_{ij}&=\sum_{k}\left(\left[\mathbf{U}\right]_{ik}\left[\mathbf{V}^{\mathrm{H}}\right]_{kj}+\left[\mathbf{V}\right]_{ik}\left[\mathbf{U}^{\mathrm{H}}\right]_{kj}\right)\\&=\sum_{k}\left(\left[\mathbf{U}\right]_{ik}\left[\mathbf{V}\right]_{jk}^{*}+\left[\mathbf{V}\right]_{ik}\left[\mathbf{U}\right]_{jk}^{*}\right).\end{aligned}$$

Thus,

$$\begin{aligned}\mathrm{tr}\left(\mathbf{U}\mathbf{V}^{\mathrm{H}}+\mathbf{V}\mathbf{U}^{\mathrm{H}}\right)&=\sum_{i}\left[\mathbf{U}\mathbf{V}^{\mathrm{H}}+\mathbf{V}\mathbf{U}^{\mathrm{H}}\right]_{ii}\\&=\sum_{i}\sum_{k}\Big(\left[\mathbf{U}\right]_{ik}\left[\mathbf{V}\right]_{ik}^{*}+\left[\mathbf{V}\right]_{ik}\left[\mathbf{U}\right]_{ik}^{*}\Big).\end{aligned} \tag{4.55}$$

The condition for the minimum implies that for any choice of complex numbers $\left[\mathbf{V}\right]_{ik}$, it must hold that

$$\sum_{i}\sum_{k}\Big(\left[\mathbf{U}\right]_{ik}\left[\mathbf{V}\right]_{ik}^{*}+\left[\mathbf{V}\right]_{ik}\left[\mathbf{U}\right]_{ik}^{*}\Big)=0.$$

In particular for the choices $\left[\mathbf{V}\right]_{ik}=\delta_{ii'}\delta_{kk'}$ and $\left[\mathbf{V}\right]_{ik}=j\delta_{ii'}\delta_{kk'}$ defined for arbitrary indices i' and k', the condition becomes

$$\left[\mathbf{U}\right]_{i'k'}+\left[\mathbf{U}\right]_{i'k'}^{*}=0 \tag{4.56}$$

$$\left[\mathbf{U}\right]_{i'k'}-\left[\mathbf{U}\right]_{i'k'}^{*}=0, \tag{4.57}$$

respectively. This, of course, can only be true if $\left[\mathbf{U}\right]_{i'k'}=0$ for any indices, which is equivalent to write that $\mathbf{U}=\mathbf{0}$. Thus, $\mathbf{B}+\mathbf{K}^{\circ}\mathbf{A}=\mathbf{0}\implies\mathbf{K}^{\circ}=-\mathbf{B}\mathbf{A}^{-1}$, where the existence of $\mathbf{A}^{-1}$ is

ensured by the assumption of its positive definiteness. Finally, this result implies in the Kalman Gain expression

$$\mathbf{K}^{\circ} = \left(\mathbf{P}^{-}\boldsymbol{\Upsilon}^{\mathrm{H}} - \mathbf{C}^{-}\right)\left(\boldsymbol{\Upsilon}\mathbf{P}^{-}\boldsymbol{\Upsilon}^{\mathrm{H}} + \mathbf{R} - \boldsymbol{\Upsilon}\mathbf{C}^{-} - \left(\boldsymbol{\Upsilon}\mathbf{C}^{-}\right)^{\mathrm{H}}\right)^{-1}. \tag{4.58}$$

With this final result, it is now possible to compute the minimum covariance $\mathbf{P}^{+}\left(\mathbf{K}^{\circ}\right)$ using Equation (4.52)

$$\begin{aligned}
\mathbf{P}^{+}\left(\mathbf{K}^{\circ}\right) &= \mathbf{P}^{-} - \mathbf{B}\mathbf{A}^{-1}\mathbf{B}^{\mathrm{H}} - \mathbf{B}\mathbf{A}^{-1}\mathbf{B}^{\mathrm{H}} + \mathbf{B}\mathbf{A}^{-1}\mathbf{A}\mathbf{A}^{-1}\mathbf{B}^{\mathrm{H}} \\
&= \mathbf{P}^{-} - \mathbf{B}\mathbf{A}^{-1}\mathbf{B}^{\mathrm{H}} \\
&= \mathbf{P}^{-} + \mathbf{K}^{\circ}\mathbf{B}^{\mathrm{H}} \\
&= \mathbf{P}^{-} - \mathbf{K}^{\circ}\left(\mathbf{P}^{-}\boldsymbol{\Upsilon}^{\mathrm{H}} - \mathbf{C}^{-}\right)^{\mathrm{H}},
\end{aligned} \tag{4.59}$$

with concludes the objective of this appendix.

Chapter 5

General Sampling

Assume that for any mode (ℓ, m), the mode coefficient function $\boldsymbol{q}_{\ell m}$ has its values known (or estimated) at a discrete set of positive frequencies, which consequently also determines $\boldsymbol{q}_{\ell m}$ at a set of negative frequencies due to Equation (3.41), and let $\{\nu_n\}_{n\in\mathbb{Z}}$ denote the union of those sets. Naturally, this scenario raises a question about the possibility of retrieving $\boldsymbol{q}_{\ell m}$ as a function, *i.e.*, $\boldsymbol{q}_{\ell m}(\nu)$ for any $\nu \in \mathbb{R}$, through its set of samples $\{\boldsymbol{q}_{\ell m}(\nu_n)\}_{n\in\mathbb{Z}}$. If the frequencies are equally spaced, meaning that $\nu_n = n \cdot \Delta\nu$ for a constant "sampling frequency" $\Delta\nu$, then it becomes even more natural to answer this question by considering the remarkable Whittaker-Nyquist-Shannon Sampling Theorem (WNSST) to perform such reconstruction as follows

$$\boldsymbol{q}_{\ell m}(\nu) = \sum_{n\in\mathbb{Z}} \boldsymbol{q}_{\ell m}(\nu_n) \cdot \operatorname{sinc}\left(\frac{\nu}{\Delta\nu} - n\right).$$

Of course this approach requires assuming that the inverse Fourier transform of $\boldsymbol{q}_{\ell m}$ is "band-limited in time" meaning that its energy must be completely concentrated within a time-domain compact whose radius must be no greater than $1/2\Delta\nu$. Although such assumption is reasonable, the said approach is still troublesome regarding the causality conditions at (3.45) – (3.48). In fact, consider those conditions in a generic form and notice that the usage of WNSST leads to

$$\sum_{n\in\mathbb{Z}} \left(\nu^a \xi_n(\nu) + \frac{1}{j\pi}\mathsf{PV}\int_{\mathbb{R}} \frac{\upsilon^a \xi_n(\upsilon)}{\upsilon - \nu} d\upsilon\right) \boldsymbol{q}_{\ell m}(\nu_n) = \mathbf{0},$$

where $\xi_n(\nu) = \operatorname{sinc}\left(\frac{\nu}{\Delta\nu} - n\right)$. Since the above condition must be valid for any set of samples $\{\boldsymbol{q}_{\ell m}(\nu_n)\}_{n\in\mathbb{Z}}$, the following must hold for any $n \in \mathbb{Z}$

$$\nu^a \xi_n(\nu) = -\frac{1}{j\pi}\mathsf{PV}\int_{\mathbb{R}} \frac{\upsilon^a \xi_n(\upsilon)}{\upsilon - \nu} d\upsilon.$$

However, once ξ_n is real for any n, the above condition cannot hold due to Property A.2. As consequence, a central result for this work is reached and synthesised at the following theorem due to its relevance.

Theorem 5.1. The usage of WNSST to reconstruct the mode coefficient functions $\boldsymbol{q}_{\ell m}$ leads to non-causal electric fields.

The impossibility of using WNSST indicates that special care must be taken in the retrieving of the mode coefficient functions through interpolation methods. From now on, this work shall

concentrate its efforts in the sought of suitable reconstructions for the $\boldsymbol{q}_{\ell m}$. In this quest, analyticity for the reconstructors is clearly an advantage in the verifying of Kramers-Kronig relations. That being said, it is suggestive seeking for a general form of WNSST that obeying the causality conditions. In this direction, this Chapter provides the fundamental concepts and results behind such generalisation process.

5.1 The General Sampling Theorem

The starting point towards that generalisation, which also comes to be the main result of this Chapter, is the General Sampling Theorem (GST). However, before diving into its formalism, it is worth introducing the motivation behind its development. For this goal, consider an unknown complex-valued function ψ defined on some real domain. Although ψ is unknown by hypothesis, also consider that it is possible to countably evaluate its values in arbitrary points of its domain by performing some sort of procedure or experiment. In other words, it is possible to measure a set of samples $\left\{\psi\left(u_n\right)\right\}_{n\in\mathbb{N}}$. The GST establishes the requirements on ψ and on the sampling points $\{u_n\}_{n\in\mathbb{N}}$ that must be satisfied in order to be possible to perfectly reconstruct ψ from its collected samples.

The following Theorem and its proof are adapted from [Kra59].

Theorem 5.2 (General Sampling)**.** Consider $\mathfrak{V}\subset\mathbb{R}$ and let $(\mathfrak{V},\Sigma_{\mathfrak{V}},\mu)$ denote a measure space such that $\mu\left(\mathfrak{V}\right)<+\infty$ (band-limited). Given a set $\mathfrak{U}\subseteq\mathbb{R}$, a number $u\in\mathfrak{U}$ and a family of u-indexed functions $K\left(u,\cdot\right)\in L^2_w\left(\mathfrak{V},\Sigma_{\mathfrak{V}},\mu\right)$, if there exists a sequence $\left(u_n\right)_{n\in\mathbb{N}}$ in $\mathfrak{U}$ such that $\left\{K\left(u_n,\cdot\right)\right\}_{n\in\mathbb{N}}$ is a complete orthonormal set on $L^2_w\left(\mathfrak{V},\Sigma_{\mathfrak{V}},\mu\right)$, then for a signal $\psi:\mathfrak{U}\to\mathbb{C}$ that can be written as

$$\psi\left(u\right)=\left\langle\Psi\middle|K\left(u,\cdot\right)^*\right\rangle_{\mathfrak{V}}\overset{\text{def}}{=}\int_{\mathfrak{V}}\Psi\cdot K\left(u,\cdot\right)\cdot w d\mu \tag{5.1}$$

for some $\Psi\in L^2_w\left(\mathfrak{V},\Sigma_{\mathfrak{V}},\mu\right)$, then the series $\sum_{n\in\mathbb{N}}\psi\left(u_n\right)\xi_n$, where

$$\xi_n\left(u\right)=\left\langle K\left(u,\cdot\right)\middle|K\left(u_n,\cdot\right)\right\rangle_{\mathfrak{V}}, \tag{5.2}$$

uniformly converges to ψ.

Proof. See appendix 5.A.

In order to contextualise the above notation with previous one, consider an invertible map $f:\mathbb{R}\to\mathbb{R}$, possibly linear, under which the frequency ν is retrieved from u in a way that $\nu=f\left(u\right)$. In this sense, u shall also be seen as a variable that carries the frequency information. Moreover, if physical meaning should be given to ψ, it must be taken in a way that either

$$q^{\text{TE}}_{\ell m}\left(\nu\right)=\psi\left(u\right)\quad\text{or}\quad q^{\text{TM}}_{\ell m}\left(\nu\right)=\psi\left(u\right) \tag{5.3}$$

holds. The function Ψ is said to be the transform of ψ with respect of the kernel K and the Theorem is is based on the existence of such function. Lastly, ξ_n is sought constructor (which becomes the sinc in the particular case of WNSST).

In the context created above, it is worth seeing GST as the conditions the mode coefficient functions must obey so they can be projected in a set of constructors pondered by their own samples.

5.2 Signal Energy

Since ψ is a signal, a mathematical notion of energy can be associated to it in the form of $\|\psi\|_{\mathfrak{U}}^2 \stackrel{\text{def}}{=} \langle\psi|\psi\rangle_{\mathfrak{U}}$. As it will be seen, such energy bears a resemblance with the radiated power per mode, *cf*. Equation (3.14), but it shall not be misinterpreted with the physical notion of electromagnetic energy even though their names share the same word. The energy can be written as

$$\|\psi\|_{\mathfrak{U}}^2 = \sum_{n\in\mathbb{N}}\sum_{n'\in\mathbb{N}} \psi\left(u_n\right)\psi\left(u_{n'}\right)^* \langle\xi_n|\xi_{n'}\rangle_{\mathfrak{U}}\,. \tag{5.4}$$

If the kernel obeys the completeness relations, then $\langle\xi_n|\xi_{n'}\rangle_{\mathfrak{U}} = C\cdot\delta_{nn'}$ holds as it has been shown in Section 5.B. For this particular case, it is true that

$$\|\psi\|_{\mathfrak{U}}^2 = C\sum_{n\in\mathbb{N}} \left|\psi\left(u_n\right)\right|^2, \tag{5.5}$$

which means that energy information lies completely in the collected samples and does not depend on the constructors in $\{\xi_n\}_{n\in\mathbb{N}}$.

On the other hand, it is also possible to calculate the energy of the transformed signal Ψ. For that, it is enough to see that, once this signal exists, it does also have a series representation from the samples. In fact, once the transformed signal $\Psi \in L_w^2\left(\mathfrak{W}, \Sigma_{\mathfrak{W}}, \mu\right)$ by hypothesis, its conjugate Ψ^* belongs to this space as well. Therefore,

$$\Psi^* = \sum_{n\in\mathbb{N}} \left\langle \Psi^* \middle| K\left(u_n,\cdot\right)\right\rangle \cdot K\left(u_n,\cdot\right).$$

Hence,

$$\begin{aligned}
\Psi &= \sum_{n\in\mathbb{N}} \left\langle \Psi^* \middle| K\left(u_n,\cdot\right)\right\rangle^* \cdot K\left(u_n,\cdot\right)^* \\
&= \sum_{n\in\mathbb{N}} \left\langle K\left(u_n,\cdot\right) \middle| \Psi^*\right\rangle \cdot K\left(u_n,\cdot\right)^* \\
&= \sum_{n\in\mathbb{N}} \left\langle \Psi \middle| K\left(u_n,\cdot\right)^*\right\rangle \cdot K\left(u_n,\cdot\right)^* \\
&= \sum_{n\in\mathbb{N}} \psi\left(u_n\right)\cdot K\left(u_n,\cdot\right)^*
\end{aligned} \tag{5.6}$$

which also implies the Parseval's identity, *cf*. [GB15, Theorem 5.3.10]. Thus,

$$\|\Psi\|_{\mathfrak{V}}^2 = \sum_{n\in\mathbb{N}} |\psi(u_n)|^2 \tag{5.7}$$

also holds.

The similarity between Equations (5.5) and (5.7) leads to the Plancherel identity

$$\|\psi\|_{\mathfrak{U}}^2 = C\,\|\Psi\|_{\mathfrak{V}}^2, \tag{5.8}$$

which is only valid when the kernel obeys the completeness relations, *i.e.*, the constructors form an orthogonal set.

5.3 Truncation Error

The practical usage of the GST depends on its performance when its series is truncated. Let $N \in \mathbb{N}$ be the number of constructors considered in the truncation and ψ_N denote the part of ψ that is projected in those constructors in a way that

$$\psi_N = \sum_{n\leqslant N} \psi(u_n)\,\xi_n. \tag{5.9}$$

Naturally, the energy of this projection is

$$\|\psi_N\|_{\mathfrak{U}}^2 = \sum_{n\leqslant N} |\psi(u_n)|^2, \tag{5.10}$$

from which is clear that $\|\psi_N\|_{\mathfrak{U}}^2 < \|\psi\|_{\mathfrak{U}}^2$. It is interesting to notice that that the difference $\|\psi\|_{\mathfrak{U}}^2 - \|\psi_N\|_{\mathfrak{U}}^2$ is precisely the residual energy $\|\psi - \psi_N\|_{\mathfrak{U}}^2$ given by

$$\|\psi - \psi_N\|_{\mathfrak{U}}^2 = \psi - \psi_N = \sum_{n>N} |\psi(u_N)|^2. \tag{5.11}$$

As conclusion, the quality of the reconstruction is constrained to $\|\psi - \psi_N\|_{\mathfrak{U}}^2$ being very small when compared to $\|\psi\|_{\mathfrak{U}}^2$ and it does not depend on the constructors ξ_n. Consequently, this method of interpolation is as good as the energy of the signal is (completely or mostly) concentrated in a frequency-domain region, which is quite reasonable, so the energy associated to samples outside this region is negligible.

5.4 WNSST as a particularisation of GST

As one might wonder, it is possible to reach the WNSST as a particular case of GST by considering the kernel $K : \mathbb{R} \times [-v_\circ, v_\circ] \to \mathbb{C}$ defined by

$$K(u, v) = \frac{e^{2\pi j u v}}{\sqrt{2v_\circ}} \tag{5.12}$$

for some $v_\circ > 0$. As it will be shown in subsection 6.3.5, the family $\left\{K\left(\frac{n}{2v_\circ}, \cdot\right)\right\}_{n\in\mathbb{Z}}$ forms a complete orthonormal set on the Lebesgue space over the compact $[-v_\circ, v_\circ]$. Furthermore

$$\left\langle K(\cdot, v) \middle| K(\cdot, s) \right\rangle = \frac{1}{2v_\circ}\int_{\mathbb{R}} e^{2\pi j(v-s)u} du = \frac{1}{2v_\circ}\delta(v-s). \tag{5.13}$$

Thus, this kernel obeys the completeness relation, ensuring the results discussed above. The following also holds

$$\left\langle K(u, \cdot) \middle| K(r, \cdot) \right\rangle = \frac{1}{2v_\circ}\int_{[-v_\circ, v_\circ]} e^{2\pi j(u-r)v} dv = \frac{\sin\big(2\pi v_\circ (u-r)\big)}{2\pi v_\circ (u-r)} = \operatorname{sinc}\Big(2v_\circ (u-r)\Big)$$

from which the constructor can hence be calculated as

$$\xi_n(u) = \operatorname{sinc}\left(2v_\circ\left(\frac{n}{2v_\circ} - u\right)\right) = \operatorname{sinc}\big(2v_\circ u - n\big). \tag{5.14}$$

The last equation completely retrieves the WNSST. Furthermore, it is also interesting to consider a simple map $\nu = \alpha u$ and notice that the constructor as a function of frequency has the form

$$\xi_n(\nu/\alpha) = \operatorname{sinc}\left(\frac{2v_\circ \nu}{\alpha} - n\right), \tag{5.15}$$

from which is clear that the sampling frequency is $\Delta\nu = \alpha/2v_\circ$.

As it has been above exemplified, the kernel is completely responsible for the nature of the constructor and , in special, its reality. Having this in mind, subsection 6.3.6 proposes an adaptation of the kernel in Equation (5.12) which yields complex-valued constructors obeying the causality conditions. Aiming this goal, the next section brings sufficient conditions over possible kernels so that they provide causal constructors.

5.5 Causal Kernels

Since frequencies may spam all over the real values, it is natural to take $\mathfrak{U} = \mathbb{R}$. In this context, once again consider the causality conditions at (3.45) – (3.48) generically synthesised as

$$u^a \psi(u) = -\frac{1}{j\pi}\mathsf{PV}\int_{\mathbb{R}} \frac{r^a \psi(r)}{r-u} dr \tag{5.16}$$

and assume that sequence of the partial sums of $\sum_{n\in\mathbb{N}} \psi(u_n)\,\xi_n$ is bounded (or dominated) by an Lebesgue integrable function, then the Dominated Convergence Theorem and it is possible to say that

$$\sum_{n\in\mathbb{N}}\left(u^a \xi_n(u) + \frac{1}{j\pi}\mathsf{PV}\int_{\mathbb{R}} \frac{r^a \xi_n(r)}{r-u} dr\right)\psi(u_n) = 0.$$

Since the above condition must hold for any set $\{\psi(u_n)\}_{n\in\mathbb{N}}$ of collected samples, it must be true that

$$u^a \xi_n(u) + \frac{1}{j\pi}\mathsf{PV}\int_{\mathbb{R}} \frac{r^a \xi_n(r)}{r-u} dr = 0$$

for any $n \in \mathbb{N}$. Moreover, assuming that the function $\frac{r^a K(r,v)}{r-u}$ is Lebesgue integrable for any $(r, v) \in \mathbb{R} \times \mathfrak{V}$, Fubini's Theorem holds and the Lebesgue integral in $\mathbb{R}$ commutes with the inner product in $\mathfrak{V}$. Hence,

$$\left\langle u^a K(u,\cdot) + \frac{1}{j\pi}\mathsf{PV}\int_{\mathbb{R}} \frac{r^a K(r,\cdot)}{r-u} dr \middle| K(u_n,\cdot) \right\rangle_{\mathfrak{V}} = 0$$

do also hold for any $n \in \mathbb{N}$. Thus, the completeness of the set $\left\{K(u_n,\cdot)\right\}_{n\in\mathbb{N}}$ immediately implies that

$$u^a K(u,v) = -\frac{1}{j\pi}\mathsf{PV}\int_{\mathbb{R}} \frac{r^a K(r,v)}{r-u} dr. \tag{5.17}$$

Even though the last result can be thought as sought condition over the kernel, it is worth going beyond and analysing the above equation in light of the values of a. In this direction, consider the application of the inverse Fourier transform, with respect to the frequency variable u, on such equation as follows

$$\mathcal{F}^{-1}\left(u^a K(u,v)\right) = \operatorname{sgn} \cdot \mathcal{F}^{-1}\left(u^a K(u,v)\right), \tag{5.18}$$

from which one can conclude that

$$\mathcal{F}^{-1}\left(u^a K(u,v)\right)(\tau) = 0, \quad \forall \tau < 0. \tag{5.19}$$

Let $\mathcal{K}$ be the inverse Fourier transform of K with respect to the frequency variable u, *i.e.*,

$$\mathcal{K}(\tau, v) = \int_{\mathbb{R}} K(u,v)\, e^{j2\pi u\tau} du. \tag{5.20}$$

For any $a \geqslant 0$, it holds that

$$\mathcal{F}^{-1}\left(u^a K(u,v)\right)(\tau) = \frac{1}{(j2\pi)^a}\frac{\partial^a \mathcal{K}}{\partial \tau^a}(\tau, v) \tag{5.21}$$

implying that $\mathcal{K}$ and all of its time derivatives must vanishes for $\tau < 0$, *i.e.*, $\mathcal{K}^{(a)}(\tau, v) = \operatorname{sgn}(\tau) \cdot \mathcal{K}^{(a)}(\tau, v)$. On the other hand, for $-\ell \leqslant a < 0$,

5.A Proof of the GST

Proof of Theorem 5.2. Once $\left\{K(u_n,\cdot)\right\}_{n\in\mathbb{N}}$ is an orthonormal set on $L^2_w(\mathfrak{V}, \Sigma_{\mathfrak{V}}, \mu)$, it holds that

$$\left\langle K(u_n,\cdot) \middle| K(u_\ell,\cdot) \right\rangle_{\mathfrak{V}} = \delta_{n\ell}, \tag{5.22}$$

and since it is also complete in that space, any function $\psi \in L^2_w(\mathfrak{V}, \Sigma_{\mathfrak{V}}, \mu)$ can be represented as

$$\psi = \sum_{n\in\mathbb{N}} \left\langle \psi \middle| K(u_n,\cdot) \right\rangle_{\mathfrak{V}} \cdot K(u_n,\cdot). \tag{5.23}$$

In particular, if ψ is taken as $K(u,\cdot)$ itself then

$$K(u,\cdot) = \sum_{n\in\mathbb{N}} \xi_n(u) \cdot K(u_n,\cdot), \tag{5.24}$$

which is just a compact notation meaning that for any $\varepsilon > 0$ and $(u, v) \in \mathfrak{U} \times \mathfrak{V}$, there exists $N \in \mathbb{N}$ such that $m > N$ implies that

$$\left| K(u,v) - \sum_{n \leqslant m} \xi_n(u) K(u,v) \right| < \varepsilon. \tag{5.25}$$

On the other hand, consider the partial sum definition

$$\psi_m = \sum_{n \leqslant m} \psi(u_n) \xi_n \tag{5.26}$$

and the following result

$$\begin{aligned} \left| \psi(u) - \psi_m(u) \right| &= \left| \left\langle \Psi \middle| K(u,\cdot)^* \right\rangle_{\mathfrak{V}} - \sum_{n \leqslant m} \left\langle \Psi \middle| K(u_n,\cdot)^* \right\rangle_{\mathfrak{V}} \cdot \xi_n(u) \right| \\ &= \left| \left\langle \Psi \middle| K(u,\cdot)^* - \sum_{n \leqslant m} K(u_n,\cdot)^* \xi_n(u)^* \right\rangle_{\mathfrak{V}} \right| \end{aligned} \tag{5.27}$$

which, from Cauchy-Schwarz inequality and (5.25), yields

$$\begin{aligned} \left| \psi(u) - \psi_m(u) \right| &\leqslant \left\| \Psi \right\|_{\mathfrak{V}} \cdot \left\| K(u,\cdot) - \sum_{n \leqslant m} K(u_n,\cdot) \xi_n(u) \right\|_{\mathfrak{V}} \\ \cdots &= \left\| \Psi \right\|_{\mathfrak{V}} \cdot \left(\int_{\mathfrak{V}} \left| K(u,\cdot) - \sum_{n \leqslant m} K(u_n,\cdot) \xi_n(u) \right|^2 w d\mu \right)^{1/2} \\ \cdots &\leqslant \left\| \Psi \right\|_{\mathfrak{V}} \cdot \left(\varepsilon^2 \cdot \sup_{\mathfrak{V}} \{w\} \cdot \int_{\mathfrak{V}} d\mu \right)^{1/2} \\ \cdots &= \varepsilon \left\| \Psi \right\|_{\mathfrak{V}} \cdot \left(\sup_{\mathfrak{V}} \{w\} \cdot \mu(\mathfrak{V}) \right)^{1/2}. \end{aligned} \tag{5.28}$$

Since $\mu(\mathfrak{V}) < +\infty$ and $\psi \in L^2_w(\mathfrak{V}, \Sigma_{\mathfrak{V}}, \mu)$, it becomes clear that ψ_m uniformly converges to ψ and one can finally write

$$\psi \overset{\text{a.e.}}{=} \sum_{n \in \mathbb{N}} \psi(u_n) \xi_n, \tag{5.29}$$

where the equality is taken in the sense that

$$\left\| \psi - \sum_{n \in \mathbb{N}} \psi(u_n) \xi_n \right\|_{\mathfrak{U}} = 0. \tag{5.30}$$

The proof is hence concluded. ■

5.B Kernels Satisfying Completeness Relations

Consider a kernel K satisfying the following completeness relation in *udomain*

$$\left\langle K\left(\cdot,v\right)\middle|K\left(\cdot,s\right)\right\rangle_{\mathfrak{U}}=\frac{C}{w\left(v\right)}\delta\left(v-s\right). \tag{5.31}$$

Hence, for some $\psi\in L^{2}\left(\mathfrak{U},\Sigma_{\mathfrak{U}},\mu\right)$, it holds that

$$\begin{aligned}\left\langle \psi|K\left(\cdot,v\right)\right\rangle_{\mathfrak{U}} &= \int_{\mathfrak{U}}\psi\left(u\right)K\left(u,v\right)^{*}\mu\left(du\right)\\ &= \int_{\mathfrak{U}}\left[\int_{\mathfrak{V}}\mathfrak{\psi}\left(s\right)K\left(u,s\right)w\left(s\right)\mathfrak{\mu}\left(ds\right)\right]K\left(u,v\right)^{*}\mu\left(du\right)\\ &= \int_{\mathfrak{V}}\mathfrak{\psi}\left(s\right)\left[\int_{\mathfrak{U}}K\left(u,s\right)K\left(u,v\right)^{*}\mu\left(du\right)\right]w\left(s\right)\mathfrak{\mu}\left(ds\right)\\ &= \frac{C}{w\left(v\right)}\int_{\mathfrak{V}}\mathfrak{\psi}\left(s\right)w\left(s\right)\delta\left(v-s\right)\mathfrak{\mu}\left(ds\right)\\ &= C\mathfrak{\psi}\left(v\right).\end{aligned}$$

Thus, $\mathfrak{V}$-transformed $\mathfrak{\psi}$ can be retrieved by the integral transform in $\mathfrak{U}$, implying those transform are each other inverse in the sense that

$$\mathfrak{\psi}\left(v\right)=\frac{1}{C}\cdot\left\langle \psi\middle|K\left(\cdot,v\right)\right\rangle_{\mathfrak{U}}. \tag{5.32}$$

Moreover, if that is the case, the constructors form an orthogonal family. In fact,

$$\begin{aligned}\left\langle \xi_{n}|\xi_{m}\right\rangle_{\mathfrak{U}} &= \int_{\mathfrak{U}}\xi_{n}\xi_{m}^{*}d\mu\\ &= \int_{\mathfrak{U}}\xi_{n}\left(u\right)\xi_{m}\left(u\right)^{*}\mu\left(du\right)\\ &= \int_{\mathfrak{U}}\left\langle K\left(u,\cdot\right)\middle|K\left(u_{n},\cdot\right)\right\rangle_{\mathfrak{V}}\left\langle K\left(u,\cdot\right)\middle|K\left(u_{m},\cdot\right)\right\rangle_{\mathfrak{V}}^{*}\mu\left(du\right)\\ &= \int_{\mathfrak{U}}\left[\int_{\mathfrak{V}}K\left(u,v\right)K\left(u_{n},v\right)^{*}w\left(v\right)\mathfrak{\mu}\left(dv\right)\right]\cdot\left[\int_{\mathfrak{V}}K\left(u_{m},s\right)K\left(u,s\right)^{*}w\left(v\right)\mathfrak{\mu}\left(ds\right)\right]\mu\left(du\right)\\ &= \int_{\mathfrak{V}\times\mathfrak{V}}\left[\int_{\mathfrak{U}}K\left(u,v\right)K\left(u,s\right)^{*}\mu\left(du\right)\right]K\left(u_{m},s\right)K\left(u_{n},v\right)^{*}w\left(v\right)w\left(s\right)\mathfrak{\mu}\left(dv\right)\mathfrak{\mu}\left(ds\right)\\ &= \int_{\mathfrak{V}\times\mathfrak{V}}\left\langle K\left(\cdot,v\right)\middle|K\left(\cdot,s\right)\right\rangle_{\mathfrak{U}}K\left(u_{m},s\right)K\left(u_{n},v\right)^{*}w\left(v\right)w\left(s\right)\mathfrak{\mu}\left(dv\right)\mathfrak{\mu}\left(ds\right),\end{aligned}$$

then

$$\begin{aligned}\left\langle \xi_{n}|\xi_{m}\right\rangle_{\mathfrak{U}} &= C\int_{\mathfrak{V}}K\left(u_{m},v\right)K\left(u_{n},v\right)^{*}w\left(v\right)\mathfrak{\mu}\left(dv\right)\\ &= C\left\langle K\left(u_{m},\cdot\right)\middle|K\left(u_{n},\cdot\right)\right\rangle_{\mathfrak{V}}\\ &= C\cdot\delta_{nm}.\end{aligned}$$

Chapter 6

Kernel Construction

Undoubtedly, Theorem 5.2 provides an elegant and useful method to reconstruct a signal from samples of itself given the existence of the kernel K and the sequence $(u_n)_{n\in\mathbb{N}}$. Nevertheless, the attainment of such mathematical objects obeying those specific conditions may become as challenging as, or even challenger than, the application of the GST itself. This Chapter provides a clever approach to construct such objects.

6.1 Spectral Theory of Compact and Self-adjoint Operators

Fortunately, a particular and well-known theory provides an insight into where to search for those special kernels: the spectral theory for compact and self-adjoint operators. Regarding this family of operators, let $\mathcal{H}$ denote an infinite-dimensional Hilbert Space, and $\mathsf{J} : \mathcal{H} \to \mathcal{H}$ be compact and self-adjoint. Then,

Property 6.1. All eigenvalues of J are real, *cf*. [GB15, Proposition 7.5.1];

Property 6.2. Eigenvectors associated with different eigenvalues of J are orthogonal, *cf*. [GB15, Proposition 7.5.1];

Property 6.3. The eigenvalues of J form a countable set at which zero is its only possible limiting point, *cf*. [GB15, Theorem 7.3.6-7.3.7];

Property 6.4. $\mathcal{H}$ admits a complete orthonormal set formed by the eigenvectors of J, *cf*. [GB15, Theorem 7.3.6-7.3.7];

Property 6.5 (Spectral Theorem). There exist a sequence $(\lambda_n)_{n\in\mathbb{N}}$ of eigenvalues of J with respective normalised eigenvectors $(\varphi_n)_{n\in\mathbb{N}}$ such that

$$\mathsf{J}\psi = \sum_{n\in\mathbb{N}} \lambda_n \langle \psi | \varphi_n \rangle \varphi_n \tag{6.1}$$

for any $\psi \in \mathcal{H}$, *cf*. [GB15, p. 7.5.6].

In light of the results above, one might be encouraged to consider $L^2_w(\mathfrak{V}, \Sigma_{\mathfrak{V}}, \mu)$ as the Hilbert space, endowed with the usual inner product $\langle \cdot | \cdot \rangle_{\mathfrak{V}}$, and $(u_n)_{n\in\mathbb{N}}$ and $(K(u_n, \cdot))_{n\in\mathbb{N}}$ as the eigenvalues and eigenfunctions of some compact and self-adjoint operator $\mathsf{J} : L^2_w(\mathfrak{V}, \Sigma_{\mathfrak{V}}, \mu) \to \mathcal{S}$, respectively, for some $\mathcal{S} \subseteq L^2_w(\mathfrak{V}, \Sigma_{\mathfrak{V}}, \mu)$ while K, as a function of u, is yet to be found.

However, the possibility of a limiting point for the frequency-related sequence $(u_n)_{n\in\mathbb{N}}$, even though it would be zero, is not actually desirable.

On the other hand, if J is such that $\lambda_n \neq 0$ for all $n \in \mathbb{N}$, it is possible to define a new operator $\mathsf{L} : \mathcal{S} \to \mathcal{D} \subset L^2_w(\mathfrak{V}, \Sigma_{\mathfrak{V}}, \mu)$ given by

$$\mathsf{L} = \sum_{n\in\mathbb{N}} \frac{\langle \cdot | \varphi_n \rangle}{\lambda_n} \varphi_n, \tag{6.2}$$

in a way that the solutions of the equation $\mathsf{L}\zeta = \psi$ are precisely given by the restriction $\zeta = \mathsf{J}|_{\mathcal{D}}\psi$, which is easily checkable. Most naturally, it should be easy to see that $\psi = \sum_{n\in\mathbb{N}} \langle \psi | \varphi_n \rangle \varphi_n$ for any $\psi \in \mathcal{H}$. Interestingly, L has eigenvalues in $\{1/\lambda_n\}_{n\in\mathbb{N}}$ and the same set of eigenvectors of J, *i.e.* $\mathsf{L}\varphi_n = \frac{1}{\lambda_n}\varphi_n$ for any $n \in \mathbb{N}$. It must be highlighted that L is neither compact nor the inverse of J, since its compactness forbids this, *cf.* [GB15, Proof of Theorem 7.3.6], even though it is also self-adjoint. Thus, it is suggestive taking $(u_n)_{n\in\mathbb{N}}$ as the eigenvalues of L rather than J.

6.2 Self-adjoint Linear Differential Operators

As it has been discussed in the last section, the function nature of the eigenvectors, henceforth called eigenfunctions, suggests taking J as an integral operator whose compactness raises as a natural consequence of its regularisation (smoothing) property on functions. In this case, L is better if taken as a self-adjoint differential operator. In this very particular context, the following results, adapted from [CL55, Chapter 7] regarding a class of self-adjoint differential operators, becomes a powerful tool to construct the kernels.

Proposition 6.1. Consider a compact interval $\mathfrak{V} = [v^-, v^+]$ and a linear differential operator $\mathsf{L} : \mathcal{S} \to L^2_w(\mathfrak{V}, \Sigma_{\mathfrak{V}}, \mu)$ on the form

$$\mathsf{L} = \sum_{m=0}^{M} s_m \frac{d^m}{dv^m} \tag{6.3}$$

for $M \geqslant 1$ and let it be self-adjoint for a subset $\mathcal{S} \subset L^2_w(\mathfrak{V}, \Sigma_{\mathfrak{V}}, \mu) \cap \mathcal{C}^M(\mathfrak{V}; \mathbb{C})$ and coefficient functions $s_m \in \mathcal{C}^m(\mathfrak{V}; \mathbb{C})$. Hence, the following results hold:

Property 6.6. The eigenvalues of L, which are real due to its self-adjointness, form a countable set with no accumulation point [CL55, Chapter 7, Theorem 2.1];

Property 6.7. The eigenfunctions of L, which also are countable due to the above property, form a complete orthogonal set on $L^2_w(\mathfrak{V}, \Sigma_{\mathfrak{V}}, \mu)$ [CL55, Chapter 7, Theorem 4.2].

Although the above results are quite compelling, neither the subset $\mathcal{S}$ nor the functions s_m are determined in the Proposition 6.1. This is most due to the fact that such analysis, which is developed in Section 6.A, is quite mathematically sophisticated to be synthesised in a general form

In light of the above properties, it is natural to consider the eigenvalues and eigenfunctions as candidates for $(u_n)_{n\in\mathbb{N}}$ and $\left\{K(u_n,\cdot)\right\}_{n\in\mathbb{N}}$ respectively, which of course depends on finding a kernel K tying these eigenfunctions together. This Chapter aims to construct those some examples of those kernels.

6.3 First Order Operators

The simplest case of Proposition 6.1 occurs, of course, for the first order differential operators ($M=1$), which shall be analysed in this section. For such end, consider the operator $\mathsf{L}:\mathcal{S}\subset L^2_w(\mathfrak{V},\Sigma_{\mathfrak{V}},\mu)\cap\mathcal{C}^1(\mathfrak{V};\mathbb{C})\to L^2_w(\mathfrak{V},\Sigma_{\mathfrak{V}},\mu)$ defined by

$$\mathsf{L}=\frac{1}{w}\left[s_1\frac{d}{dv}+s_2\right]. \tag{6.4}$$

The construction of the adjoint, as shown in Section 6.A, implies that

$$\mathsf{L}^\dagger=\frac{1}{w}\left[-s_1^*\frac{d}{dv}+(s_2-s_1')^*\right] \tag{6.5}$$

and

$$\mathcal{S}=\left\{\psi\in L^2_w(\mathfrak{V},\Sigma_{\mathfrak{V}},\mu)\cap\mathcal{C}^1(\mathfrak{V};\mathbb{C});\ C^-\Psi\left(v^-\right)+C^+\Psi\left(v^+\right)=\mathbf{0}\right\} \tag{6.6}$$

where the complex constants C^- and C^+ are such that $\psi_A,\psi_B\in\mathcal{S}\implies[s_1\psi_A\psi_B^*]_{\mathfrak{V}}=0\implies s_1(v^+)\left|C^-\right|^2=s_1(v^-)\left|C^+\right|^2$, after some simple algebraic manipulation. L will hence be self-adjoint when

$$-s_1^*=s_1\quad\text{and}\quad(s_2-s_1')^*=s_2 \tag{6.7}$$

which implies in $\mathrm{Re}(s_1)=0\implies s_1=jp$ and $s_2-s_1'=s_2^*\implies s_1'=s_2-s_2^*=2j\,\mathrm{Im}(s_2)\implies\mathrm{Im}(s_2)=\frac{p'}{2}$. Thus,

$$\mathsf{L}=\frac{1}{w}\left[jp\frac{d}{dv}+\left(q+j\frac{p'}{2}\right)\right] \tag{6.8}$$

for arbitrary functions $p\in\mathcal{C}^1(\mathfrak{V};\mathbb{C})$ and $q\in\mathcal{C}^0(\mathfrak{V};\mathbb{C})$.

6.3.1 Unbounded Eigenfunctions

In the context described above, consider the real eigenvalue problem for the case where Equation (6.8) is extended to $L^2_w(\mathfrak{V},\Sigma_{\mathfrak{V}},\mu)\cap\mathcal{C}^1(\mathfrak{V};\mathbb{C})$, *i.e.*, without the boundary conditions. In this direction, the solutions of

$$\frac{1}{w}\left[jp\varphi'+\left(q+j\frac{p'}{2}\right)\varphi\right]=\lambda\varphi \tag{6.9}$$

must be studied where $\varphi(\lambda,\cdot)\in L^2_w(\mathfrak{V},\Sigma_{\mathfrak{V}},\mu)\cap\mathcal{C}^1(\mathfrak{V};\mathbb{C})$ is the eigenfunction associated with the eigenvalue $\lambda\in\mathbb{R}$. Such solutions can be easily achieved by rearranging the last equation as

$$\frac{\varphi'}{\varphi}+\frac{1}{2}\frac{p'}{p}+\frac{q-\lambda w}{jp}=0,$$

which can be integrated yielding

$$\log\frac{\varphi(v)}{\varphi(v^-)}+\frac{1}{2}\log\frac{p(v)}{p(v^-)}+\int_{[v^-,v]}\frac{q-\lambda w}{jp}d\mu=0$$

and, finally,

$$\varphi(\lambda,v)=\varphi\left(\lambda,v^-\right)\sqrt{\frac{p(v^-)}{p(v)}}e^{j(Q(v)+\lambda W(v))}, \tag{6.10}$$

where

$$W(v)=\int_{[v^-,v]}\frac{w}{p}d\mu \quad \text{and} \quad Q(v)=\int_{[v^-,v]}\frac{q}{p}d\mu. \tag{6.11}$$

Of course, one is mostly interested in normalised eigenfunctions. Thus, let $W^+=W(v^+)$ and consider the inner product

$$\begin{aligned}\left\langle\varphi(\lambda_1,\cdot)\middle|\varphi(\lambda_2,\cdot)\right\rangle_{\mathfrak{V}}&=\int_{\mathfrak{V}}\varphi(\lambda_1,\cdot)\,\varphi(\lambda_2,\cdot)^*\,wd\mu\\&=\varphi\left(\lambda_1,v^-\right)\varphi\left(\lambda_2,v^-\right)^*p\left(v^-\right)\int_{\mathfrak{V}}\exp\left(j(\lambda_2-\lambda_1)\int_{[v^-,v]}\frac{w}{p}d\mu\right)\frac{w}{p}d\mu\\&=\varphi\left(\lambda_1,v^-\right)\varphi\left(\lambda_2,v^-\right)^*p\left(v^-\right)\int_{\mathfrak{V}}e^{j(\lambda_2-\lambda_1)W}W'd\mu\\&=\varphi\left(\lambda_1,v^-\right)\varphi\left(\lambda_2,v^-\right)^*p\left(v^-\right)\int_{[0,W^+]}e^{j(\lambda_2-\lambda_1)W}dW\\&=\varphi\left(\lambda_1,v^-\right)\varphi\left(\lambda_2,v^-\right)^*p\left(v^-\right)\cdot W^+e^{j\left(\frac{\lambda_2-\lambda_1}{2}\right)W^+}\operatorname{sinc}\left(\frac{(\lambda_2-\lambda_1)W^+}{2\pi}\right).\end{aligned} \tag{6.12}$$

Thus, $\left\|\varphi(\lambda,\cdot)\right\|_{\mathfrak{V}}^2=\left|\varphi(\lambda,v^-)\right|^2p(v^-)W^+$ and, by considering the abuse of notation $\varphi\leftarrow\varphi/\|\varphi\|_{\mathfrak{V}}$, the normalised eigenfunction is given by

$$\varphi(\lambda,v)=\frac{1}{\sqrt{p(v)W^+}}e^{j\left(Q(v)-\lambda W(v)+\theta(\lambda)\right)}, \tag{6.13}$$

where $\theta(\lambda)$ is an arbitrary phase that rose during the normalisation from the term $\varphi(\lambda,v^-)/|\varphi(\lambda,v^-)|$ and may be seen as a degree of freedom in the eigenfunction.

6.3.2 Completeness Relation

An important aspect of the eigenfunction (6.13) is the fact that it obeys a Completeness relation regarding the eigenvalues. In fact,

$$\begin{aligned}
\left\langle \varphi\left(\cdot, v\right) \middle| \varphi\left(\cdot, s\right) \right\rangle_{\mathfrak{U}} &\stackrel{\text{def}}{=} \int_{\mathfrak{U}} \varphi\left(\cdot, v\right) \varphi\left(\cdot, s\right)^{*} d\mu \\
&= \frac{e^{j(Q(v)-Q(s))}}{W^{+}\sqrt{p\left(v\right) \cdot p\left(s\right)}} \int_{\mathfrak{U}} e^{j(W(s)-W(v))\lambda} d\mu\left(\lambda\right) \\
&= \frac{2\pi e^{j(Q(v)-Q(s))}}{W^{+}\sqrt{p\left(v\right) \cdot p\left(s\right)}} \delta\left(W\left(s\right) - W\left(v\right)\right) \\
&= \frac{2\pi}{p\left(v\right) \cdot W^{+}} \delta\big(W\left(s\right) - W\left(v\right)\big) \\
&= \frac{2\pi}{p\left(v\right) \cdot W^{+} \cdot W'\left(v\right)} \delta\big(s - v\big) \\
&= \frac{2\pi}{w\left(v\right) \cdot W^{+}} \delta\big(v - s\big). \qquad (6.14)
\end{aligned}$$

As discussed in Section 5.B, such result provides several desirable consequences as the orthogonality of the constructors and the Plancherel identity for the reconstructed signal.

6.3.3 Bounded Eigenvalues

The background developed in the last subsections provides the tools to easily determine the eigenvalues and eigenfunctions of the original operator L, which is restricted to $\mathcal{S}$. In this context, the eigenfunctions must obey the boundary conditions

$$C^{-}\varphi\left(\lambda, v^{-}\right) + C^{+}\varphi\left(\lambda, v^{+}\right) = 0, \qquad (6.15)$$

which, from the Equation (6.13), implies that

$$\frac{C^{-}}{\sqrt{p\left(v^{-}\right) W^{+}}} e^{j\left(\theta(\lambda)\right)} + \frac{C^{+}}{\sqrt{p\left(v^{+}\right) W^{+}}} e^{j\left(Q^{+} - \lambda W^{+} + \theta(\lambda)\right)} = 0,$$

since by definition $Q\left(v^{-}\right) = W\left(v^{-}\right) = 0$ and $Q^{+} = Q\left(v^{+}\right)$ and $W^{+} = W\left(v^{+}\right)$. By rearranging the terms, it becomes

$$-\frac{C^{+}}{C^{-}} \sqrt{\frac{p\left(v^{-}\right)}{p\left(v^{+}\right)}} e^{j\left(Q^{+} - \lambda W^{+}\right)} = 1.$$

The self-adjointness condition, as stated in the beginning of this section, requires that $p\left(v^{+}\right)\left|C^{-}\right|^{2} = p\left(v^{-}\right)\left|C^{+}\right|^{2}$. Thus,

$$-\frac{C^{+}}{C^{-}} \sqrt{\frac{p\left(v^{-}\right)}{p\left(v^{+}\right)}} = -\frac{C^{+}}{C^{-}} \sqrt{\frac{\left|C^{-}\right|^{2}}{\left|C^{+}\right|^{2}}} = -\frac{C^{+}/\left|C^{+}\right|}{C^{-}/\left|C^{-}\right|} = e^{j\alpha} \qquad (6.16)$$

where $\alpha - \pi$ is the phase difference between the constants C^{+} and C^{-}. Therefore,

$$e^{j\left(\alpha + Q^{+} - \lambda W^{+}\right)} = 1, \qquad (6.17)$$

whose solutions are, as expected, quantised and given by

$$\alpha + Q^+ - \lambda W^+ = -2n\pi \implies \lambda_n = \frac{2\pi}{W^+}n + \frac{\alpha + Q^+}{W^+} \tag{6.18}$$

where $n \in \mathbb{Z}$.

6.3.4 The Kernel

At this point, it must be already clear that the GST kernel will be given by the unbounded eigenfunction, Equation (6.13), while the sampling points will precisely be the eigenvalues of the self-adjoint operator. In other words,

$$K(u,v) = \frac{1}{\sqrt{p(v)\,W(v^+)}} e^{j\left(Q(v) - uW(v) + \theta(u)\right)} \quad \text{and} \quad u_n = \frac{2\pi}{W(v^+)}n + \frac{\alpha + Q(v^+)}{W(v^+)}, \tag{6.19}$$

where

$$W(v) = \int_{[v^-,v]} \frac{w}{p} d\mu \quad \text{and} \quad Q(v) = \int_{[v^-,v]} \frac{q}{p} d\mu$$

and $p \in L^2_w(\mathfrak{V}, \Sigma_{\mathfrak{V}}, \mu) \cap \mathcal{C}^1(\mathfrak{V}; \mathbb{R}_{>0})$, $q \in L^2_w(\mathfrak{V}, \Sigma_{\mathfrak{V}}, \mu) \cap \mathcal{C}^0(\mathfrak{V}; \mathbb{R})$, $w \in L^2_w(\mathfrak{V}, \Sigma_{\mathfrak{V}}, \mu) \cap \mathcal{C}^0(\mathfrak{V}; \mathbb{R}_{>0})$, whilst $\theta : \mathbb{R} \to \mathbb{R}$ are arbitrary functions and α, v^- and $v^+ > v^-$ are arbitrary real parameters.

The constructor can now be easily calculated as

$$\begin{aligned}
\xi_n(u) &= \left\langle K(u,\cdot) \middle| K(u_n,\cdot) \right\rangle_{\mathfrak{V}} \\
&= \int_{\mathfrak{V}} K(u,\cdot)\, K(u_n,\cdot)\, w d\mu \\
&= \frac{e^{j(\theta(u)-\theta(u_n))}}{W(v^+)} \int_{[0,W(v^+)]} e^{j(u_n-u)W} dW \\
&= \frac{e^{j(\theta(u)-\theta(u_n))}}{W(v^+)} W\left(v^+\right) e^{j\frac{u_n-u}{2}W\left(v^+\right)} \operatorname{sinc}\left(\frac{u_n-u}{2\pi} W\left(v^+\right)\right) \\
&= e^{j(\theta(u)-\theta(u_n))} e^{j\frac{u_n-u}{2}W\left(v^+\right)} \operatorname{sinc}\left(\frac{u_n-u}{2\pi} W\left(v^+\right)\right).
\end{aligned}$$

Since $\frac{u_n-u}{2}W(v^+) = n\pi - \frac{uW\left(v^+\right) - Q\left(v^+\right) - \alpha}{2}$, the constructor can be simply expressed as

$$\xi_n(u) = (-1)^n e^{-j\left(\frac{uW\left(v^+\right) - Q\left(v^+\right) - \alpha}{2} - \theta(u) + \theta(u_n)\right)} \operatorname{sinc}\left(n - \frac{uW(v^+) - Q(v^+) - \alpha}{2\pi}\right). \tag{6.20}$$

6.3.5 WNSST Particularisation

Of course the results of WNSST can be found as a particularisation of the results from the last subsection. In fact, for the following choices

$$p = \frac{1}{2\pi}, \quad w = 1, \quad q = 0, \quad \theta(u) = \frac{uW(v^+) - Q(v^+) - \alpha}{2}, \quad \alpha = 0 \quad \text{and} \quad v^- = -v^+$$

it is easy to show that $W\left(v\right)=2\pi\left(v+v^{+}\right)$, thus $W\left(v^{+}\right)=4\pi v^{+}$, $Q\left(v^{+}\right)=0$ and $\theta\left(u_{n}\right)=n\pi$. Thus, the constructor at Equation (6.20) simply becomes

$$\xi_{n}\left(u\right)=\operatorname{sinc}\left(n-2v^{+}u\right), \tag{6.21}$$

hence retrieving the formula Equation (5.14) as expected. As curiosity, it is interesting to see that the operator L for this very particular case is

$$\mathsf{L}=-\frac{1}{2\pi j}\frac{d}{dv} \tag{6.22}$$

and it operates at the very particular set

$$\mathcal{S}=\left\{\psi\in L_{w}^{2}\left(\mathfrak{V},\Sigma_{\mathfrak{V}},\mu\right)\cap\mathcal{C}^{1}(\mathfrak{V};\mathbb{R})\,;\;\psi\left(-v^{+}\right)=\psi\left(v^{+}\right)\right\}.$$

In other words, it can be said that WNSST is a simple particularisation from the simplest case of the application of GST.

6.3.6 Causal Constructors

The objective of this section is to tune the constructor parameters in order to ensure its causality. For this goal, it will be necessary to beforehand calculate the inverse Fourier Transform Ξ_{n} of the constructor at Equation (6.20). To simplify the equations, consider $\alpha=0$, since it has the same influence of $Q\left(v^{+}\right)$, and $\theta\left(u\right)=0$. Thus,

$$\xi_{n}\left(u\right)=\left(-1\right)^{n}e^{-j\left(\frac{uW\left(v^{+}\right)-Q\left(v^{+}\right)}{2}\right)}\operatorname{sinc}\left(n-\frac{uW\left(v^{+}\right)-Q\left(v^{+}\right)}{2\pi}\right) \tag{6.23}$$

and

$$\begin{aligned}\Xi_{n}\left(\tau\right)&=\int_{\mathbb{R}}\xi_{n}\left(u\right)e^{2\pi ju\tau}du\\&=\left(-1\right)^{n}\int_{\mathbb{R}}\operatorname{sinc}\left(\frac{W\left(v^{+}\right)}{2\pi}u-\frac{Q\left(v^{+}\right)}{2\pi}-n\right)e^{-j\left(\frac{W\left(v^{+}\right)}{2}u-\frac{Q\left(v^{+}\right)}{2}\right)}e^{2\pi ju\tau}du\\&=\left(-1\right)^{n}e^{j\frac{Q\left(v^{+}\right)}{2}}\int_{\mathbb{R}}\operatorname{sinc}\left(\frac{W\left(v^{+}\right)}{2\pi}u-\frac{Q\left(v^{+}\right)}{2\pi}-n\right)e^{2\pi ju\left(\tau-\frac{W\left(v^{+}\right)}{4\pi}\right)}du\end{aligned}$$

By considering a simple change of variable $\mathsf{u} = \frac{W\left(v^+\right)}{2\pi}u - \frac{Q\left(v^+\right)}{2\pi} - n$, the above integral becomes

$$\begin{aligned}
\Xi_n(\tau) &= \frac{2\pi}{W(v^+)}(-1)^n e^{j\frac{Q\left(v^+\right)}{2}} \int_{\mathbb{R}} \operatorname{sinc}(\mathsf{u})\, e^{2\pi j\left(\frac{2\pi}{W\left(v^+\right)}\mathsf{u}+\frac{Q\left(v^+\right)+2\pi n}{W\left(v^+\right)}\right)\left(\tau-\frac{W\left(v^+\right)}{4\pi}\right)} d\mathsf{u} \\
&= \frac{2\pi}{W(v^+)}(-1)^n e^{2\pi j\left(\frac{Q\left(v^+\right)}{4\pi}+\frac{Q\left(v^+\right)+2\pi n}{W\left(v^+\right)}\left(\tau-\frac{W\left(v^+\right)}{4\pi}\right)\right)} \int_{\mathbb{R}} \operatorname{sinc}(\mathsf{u})\, e^{2\pi j\mathsf{u}\left(\frac{2\pi}{W\left(v^+\right)}\tau-\frac{1}{2}\right)} d\mathsf{u} \\
&= \frac{2\pi}{W(v^+)}(-1)^n e^{2\pi j\left(\frac{Q\left(v^+\right)+2\pi n}{W\left(v^+\right)}\tau-\frac{n}{2}\right)} \int_{\mathbb{R}} \operatorname{sinc}(\mathsf{u})\, e^{2\pi j\mathsf{u}\left(\frac{2\pi}{W\left(v^+\right)}\tau-\frac{1}{2}\right)} d\mathsf{u} \\
&= \frac{2\pi}{W(v^+)} e^{2\pi j\frac{Q\left(v^+\right)+2\pi n}{W\left(v^+\right)}\tau} \operatorname{rect}\left(\frac{2\pi}{W(v^+)}\tau - \frac{1}{2}\right). \qquad (6.24)
\end{aligned}$$

The result above is enough to conclude that $\tau < 0$ implies in $\Xi_n(\tau) = 0$, since Ξ_n does not vanish only if $0 < \tau < {}^{W\left(v^+\right)}/_{2\pi}$. Hence, the particular choice of the phase function θ was enough to create a causal constructor.

In light of such result, it is suggestive tuning the parameters in a way that

$$\nu_n = \frac{2\pi}{W(v^+)}n + \frac{Q(v^+)}{W(v^+)}, \qquad (6.25)$$

where $\frac{2\pi}{W\left(v^+\right)}$ is the distance between consecutive sampling frequencies and $Q(v^+)$ is better if taken in a way that $n = 0$ implies in the central frequency of the sampling band, *i.e.* ${}^{Q\left(v^+\right)}/_{W\left(v^+\right)}$ is the central frequency. It is worth highlighting, nevertheless, that since negative frequencies must be considered to reach the causality of the electric field as a whole, the centre of such band is commonly zero implying that $Q(v^+) = 0$ is the better choice and also that Q and q are both the zero function. However, since this choice is not mandatory in the context of the causality of the constructor itself, Q is then kept for completeness. Thus, τ can be taken as the time itself and the time-domain constructor is given by

$$\Xi_n(t) = \frac{2\pi}{W(v^+)} \cdot e^{2\pi j\nu_n t} \cdot \operatorname{rect}\left(\frac{2\pi}{W(v^+)}t - \frac{1}{2}\right). \qquad (6.26)$$

Lastly, it is important to remember from Theorem 5.2 that the constructor above can only be used to represent signals ψ that can be written in the form

$$\psi(\nu) = \frac{1}{\sqrt{W(v^+)}} \int_{v^-}^{v^+} \Psi(v)\, e^{j(Q(v)-\nu W(v))} \frac{w(v)}{\sqrt{p(v)}} dv, \qquad (6.27)$$

for some $\Psi \in L^2_w(\mathfrak{V}, \Sigma_{\mathfrak{V}}, \mu)$. If this is not the case and Equations (6.23) and (6.26) are still used as an attempt to reconstruct the signal, then the result would be a different signal which is commonly interpreted as the original but suffering from undersampling effects. Moreover, if

the inverse Fourier transform Ψ of ψ is taken, then

$$\begin{aligned}\Psi(t) &= \int_{\mathbb{R}} \psi(\nu)\, e^{j2\pi\nu t} d\nu \\ &= \frac{1}{\sqrt{W(v^+)}} \int_{\mathbb{R}} \left[\int_{v^-}^{v^+} \Psi(v)\, e^{j(Q(v)-\nu W(v))} \frac{w(v)}{\sqrt{p(v)}} dv \right] e^{j2\pi\nu t} d\nu \\ &= \frac{1}{\sqrt{W(v^+)}} \int_{v^-}^{v^+} \Psi(v) \left[\int_{\mathbb{R}} e^{j2\pi\nu\left(t-\frac{W(v)}{2\pi}\right)} d\nu \right] e^{jQ(v)} \frac{w(v)}{\sqrt{p(v)}} dv \\ &= \frac{1}{\sqrt{W(v^+)}} \int_{v^-}^{v^+} \Psi(v)\, \delta\left(t - \frac{W(v)}{2\pi}\right) e^{jQ(v)} \frac{w(v)}{\sqrt{p(v)}} dv.\end{aligned}$$

It must be noticed that W is a strictly increasing function since $W' = {}^{w}/_{p} > 0$. Thus, if $t - \frac{W(v)}{2\pi}$ reaches zero, it happens only once and then, from the composition property of delta distribution, it holds that

$$\delta\left(t - \frac{W(v)}{2\pi}\right) = \frac{2\pi}{W'(v)} \delta\left(v - W^{-1}(2\pi t)\right) = \frac{2\pi p(v)}{w(v)} \delta\left(v - W^{-1}(2\pi t)\right). \tag{6.28}$$

Therefore,

$$\begin{aligned}\Psi(t) &= \frac{1}{\sqrt{W(v^+)}} \int_{v^-}^{v^+} \Psi(v) \frac{2\pi p(v)}{w(v)} \delta\left(v - W^{-1}(2\pi t)\right) e^{jQ(v)} \frac{w(v)}{\sqrt{p(v)}} dv \\ &= \frac{2\pi}{\sqrt{W(v^+)}} \int_{v^-}^{v^+} \Psi(v)\, \delta\left(v - W^{-1}(2\pi t)\right) e^{jQ(v)} \sqrt{p(v)} dv \\ &= \begin{cases} 2\pi \sqrt{\frac{p\left(W^{-1}(2\pi t)\right)}{W(v^+)}} \Psi\left(W^{-1}(2\pi t)\right) e^{jQ\left(W^{-1}(2\pi t)\right)}, & \text{if} \quad t \in \left(0, \frac{W(v^+)}{2\pi}\right) \\ 0, & \text{if} \quad t \notin \left(0, \frac{W(v^+)}{2\pi}\right) \end{cases}.\end{aligned} \tag{6.29}$$

As conclusion, this method can only be used to represent signals "band-limited" in time-domain, *i.e.*, the signal must vanish outside the interval $\left(0, \frac{W(v^+)}{2\pi}\right)$.

6.A Contruction of the Adjoint

Consider the differential operator L in Proposition 6.1. The objective of this appendix is to construct the adjoint $\mathsf{L}^\dagger$ and study over which conditions $\mathsf{L} = \mathsf{L}^\dagger$, *i.e.*, L is self-adjoint. For this goal, consider $\psi_A, \psi_B \in \mathcal{S}$ and the following

$$\left\langle \mathsf{L}\psi_A \middle| \psi_B \right\rangle_{\mathfrak{V}} = \int_{\mathfrak{V}} \mathsf{L}\psi_A\ \psi_B^* w d\mu = \sum_{m=0}^{M} \int_{\mathfrak{V}} s_m \psi_A^{(m)} \psi_B^* d\mu. \tag{6.30}$$

For simplicity, also consider the family of auxiliary functions $\zeta_m = s_m\psi_B^*$, from which the integral in the last summation becomes

$$\begin{aligned}
\int_{\mathfrak{V}} s_m\psi_A^{(m)}\psi_B^* d\mu &= \int_{\mathfrak{V}} \psi_A^{(m)}\zeta_m d\mu \\
&= \left[\psi_A^{(m-1)}\zeta_m^{(0)}\right]_{\mathfrak{V}} - \int_{\mathfrak{V}} \psi_A^{(m-1)}\zeta_m^{(1)} d\mu \\
&= \left[\psi_A^{(m-1)}\zeta_m^{(0)}\right]_{\mathfrak{V}} - \left[\psi_A^{(m-2)}\zeta_m^{(1)}\right]_{\mathfrak{V}} + \int_{\mathfrak{V}} \psi_A^{(m-2)}\zeta_m^{(2)} d\mu \\
&= \left[\psi_A^{(m-1)}\zeta_m^{(0)}\right]_{\mathfrak{V}} - \left[\psi_A^{(m-2)}\zeta_m^{(1)}\right]_{\mathfrak{V}} + \cdots + (-1)^{m-1}\left[\psi_A^{(0)}\zeta_m^{(m-1)}\right]_{\mathfrak{V}} + (-1)^m \int_{\mathfrak{V}} \psi_A^{(0)}\zeta_m^{(m)} d\mu \\
&= \left[\sum_{p=0}^{m-1} (-1)^p \psi_A^{(m-1-p)}\zeta_m^{(p)}\right]_{\mathfrak{V}} + (-1)^m \int_{\mathfrak{V}} \psi_A^{(0)}\zeta_m^{(m)} d\mu. \qquad (6.31)
\end{aligned}$$

To simplify the notation on the last equation, it is interesting to define the function matrices

$$\Psi_A = \begin{bmatrix}\psi_A^{(0)} & \psi_A^{(1)} & \psi_A^{(2)} & \cdots & \psi_A^{(M-1)}\end{bmatrix}^{\mathrm{T}} \quad \text{and} \quad Z_m = \begin{bmatrix}\zeta_m^{(0)} & \zeta_m^{(1)} & \zeta_m^{(2)} & \cdots & \zeta_m^{(M-1)}\end{bmatrix}^{\mathrm{T}} \qquad (6.32)$$

and the M-order square matrix

$$W_m = \begin{bmatrix}
0 & 0 & \cdots & 0 & (-1)^{m-1} & \cdots & 0 \\
0 & 0 & \cdots & (-1)^{m-2} & 0 & \cdots & 0 \\
\vdots & \vdots & \ddots & \vdots & \vdots & \ddots & \vdots \\
0 & -1 & \cdots & 0 & 0 & \cdots & 0 \\
1 & 0 & \cdots & 0 & 0 & \cdots & 0 \\
\vdots & \vdots & \ddots & \vdots & \vdots & \ddots & \vdots \\
0 & 0 & \cdots & 0 & 0 & \cdots & 0
\end{bmatrix} \qquad (6.33)$$

so that the last equation can now be rewritten using the quadratic form

$$\int_{\mathfrak{V}} s_m\psi_A^{(m)}\psi_B^* d\mu = \left[\Psi_A^{\mathrm{T}} W_m Z_m\right]_{\mathfrak{V}} + (-1)^m \int_{\mathfrak{V}} \psi_A^{(0)}\zeta_m^{(m)} d\mu. \qquad (6.34)$$

Since the k-derivative of the auxiliary function ζ_m is given by

$$\begin{aligned}
\zeta_m^{(k)} &= \left(s_m\psi_B^*\right)^{(k)} \\
&= \sum_{q=0}^{k} \binom{k}{q} s_m^{(k-q)}\psi_B^{(q)*} \qquad (6.35) \\
&= \left[\binom{k}{0}s_m^{(k)} \quad \binom{k}{1}s_m^{(k-1)} \quad \cdots \quad \binom{k}{k}s_m^{(0)} \quad \cdots \quad 0\right]\Psi_B^*,
\end{aligned}$$

then

$$Z_m = \begin{bmatrix} \binom{0}{0} s_m^{(0)} & 0 & 0 & \cdots & 0 \\ \binom{1}{0} s_m^{(1)} & \binom{1}{1} s_m^{(0)} & 0 & \cdots & 0 \\ \binom{2}{0} s_m^{(2)} & \binom{2}{1} s_m^{(1)} & \binom{2}{2} s_m^{(0)} & \cdots & 0 \\ \vdots & \vdots & \vdots & \ddots & \vdots \\ \binom{M-1}{0} s_m^{(M-1)} & \binom{M-1}{1} s_m^{(M-2)} & \binom{M-1}{2} s_m^{(M-3)} & \cdots & \binom{M-1}{M-1} s_m^{(0)} \end{bmatrix} \Psi_B^* = S_m \Psi_B^*. \tag{6.36}$$

Thus,

$$\int_{\mathfrak{V}} s_m \psi_A^{(m)} \psi_B^* d\mu = \left[\Psi_A^{\mathrm{T}} W_m S_m \Psi_B^* \right]_{\mathfrak{V}} + \int_{\mathfrak{V}} \psi_A \left[\sum_{q=0}^{m} (-1)^m \binom{m}{q} s_m^{(m-q)} \psi_B^{(q)*} \right] d\mu$$

and

$$\begin{aligned} \left\langle \mathsf{L}\psi_A \middle| \psi_B \right\rangle_{\mathfrak{V}} &= \left[\Psi_A^{\mathrm{T}} \left(\sum_{m=0}^{M} W_m S_m \right) \Psi_B^* \right]_{\mathfrak{V}} + \int_{\mathfrak{V}} \psi_A \left[\sum_{m=0}^{M} \sum_{q=0}^{m} (-1)^m \binom{m}{q} s_m^{(m-q)} \psi_B^{(q)*} \right] d\mu \\ &= \left[\Psi_A^{\mathrm{T}} \left(\sum_{m=0}^{M} W_m S_m \right) \Psi_B^* \right]_{\mathfrak{V}} + \int_{\mathfrak{V}} \psi_A \left[\frac{1}{w} \sum_{m=0}^{M} \sum_{q=0}^{m} (-1)^m \binom{m}{q} s_m^{(m-q)*} \psi_B^{(q)} \right]^* w d\mu \\ &= \left[\Psi_A^{\mathrm{T}} \left(\sum_{m=0}^{M} W_m S_m \right) \Psi_B^* \right]_{\mathfrak{V}} + \int_{\mathfrak{V}} \psi_A \left[\frac{1}{w} \sum_{m=0}^{M} \sum_{q=m}^{M} (-1)^q \binom{q}{m} s_q^{(q-m)*} \psi_B^{(m)} \right]^* w d\mu \\ &= \left[\Psi_A^{\mathrm{T}} \left(\sum_{m=0}^{M} W_m S_m \right) \Psi_B^* \right]_{\mathfrak{V}} + \int_{\mathfrak{V}} \psi_A \big(\mathsf{G}\psi_B \big)^* w d\mu \\ &= \left[\Psi_A^{\mathrm{T}} \left(\sum_{m=0}^{M} W_m S_m \right) \Psi_B^* \right]_{\mathfrak{V}} + \left\langle \psi_A \middle| \mathsf{G}\psi_B \right\rangle_{\mathfrak{V}}, \end{aligned} \tag{6.37}$$

where the operator G is defined as

$$\mathsf{G} = \frac{1}{w} \sum_{m=0}^{M} \left[\sum_{q=m}^{M} (-1)^q \binom{q}{m} s_q^{(q-m)*} \right] \frac{d^m}{dv^m}. \tag{6.38}$$

From Equation (6.37), it is possible to conclude that $\mathsf{G} = \mathsf{L}^\dagger$ if the set $\mathcal{S} \subset L_w^2(\mathfrak{V}, \Sigma_{\mathfrak{V}}, \mu) \cap \mathcal{C}^M(\mathfrak{V}; \mathbb{C})$ is such that

$$\psi_A, \psi_B \in \mathcal{S} \implies \left[\Psi_A^{\mathrm{T}} \left(\sum_{m=0}^{M} W_m S_m \right) \Psi_B^* \right]_{\mathfrak{V}} = 0. \tag{6.39}$$

The condition above, although necessary, is not sufficient to determine the set $\mathcal{S}$ and shall hence be thought as a test used to characterise it. In this context, [CL55, Ch. 11, Theorem 3.2] ensures the existence of complex-valued square matrices $C^+, C^- \in \mathbb{C}^{M \times M}$ such that $\mathcal{S}$ can be

taken as the set of all function in $L^2_w(\mathfrak{V}, \Sigma_{\mathfrak{V}}, \mu) \cap \mathcal{C}^M(\mathfrak{V}; \mathbb{C})$ obeying the boundary conditions $C^- \Psi(v^-) + C^+ \Psi(v^+) = \mathbf{0}$. In other words, there exist $C^+, C^- \in \mathbb{C}^{M \times M}$ such that

$$\mathcal{S} = \left\{ \psi \in L^2_w(\mathfrak{V}, \Sigma_{\mathfrak{V}}, \mu) \cap \mathcal{C}^M(\mathfrak{V}; \mathbb{C}) \,;\; C^- \Psi\left(v^-\right) + C^+ \Psi\left(v^+\right) = \mathbf{0} \right\} \tag{6.40}$$

satisfies the condition (6.39), hence ensuring the existence of the adjoint $\mathsf{L}^\dagger$. It must be noticed that $\mathcal{S}$ is actually a subspace of $\psi \in L^2_w(\mathfrak{V}, \Sigma_{\mathfrak{V}}, \mu) \cap \mathcal{C}^M(\mathfrak{V}; \mathbb{C})$ since the null function clearly figures in $\mathcal{S}$ and $\psi_A, \psi_B \in \mathcal{S} \implies \alpha\psi_A + \beta\psi_B \in \mathcal{S}$ for $\alpha, \beta \in \mathbb{C}$.

Once the adjoint exists, it is possible to study how to the family of functions s_m may lead to a self-adjoint differential operator L. In fact, by comparing Equation (6.3) and Equation (6.38), L will be self-adjoint if

$$s_m = \sum_{q=m}^{M} (-1)^q \binom{q}{m} s_q^{(q-m)*}. \tag{6.41}$$

It is important to notice that the condition above is not enough to determine the coefficient functions, but only provides some constraints over them. In fact, it is easy to see that every function s_m has a degree of freedom on its either real or imaginary part depending on M parity.

Chapter 7

Green's Function Construction

Although most of the achieved results in the past chapters have their own meaning and relevance, all of them are actually intermediary conclusions towards the main goal of this work. This chapter is hence dedicated to finally assemble them in a proposed form for the antenna Green's function. In this way, special care must be taken regarding the interpretation of some auxiliary results and the mathematical complexity of such delicate procedure, at which organisation is a valuable asset.

7.1 The Time-domain Modal Basis

From chapter 1, record that the Green's function of the antenna setup has the form

$$\boldsymbol{\mathcal{G}}(\boldsymbol{r},t)=\sum_{n\in\mathbb{Z}}\sum_{\ell\in\mathbb{N}}\sum_{|m|\leqslant\ell}\boldsymbol{\mathcal{G}}_{\ell mn}(\boldsymbol{r},t)\,\boldsymbol{q}_{\ell m}(\nu_n) \tag{7.1}$$

where $\boldsymbol{\mathcal{G}}_{\ell mn}(\boldsymbol{r},t)$ can be thought as an abstract TE and TM response associated with the mode (ℓ,m) and with the frequency ν_n, hence working as a basis for any antenna Green's function that might come to be observed in the same set of $\{\nu_n\}_{n\in\mathbb{Z}}$. In fact, those responses are even orthogonal since

$$\begin{aligned}\boldsymbol{\mathcal{G}}_{\ell mn}(\boldsymbol{r},t)&=\frac{\sqrt{\eta}}{\mathcal{U}_0}\int_{\mathbb{R}}\Big(\kappa(\nu)\,\boldsymbol{Y}_{\ell m}(\theta,\phi)\,\boldsymbol{Z}_\ell\big(\kappa(\nu)\cdot r\big)\cdot\xi_n(\nu)\Big)e^{j2\pi\nu t}d\nu\\&=\frac{2\pi\sqrt{\eta}}{\mathcal{U}_0 c}\,\boldsymbol{Y}_{\ell m}(\theta,\phi)\int_{\mathbb{R}}\nu\boldsymbol{Z}_\ell\left(\frac{2\pi r}{c}\nu\right)\cdot\xi_n(\nu)\,e^{j2\pi\nu t}d\nu,\end{aligned}$$

which inherits the orthogonality of $\boldsymbol{Y}_{\ell m}$. Morover, as it is already suggestive and will soon be seen, each $\boldsymbol{\mathcal{G}}_{\ell mn}$ can be split in a propagating component, hence associated with the far field, and in a reactive component, associated with the near field, in a way that

$$\boldsymbol{\mathcal{G}}_{\ell mn}=\boldsymbol{\mathcal{G}}^{\text{far}}_{\ell mn}+\boldsymbol{\mathcal{G}}^{\text{near}}_{\ell mn}. \tag{7.2}$$

As it has been shown in Section 3.5, such split comes from the a decomposition of the matrix $\boldsymbol{Z}_\ell$ in its radius-decaying degree.

In order to computationally implement such basis, the objective of this section is to analytically calculate the above integral. The best approach to reach such goal is most certainly use

the convolution property of the Fourier transform, inasmuch as $\boldsymbol{Z}_\ell$ and ξ_n come from completely different backgrounds. By doing this, the last equation becomes

$$\boldsymbol{\mathcal{G}}_{\ell mn}(\boldsymbol{r},t) = \frac{2\pi\sqrt{\eta}}{\mathcal{U}_0 c}\,\boldsymbol{Y}_{\ell m}(\theta,\phi)\int_{\mathbb{R}}\mathcal{F}^{-1}(\nu\boldsymbol{Z}_\ell)(t')\cdot\Xi_n(t-t')\,dt', \tag{7.3}$$

where the inverse Fourier transforms $\mathcal{F}^{-1}(\nu\boldsymbol{Z}_\ell)$ and Ξ_n have already been calculated in Equation (3.64) and Equation (6.26), respectively. From first result, it must be noticed that

$$\begin{aligned}\int_{\mathbb{R}}\mathcal{F}^{-1}(\nu\boldsymbol{Z}_\ell)(t')\cdot\Xi_n(t-t')\,dt' &= \frac{c}{j4\pi^2 r}\int_{\mathbb{R}}\partial_t\boldsymbol{Z}_\ell\left(r,\frac{ct'}{2\pi r}-\frac{1}{2\pi}\right)\cdot\operatorname{sgn}\left(\frac{ct'}{2\pi r}-\frac{1}{2\pi}\right)\cdot\Xi_n(t-t')\,dt'\\ &\quad+\frac{1}{j\pi}\int_{\mathbb{R}}\boldsymbol{Z}_\ell\left(r,\frac{ct'}{2\pi r}-\frac{1}{2\pi}\right)\cdot\delta\left(t'-\frac{r}{c}\right)\cdot\Xi_n(t-t')\,dt'\\ &= \frac{c}{j4\pi^2 r}\int_{r/c}^{\infty}\partial_t\boldsymbol{Z}_\ell\left(r,\frac{ct'}{2\pi r}-\frac{1}{2\pi}\right)\cdot\Xi_n(t-t')\,dt'\\ &\quad+\frac{1}{j\pi}\boldsymbol{Z}_\ell(r,0)\cdot\Xi_n\left(t-\frac{r}{c}\right).\end{aligned}$$

Thus,

$$\boldsymbol{\mathcal{G}}_{\ell mn}(\boldsymbol{r},t) = \frac{2\sqrt{\eta}}{j\mathcal{U}_0 c}\,\boldsymbol{Y}_{\ell m}(\theta,\phi)\left[\boldsymbol{Z}_\ell(r,0)\cdot\Xi_n\left(t-\frac{r}{c}\right)+\frac{c}{4\pi r}\int_{r/c}^{\infty}\partial_t\boldsymbol{Z}_\ell\left(r,\frac{ct'}{2\pi r}-\frac{1}{2\pi}\right)\cdot\Xi_n(t-t')\,dt'\right]. \tag{7.4}$$

Each of the two terms of the right hand side of the equation above will now be separately studied.

7.1.1 First Term

The definition of the matrix $\boldsymbol{Z}_\ell(r,\tau)$, Equation (3.62), yields that

$$\boldsymbol{Z}_\ell(r,0) = j^\ell\frac{c}{2r}\begin{bmatrix}0 & 0\\ -1 & 0\\ 0 & j\end{bmatrix}$$

and, from Equation (6.26), it holds that

$$\boldsymbol{Z}_\ell(r,0)\cdot\Xi_n\left(t-\frac{r}{c}\right)\overset{\text{a.e.}}{=}\begin{cases}\dfrac{\pi c j^\ell}{W(v^+)}\begin{bmatrix}0 & 0\\ -1 & 0\\ 0 & j\end{bmatrix}\dfrac{e^{2\pi j\nu_n\left(t-\frac{r}{c}\right)}}{r}, & \text{if}\quad t\in\left(\frac{r}{c},\frac{r}{c}+\frac{W(v^+)}{2\pi}\right)\\ 0, & \text{if}\quad t\notin\left(\frac{r}{c},\frac{r}{c}+\frac{W(v^+)}{2\pi}\right)\end{cases}. \tag{7.5}$$

The above equation makes it clear the local characteristic of the sampling method used, *i.e.*, the impulse response has a pulse-like aspect as already expected. Moreover, it is straightforward to conclude that such term is associated with the propagation of the far-field.

7.1.2 Second Term

The calculation of the integral term is slightly more sophisticated and requires more steps. Firstly, it must be noticed that

$$\frac{c}{4\pi r}\int_{r/c}^{\infty}\partial_t\boldsymbol{\mathcal{Z}}_\ell\left(r,\frac{ct'}{2\pi r}-\frac{1}{2\pi}\right)\cdot\Xi_n\left(t-t'\right)dt' = \frac{c}{2W\left(v^+\right)}\frac{e^{2\pi j\nu_n t}}{r}\cdot\text{step}\left(t-\frac{r}{c}\right)\cdot\int_{t_0}^{t}\partial_t\boldsymbol{\mathcal{Z}}_\ell\left(r,\frac{ct'}{2\pi r}-\frac{1}{2\pi}\right)\cdot e^{-2\pi j\nu_n t'}dt' \quad (7.6)$$

where $t_0=\max\left(\frac{r}{c},t-\frac{W\left(v^+\right)}{2\pi}\right)$. By taking $\tau'=\frac{ct'}{2\pi r}-\frac{1}{2\pi}$, it holds that $t'=\frac{2\pi r}{c}\left(\tau'+\frac{1}{2\pi}\right)$ and the last integral becomes

$$\int_{t_0}^{t}\partial_t\boldsymbol{\mathcal{Z}}_\ell\left(r,\frac{ct'}{2\pi r}-\frac{1}{2\pi}\right)\cdot e^{-2\pi j\nu_n t'}dt' = \frac{2\pi r}{c}\int_{\tau_0}^{\tau}\partial_t\boldsymbol{\mathcal{Z}}_\ell\left(r,\tau'\right)\cdot e^{-2\pi j\nu_n\cdot\frac{2\pi r}{c}\left(\tau'+\frac{1}{2\pi}\right)}d\tau'$$
$$= \frac{2\pi r}{c}e^{-2\pi j\nu_n\cdot\frac{r}{c}}\int_{\tau_0}^{\tau}\partial_t\boldsymbol{\mathcal{Z}}_\ell\left(r,\tau'\right)\cdot e^{-j\frac{4\pi^2 r}{c}\nu_n\tau'}d\tau'$$

where

$$\tau_0=\frac{c}{2\pi r}\max\left(\frac{r}{c},t-\frac{W\left(v^+\right)}{2\pi}\right)-\frac{1}{2\pi}\quad\text{and}\quad\tau=\frac{c}{2\pi r}t-\frac{1}{2\pi}. \quad (7.7)$$

Thus,

$$\frac{c}{4\pi r}\int_{r/c}^{\infty}\partial_t\boldsymbol{\mathcal{Z}}_\ell\left(r,\frac{ct'}{2\pi r}-\frac{1}{2\pi}\right)\cdot\Xi_n\left(t-t'\right)dt' = \frac{\pi e^{2\pi j\nu_n\left(t-\frac{r}{c}\right)}}{W\left(v^+\right)}\text{step}\left(t-\frac{r}{c}\right)\int_{\tau_0}^{\tau}\partial_t\boldsymbol{\mathcal{Z}}_\ell\left(r,\tau'\right)\cdot e^{-j\frac{4\pi^2 r}{c}\nu_n\tau'}d\tau'. \quad (7.8)$$

The polynomial nature of $\partial_t\boldsymbol{\mathcal{Z}}_\ell\left(r,\cdot\right)$ at its definition and the result registered in Equation (7.39) implies that

$$\frac{c}{4\pi r}\int_{r/c}^{\infty}\partial_t\boldsymbol{\mathcal{Z}}_\ell\left(r,\frac{ct'}{2\pi r}-\frac{1}{2\pi}\right)\cdot\Xi_n\left(t-t'\right)dt' = \frac{\pi}{W\left(v^+\right)}\frac{e^{2\pi j\nu_n\left(t-\frac{r}{c}\right)}}{r^2}\text{step}\left(t-\frac{r}{c}\right)\left[\mathsf{Z}_{\ell n}\left(r,\tau\right)e^{-\frac{j4\pi^2 r\nu_n}{c}\tau}-\mathsf{Z}_{\ell n}\left(r,\tau_0\right)e^{-\frac{j4\pi^2 r\nu_n}{c}\tau_0}\right], \quad (7.9)$$

for a function matrix $\mathsf{Z}_{\ell n}$ that does not have zeros at $r=0$, but bears poles at all orders less than or equal to ℓ. With the last conclusion, it becomes clear tha the second term is the one associated with the near field, as expected.

7.2 Time-domain Propagating Wave

A quick consideration of the first term of $\boldsymbol{\mathcal{G}}_{\ell mn}$ leads to the conclusion that

$$\boldsymbol{\mathcal{G}}^{\text{far}}_{\ell mn}(\boldsymbol{r},t) \overset{\text{a.e.}}{=} \begin{cases} \dfrac{2\pi}{\mathcal{U}_0 W(v^+)} \dfrac{e^{2\pi j\nu_n\left(t-\frac{r}{c}\right)}}{r} \boldsymbol{T}_{\ell m}(\theta,\phi), & \text{if} \quad t \in \left(\frac{r}{c}, \frac{r}{c}+\frac{W\left(v^+\right)}{2\pi}\right) \\ 0, & \text{if} \quad t \notin \left(\frac{r}{c}, \frac{r}{c}+\frac{W\left(v^+\right)}{2\pi}\right) \end{cases} \tag{7.10}$$

and, consequently that

$$\begin{aligned} \boldsymbol{\mathcal{G}}^{\text{far}}(\boldsymbol{r},t) &= \sum_{n\in\mathbb{Z}} \sum_{\ell\in\mathbb{N}} \sum_{|m|\leqslant\ell} \boldsymbol{\mathcal{G}}^{\text{far}}_{\ell mn}(\boldsymbol{r},t)\, \boldsymbol{q}_{\ell m}(\nu_n) \\ &= \begin{cases} \dfrac{2\pi}{\mathcal{U}_0 W(v^+)} \dfrac{1}{r} \displaystyle\sum_{n\in\mathbb{Z}} \mathtt{E}(\theta,\phi,\nu_n)\, e^{2\pi j\nu_n\left(t-\frac{r}{c}\right)}, & \text{if} \quad t \in \left(\frac{r}{c}, \frac{r}{c}+\frac{W\left(v^+\right)}{2\pi}\right) \\ 0, & \text{if} \quad t \notin \left(\frac{r}{c}, \frac{r}{c}+\frac{W\left(v^+\right)}{2\pi}\right) \end{cases}. \end{aligned} \tag{7.11}$$

Several interesting conclusions can be taken from the last result.

The first, and most obvious, regards the causality where the fact that both r and $W(v^+)$ are positive implies that a non-positive time will never figure in the interval $\left(\frac{r}{c}, \frac{r}{c}+\frac{W\left(v^+\right)}{2\pi}\right)$ and, therefore, $t \leqslant 0 \implies \boldsymbol{\mathcal{G}}^{\text{far}}(\boldsymbol{r},t) = 0$, as requested by design.

A second interesting result is the pulse-like form of such field whose energy at the time $t > 0$ is completely concentrated at the spherical shell defined by

$$ct - c\frac{W(v^+)}{2\pi} < r < ct. \tag{7.12}$$

From which it becomes clear that the term ct determines the distance of the wavefront at the time t, as expected, but naturally obtained, while $ct - {}^{cW\left(v^+\right)}/_{2\pi}$ must be understood as how far into the future of the wave it is possible to see with the frequency resolution of $\frac{2\pi}{W(v^+)}$ (refer to the final comments of subsection 6.3.6), hence working as a "spatial prediction horizon" of the sampling method.

Moreover, since $\nu_n = \frac{2\pi}{W(v^+)} n$ linearly depends on n (refer to Equation (6.25)), the expression

$$\frac{2\pi}{\mathcal{U}_0 W(v^+)} \frac{1}{r} \sum_{n\in\mathbb{Z}} \mathtt{E}(\theta,\phi,\nu_n)\, e^{2\pi j\nu_n\left(t-\frac{r}{c}\right)}$$

is precisely the Fourier series of the far-field Green's function $\boldsymbol{\mathcal{G}}^{\text{far}}(\boldsymbol{r},\cdot)$ inside the prediction interval. Besides, the hermitianess of $\mathtt{E}$ implies that positive and negative frequencies can be

combined as

$$\begin{aligned}\sum_{n\in\mathbb{Z}}\mathtt{E}\left(\theta,\phi,\nu_n\right)e^{2\pi j\nu_n\left(t-\frac{r}{c}\right)} &= \sum_{n\in\mathbb{N}}\mathtt{E}\left(\theta,\phi,\nu_n\right)e^{2\pi j\nu_n\left(t-\frac{r}{c}\right)}+\sum_{n\in\mathbb{N}}\mathtt{E}\left(\theta,\phi,-\nu_n\right)e^{-2\pi j\nu_n\left(t-\frac{r}{c}\right)}\\ &= \sum_{n\in\mathbb{N}}\mathtt{E}\left(\theta,\phi,\nu_n\right)e^{2\pi j\nu_n\left(t-\frac{r}{c}\right)}+\sum_{n\in\mathbb{N}}\left[\mathtt{E}\left(\theta,\phi,\nu_n\right)e^{2\pi j\nu_n\left(t-\frac{r}{c}\right)}\right]^*\\ &= \sum_{n\in\mathbb{N}}\mathtt{E}\left(\theta,\phi,\nu_n\right)e^{2\pi j\nu_n\left(t-\frac{r}{c}\right)}+\left[\sum_{n\in\mathbb{N}}\mathtt{E}\left(\theta,\phi,\nu_n\right)e^{2\pi j\nu_n\left(t-\frac{r}{c}\right)}\right]^*\\ &= 2\,\mathrm{Re}\left(\sum_{n\in\mathbb{N}}\mathtt{E}\left(\theta,\phi,\nu_n\right)e^{2\pi j\nu_n\left(t-\frac{r}{c}\right)}\right).\end{aligned}$$

Finally, the propagating Green's function of the antenna has the form

$$\boldsymbol{\mathcal{G}}^{\mathrm{far}}\left(\boldsymbol{r},t\right)=\frac{4\pi}{\mathcal{U}_0W\left(v^+\right)}\frac{1}{r}\,\mathrm{Re}\left(\sum_{n\in\mathbb{N}}\mathtt{E}\left(\theta,\phi,\nu_n\right)e^{2\pi j\nu_n\left(t-\frac{r}{c}\right)}\right),\quad t\in\left(\frac{r}{c},\frac{r}{c}+\frac{W\left(v^+\right)}{2\pi}\right).\tag{7.13}$$

Although the result above seems to be quite simple, it is important to stress that it can only be directly used when (θ,ϕ) lies in the set $\{(\theta_i,\phi_i)\}_{i\in\mathbb{N}_{\leqslant M}}$ of collected directions as described at Section 4.2.For any other case, it is worth using again the definition of $\mathtt{E}$, Equation (3.29), to see that

$$\begin{aligned}\boldsymbol{\mathcal{G}}^{\mathrm{far}}\left(\boldsymbol{r},t\right) &= \frac{4\pi}{\mathcal{U}_0W\left(v^+\right)}\frac{1}{r}\,\mathrm{Re}\left(\sum_{n\in\mathbb{N}}\sum_{\ell\in\mathbb{N}}\sum_{|m|\leqslant\ell}\boldsymbol{T}_{\ell m}\left(\theta,\phi\right)\boldsymbol{q}_{\ell m}\left(\nu_n\right)e^{2\pi j\nu_n\left(t-\frac{r}{c}\right)}\right)\\ &= \frac{4\pi}{\mathcal{U}_0W\left(v^+\right)}\frac{1}{r}\,\mathrm{Re}\left(\sum_{\ell\in\mathbb{N}}\sum_{|m|\leqslant\ell}\boldsymbol{T}_{\ell m}\left(\theta,\phi\right)\sum_{n\in\mathbb{N}}\boldsymbol{q}_{\ell m}\left(\nu_n\right)e^{2\pi j\nu_n\left(t-\frac{r}{c}\right)}\right).\end{aligned}$$

Finally, it is possible to conclude that

$$\boldsymbol{\mathcal{G}}^{\mathrm{far}}\left(\boldsymbol{r},t\right)=\begin{cases}\dfrac{4\pi}{\mathcal{U}_0W\left(v^+\right)}\dfrac{1}{r}\,\mathrm{Re}\left(\displaystyle\sum_{\ell\in\mathbb{N}}\sum_{|m|\leqslant\ell}\boldsymbol{T}_{\ell m}\left(\theta,\phi\right)\boldsymbol{Q}_{\ell m}\left(t-\frac{r}{c}\right)\right), & \text{if}\quad t\in\left(\frac{r}{c},\frac{r}{c}+\frac{W\left(v^+\right)}{2\pi}\right)\\ 0, & \text{if}\quad t\notin\left(\frac{r}{c},\frac{r}{c}+\frac{W\left(v^+\right)}{2\pi}\right)\end{cases}\tag{7.14}$$

where

$$\boldsymbol{Q}_{\ell m}\left(t\right)=\sum_{n\in\mathbb{N}}\boldsymbol{q}_{\ell m}\left(\nu_n\right)e^{2\pi j\nu_n t}\tag{7.15}$$

is the retarded Fourier series of the mode $\boldsymbol{q}_{\ell m}$. The Equations (7.14) and (7.15) can be seen as the main results of this work regarding the propagating Green's function of the antenna.

7.3 Signal Wave

In this section, the obtained propagating Green's function will be used to determine the antenna response $\boldsymbol{\mathcal{E}}\left(\boldsymbol{r},t\right)$ to an arbitrary time-domain put $\mathcal{U}:\mathbb{R}\to\mathbb{R}$. For such goal, record

from Equation (1.2) that

$$\boldsymbol{\mathcal{E}}\left(\boldsymbol{r},t\right)=\int_{\mathbb{R}}\boldsymbol{\mathcal{G}}\left(\boldsymbol{r},t'\right)\mathcal{U}\left(t-t'\right)dt'. \tag{7.16}$$

Therefore and since $\mathcal{U}$ is a real signal, it holds that

$$\begin{aligned}\boldsymbol{\mathcal{E}}\left(\boldsymbol{r},t\right)&=\frac{4\pi}{\mathcal{U}_0W\left(v^+\right)}\frac{1}{r}\operatorname{Re}\left(\sum_{\ell\in\mathbb{N}}\sum_{|m|\leqslant\ell}\boldsymbol{T}_{\ell m}\left(\theta,\phi\right)\int_{r/c}^{r/c+W\left(v^+\right)/2\pi}\boldsymbol{Q}_{\ell m}\left(t'-\frac{r}{c}\right)\mathcal{U}\left(t-t'\right)dt'\right)\\&=\frac{4\pi}{\mathcal{U}_0W\left(v^+\right)}\frac{1}{r}\operatorname{Re}\left(\sum_{\ell\in\mathbb{N}}\sum_{|m|\leqslant\ell}\boldsymbol{T}_{\ell m}\left(\theta,\phi\right)\sum_{n\in\mathbb{N}}\boldsymbol{q}_{\ell m}\left(\nu_n\right)\int_{\frac{r}{c}}^{\frac{r}{c}+\frac{W\left(v^+\right)}{2\pi}}\mathcal{U}\left(t-t'\right)e^{2\pi j\nu_n\left(t'-\frac{r}{c}\right)}dt'\right)\\&=\frac{4\pi}{\mathcal{U}_0W\left(v^+\right)}\frac{1}{r}\operatorname{Re}\left(\sum_{\ell\in\mathbb{N}}\sum_{|m|\leqslant\ell}\boldsymbol{T}_{\ell m}\left(\theta,\phi\right)\sum_{n\in\mathbb{N}}\boldsymbol{q}_{\ell m}\left(\nu_n\right)e^{2\pi j\nu_n\left(t-\frac{r}{c}\right)}\int_{t-\frac{r}{c}-\frac{W\left(v^+\right)}{2\pi}}^{t-\frac{r}{c}}\mathcal{U}\left(\tau\right)e^{-2\pi j\nu_n\tau}d\tau\right).\end{aligned}$$

To simplify the above result, consider the definition of auxiliary time-domain functions:

$$\mathscr{U}_n\left(t\right)=\int_{t-\frac{W\left(v^+\right)}{2\pi}}^{t}\mathcal{U}\left(\tau\right)e^{-2\pi j\nu_n\tau}d\tau \tag{7.17}$$

and

$$\boldsymbol{\mathcal{U}}_{\ell m}\left(t\right)=\sum_{n\in\mathbb{N}}\boldsymbol{q}_{\ell m}\left(\nu_n\right)\mathscr{U}_n\left(t\right)e^{2\pi j\nu_nt}. \tag{7.18}$$

Finally, the electric field will be hence given by

$$\boldsymbol{\mathcal{E}}\left(\boldsymbol{r},t\right)=\frac{4\pi}{\mathcal{U}_0W\left(v^+\right)}\frac{1}{r}\operatorname{Re}\left(\sum_{\ell\in\mathbb{N}}\sum_{|m|\leqslant\ell}\boldsymbol{T}_{\ell m}\left(\theta,\phi\right)\boldsymbol{\mathcal{U}}_{\ell m}\left(t-\frac{r}{c}\right)\right). \tag{7.19}$$

From a mathematical or theoretical perspective, the last three equations, as an algorithm, shall be considered the main result of this work. In practice, nevertheless, some aspects must be punctuated. The most obvious, regarding the fact the ℓ must be truncated has already be discussed in chapter 4. Another issue regards not only the truncation of the frequency, but also the fact that the lowest collected frequency is certainly different from $2\pi/W\left(v^+\right)$. Such issue is discussed in the next section.

As a final thought regarding the above equations, it is interesting to notice that $2\pi/W\left(v^+\right)$ works as a time-resolution of the method in the sense that it is only sensible to inputs whose dynamics change faster than that value. In order to clarify this fact, consider once again Equation (7.17) and notice that if the input is practically constant at the interval $\left[t-W\left(v^+\right)/2\pi,t\right]$,

then the integral can be approximated as

$$\begin{aligned}\mathscr{U}_n(t) &= \mathcal{U}(t)\left(-\frac{e^{-2\pi j\nu_n t}}{2\pi j\nu_n} + \frac{e^{-2\pi j\nu_n\left(t-\frac{W\left(v^+\right)}{2\pi}\right)}}{2\pi j\nu_n}\right)\\ &= \mathcal{U}(t)\frac{e^{-2\pi j\nu_n t}}{2\pi j\nu_n}\left(e^{j\nu_n W\left(v^+\right)}-1\right)\\ &= 0\end{aligned} \tag{7.20}$$

since $\nu_n W(v^+) = 2\pi n$. Thus, $\boldsymbol{\mathcal{U}}_{\ell m}(t) = 0$ and $\boldsymbol{\mathcal{E}}(\boldsymbol{r}, t) = \mathbf{0}$, as expected, highlighting the fact that the antenna works as a band-pass filter which is sensible to changes in its input. In other words, if the sampling frequencies are poorly chosen, *i.e.*, ${}^{2\pi}/_{W\left(v^+\right)}$ is high, then ${}^{W\left(v^+\right)}/_{2\pi}$ could be so small that the method could not perceive changes in the input.

7.4 Pulse-like Inputs

Commonly, it is the case where the input $\mathcal{U}$ bears a pulse-like form in a way that it can be rewritten as

$$\mathcal{U}(t) = \widetilde{\mathcal{U}}(t)\,\mathrm{rect}\left(\frac{t-t_\circ}{T}-\frac{1}{2}\right) \overset{\text{a.e.}}{=} \begin{cases}\widetilde{\mathcal{U}}(t), & \text{if} \quad t\in(t_\circ, t_\circ+T)\\ 0, & \text{if} \quad t\notin(t_\circ, t_\circ+T)\end{cases} \tag{7.21}$$

for some $\widetilde{\mathcal{U}}:\mathbb{R}\to\mathbb{R}$ where $t_\circ\in\mathbb{R}$ is the initial time of the pulse and T is its duration, which must be less than ${}^{W\left(v^+\right)}/_{2\pi}$ to avoid overlapping as it has been explained in subsection 6.3.6. In that case, it is worth developing Equation (7.17) a bit further by noticing that

$$\mathscr{U}_n(t) = \begin{cases}\displaystyle\int_{t_{\min}}^{t_{\max}}\widetilde{\mathcal{U}}(\tau)\,e^{-2\pi j\nu_n\tau}d\tau, & \text{if} \quad t_{\min}<t_{\max}\\ 0, & \text{if} \quad t_{\min}\geqslant t_{\max}\end{cases} = \mathrm{step}\left(\frac{t_{\max}}{t_{\min}}-1\right)\int_{t_{\min}}^{t_{\max}}\widetilde{\mathcal{U}}(\tau)\,e^{-2\pi j\nu_n\tau}d\tau \tag{7.22}$$

where

$$t_{\min} = \max\left(t-\frac{W(v^+)}{2\pi}, t_\circ\right) \quad \text{and} \quad t_{\max} = \min\left(t, t_\circ+T\right). \tag{7.23}$$

The last result makes it clear that it is important to beforehand calculate, or at least computationally estimate, integrals on the form

$$I_n(a,b) = \mathrm{step}\left(\frac{b}{a}\right)\int_a^{a+b}\widetilde{\mathcal{U}}(\tau)\,e^{-2\pi j\nu_n\tau}d\tau \tag{7.24}$$

to precisely apply the algorithm. For example, for the particular case where

$$\widetilde{\mathcal{U}}(t) = \cos\left(2\pi\nu t+\beta\right), \tag{7.25}$$

it holds that

$$
\begin{aligned}
I_n(a,b) &= \text{step}\left(\frac{b}{a}\right)\int_a^{a+b}\cos\left(2\pi\nu\tau+\beta\right)e^{-2\pi j\nu_n\tau}d\tau \\
&= \text{step}\left(\frac{b}{a}\right)\int_a^{a+b}\left(\frac{e^{j(2\pi\nu\tau+\beta)}+e^{-j(2\pi\nu\tau+\beta)}}{2}\right)e^{-2\pi j\nu_n\tau}d\tau \\
&= \text{step}\left(\frac{b}{a}\right)\int_a^{a+b}\left(\frac{e^{j(2\pi(\nu-\nu_n)\tau+\beta)}+e^{-j(2\pi(\nu+\nu_n)\tau+\beta)}}{2}\right)d\tau \\
&= \text{step}\left(\frac{b}{a}\right)\left(\frac{e^{j\beta}}{2}\left[\frac{e^{2\pi j(\nu-\nu_n)\tau}}{j\left(2\pi\left(\nu-\nu_n\right)\right)}\right]_a^{a+b}-\frac{e^{-j\beta}}{2}\left[\frac{e^{-2\pi j(\nu+\nu_n)\tau}}{j\left(2\pi\left(\nu+\nu_n\right)\right)}\right]_a^{a+b}\right) \\
&= \frac{b}{2}\text{step}\left(\frac{b}{a}\right)\left[e^{j\left(2\pi(\nu-\nu_n)\left(a+\frac{b}{2}\right)+\beta\right)}\text{sinc}\big(\left(\nu-\nu_n\right)b\big)+e^{-j\left(2\pi(\nu+\nu_n)\left(a+\frac{b}{2}\right)+\beta\right)}\text{sinc}\big(\left(\nu+\nu_n\right)b\big)\right]
\end{aligned}
\tag{7.26}
$$

7.5 Phase Correction at Implementation

Although the frequencies $\{\nu_n\}_{n\in\mathbb{N}}$ of the samples are known beforehand, it is most likely that during the implementation of Equations (7.17) and (7.18) the formula $\nu_n = \frac{2\pi}{W(v^+)}n$ is preferred. In this scenario, one might be led to think that $n=1$ correspond to the first frequency on the collected data and so on. However, this is not true. It important to remember that due to the causality requirements, negative frequencies had to be included in the frequency band. In this case, the band becomes symmetric with respect to zero and the collected frequencies figure at the edges of this band. Therefore, the minimum collected frequency probably has a very high index.

In order to prevent confusion, it is interesting to normalise those indices. Firstly, let n_1 denote the index of the lowest collected sample and notice that for any frequency less than the ν_{n_1}, $\boldsymbol{q}_{\ell m}$ is taken as zero since no energy is associated with such frequency. Then, Equation (7.18) can be rewritten as

$$
\boldsymbol{\mathcal{U}}_{\ell m}(t) = \sum_{n\in\mathbb{N}_{\geqslant n_1}}\boldsymbol{q}_{\ell m}(\nu_n)\,\mathscr{U}_n(t)\,e^{2\pi j\nu_n t}
$$

and to avoid the inconvenient of dealing with those high indices, a shift is performed on them in a way that the frequency is redefined as

$$
\nu_n = \nu_{n_1} + \frac{2\pi}{W(v^+)}(n-1). \tag{7.27}
$$

With this new definition, Equations (7.17) and (7.18) became valid once again.

7.6 Results

To analyse the obtained algorithm, it has been used the same set of data considered in the estimation at Section 4.5. For those data, $^{2\pi}/_{W(v^+)} = 1\,\text{GHz}$ hence implying a temporal resolution of 1 ns for the method. Moreover, an input of the form

$$\mathcal{U}(t) = 1\,\text{V} \cdot \cos\left(2\pi \cdot 260\,\text{GHz} \cdot t + \frac{\pi}{2}\right) \cdot \text{rect}\left(\frac{t - t_\circ}{T} - \frac{1}{2}\right) \tag{7.28}$$

where $t_\circ = {}^{2}/_{260\,\text{GHz}} = 7.69\,\text{ps}$ and $T = {}^{5}/_{260\,\text{GHz}} = 19.23\,\text{ps}$.

The vertical and horizontal components of the time-domain electric field were then evaluated over a period of 9 ns at the direction $(\theta, \phi) = (36.0°, 0.0°)$ and at a distance $r = 2\,\text{m}$ from the antenna. As result, Figure 7.1 shows the overall panorama, from which it is clear the that the causality of the antenna model is preserved, while figures 7.2 and 7.3 care to show the a time-zoomed form of Figure 7.1 focused on the input and output respectively.

It is interesting noticing the time-width of the response in comparison to the input, highlighting the fact that the field in that particular point is the resulted filed produced by infinitely many emitters on the antenna surface hence spanning from the time when the closest emitter starts to emit to the time where the furthest emitter cease its emission.

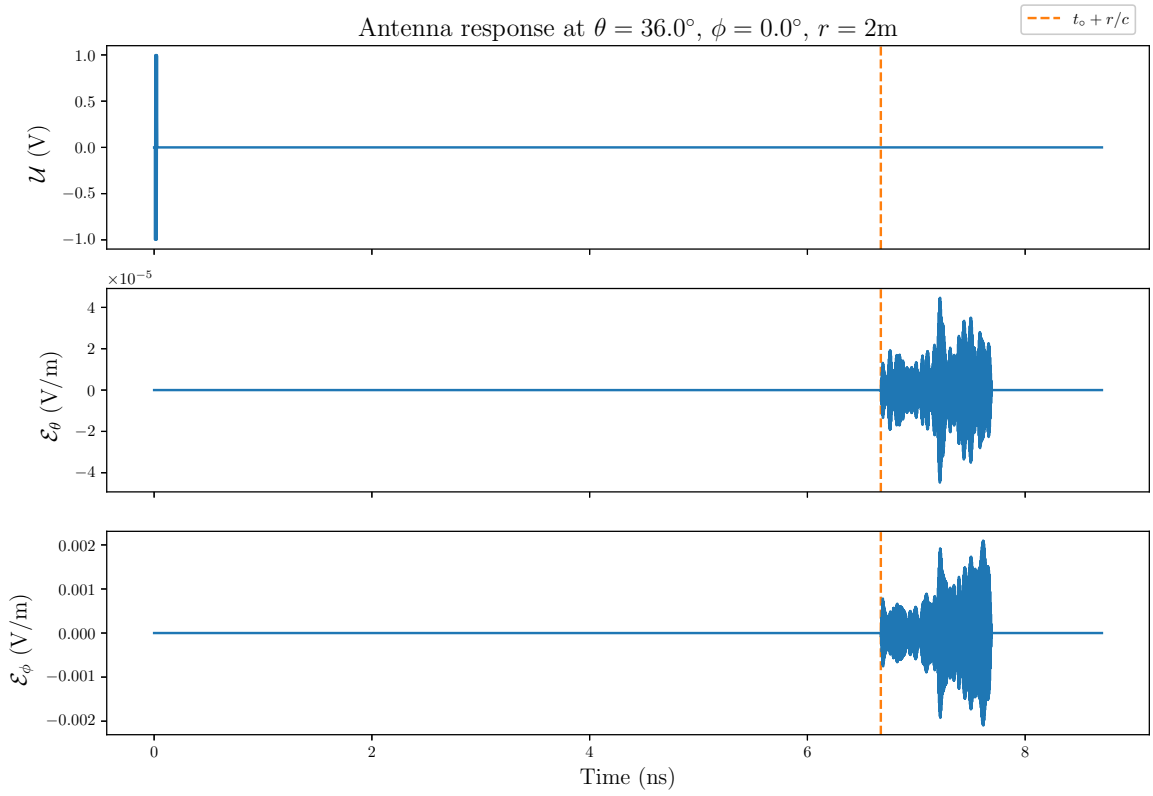

Figure 7.1: Overall depiction of the Antenna response at a distance of 2 m.

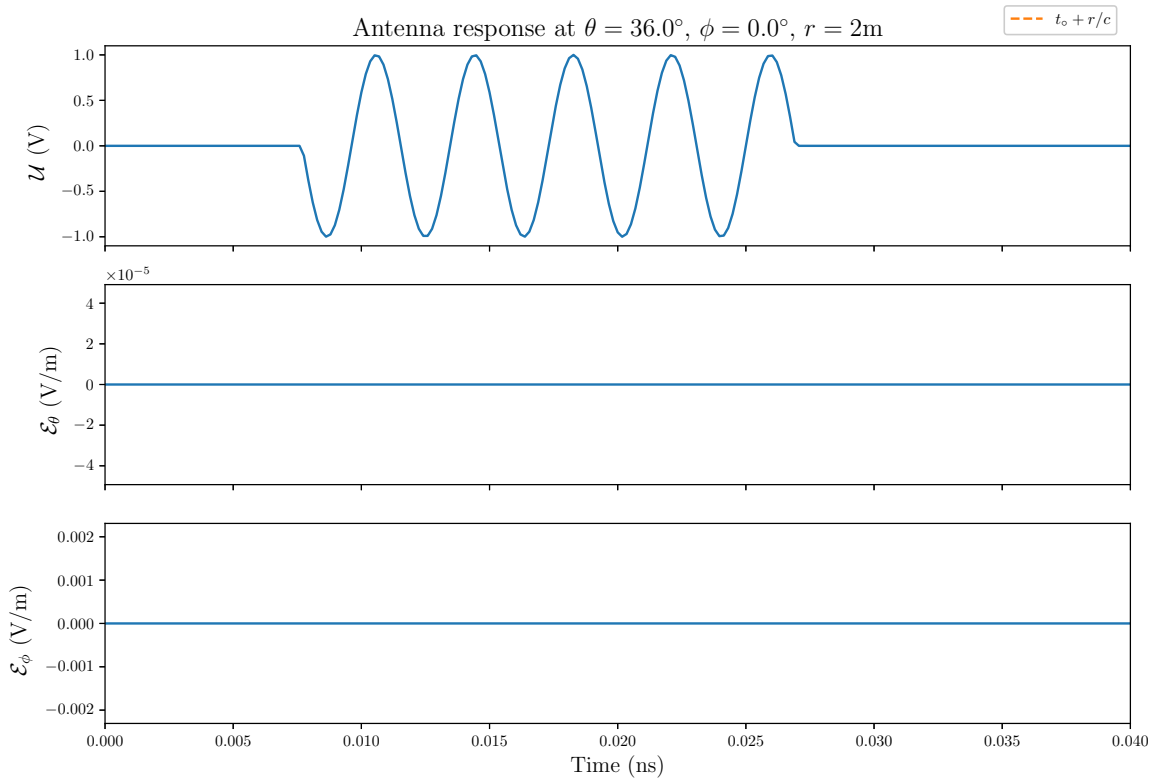

Figure 7.2: Behaviour of the considered input.

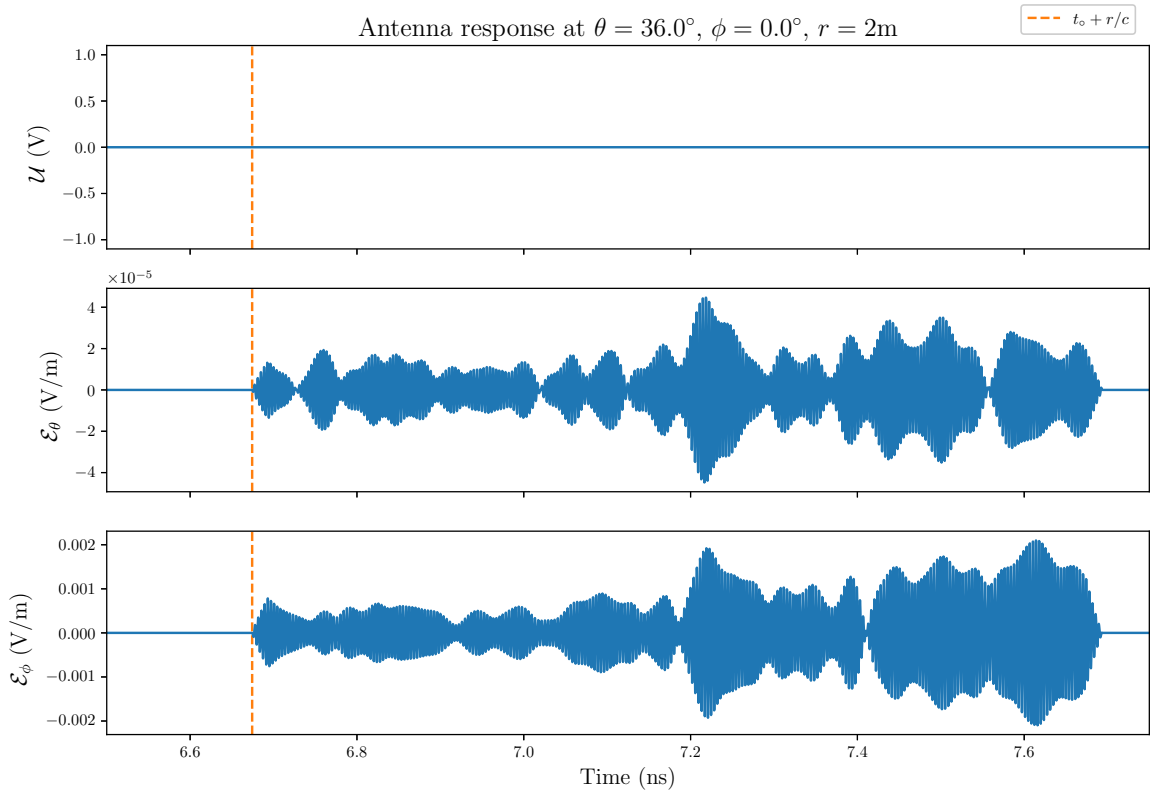

Figure 7.3: Behaviour of the vertical and the horizontal components of the time-domain electric field at a distance of 2 m.

Figure 7.4 offers another point of view of the previous described process where now the magnitude $\mathcal{E}(\boldsymbol{r}, t)$ of the time-domain electric field is shown over a range of distance at different instants. It is worth noting the pulse-like response of the field, which delimits its wavefront, and its free-space attenuation.

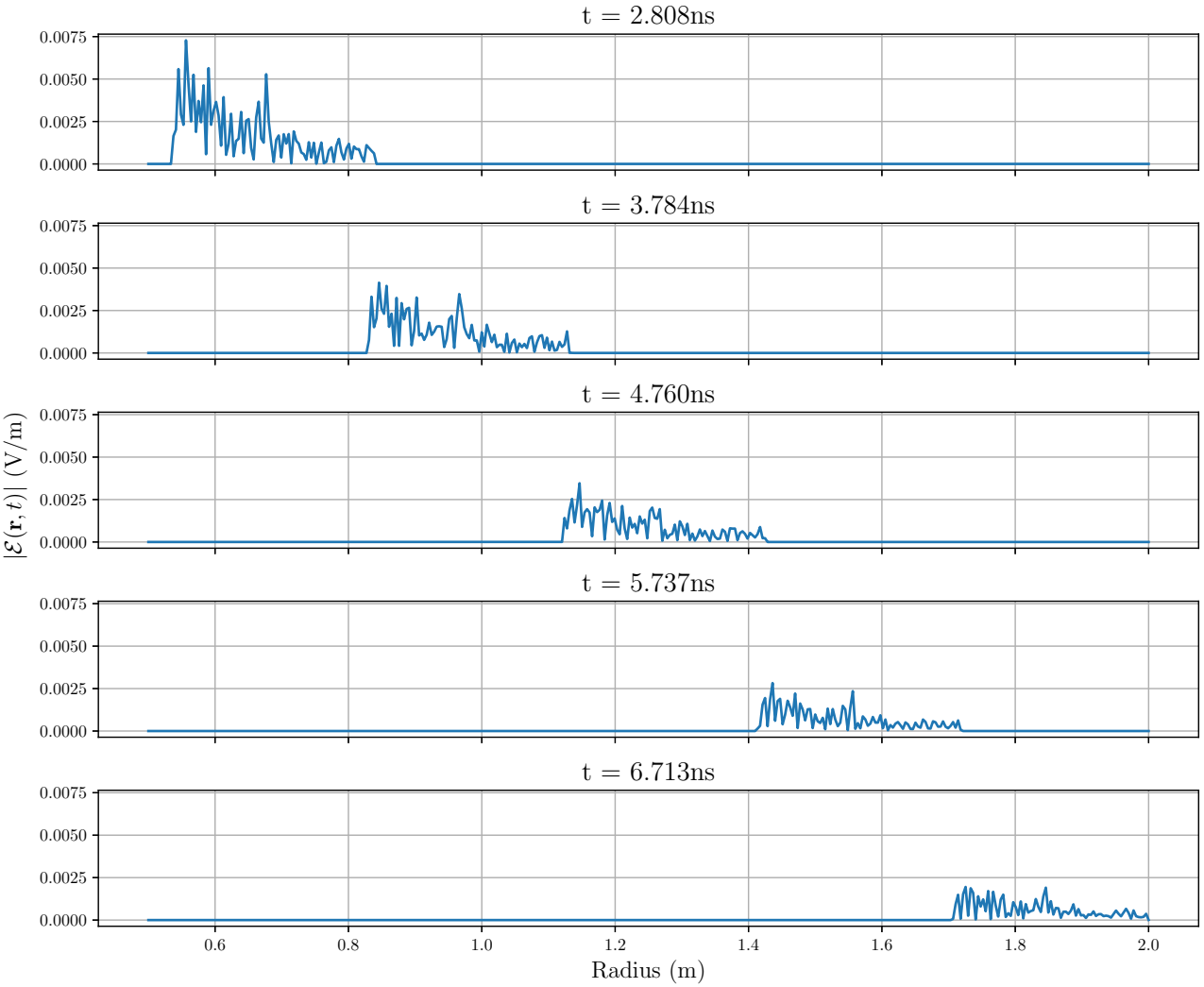

Figure 7.4: Sequential graphs depicting the emitting pulse magnitude as time goes on.

7.A Green's Function Formalism

Consider an antenna fed by a time-domain input signal $\mathcal{U} : \mathbb{R} \to \mathbb{R}$. The time-domain electric field produced will have the form

$$\boldsymbol{\mathcal{E}}(\boldsymbol{r}, t) = \int_{\mathbb{R}} \boldsymbol{\mathcal{G}}(\boldsymbol{r}, \tau)\, \mathcal{U}(t - \tau)\, d\tau \tag{7.29}$$

where the causality is ensured by requiring that $\boldsymbol{\mathcal{G}}(\boldsymbol{r}, \tau) = 0$ for $\tau < 0$.

$$\begin{aligned}\mathbf{E}(\boldsymbol{r},\nu) &= \int_{\mathbb{R}}\left(\int_{\mathbb{R}}\boldsymbol{\mathcal{G}}(\boldsymbol{r},\tau)\,\mathcal{U}(t-\tau)\,d\tau\right)e^{-j2\pi\nu t}dt \\ &= \int_{\mathbb{R}}\boldsymbol{\mathcal{G}}(\boldsymbol{r},\tau)\left(\int_{\mathbb{R}}\mathcal{U}(t-\tau)\,e^{-j2\pi\nu t}dt\right)d\tau \\ &= \int_{\mathbb{R}}\boldsymbol{\mathcal{G}}(\boldsymbol{r},\tau)\,e^{-j2\pi\nu\tau}d\tau\cdot\mathrm{U}(\nu) \\ &= \mathbf{G}(\boldsymbol{r},\nu)\cdot\mathrm{U}(\nu)\end{aligned}$$

Consider an input

$$\mathcal{U}(t) = \mathcal{U}_0\cos(2\pi\nu' t) \tag{7.30}$$

Hence

$$\mathrm{U}_n(\nu) = \mathcal{U}_0\cdot\frac{\delta(\nu-\nu')+\delta(\nu+\nu')}{2} \tag{7.31}$$

The electric field will be

$$\mathbf{E}(\boldsymbol{r},\nu) = \mathbf{G}(\boldsymbol{r},\nu)\,\mathcal{U}_0\cdot\frac{\delta(\nu-\nu')+\delta(\nu+\nu')}{2} \tag{7.32}$$

Thus,

$$\boldsymbol{E}(\boldsymbol{r},\nu') = \mathbf{G}(\boldsymbol{r},\nu')\,\mathcal{U}_0 \tag{7.33}$$

Therefore

$$\mathbf{G}(\boldsymbol{r},\nu') = \frac{\boldsymbol{E}(\boldsymbol{r},\nu')}{\mathcal{U}_0} \tag{7.34}$$

Finally

$$\boldsymbol{\mathcal{G}}(\boldsymbol{r},t) = \frac{1}{\mathcal{U}_0}\int_{\mathbb{R}}\boldsymbol{E}(\boldsymbol{r},\nu)\,e^{j2\pi\nu t}d\nu \tag{7.35}$$

7.B The Incomplete Gamma Function

The objective of this appendix is calculate the integral

$$\int_{\tau_0}^{\tau}\tau'^{k}e^{-j\frac{4\pi^2 r}{c}\nu_n\tau'}d\tau' \tag{7.36}$$

where k is a non-negative integer. For such goal, consider the incomplete Gamma function $\Gamma(\cdot,x)$ defined by

$$\Gamma(\alpha,x_0) = \int_{x_0}^{\infty}x^{\alpha-1}e^{-x}dx. \tag{7.37}$$

If α is a non-negative integer k, a simple process of integration by parts yields that

$$\Gamma(k+1,x_0) = k!e^{-x_0}\sum_{a=0}^{k}\frac{x_0^a}{a!}. \tag{7.38}$$

Regarding the original integral, consider the change of variable $\tau' = \frac{c}{j4\pi^2 r\nu_n}x$. Then,

$$\begin{aligned}
\int_{\tau_0}^{\tau} \tau'^k e^{-j\frac{4\pi^2 r}{c}\nu_n\tau'} d\tau' &= \left(\frac{c}{j4\pi^2 r\nu_n}\right)^{k+1} \int_{\frac{j4\pi^2 r\nu_n}{c}\tau_0}^{\frac{j4\pi^2 r\nu_n}{c}\tau} x^k e^{-x} dx \\
&= \left(\frac{c}{j4\pi^2 r\nu_n}\right)^{k+1} \cdot \left[\int_{\frac{j4\pi^2 r\nu_n}{c}\tau}^{\infty} x^k e^{-x} dx - \int_{\frac{j4\pi^2 r\nu_n}{c}\tau_0}^{\infty} x^k e^{-x} dx\right] \\
&= \left(\frac{c}{j4\pi^2 r\nu_n}\right)^{k+1} \cdot \left[\Gamma\left(k+1, \frac{j4\pi^2 r\nu_n}{c}\tau\right) - \Gamma\left(k+1, \frac{j4\pi^2 r\nu_n}{c}\tau_0\right)\right] \\
&= \left(\frac{c}{j4\pi^2 r\nu_n}\right)^{k+1} \cdot \sum_{a=0}^{k} \frac{k!}{a!} \left(\frac{j4\pi^2 r\nu_n}{c}\right)^a \left[\tau^a e^{-\frac{j4\pi^2 r\nu_n}{c}\tau} - \tau_0^a e^{-\frac{j4\pi^2 r\nu_n}{c}\tau_0}\right] \\
&= \frac{c}{j4\pi^2 r\nu_n} \sum_{a=0}^{k} \frac{k!}{a!} \left(\frac{c}{j4\pi^2 r\nu_n}\right)^{k-a} \left[\tau^a e^{-\frac{j4\pi^2 r\nu_n}{c}\tau} - \tau_0^a e^{-\frac{j4\pi^2 r\nu_n}{c}\tau_0}\right]. \\
&= \mathsf{h}_n^k(r,\tau) \frac{e^{-\frac{j4\pi^2 r\nu_n}{c}\tau}}{r} - \mathsf{h}_n^k(r,\tau_0) \frac{e^{-\frac{j4\pi^2 r\nu_n}{c}\tau_0}}{r}, \qquad (7.39)
\end{aligned}$$

where it is important to notice that the function h_n^k does not have zeros at $r = 0$·

Chapter 8

Conclusions

Taking into consideration the achieved results, specially those that came to fruition regarding the obtained expression for the time-domain electric field, it can be said that this has reached its main objective, as described in the Introduction. Nevertheless, it is convenient to make some comments about its secondary goals.

Initially, it had been intended to develop a new sampling method for reducing the number of collected samples while keeping the same reconstruction performance of WNSST. In the search of such method, a new class of sampling theorems, derived from Theorem 5.2 and based on regular Sturm-Liouville operators, self-adjoint for separated boundary conditions has been developed. Some of them performed better than WNSST for a class of functions, in particular those with rapid variations, which can hence be considered as a byproduct of this research. For this reason their kernel were considered to produce constructors. The main difficulty with those kernels arose from the causality requirement since all of them were real-valued. However, it is known that by loosing some constraints on the Sturm-Liouville Theory, it is possible to reach complex-valued kernels, which could certainly be used improve the performance of the algorithm. Since no more time could be spending on that direction, such problem is then left as suggestion for future research.

Appendices

Appendix A

Fourier Analysis of Causality

Let $\hbar$ and h denote a pair of time/frequency-domain Fourier transform. Moreover, consider $\hbar$ to be the impulse response of a PLTI system, *i.e.*, $\hbar$ is real-valued and the condition $t < 0$ must imply $\hbar(t) = 0$ to prevent any advanced response from the system. This appendix brings forth sufficient conditions one must impose over h to ensure the causality of the said system.

A.1 Cauchy Principal Value

Definition A.1 (Cauchy Principal Value)**.** Let the function $f : \mathbb{R} \setminus \{\upsilon_\circ\} \to \mathbb{C}$ not be Lebesgue integrable on its domain. If, nevertheless, the limit

$$\lim_{\varepsilon \to 0^+} \left[\int_{(-\infty, \upsilon_\circ - \varepsilon]} f(\upsilon)\, d\upsilon + \int_{[\upsilon_\circ + \varepsilon, +\infty)} f(\upsilon)\, d\upsilon \right]$$

exists, then it is said to be the Cauchy Principal Value of the integral of f and it is denoted by

$$\mathsf{PV} \int_{\mathbb{R}} f(\upsilon)\, d\upsilon.$$

Definition A.2. The signum function $\operatorname{sgn} : \mathbb{R} \to \{-1, 0, +1\}$ is defined as

$$\operatorname{sgn}(t) = \begin{cases} -1, & \text{if } t < 0 \\ 0, & \text{if } t = 0 \\ +1, & \text{if } t > 0 \end{cases} \tag{A.1}$$

As stated in [Kam08, Ch. 7, Eq. 69, Page 395], the Fourier transform of the signum function is the tempered distribution

$$\mathcal{F}(\operatorname{sgn})(\nu) = \frac{1}{j\pi} \mathsf{PV}\left(\frac{1}{\nu}\right). \tag{A.2}$$

A.2 Kramers-Kronig Relations

A function $f : D \subseteq \mathbb{R} \to \mathbb{C}$ is said to obey the Kramers-Kronig relations at $\upsilon_\circ \in D$ when it holds that

$$f(\upsilon_\circ) = \frac{1}{j\pi} \mathsf{PV} \int_{\mathbb{R}} \frac{f(\upsilon)}{\upsilon - \upsilon_\circ} d\upsilon. \tag{A.3}$$

The plural in the word relations is due to the fact that the last equation, when its real and imaginary parts are taken, leads to the following real conditions

$$\operatorname{Re} f(\upsilon_\circ) = \frac{1}{\pi}\mathsf{PV}\int_{\mathbb{R}} \frac{\operatorname{Im} f(\upsilon)}{\upsilon - \upsilon_\circ} d\upsilon \tag{A.4}$$

$$\operatorname{Im} f(\upsilon_\circ) = -\frac{1}{\pi}\mathsf{PV}\int_{\mathbb{R}} \frac{\operatorname{Re} f(\upsilon)}{\upsilon - \upsilon_\circ} d\upsilon, \tag{A.5}$$

which actually comes to be known as Kramers-Kronig relations. Commonly, one is most interested in the case where f is well defined for any real value, *i.e.*, $D = \mathbb{R}$, and it obeys Kramers-Kronig relations at any $\upsilon_\circ \in \mathbb{R}$. At the desired case when it does happen, the function is simply said to obey Kramers-Kronig relations.

As the firsts conclusions on this matter, consider the following easily checkable statements:

Property A.1. A function obeys Kramers-Kronig relations if, and only if, its real and imaginary parts are a pair of Hilbert transform, *i.e.*, $\operatorname{Re} f = -\mathsf{H}(\operatorname{Im} f)$ and $\operatorname{Im} f = \mathsf{H}(\operatorname{Re} f)$.

Property A.2. A pure real function f, *i.e.*, $\operatorname{Im} f = 0$, does not obey Kramers-Kronig relations unless it is zero everywhere.

Property A.3. A pure imaginary function f, *i.e.*, $\operatorname{Re} f = 0$, does not obey Kramers-Kronig relations unless it is zero everywhere.

As it will soon be shown, there is a close relationship between causality and the Kramers-Kronig relation. For this reason, it becomes interesting to ensure that those relations hold. This section is mainly meant to present, in the following results, a sufficient condition for this to happen.

Proposition A.1. Let $\mathbb{C}_+ = \left\{\upsilon \in \mathbb{C};\ \operatorname{Im}(\upsilon) > 0\right\}$ denote the upper half-plane, $D \subseteq \mathbb{C}$ be open, $\zeta : D \to \mathbb{C}$ be holomorphic in its domain and $\Gamma \subset \overline{\mathbb{C}_+}$ be the set of all isolated singularities of ζ in the upper half-plane and in the real line, which is assumed to be finite. If $\overline{\mathbb{C}_+} \setminus \Gamma \subset D$; and every $\upsilon \in \Gamma \cap \mathbb{R}$ is a pole of order 1; and $\lim\limits_{r\to\infty} r \cdot \sup\left\{|\zeta(\upsilon)|;\ |\upsilon| = r \wedge \upsilon \in \overline{C}_+\right\} = 0$, then

$$\mathsf{PV}\int_{\mathbb{R}} \zeta(\upsilon)\, d\upsilon = 2\pi j \sum_{\upsilon\in\Gamma\setminus\mathbb{R}} \operatorname{Res}(\zeta, \upsilon) + \pi j \sum_{\upsilon\in\Gamma\cap\mathbb{R}} \operatorname{Res}(\zeta, \upsilon). \tag{A.6}$$

Proof. *Cf*. [Net05, Sec. 4.4, page 242].

Lemma A.1. Let $D \subseteq \mathbb{C}$ be open, $f : D \to \mathbb{C}$ be holomorphic in its domain and $\Gamma \in \overline{\mathbb{C}_+}$ denote the set of all isolated singularities of f, which is assumed to be finite. If $\overline{\mathbb{C}_+} \setminus \Gamma \subset D$; and every element in $\Gamma \cap \mathbb{R}$ is pole of order 1; and $\lim\limits_{r\to\infty} f\left(re^{j\theta}\right) = 0$ for any $\theta \in [0, \pi]$; then for any real value $\upsilon_\circ \in \mathbb{R} \setminus \Gamma$, it holds that

$$f(\upsilon_\circ) = \frac{1}{j\pi}\mathsf{PV}\int_{\mathbb{R}} \frac{f(\upsilon)}{\upsilon - \upsilon_\circ} d\upsilon - 2\sum_{\upsilon\in\Gamma\setminus\mathbb{R}} \frac{\operatorname{Res}(f, \upsilon)}{\upsilon - \upsilon_\circ} - \sum_{\upsilon\in\Gamma\cap\mathbb{R}} \frac{\operatorname{Res}(f, \upsilon)}{\upsilon - \upsilon_\circ}. \tag{A.7}$$

Proof. The result is a direct consequence of the order of the real poles in Proposition A.1. In fact, take $\zeta(\upsilon) = \frac{f(\upsilon)}{\upsilon-\upsilon_\circ}$ and notice that $\Gamma = \Gamma \cup \{\upsilon_\circ\}$, $\Gamma \cap \mathbb{R} = (\Gamma \cap \mathbb{R}) \cup \{\upsilon_\circ\}$, $\Gamma \setminus \mathbb{R} = \Gamma \setminus \mathbb{R}$ and

$$\operatorname{Res}(\zeta, \upsilon) = \begin{cases} \frac{\operatorname{Res}(f,\upsilon)}{\upsilon-\upsilon_\circ}, & \text{if } \upsilon \neq \upsilon_\circ \\ f(\upsilon_\circ), & \text{if } \upsilon = \upsilon_\circ \end{cases}.$$

Hence,

$$\begin{aligned} \mathsf{PV}\int_{\mathbb{R}} \frac{f(\upsilon)}{\upsilon-\upsilon_\circ} d\upsilon &= 2\pi j \sum_{\upsilon\in\Gamma\setminus\mathbb{R}} \operatorname{Res}(\zeta,\upsilon) + \pi j \sum_{\upsilon\in\Gamma\cap\mathbb{R}} \operatorname{Res}(\zeta,\upsilon) + \pi j \cdot \operatorname{Res}(\zeta,\upsilon_\circ) \\ &= 2\pi j \sum_{\upsilon\in\Gamma\setminus\mathbb{R}} \frac{\operatorname{Res}(f,\upsilon)}{\upsilon-\upsilon_\circ} + \pi j \sum_{\upsilon\in\Gamma\cap\mathbb{R}} \frac{\operatorname{Res}(f,\upsilon)}{\upsilon-\upsilon_\circ} + \pi j \cdot f(\upsilon_\circ), \end{aligned}$$

which yields the result. ■

Theorem A.1 (Holomorphism $\implies$ Kramers-Kronig)**.** Let $D \subseteq \mathbb{C}$ be open with $\overline{\mathbb{C}_+} \subset D$, and consider a function $f : D \to \mathbb{C}$ such that $\lim_{r\to\infty} f\left(re^{j\theta}\right) = 0$ for any $\theta \in [0, \pi]$. If f is holomorphic in D, then it obeys the Kramers-Kronig relations. *I.e.*,

$$f \text{ is holomorphic in } D \implies f(\upsilon_\circ) = \frac{1}{j\pi}\mathsf{PV}\int_{\mathbb{R}} \frac{f(\upsilon)}{\upsilon-\upsilon_\circ} d\upsilon, \ \ \forall \upsilon_\circ \in \mathbb{R}. \tag{A.8}$$

Proof. The result comes as a particular case of Lemma A.1 where $\Gamma = \varnothing$. ■

Theorem A.1 is the sought result and it can quickly be summed up as: if a function f is holomorphic everywhere in an open set containing the upper half-plane and the real line and it goes to zero in their edges, then its restriction to the real line $f|_{\mathbb{R}}$ obeys the Kramers-Kronig relations. As consequence, if such function has singularities, then they must figure in the lower half-plane.

Lastly, it must be highlighted that the converse of Theorem A.1 is not true. Which, in other words, means that obeying Kramers-Kronig is not a sufficient condition to Holomorphism. In fact, it is possible to construct a non-analytic (hence non-holomorphic) function for which Kramers-Kronig is still valid. To illustrate this possibility, in the context of Lemma A.1, take for example $f(z) = \frac{1}{(z-j)^2}$, whose only one pole lies in upper half-plane and clearly $\operatorname{Res}(f, j) = 0$. Thus, f obeys Kramers-Kronig even though it is not holomorphic.

A.3 Parity and Hermitianness on Fourier transform Pairs

Throughout this section, let $\mathcal{f}$ and f denote a generic pair of time/frequency-domain Fourier transform where $\mathcal{f}$ is real. In this context, consider the following definitions and results.

Property A.4. $\mathcal{f}$ is even $\iff$ f is real and even;

Property A.5. f is odd $\iff$ f is imaginary and odd.

The above properties are easily verified by considering a simple application of Euler's formula in the Fourier transform, as follows

$$f(\nu) = \int_{\mathbb{R}} f(t) \cdot \cos(2\pi\nu t)\, dt - j \int_{\mathbb{R}} f(t) \cdot \sin(2\pi\nu t)\, dt, \tag{A.9}$$

$$\begin{aligned} f(t) = \int_{\mathbb{R}} \Big(\operatorname{Re} f(\nu) \cdot \cos(2\pi\nu t) - \operatorname{Im} f(\nu) \cdot \sin(2\pi\nu t) \Big) d\nu \\ + j \int_{\mathbb{R}} \Big(\operatorname{Re} f(\nu) \cdot \sin(2\pi\nu t) + \operatorname{Im} f(\nu) \cdot \cos(2\pi\nu t) \Big) d\nu. \end{aligned} \tag{A.10}$$

Definition A.3 (Even and odd parts of a time-domain function)**.** The even and odd parts of f are the time-domain functions $f_e, f_o : \mathbb{R} \to \mathbb{R}$, respectively, defined by

$$f_e(t) = \frac{f(t) + f(-t)}{2} \quad \text{and} \quad f_o(t) = \frac{f(t) - f(-t)}{2}.$$

Property A.6. $f = f_e + f_o$.

Property A.7. The Fourier transform of f_e is even and real.

Property A.8. The Fourier transform of f_o is odd and imaginary.

Motivated by the last two properties, consider the following definition.

Definition A.4 (Even and odd parts of a frequency-domain function)**.** The even and odd parts of f are the frequency-domain functions $f_e, f_o : \mathbb{R} \to \mathbb{R}$, respectively, defined by $f_e = \mathcal{F}(f_e)$ and $j f_o = \mathcal{F}(f_o)$.

Property A.9. $f = f_e + j f_o$.

Property A.10. $f_e(t) = \frac{f(t)+f(-t)}{2}$.

Property A.11. $f_o(t) = \frac{f(t)-f(-t)}{2j}$.

More generally, it holds that

Proposition A.2. f is real $\iff$ f is hermitian.

Proof. ($\Longrightarrow$) It is a direct consequence of the parities of f_e and f_o and Property A.9. ($\Longleftarrow$) It can be easily verified from Equation (A.10). ■

A.4 Results on Causality

Consider once again a PLTI system and let $\hbar$ be its time-domain impulse response, meaning that $\hbar$ must be real and $\hbar(t) = 0$ if $t < 0$, while h denotes the Fourier transform of $\hbar$. In this context, the following results hold.

Lemma A.2 (Causality $\implies$ Hermitianness)**.** If h is the Fourier transform of the impulse response $\hbar$ of a PLTI system, then h is hermitian.

Proof. Since $\hbar$ is real, the Proposition A.2 yields the result. ■

Lemma A.3. $\hbar_o = \operatorname{sgn} \cdot \hbar_e$ and $\hbar_e \overset{\text{a.e.}}{=} \operatorname{sgn} \cdot \hbar_o$.

Proof. Initially, one must be able to notice that given $t \in \mathbb{R} \setminus \{0\}$, either $\hbar(t)$ or $\hbar(-t)$ is zero. Hence, by studying the Definition A.3, the even and odd parts of $\hbar$ can be rewritten as

$$\hbar_e(t) = \frac{1}{2}\begin{cases} \hbar(-t), & \text{if } t < 0 \\ 2\hbar(0), & \text{if } t = 0 \\ \hbar(t), & \text{if } t > 0 \end{cases} \quad \text{and} \quad \hbar_o(t) = \frac{1}{2}\begin{cases} -\hbar(-t), & \text{if } t < 0 \\ 0, & \text{if } t = 0 \\ \hbar(t), & \text{if } t > 0 \end{cases},$$

from which it is now easy to notice that $\hbar_o(t) = \operatorname{sgn}(t) \cdot \hbar_e(t)$, yielding the first result. For the second result, consider multiplying both sides of the first by sgn, which would lead to

$$\operatorname{sgn}(t)\,\hbar_o(t) = \operatorname{sgn}(t)^2 \cdot \hbar_e(t) = \begin{cases} \hbar_e(t), & \text{if } t \neq 0 \\ 0, & \text{if } t = 0 \end{cases}.$$

Thus, $\hbar_e(t) = \operatorname{sgn}(t)\,\hbar_o(t)$ for any $t \in \mathbb{R} \setminus \{0\}$, and since $\{0\}$ has zero measure, the equality holds almost everywhere, yielding the second result. ■

Lemma A.4. $\hbar \overset{\text{a.e.}}{=} \operatorname{sgn} \cdot \hbar$.

Proof. It is enough to sum the two results from Lemma A.3. ■

Corollary A.1. For any frequency $\nu \in \mathbb{R}$, h must be such that

$$h(\nu) = -\frac{1}{j\pi}\mathsf{PV}\int_{\mathbb{R}} \frac{h(\upsilon)}{\upsilon - \nu} d\upsilon. \tag{A.11}$$

Theorem A.2 (Causality $\iff$ Kramers-Kronig + Hermitianness)**.** A frequency-domain function $h : \mathbb{R} \to \mathbb{C}$ is the Fourier transform of the impulse response of a PLTI system if, and only if, it is hermitian and h^* obeys Kramers-Kronig relations.

Proof. ($\Longrightarrow$) The hermitianness of h is ensured by Lemma A.2, while the fact that h^* obeys Kramers-Kronig relations is a direct consequence of Corollary A.1. ($\Longleftarrow$) Since h^* obeys Kramers-Kronig relations, it holds that

$$h(\nu)^* = \frac{1}{j\pi}\mathsf{PV}\int_{\mathbb{R}} \frac{h(\upsilon)^*}{\upsilon-\nu}d\upsilon \implies h(\nu) = -\frac{1}{j\pi}\mathsf{PV}\int_{\mathbb{R}} \frac{h(\upsilon)}{\upsilon-\nu}d\upsilon, \quad \forall \nu \in \mathbb{R}.$$

If the inverse Fourier transform is taken on the above equation, it yields $\hbar(t) = \operatorname{sgn}(t) \cdot \hbar(t)$, which makes it clear that $\hbar(t) = 0$ for any $t < 0$. The reality of $\hbar$ is ensured by the hermitianness of h. Thus, $\hbar$ has what is needed to be the impulse response of a PLTI system. ■

Theorem A.3 (Holomorphism + Hermitianness $\implies$ Causality)**.** Consider an open set $D \subseteq \mathbb{C}$ such that $\overline{\mathbb{C}_+} \in D$ and let $h^* : D \to \mathbb{C}$ be holomorphic in D and $\lim\limits_{r\to\infty} h^*\left(re^{j\theta}\right) = 0$ for any $\theta \in [0, \pi]$. If the restriction $h|_{\mathbb{R}}$ is hermitian, then it also is the frequency-domain impulse response of a PLTI system.

Proof. The holomorphism implies Kramers-Kronig relations (Theorem A.1), which with the hermitianness implies the causality (Theorem A.2). ■

The last result establishes sufficient conditions over h so it correspond to a causal system and hence it may be seen as the main conclusion of this appendix. It must be stressed, nevertheless, that this result is not actually necessary for causality, by reasons that have been explained in the end of Section A.2. Thus, it is possible that holomorphism in the upper half-plane and in the real line cannot be ensured, hence making the requirements quite restrictive. If it were the case, chances are that Theorem A.2 is the attained result to guarantee causality.

Appendix B

Spherical Coordinate System

This appendix aims to document some conversion results between spherical and cartesian coordinates. The figure B.1 conveniently depicts the parameters (r, θ, ϕ) and the unit vectors $(\hat{r}, \hat{\theta}, \hat{\phi})$ with respect to the cartesian frame. As usual, $r \in [0, \infty)$ is radius; $\theta \in [0, \pi]$ is the polar angle; and $\phi \in [-\pi, \pi]$ is the azimuthal angle.

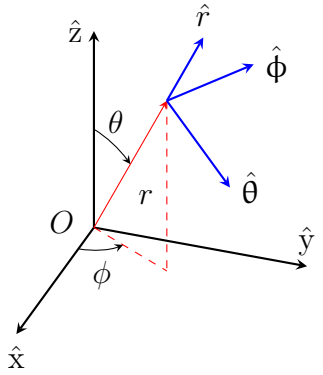

Figure B.1: Spherical Coordinates parameters and unit vectors depiction.

B.1 Position Parameters conversion

A vector position $\boldsymbol{r} \in \mathbb{R}^3$ can either be represented at the cartesian basis using the coordinates (x, y, z) or spherically by the triple (r, θ, ϕ). The conversion between those coordinates is given by

- Spherical to cartesian:

$$\begin{cases} x = r\cos\phi\sin\theta & \text{(B.1)} \\ y = r\sin\phi\sin\theta & \text{(B.2)} \\ z = r\cos\theta & \text{(B.3)} \end{cases}$$

- Cartesian to Spherical:

$$\begin{cases} r = \sqrt{x^2 + y^2 + z^2} & \text{(B.4)} \\ \theta = \arccos\left(\dfrac{z}{r}\right) & \text{(B.5)} \\ \phi = \operatorname{sgn}(y) \cdot \arccos\left(\dfrac{x}{r\sin\theta}\right) & \text{(B.6)} \end{cases}$$

B.2 Vector Components Conversion

Given a vector $\overrightarrow{F}$ in a tridimensional euclidean space, it can then be represented by its cartesian and spherical components as follows

$$\overrightarrow{F} = F_x\hat{\mathrm{x}} + F_y\hat{\mathrm{y}} + F_z\hat{\mathrm{z}} = F_r\hat{r} + F_\theta\hat{\boldsymbol{\theta}} + F_\phi\hat{\boldsymbol{\phi}}. \tag{B.7}$$

The conversion between these components is given by

$$\begin{bmatrix} F_x \\ F_y \\ F_z \end{bmatrix} = \boldsymbol{M}\left(\theta, \phi\right) \begin{bmatrix} F_r \\ F_\theta \\ F_\phi \end{bmatrix} \tag{B.8}$$

where the rotation matrix

$$\boldsymbol{M}\left(\theta, \phi\right) = \begin{bmatrix} \sin\theta\cos\phi & \cos\theta\cos\phi & -\sin\phi \\ \sin\theta\sin\phi & \cos\theta\sin\phi & \cos\phi \\ \cos\theta & -\sin\theta & 0 \end{bmatrix} \tag{B.9}$$

is, of course, orthogonal.

Appendix C

Special Functions

C.1 Spherical Bessel Functions

C.2 Associated Legendre Polynomials

As it will be clear in the next appendices, the associated Legendre polynomials play an important role in describing the spherical harmonics and, therefore, the solutions of scalar and vector HHE.

Definition C.1. Given $\ell \in \mathbb{N}_0$ and $m \in \left\{m' \in \mathbb{Z};\ |m'| \leqslant \ell\right\}$, the ℓ-degree m-order associated Legendre polynomial $P_\ell^m : [-1,1] \to \mathbb{R}$ is defined[1] as

$$P_\ell^m(u) = \frac{(-1)^m}{2^\ell \ell!} \left(1-u^2\right)^{m/2} \frac{d^{\ell+m}}{du^{\ell+m}} \left(u^2-1\right)^\ell. \tag{C.1}$$

Property C.1. $|m| > \ell \implies P_\ell^m = 0$.

Property C.2. $P_\ell^{-m} = (-1)^m \dfrac{(\ell-m)!}{(\ell+m)!} P_\ell^m$.

Proposition C.1. P_ℓ^m is a solution of the associated Legendre equation

$$\left[\left(1-u^2\right) y'\right]' + \left[\ell(\ell+1) - \frac{m^2}{1-u^2}\right] y = 0. \tag{C.2}$$

Proof. See [Bel04, Sec. 3.8]

Proposition C.2 (Orthogonality in degree)**.**

$$\int_{-1}^{1} P_\ell^m(u)\, P_{\ell'}^m(u)\, du = \frac{2}{2\ell+1} \frac{(\ell+m)!}{(\ell-m)!} \delta_{\ell\ell'}. \tag{C.3}$$

Proof. See [Bel04, Theorem 3.11]

[1] Commonly, P_ℓ^m is defined from the m-th derivative of the ℓ-degree Legendre polynomial P_ℓ and (C.1) becomes a consequence of such definition and Rodrigue's Formula. However, since this approach is not able to accommodate negative values of m, the property C.2 becomes hence a definition.

Proposition C.3 (Orthogonality in order)**.**

$$\int_{-1}^{1} \frac{mm'}{1-u^2} P_\ell^m(u)\, P_\ell^{m'}(u)\, du = m \frac{(\ell+m)!}{(\ell-m)!} \delta_{mm'}. \tag{C.4}$$

Proposition C.4 (Orthogonality in degree)**.**

$$\begin{aligned} &\int_{-1}^{1} \left(\frac{m^2}{1-u^2} P_\ell^m P_{\ell'}^m + \left(1-u^2\right) \frac{dP_\ell^m}{du} \frac{dP_{\ell'}^m}{du} \right) du \\ &\qquad = \ell\left(\ell+1\right) \frac{2}{2\ell+1} \frac{(\ell+m)!}{(\ell-m)!} \delta_{\ell\ell'} \end{aligned} \tag{C.5}$$

Appendix D

Spherical Scalar Solutions of HHE

D.1 Separation of Variables

The starting point for reaching spherical vector solutions of the HHE is to study its spherical scalar solutions. In this direction, let $\psi \in \mathcal{C}^2(\mathbb{R}^3;\mathbb{C}) \cap \mathcal{L}^2(\mathbb{R}^3,\Sigma,\nu)$, where Σ denotes the $\mathbb{R}^3$ Borel σ-algebra and $\nu : \Sigma \to \mathbb{R}_{\geqslant 0}$ represents the $\mathbb{R}^3$ Lebesgue measure, be a nontrivial scalar solution of the HHE:

$$\nabla^2\psi + k^2\psi = 0. \tag{D.1}$$

Since the above PDE is linear, the method of separation of variables is of course the most traditional approach, in which solutions of the form $\psi(r,\theta,\phi) = R(r)\,\Theta(\theta)\,\Phi(\phi)$ are studied. After some algebraic work, the following three ordinary differential equations are isolated:

$$\Phi'' + m^2\Phi = 0, \tag{D.2}$$

$$\frac{(\sin\theta\cdot\Theta')'}{\sin\theta} + \left(\ell(\ell+1) - \frac{m^2}{\sin^2\theta}\right)\Theta = 0, \tag{D.3}$$

$$\left(r^2R'\right)' + \left(k^2r^2 - \ell(\ell+1)\right)R = 0, \tag{D.4}$$

where ℓ and m are eigenvalues-related coupling constants.

D.2 Solutions of Equation (D.2)

It is straightforward to see that the solutions of (D.2) are $\Phi_m(\phi) = e^{jm\phi}$, where it must be required that $m \in \mathbb{Z}$ to ensure the continuity and differentiability of Φ at $\phi = 0$ and $\phi = 2\pi$.

D.3 Solutions of Equation (D.4)

Finally, by taking $v = kr$, the equation (D.4) becomes the ℓ-order Spherical Bessel Differential Equation [Nis, Sec. 10.47], whose standard pairwise linearly independent solutions

are

$$
\begin{aligned}
z_\ell^1 &= j_\ell, && \text{(Bessel function of the first kind)}\\
z_\ell^2 &= y_\ell, && \text{(Bessel function of the second kind)}\\
z_\ell^3 &= h_\ell^{(1)}, && \text{(Hankel function of the first kind)}\\
z_\ell^4 &= h_\ell^{(2)}. && \text{(Hankel function of the second kind)}
\end{aligned}
$$

For convenience, these solutions shall be compactly represented in the single notation z_ℓ^s labelled by the superscript $s \in \{1, 2, 3, 4\}$ as above shown. Thus, $R_{\ell s}(r) = z_\ell^s(kr)$.

D.4 Solutions of Equation (D.3)

Moreover, by defining $u = \cos\theta$, (D.3) reveals itself as the Associated Legendre Equation [Nis, Subsec. 14.2.ii], whose solutions at the poles $u = \pm 1$ converge only if $\ell \in \mathbb{N}_0$ [Bel04, Sec. 3.1]. Hence, $\Theta_{\ell m}(\theta) = P_\ell^m(\cos\theta)$, which vanishes if $|m| > \ell$.

The complete solution will hence be given by

$$\psi(r,\theta,\phi) = \sum_{\ell\in\mathbb{N}} \sum_{|m|\leqslant\ell} \sum_{s\in\mathcal{B}} c_{\ell ms} z_\ell^s(kr)\, Y_\ell^m(\theta,\phi). \tag{D.5}$$

D.5 Spherical Harmonics

Definition D.1.

$$Y_\ell^m(\theta,\phi) = \sqrt{\frac{2\ell+1}{4\pi}}\sqrt{\frac{(l-m)!}{(l+m)!}} P_\ell^m(\cos\theta)\, e^{jm\phi} \tag{D.6}$$

Proposition D.1. $Y_\ell^{m*} = (-1)^m Y_\ell^{-m}$.

Proof. In light of the Property C.2, consider the following

$$\begin{aligned}
Y_\ell^{m*}(\theta,\phi) &= \sqrt{\frac{2\ell+1}{4\pi}}\sqrt{\frac{(l-m)!}{(l+m)!}} P_\ell^m(\cos\theta)\, e^{-jm\phi} \\
&= \sqrt{\frac{2\ell+1}{4\pi}}\sqrt{\frac{(l-m)!}{(l+m)!}} (-1)^m \frac{(\ell+m)!}{(\ell-m)!} P_\ell^{-m}(\cos\theta)\, e^{-jm\phi} \\
&= (-1)^m \sqrt{\frac{2\ell+1}{4\pi}}\sqrt{\frac{(l+m)!}{(l-m)!}} P_\ell^{-m}(\cos\theta)\, e^{-jm\phi} \\
&= (-1)^m Y_\ell^{-m}(\theta,\phi).
\end{aligned}$$

■

Proposition D.2. *Proof.*

$$\begin{aligned}
\frac{\partial Y_\ell^m}{\partial\theta}(\theta,\phi) &= \sqrt{\frac{2\ell+1}{4\pi}}\sqrt{\frac{(\ell-m)!}{(\ell+m)!}} \frac{\partial}{\partial\theta}\Big(P_\ell^m(\cos\theta)\Big) e^{jm\phi} \\
&= -\sqrt{\frac{2\ell+1}{4\pi}}\sqrt{\frac{(l-m)!}{(l+m)!}} P_\ell^{m\prime}(\cos\theta)\sin\theta e^{jm\phi}
\end{aligned}$$

Thus,

$$\frac{\partial Y_\ell^m}{\partial\theta}(0,\phi) = \frac{\partial Y_\ell^m}{\partial\theta}(\pi,\phi) = 0.$$

If $\theta \neq 0$, [Nis, Eq. 14.10.5] can be used as

$$\sin\theta P_\ell^{m\prime}(\cos\theta) = (\ell+m)\frac{1}{\sin\theta} P_{\ell-1}^m(\cos\theta) - \ell\frac{\cos\theta}{\sin\theta} P_\ell^m(\cos\theta).$$

Hence,

$$\begin{aligned}\frac{\partial Y_\ell^m}{\partial\theta}(\theta,\phi) &= \sqrt{\frac{2\ell+1}{4\pi}}\sqrt{\frac{(\ell-m)!}{(\ell+m)!}}\left[\ell\frac{\cos\theta}{\sin\theta}P_\ell^m(\cos\theta) - (\ell+m)\frac{1}{\sin\theta}P_{\ell-1}^m(\cos\theta)\right]e^{jm\phi}\\ &= \ell\frac{\cos\theta}{\sin\theta}Y_\ell^m(\theta,\phi) - \sqrt{\frac{2\ell+1}{4\pi}}\sqrt{\frac{(\ell-m)!}{(\ell+m)!}}\left[(\ell+m)\frac{1}{\sin\theta}P_{\ell-1}^m(\cos\theta)\right]e^{jm\phi}\\ &= \ell\frac{\cos\theta}{\sin\theta}Y_\ell^m(\theta,\phi) - \sqrt{\frac{2\ell+1}{2\ell-1}}\frac{\sqrt{\ell^2-m^2}}{\sin\theta}Y_{\ell-1}^m(\theta,\phi)\end{aligned}$$

■

Proposition D.3.

$$\oiint Y_\ell^{m*}Y_{\ell'}^{m'}d\Omega = \delta_{\ell\ell'}\delta_{mm'} \tag{D.7}$$

Proposition D.4.

$$\oiint\left(\frac{mm'Y_\ell^{m*}Y_{\ell'}^{m'}}{\sin^2\theta} + \frac{\partial Y_\ell^{m*}}{\partial\theta}\frac{\partial Y_{\ell'}^{m'}}{\partial\theta}\right)d\Omega = \ell(\ell+1)\delta_{\ell\ell'}\delta_{mm'} \tag{D.8}$$

Proposition D.5.

$$\oiint\left(\frac{mY_\ell^{m*}}{\sin\theta}\frac{\partial Y_{\ell'}^{m'}}{\partial\theta} + \frac{\partial Y_\ell^{m*}}{\partial\theta}\frac{m'Y_{\ell'}^{m'}}{\sin\theta}\right)d\Omega = 0 \tag{D.9}$$

Definition D.2.

$$\boldsymbol{Y}_{\ell m} = \frac{1}{\sqrt{\ell(\ell+1)}}\begin{bmatrix}\sqrt{\ell(\ell+1)}Y_\ell^m & 0 & 0\\ 0 & \dfrac{jmY_\ell^m}{\sin\theta} & \dfrac{\partial Y_\ell^m}{\partial\theta}\\ 0 & -\dfrac{\partial Y_\ell^m}{\partial\theta} & \dfrac{jmY_\ell^m}{\sin\theta}\end{bmatrix} \tag{D.10}$$

Proposition D.6. $\boldsymbol{Y}_{\ell m}^* = (-1)^m\boldsymbol{Y}_{\ell,-m}$

Proof.

$$\begin{aligned}
\boldsymbol{Y}^*_{\ell m} &= \frac{1}{\sqrt{\ell\,(\ell+1)}} \begin{bmatrix} \sqrt{\ell\,(\ell+1)}Y_\ell^{m*} & 0 & 0 \\ 0 & \dfrac{-jmY_\ell^{m*}}{\sin\theta} & \dfrac{\partial Y_\ell^{m*}}{\partial\theta} \\ 0 & -\dfrac{\partial Y_\ell^{m*}}{\partial\theta} & \dfrac{-jmY_\ell^{m*}}{\sin\theta} \end{bmatrix} \\
&= \frac{(-1)^m}{\sqrt{\ell\,(\ell+1)}} \begin{bmatrix} \sqrt{\ell\,(\ell+1)}Y_\ell^{-m} & 0 & 0 \\ 0 & \dfrac{-jmY_\ell^{-m}}{\sin\theta} & \dfrac{\partial Y_\ell^{-m}}{\partial\theta} \\ 0 & -\dfrac{\partial Y_\ell^{-m}}{\partial\theta} & \dfrac{-jmY_\ell^{-m}}{\sin\theta} \end{bmatrix} \\
&= (-1)^m \boldsymbol{Y}_{\ell,-m}.
\end{aligned}$$

■

Proposition D.7.

$$\oiint \boldsymbol{Y}^{\mathrm{H}}_{\ell m} \boldsymbol{Y}_{\ell' m'} d\Omega = \mathbf{I}_3 \delta_{\ell\ell'} \delta_{mm'}. \tag{D.11}$$

Appendix E

Spherical Vector Solutions of HHE

E.1 Vector Spherical Harmonics

The Vector Spherical Harmonics are three vector solutions of the HHE. Here lies an outline description of them and some of their properties.

E.1.1 The $\boldsymbol{L}$ Field

Definition E.1. Let ψ be a nontrivial scalar solution of the HHE

$$\boldsymbol{L} = \nabla\psi \tag{E.1}$$

Property E.1. $\nabla\times\boldsymbol{L} = 0$.

Property E.2. $\nabla\cdot\boldsymbol{L} = -k^2\psi$.

Property E.3. $\nabla^2\boldsymbol{L} + k^2\boldsymbol{L} = 0$.

E.1.2 The $\boldsymbol{M}$ Field

Definition E.2. $\boldsymbol{M} = \nabla\times(\psi\boldsymbol{r})$

Property E.4. $\nabla\cdot\boldsymbol{M} = 0$

Property E.5. $\boldsymbol{M} = \boldsymbol{L}\times\boldsymbol{r}$

Property E.6. $\nabla^2\boldsymbol{M} + k^2\boldsymbol{M} = 0$.

Property E.7. $\nabla\times(\nabla\times\boldsymbol{M}) = k^2\boldsymbol{M}$.

E.1.3 The $\boldsymbol{N}$ Field

Definition E.3. $\boldsymbol{N} = \dfrac{1}{k}\nabla\times\boldsymbol{M}$

Property E.8. $\nabla\cdot\boldsymbol{N} = 0$

Property E.9. $\nabla\times\boldsymbol{N} = k\boldsymbol{M}$

Property E.10. $\nabla\times(\nabla\times\boldsymbol{N}) = k^2\boldsymbol{N}$.

Property E.11. $\nabla^2\boldsymbol{N} + k^2\boldsymbol{N} = 0$.

E.1.4 Linear Independence

Since $\boldsymbol{L}$, $\boldsymbol{M}$ and $\boldsymbol{N}$ are meant to generate any solution of the vector Helmholtz equation. It is usual to ask if they are in fact linearly independent in the euclidian space $\mathbb{R}^3$. In this sense, it can be shown that only when they derive from ψ^s_{00}, the vectors $\boldsymbol{M}$ and $\boldsymbol{N}$ are both zero. Hence, those vectors are not able to generate spherically symmetric vector solutions of the Helmholtz Equation.

E.1.5 Spherically Symmetric Solutions

Since the vectors $\boldsymbol{L}$, $\boldsymbol{M}$ and $\boldsymbol{N}$ are not able to provide spherically symmetric solutions to the vector HHE, those solutions shall be find in another fashion. In other words, it must be found vector fields with no dependence on θ or ϕ, hence of the form

$$\boldsymbol{F}(r) = F_r(r)\,\hat{r} + F_\theta(r)\,\hat{\theta} + F_\phi(r)\,\hat{\phi}, \tag{E.2}$$

such that

$$\nabla^2\boldsymbol{F}(r) + k^2\boldsymbol{F}(r). \tag{E.3}$$

For this particular case, it is possible to shown, by using the vector laplacian in spherical coordinates, that the only possible solution is

$$\boldsymbol{F}(r) = z^s_1(kr)\,\hat{r}. \tag{E.4}$$

E.2 Vector Spherical Solutions of the HHE

It is finally possible to discuss the general vector solutions of the HHE given by

$$\nabla^2\boldsymbol{\Psi} + k^2\boldsymbol{\Psi} = 0. \tag{E.5}$$

The complete solution would have the form

$$\begin{aligned}
\boldsymbol{\Psi}(r,\theta,\phi) &= \sum_{\ell\in\mathbb{N}}\sum_{|m|\leqslant\ell}\sum_{s\in\mathcal{B}}\left(\lambda^s_{\ell m}\boldsymbol{L}^s_{\ell m} + \mu^s_{\ell m}\boldsymbol{M}^s_{\ell m} + \nu^s_{\ell m}\boldsymbol{N}^s_{\ell m}\right)\\
&= \sum_{\ell\in\mathbb{N}}\sum_{|m|\leqslant\ell}\sum_{s\in\mathcal{B}}\begin{bmatrix}\boldsymbol{L}^s_{\ell m} & \boldsymbol{M}^s_{\ell m} & \boldsymbol{N}^s_{\ell m}\end{bmatrix}\begin{bmatrix}\lambda^s_{\ell m}\\ \mu^s_{\ell m}\\ \nu^s_{\ell m}\end{bmatrix}\\
&= \sum_{\ell\in\mathbb{N}}\sum_{|m|\leqslant\ell}\sum_{s\in\mathcal{B}}\boldsymbol{Y}_{\ell m}(\theta,\phi)\,\boldsymbol{Z}_{\ell s}(kr)\,\boldsymbol{q}_{\ell m s}
\end{aligned}$$

Where the matrix $\boldsymbol{Z}_{\ell s}$ would then be given by

$$\boldsymbol{Z}_{\ell s}(kr) = \begin{bmatrix} \dfrac{kz_\ell^{s\prime}(kr)}{\sqrt{\ell(\ell+1)}} & 0 & \sqrt{\ell(\ell+1)}\dfrac{z_\ell^s(kr)}{kr} \\ 0 & z_\ell^s(kr) & 0 \\ \dfrac{z_\ell^s(kr)}{r} & 0 & \dfrac{1}{kr}\dfrac{d}{dr}\Big(rz_\ell^s(kr)\Big) \end{bmatrix}$$

However, for the particular case where the $\boldsymbol{\Psi}$ is a solenoidal field, $\nabla\cdot\boldsymbol{\Psi} = 0$, which will be the case for the electromagnetic field in this report, it can be easily shown that $\lambda_{\ell m}^s = 0$. Hence, it is convenient to redefine

$$\boldsymbol{q}_{\ell m s} = \begin{bmatrix} \mu_{\ell m}^s \\ \nu_{\ell m}^s \end{bmatrix} \tag{E.6}$$

and

Definition E.4.

$$\boldsymbol{Z}_{\ell s}(kr) = \begin{bmatrix} 0 & \sqrt{\ell(\ell+1)}\dfrac{z_\ell^s(kr)}{kr} \\ z_\ell^s(kr) & 0 \\ 0 & \dfrac{1}{kr}\dfrac{d}{dr}\Big(rz_\ell^s(kr)\Big) \end{bmatrix}. \tag{E.7}$$

Proposition E.1 (Analytic continuation)**.** $\boldsymbol{Z}_{\ell s}(-kr) = (-1)^\ell \boldsymbol{Z}_{\ell s}(kr)^* \begin{bmatrix} 1 & 0 \\ 0 & -1 \end{bmatrix}$

Proof. It is enough to consider the analytic continuation of Hankel functions: $z_\ell^s(-u) = (-1)^\ell z_\ell^s(u)^*$, *cf*. [AS13, Eq. 10.1.36-37, page 439]. ■

E.3 Particularisation For Solenoidal Fields

E.4 Asymptotic Behaviour

Appendix F

Definitions and Results in Vector Calculus

F.1 First Derivatives

$$\nabla(\varphi\psi) = \psi\nabla\varphi + \varphi\nabla\psi \qquad \text{(Gradient of Product)}$$

$$\nabla\cdot(\varphi\boldsymbol{F}) = \varphi\nabla\cdot\boldsymbol{F} + \boldsymbol{F}\cdot\nabla\varphi \qquad \text{(Divergence of Product)}$$

$$\nabla\cdot(\boldsymbol{F}\times\boldsymbol{G}) = (\nabla\times\boldsymbol{F})\cdot\boldsymbol{G} - \boldsymbol{F}\cdot(\nabla\times\boldsymbol{G}) \qquad \text{(Divergence of Cross Prod.)}$$

$$\nabla\times(\varphi\boldsymbol{F}) = \varphi\nabla\times\boldsymbol{F} + \nabla\varphi\times\boldsymbol{F} \qquad \text{(Curl of Product)}$$

F.2 Second Derivatives

$$\nabla^2\varphi = \nabla\cdot(\nabla\varphi) \qquad \text{(Scalar Laplacian Definition)}$$

$$\nabla^2\boldsymbol{F} = \nabla(\nabla\cdot\boldsymbol{F}) - \nabla\times(\nabla\times\boldsymbol{F}) \qquad \text{(Vector Laplacian Definition)}$$

$$\nabla\cdot(\nabla\times\boldsymbol{F}) = 0 \qquad \text{(Divergence of Curl)}$$

$$\nabla\times(\nabla\varphi) = 0 \qquad \text{(Curl of Gradient)}$$

$$\nabla^2(\varphi\psi) = \psi\nabla^2\varphi + \varphi\nabla^2\psi + 2\nabla\varphi\cdot\nabla\psi \qquad \text{(Scalar Laplacian of Prod.)}$$

$$\nabla^2(\varphi\boldsymbol{F}) = \boldsymbol{F}\nabla^2\varphi + \varphi\nabla^2\boldsymbol{F} + 2(\nabla\varphi\cdot\nabla)\,\boldsymbol{F} \qquad \text{(Vector Laplacian of Prod.)}$$

F.3 Third Derivatives

$$\nabla^2(\nabla\varphi) = \nabla\left(\nabla^2\varphi\right) \qquad \text{(Laplacian of Gradient)}$$

$$\nabla^2(\nabla\cdot\boldsymbol{F}) = \nabla\cdot\left(\nabla^2\boldsymbol{F}\right) \qquad \text{(Laplacian of Divergence)}$$

$$\nabla^2(\nabla\times\boldsymbol{F}) = \nabla\times\left(\nabla^2\boldsymbol{F}\right) \qquad \text{(Laplacian of Curl)}$$

F.4 ∇ in Spherical Coordinates

$$\nabla\varphi = \frac{\partial\varphi}{\partial r}\hat{r} + \frac{1}{r}\frac{\partial\varphi}{\partial\theta}\hat{\theta} + \frac{1}{r\sin\theta}\frac{\partial\varphi}{\partial\phi}\hat{\phi} \qquad \text{(Gradient in Spherical Coord.)}$$

$$\nabla\cdot\boldsymbol{F} = \frac{1}{r^2}\frac{\partial}{\partial r}\left(r^2F_r\right) + \frac{1}{r\sin\theta}\frac{\partial}{\partial\theta}\left(\sin\theta\cdot F_\theta\right) + \frac{1}{r\sin\theta}\frac{\partial F_\phi}{\partial\phi} \qquad \text{(Divergence in Spherical Coord.)}$$

$$\begin{aligned}\nabla\times\boldsymbol{F} = {} & \frac{1}{r\sin\theta}\left(\frac{\partial}{\partial\theta}\left(\sin\theta\cdot F_\phi\right) - \frac{\partial F_\theta}{\partial\phi}\right)\hat{r} \\ & + \frac{1}{r}\left(\frac{1}{\sin\theta}\frac{\partial F_r}{\partial\phi} - \frac{\partial}{\partial r}\left(rF_\phi\right)\right)\hat{\theta} \\ & + \frac{1}{r}\left(\frac{\partial}{\partial r}\left(rF_\theta\right) - \frac{\partial F_r}{\partial\theta}\right)\hat{\phi}\end{aligned} \qquad \text{(Curl in Spherical Coord.)}$$

$$\nabla^2\varphi = \frac{1}{r^2}\frac{\partial}{\partial r}\left(r^2\frac{\partial\varphi}{\partial r}\right) + \frac{1}{r^2\sin\theta}\frac{\partial}{\partial\theta}\left(\sin\theta\frac{\partial\varphi}{\partial\theta}\right) + \frac{1}{r^2\sin^2\theta}\frac{\partial^2\varphi}{\partial\phi^2}$$

(Scalar Laplacian in Spherical Coord.)

$$\begin{aligned}\nabla^2\boldsymbol{F} = {} & \left(\nabla^2F_r - \frac{2F_r}{r^2} - \frac{2}{r^2\sin\theta}\left(\frac{\partial F_\theta\sin\theta}{\partial\theta} + \frac{\partial F_\phi}{\partial\phi}\right)\right)\hat{r} \\ & + \left(\nabla^2F_\theta - \frac{F_\theta}{r^2\sin^2\theta} + \frac{2}{r^2}\frac{\partial F_r}{\partial\theta} - \frac{2\cos\theta}{r^2\sin^2\theta}\frac{\partial F_\phi}{\partial\phi}\right)\hat{\theta} \\ & + \left(\nabla^2F_\phi - \frac{F_\phi}{r^2\sin^2\theta} + \frac{2}{r^2\sin^2\theta}\frac{\partial F_r}{\partial\phi} + \frac{2\cos\theta}{r^2\sin^2\theta}\frac{\partial F_\theta}{\partial\phi}\right)\hat{\phi}\end{aligned}$$

(Vector Laplacian in Spherical Coord.)

References

[CL55] Earl A. Coddington and Norman Levinson. *Theory of ordinary differential equations*. McGraw-Hill, 1955.

[Kra59] H. P. Kramer. "A Generalized Sampling Theorem". In: *Journal of Mathematics and Physics* 38.1-4 (1959), 68–72. DOI: 10.1002/sapm195938168.

[Zem87] A. H. Zemanian. *Distribution theory and transform analysis: An introduction to generalized functions, with applications*. Dover Publications, 1987.

[Rud91] Walter Rudin. *Functional analysis*. 2nd ed. McGraw-Hill, 1991.

[Tro96] John L. Troutman. *Variational Calculus and Optimal Control*. Springer, 1996.

[Jac99] John David Jackson. *Classical electrodynamics*. third. Wiley, 1999.

[Lju99] Lennart Ljung. *System identification: Theory for the user*. Prentice Hall PTR, 1999.

[BN00] George Bachman and Lawrence Narici. *Functional analysis*. Dover Publications, 2000.

[Bel04] W. W. Bell. *Special Functions for Scientists and Engineers*. Dover Publications, 2004.

[Net05] Alcides Neto. *Funções de Uma variável Complexa*. IMPA, 2005.

[Kam08] David W. Kammler. *A first course in Fourier analysis*. Cambridge University Press, 2008.

[Kli10] Ludger Klinkenbusch. "Spherical-multipole based time-domain near-field to near-field transformation". In: *2010 URSI International Symposium on Electromagnetic Theory* (2010). DOI: 10.1109/ursi-emts.2010.5637254.

[AS13] Milton Abramowitz and Irene A. Stegun. *Handbook of Mathematical Functions with formulas, graphs, and mathematical tables*. Dover Publ, 2013.

[MAU13] Meriem Mhedhbi, Stephane Avrillon, and Bernard Uguen. "Comparison of vector and scalar spherical harmonics expansions of UWB antenna patterns". In: *2013 International Conference on Electromagnetics in Advanced Applications (ICEAA)* (2013). DOI: 10.1109/iceaa.2013.6632401.

[RRF14] Glaucio L. Ramos, Cassio G. Rego, and Alexandre R. Fonseca. "Parallel implementation of a combined moment expansion and spherical-multipole time-domain near-field to far-field transformation". In: *IEEE Transactions on Magnetics* 50.2 (2014), 609–612. DOI: 10.1109/tmag.2013.2280796.

[GB15] Eduardo Teixeira Geraldo Botelho Daniel Pellegrino. *Fundamentos de Análise Funcional*. 2nd ed. Rio de Janeiro: Sociedade Brasileira de Matemática, 2015.

[Lag21] I. E. Lager. "Causal excitation in antenna simulations". In: *Radioengineering* 30.1 (2021), 1–9. DOI: 10.13164/re.2021.0001.

[Mé21] Nicolas Mézières. “Contributions to Fast and Accurate Antenna Characterization”. PhD thesis. Rennes, France: L’UNIVERSITE DE RENNES 1, Aug. 2021.

[Nis] *NIST Digital Library of Mathematical Functions*. http://dlmf.nist.gov/, Release 1.1.1 of 2021-03-15. F. W. J. Olver, A. B. Olde Daalhuis, D. W. Lozier, B. I. Schneider, R. F. Boisvert, C. W. Clark, B. R. Miller, B. V. Saunders, H. S. Cohl, and M. A. McClain, eds. URL: `http://dlmf.nist.gov/`.